



TECHNICKÁ UNIVERZITA V LIBERCI

Fakulta textilní



Hybridní tkané struktury

Disertační práce

Studijní program: P3106 – Textile Engineering
Studijní obor: 3106V015 – Textilní technika a materiálové inženýrství
Autor práce: **Hafsa Jamshaid, MS.**
Vedoucí práce: doc. Rajesh Mishra, Ph.D.
Vedoucí specialista: prof. Ing. Jiří Militký, CSc, EURING.





HYBRID WOVEN STRUCTURES

Dissertation

Study programme: P3106 – Textile Engineering
Study branch: 3106V015 – Textile Technics and Materials Engineering
Author: **Hafsa Jamshaid, MS**
Supervisor: doc. Rajesh Mishra, Ph.D.
Supervisor specialist: prof. Ing. Jiří Militký, CSc, EURING.



Prohlášení

Byla jsem seznámena s tím, že na mou disertační práci se plně vztahuje zákon č. 121/2000 Sb., o právu autorském, zejména § 60 – školní dílo.

Beru na vědomí, že Technická univerzita v Liberci (TUL) nezasahuje do mých autorských práv užitím mé disertační práce pro vnitřní potřebu TUL.

Užiji-li disertační práci nebo poskytnu-li licenci k jejímu využití, jsem si vědoma povinnosti informovat o této skutečnosti TUL; v tomto případě má TUL právo ode mne požadovat úhradu nákladů, které vynaložila na vytvoření díla, až do jejich skutečné výše.

Disertační práci jsem vypracovala samostatně s použitím uvedené literatury a na základě konzultací s vedoucím mé disertační práce a konzultantem.

Současně čestně prohlašuji, že tištěná verze práce se shoduje s elektronickou verzí, vloženou do IS STAG.

Datum:

Podpis:

"My work is dedicated to all the wonderful people around me, who were always helpful, encouraging and became a motivation for me to successfully conduct this research work. I can never mention all the names but I have everybody's name engraved on my heart, no matter where I go, what I do, I shall always try and adopt few of traits of some of the best people I ever met."

Acknowledgement

"Seek Knowledge, gain wisdom and keep learning, no matter how far you have to travel."

- Hazrat Muhammad P.B.U.H (*Prophet, Motivator*)

In your life there are few quotes that inspire you and the inspiration I had, made me see a dream, all the efforts I did, all the hard work I had gone through were to live that dream. I am thankful to Almighty Allah for providing me with the opportunities and support of so many beautiful minds who understood meanings of a dream. I am thankful to Technical University of Liberec for providing the platform and doc. Rajesh Mishra for providing me the path and direction. My supervisor deserves the credit as his monumental guidance; support and patience made everything grow into reality. I really appreciate the way he guided me, took care of difficult things and made them look easy and above all motivated me all the times, I am so thankful to him. Professor Ing. Jiri Militky, CSc for his support and guidance, he was very kind to share his ocean of knowledge and inspired me with his infectious fervor to share his genius.

My heart is full of thanks to management for their continuous support and facilities that helped me to pursue my PhD degree in this esteemed institution. My special thanks to the Dean of Faculty of Textile Engineering, Ing. Jana Drašarová, PhD for her continuous support and Vice Dean Ing. Gabriela Krupincová, PhD for their kind support. I thank Secretaryies Kateřina Štruplová and Kateřina Nohýnková, for their coordination. My grateful appreciation to the lab-incharges who were kind enough to provide access to laboratory facilities at any hour of the day. This thesis may not have been possible without the contribution, support, help and coordination of the faculty and staff of Textile Engineering. I thank all my friends and colleagues who were supportive throughout the research period.

I am extremely lucky to have a family who always supported me, my husband Jamshaid Babar and my two sons ' Uzair Jamshaidand , Taha Jamshaid are my world. They were always supportive for my studies. They patiently waited for my work to finish. I can proudly say no matter how much time we spent without each other, our bonding is ever strong, stronger than before. I love my small family more than anything else in this world. I want to dedicate this to my late parents, Sheikh Muhammad Riaz and Naeem Akhter, they helped and guided me on every level of my studies.

My little journey to PhD has been a full of experiences, I know this little path is coming to an end but the knowledge I gained from this, I am sure I will not stop learning. In these past years, I woke up every day like a new born baby and watched this world of wonders with open eyes. I never imagined learning can be so much fun. I have experienced this in the company of some of world's finest and I am proud of it.

I can proudly say, dreams can come true with dedication and support.

ABSTRACT

With the advancement and continuing integration of composite materials and technology in today's modern industries, research in this field is becoming more and more significant. Most research exercises production of composites, testing of composites, attempts to find ways of prediction of properties etc. Others use entire fiber bundles or fiber/resin blocks and combine their properties in the layers/plies during forming of composites. However, the properties of the fibers in the fiber bundle/yarn can be used to predict the properties of final composite product accurately.

This thesis conveys a better insight into characteristics of Basalt fibers specifically, alongside commonly used fibers to design and develop hybrid woven fabrics for TRC composite materials. Various combinations of basalt hybrid fabrics are investigated with respect to mechanical, thermal, acoustic, electrical and other functional properties. The influence of hybridization and structure of woven fabric is studied in detail. The tensile properties are predicted by using structural model and correlated to the results obtained through experiments.

Basalt fibers are very promising materials due to their fire resistance related to magmatic origin, superior mechanical properties and relatively low cost. On the other hand, being a relatively new kind of fiber, they are still not studied extensively. There are very few indications in technical papers about their behavior after aging treatments. The current study investigates the possibility of using basalt with other types of yarns and consequently the effect of hybrid woven structure on load bearing capacity and durability. In the present work, the load-bearing behavior of Textile Reinforced Concrete (TRC), which is a composite of a fine-grained concrete matrix and a reinforcement of high-performance fibers processed to textiles, when exposed to uniaxial tensile loading was investigated. The investigations are focused on reinforcement of hybrid woven fabrics.

When textile yarns are embedded in concrete, they are not entirely impregnated with cementitious matrix, which leads to associated heterogeneity of the concrete and the yarns to a complex load-bearing and failure behavior of the composite system. The main objective of the work is the investigation of hybridization effects in the load-bearing behavior of TRC.

The interfacial bond between textile reinforcement and the concrete matrix is greatly heterogeneous. The characterization of the bond behavior is thus critical in order to understand the global structural behavior of TRC. The bond behavior of textile reinforcement embedded in a concrete matrix was experimentally investigated in this work. The force-displacement curves obtained from tensile tests demonstrated clearly the positive influence of basalt yarn on the mechanical performance of TRC. The bond behavior of textile reinforced concrete was characterized in this work by means of direct pull-out tests.

This thesis also aims to investigate structural performance and durability aspects of TRC for its usability in the built environment. The present work provides a direction to study durability of different fiber-reinforced cement composites which can be ascertained/forecast by interfacial

bonds and accelerated aging conditions. This study helps in gaining better insight into the specific material behavior of the concrete with hybrid reinforcement.

According to the results obtained, it can be concluded that the accelerated ageing test was too aggressive for textiles made of jute and PET, leading to extensive degradation; however, basalt and PP textiles were found to be a promising alternative as they have superior durability properties in an alkaline environment without undergoing much strength loss. Despite the hydrophobic characteristics of PP fibers and their poor bond with the cement matrix, these fibers are considered as attractive for the reinforcement of cement matrices because of their high resistance to the alkaline environment of the cement matrix and a relatively lower cost.

In general the use of high strength fibers like basalt increases the strength and toughness of the cement composites providing strain-hardening behavior. Low modulus fiber such as PP and PET enhance mainly the ductility of the cement composites, but not its strength in a strain softening behavior. The PP/PET structure did not bond strongly with the cement matrix, resulting in relatively low composite performance. The B/PP or B/PET yarn combination in a hybrid fabric should be considered as reinforcement for cement composites. By the hybridization of PP/PET yarn with basalt, this problem can be solved.

Keywords: Hybrid woven fabrics, basalt, weavability, structural models, shear, yarn pull-out, accelerated aging, DMA, acoustic properties, electrical properties

Abstrakt

Se zdokonalováním a trvalým začleňováním kompozitních materiálů a technologií v současném moderním průmyslu se výzkum v této oblasti stává čím dál více významnějším. Většina výzkumných prací se zabývá výrobou kompozitních materiálů, jejich testováním a přístupy jak predikovat vlastnosti atd. Další vědecká činnost je směřována na použití vlákných svazků nebo celků vlákno / pryskyřice kombinujících jejich vlastnosti vrstvením během formování kompozitu. Charakteristiky vláken ve vlákných svazcích resp. přízích mohou být nicméně použity pro přesné předpovězení vlastností finálního kompozitního produktu.

Tato disertační práce poskytuje podrobnější informace o vlastnostech čedičových vláken vedle běžně používaných vláken, a to pro návrh a vývoj hybridních tkaných textilií určených pro výrobu kompozitních materiálů, zejména betonu vyztuženého textilií (TRC). Zkoumány jsou různé kombinace čedičové hybridní tkaniny s ohledem na mechanické, tepelné, akustické, elektrické a jiné vlastnosti, přičemž vliv hybridizace a struktury tkaných textilií je studován detailněji. Mechanické vlastnosti jsou predikovány s použitím a strukturální modely korelovány s výsledky získanými z provedených experimentů.

Čedičová vlákna jsou velmi perspektivním materiálem díky jejich ohnivzdornosti spojené s lávovým původem, vynikajícím mechanickým vlastnostem a relativně nízké ceně. Na druhou stranu, tato vlákna doposud nebyla podrobena rozsáhlejšímu průzkumu, protože je možno je považovat za relativně nový typ vlákna. V technických člancích je možno nalézt jen omezené množství údajů o jejich chování po zpracování, jež je spojeno se stárnutím materiálu. Disertační práce prozkoumává možnosti využití čedičových vláken v kombinaci s jinými typy příze a následně také vliv hybridní tkané struktury na nosnost kompozitu a dobu jeho životnosti. V této studii je vyšetřeno nosné chování TRC kompozitu (kompozitní systém tvořený jemnozrnnou betonovou maticí a výztuží složenou z vysoce funkčních vláken zpracovaných do plošné textilie) při jednoosém namáhání tahem. Průzkum je zaměřen na výztužnou schopnost hybridní tkané struktury.

Při začleňování textilní struktury do betonu je zřejmé, že veškeré příze nejsou impregnovány cementovou maticí kompletně, což vede k heterogenitě systému beton – příze přispívajícímu ke komplexní nosnosti a defektnímu chování TRC kompozitu. Hlavním cílem této práce je tedy průzkum hybridizačních efektů na nosné chování TRC kompozitu.

Mezifázová síla mezi textilní výztuží a betonovou maticí je významně heterogenní. Charakterizace vazebného chování je proto rozhodující pro pochopení globálního strukturálního chování TRC kompozitů. V této práci bylo tedy experimentálně prozkoumáno vazebné chování textilní výztuže začleněné do betonové matrice. Pracovní křivky získané z testů jednoosého namáhání vzorků tahem jednoznačně ukazují pozitivní efekt čedičové příze na mechanické vlastnosti TRC kompozitů. Toto vazebné chování betonu vyztuženého textilií bylo sledováno v práci přímo pomocí vytrhávacího testu.

Tato disertační práce dále cílí na vyšetření aspektů strukturální funkčnosti a životnosti TRC kompozitů pro jejich použití ve stavebnictví. Práce udává směr studia životnosti různých, vlákných

vyztužených cementových kompozitů, která může být zjišťována resp. předpovídána na základě znalosti mezifázových vazeb a podmínek zrychleného stárnutí.

Na základě získaných výsledků může být shrnuto, že testy zrychleného stárnutí byly příliš agresivní pro textilie vyrobené z juty a polyesteru (PET) vedoucí k jejich významné degradaci. Čedičové (B) a polypropylenové (PP) textilie však byly shledány slibnou alternativou ke zmíněným vláknům díky jejich výjimečné životnosti v alkalickém prostředí bez významných ztrát pevnosti. I přes hydrofobní charakter polypropylenových vláken a tedy jejich slabé interakci s cementovou maticí byla tato vlákna shledána jako atraktivní pro výztuž cementové matrice, a to díky jejich vysoké odolnosti k alkalickému prostředí cementové matrice a relativně nízké ceně. Použití vysoce-pevnostních vláken jako jsou čedičová, obecně zvyšuje pevnost a tuhost cementových kompozitů poskytující mechanické zpevnění. Vlákná s nízkým modulem jako jsou polypropylen a polyester zlepšují zejména tažnost cementových kompozitů, ne však jejich pevnostně deformační chování. Struktury založené na kombinaci PP/PET se nepojí silně s cementovou maticí, což vede k relativně nízké funkčnosti kompozitu. Na druhou stranu kombinace B/P nebo B/PET v hybridní plošné textilií se zdá být dobrou volnou pro výztuž cementových kompozitů. Je tedy zřejmé, že hybridizace PP/PET příze s čedičem přináší řešení problému.

Klíčová slova: Hybridní tkaniny, čedič, zpracovatelnost tkaním, strukturální modely, smyk, vytrhávání příze, zrychlené stárnutí, DMA, akustické vlastnosti, elektrické vlastnosti

Table of Contents

| | | |
|-------------------|---|-----|
| | List of Symbols and abbreviations | 13 |
| | List of Tables | 15 |
| | List of Figures | 16 |
| | Research Objectives | 18 |
| A | To analyze the weavability problem during production of basalt hybrid fabrics | |
| B | To predict structural parameters and mechanical properties by using suitable geometrical/computational tools and verify the predictability | |
| C | To investigate the effect of weave and fiber composition on mechanical, thermal and functional properties in basalt based hybrid woven structures | |
| D | Study of thermo-mechanical characteristics of basalt hybrid fabrics | |
| E | Study of acoustic properties of basalt hybrid fabrics | |
| F | Study of durability under accelerated aging conditions | |
| G | Compatibility study of basalt and other yarns with cement | |
| Chapter 1. | Introduction | |
| 1.1 | General Introduction | 20 |
| 1.2 | The scope of this research | 23 |
| 1.3 | Dissertation Outline | 24 |
| Chapter 2. | State of the Art | |
| 2.1 | General aspects of composites | 25 |
| 2.2 | Classification of textile reinforcement | 28 |
| 2.2.1 | Woven fabric | 30 |
| 2.3 | Basalt fiber | 31 |
| 2.4 | TRC | 39 |
| 2.5 | Limitations | 42 |
| Chapter 3. | Experimental Materials and Methods | |
| 3.1 | Materials | 56 |
| 3.2 | Methods | 57 |
| 3.2.1 | Preparation of samples on CCI sample loom | 57 |
| 3.2.2 | Characterization of the raw materials | 60 |
| 3.2.3 | Testing methods for fabrics | 61 |
| 3.3 | Characterization of load bearing capacity and durability of yarns in cement composites | 76 |
| 3.4 | Statistical Analysis with ANOVA | 78 |
| Chapter 4. | Results & Discussion | |
| 4.1 | Weavability study for Basalt yarn | 79 |
| 4.1.1 | Production of hybrid and non-hybrid fabrics | 79 |
| 4.2 | Characterization of fiber and cement raw material | 89 |
| 4.3 | Accelerated aging in alkaline solution | 91 |
| 4.4 | Yarn pull out test from cement matrix | 97 |
| 4.5 | Testing of Fabric samples | 101 |
| 4.5.1 | Physical Properties | 101 |
| 4.5.2 | Static Mechanical Properties | 104 |

| | | |
|-------------------|-------------------------------------|-----|
| 4.5.3 | Dynamic Mechanical Properties | 117 |
| 4.5.4 | Transmission and Thermal Properties | 120 |
| 4.5.5 | Electrical Properties | 132 |
| 4.5.6 | Acoustic Properties | 137 |
| 4.5.7 | Thermal Stability | 145 |
| Chapter 5. | Summary & Conclusion | |
| | Summary and conclusion | 149 |
| | Future Direction | 151 |
| | Research Outputs | 152 |
| | Journal Publications | |
| | Book Chapters | |
| | Conference Publications | |
| | References | 155 |

List of Symbols and Abbreviations

| Symbol | Description |
|---------------------------|-------------------------------|
| E [MPa] | Initial modulus |
| E'' [MPa] | Loss modulus |
| G [MPa] | Shear rigidity |
| r [Pa.m ⁻² .s] | Air flow resistivity |
| R [m ² .K/W] | Thermal resistance |
| R _v [Ω] | Electrical volume resistance |
| h [m] | Thickness |
| tan δ [-] | Loss factor |
| Z [Pa·s/m ³] | Specific acoustic impedance |
| α [-] | Sound absorption coefficient |
| Γ [-] | Shear strain |
| λ [W/(mK)] | Thermal conductivity |
| τ [MPa] | Shear stress |
| ρ _v [Ω.cm] | Electrical volume resistivity |

| Abbreviations | Description |
|----------------------|---|
| ASTM | American Society for Testing and Materials |
| ATR | Attenuated total reflection |
| B/J | Basalt/jute |
| B/PET | Basalt/Polyester |
| B/PP | Basalt/Polypropylene |
| CTE | Coefficient of thermal expansion |
| CFRP | Carbon fiber reinforced plastic |
| CMCs | Ceramic matrix composites |
| EDXA | Energy dispersive X-ray analysis |
| EN ISO | European standards International Organization for Standardization |
| FRP | Fiber Reinforced Plastic |
| FTIR | Fourier Transform Infra-Red |
| FEM | Finite element method |
| FRCs | Fiber Reinforced composites |
| GFRP | Glass fiber reinforced plastic |
| GPC | Geo polymer cement |
| HFRP | Hybrid Fiber Reinforcement Plastics |
| HM | High modulus |
| HT | High tenacity |
| ICP | Inductively Coupled Plasma |
| IFSS | Interfacial shear strength |
| MMCs | Metal matrix composites |
| MTPS | Modified transient plane source |
| NRC | Noise Reduction coefficient |
| OPC | Ordinary Portland cement |
| OES | Optical emission spectroscopy |

| | |
|-----------|--|
| PMCs | Polymer matrix composites |
| SNK | Student-Newman-Keuls |
| SAC | sound absorption coefficient |
| TCI | Thermal conductivity analyzer |
| TRC | Textile Reinforced composites/Concrete |
| TPM | Twist/meter |
| <i>UD</i> | Uni-directional/dimensional |
| XRF | X-ray fluorescence spectroscopy |

List of Tables

| | | |
|-------------------|---|-----|
| Table 2.1 | Mechanical properties of structural materials | 35 |
| Table 2.2 | Mechanical properties of selected fibers | 36 |
| Table 2.3 | Physical and mechanical properties | 37 |
| Table 2.4 | Electrical properties Basalt Vs. Glass | 51 |
| Table 3.1 | Properties of fibers and yarns used | 56 |
| Table 3.2 | Production parameters | 58 |
| Table 3.3 | Fabric structure developed | 59 |
| Table 3.4 | Weave factors for various weaves | 62 |
| Table 4.1 | Machine settings for Basalt/Basalt | 80 |
| Table 4.2 | Machine settings for Basalt/Polypropylene | 81 |
| Table 4.3 | Machine settings for Basalt/Polyester | 82 |
| Table 4.4 | Machine settings for Basalt/Jute | 83 |
| Table 4.5 | Machine settings for polypropylene/basalt | 83 |
| Table 4.6 | Machine settings for polyester/basalt | 84 |
| Table 4.7 | Machine settings for Polypropylene/Polypropylene | 85 |
| Table 4.8 | Machine settings for Polyester/Polyester | 85 |
| Table 4.9 | Machine settings for Jute/Jute | 86 |
| Table 4.10 | Production parameters for weavability study on commercial loom | 87 |
| Table 4.11 | Analysis of variance output for Efficiency | 88 |
| Table 4.12 | Elemental composition of basalt | 89 |
| Table 4.13 | Metal contents (concentration) of used cements | 90 |
| Table 4.14 | % Weight loss | 92 |
| Table 4.15 | Mean tensile strength after 1 week of alkali treatment | 92 |
| Table 4.16 | Mean tensile strength after 2 week of alkali treatment | 92 |
| Table 4.17 | Apparent interfacial shear strength (τ_{app}) for different fibers in cement | 98 |
| Table 4.18 | Experimental findings of the pull out study | 99 |
| Table 4.19 | Physical Parameters of Fabrics | 102 |
| Table 4.20 | Mechanical Properties of Fabric | 105 |
| Table 4.21 | Thermal Properties of Fabrics | 132 |
| Table 4.22 | Calculated porosity and measured resistance of samples | 133 |
| Table 4.23 | NRC and others parameters | 139 |

List of Figures

| | | |
|--------------------|---|-----|
| Figure 2.1 | Classification of composites | 27 |
| Figure 2.2 | Classification of fibers | 29 |
| Figure 2.3 | Classification of reinforcement according to their architecture | 30 |
| Figure 2.4 | Woven structures | 31 |
| Figure 2.5 | Basalt fiber spinning | 34 |
| Figure 2.6 | Pedestrian Bridge in Okinawa, Japan made of Hybrid Composite | 42 |
| Figure 2.7 | Limit arrangement of polymeric phase (gray) and air phase (white) in conductivity model | 48 |
| Figure 2.8 | Acoustic characteristics of textile materials | 53 |
| Figure 3.1 | CCI sample loom and commercial rapier loom for running the fabric samples | 57 |
| Figure 3.2 | Photographs (Dinolite) of the structures developed with magnification 1280 x1024 | 60 |
| Figure 3.3 | TIRA tester for tensile properties | 63 |
| Figure 3.4 | Weave structure (a-c) 3D image, (d-f) code editor and (g-i) graphical editor | 64 |
| Figure 3.5 | Fabric parameters: yarn spacing | 65 |
| Figure 3.6 | Picture frame fixture design | 66 |
| Figure 3.7 | Clamping of sample in fixture | 67 |
| Figure 3.8 | Determination of shear angle using image analysis | 68 |
| Figure 3.9 | Detected lines and points in Hough's histogram | 68 |
| Figure 3.10 | Schematic diagram of the experimental set up of DMA | 69 |
| Figure 3.11 | Schematic diagram of the experimental set up to measure air permeability | 71 |
| Figure 3.12 | Schematic diagram of the experimental set up to measure thermal properties | 71 |
| Figure 3.13 | Schematic diagram of the experimental set up to measure thermal properties | 71 |
| Figure 3.14 | (a) Resistivity measurement system and (b) schematic diagram of an experimental set-up to measure electrical resistance | 72 |
| Figure 3.15 | (a) Impedance tube method and (b) schematic diagram of an experimental set-up | 74 |
| Figure 3.16 | Schematic diagram Perkin Elmer Differential Scanning Calorimeter DSC6 | 75 |
| Figure 3.17 | Mettler Toledo TGA/SDTA851 | 76 |
| Figure 3.18 | Yarn pull out test | 77 |
| Figure 4.1 | Residual Plots for Efficiency % | 88 |
| Figure 4.2 | Energy-Dispersive X-Ray Analysis of Basalt | 89 |
| Figure 4.3 | FTIR spectra of used cement materials (a) OPC, (b) GPC | 90 |
| Figure 4.4 | Effect of pH on degradation of yarn after alkali treatment | 93 |
| Figure 4.5 | Effect of time on degradation of yarn after alkali treatment | 94 |
| Figure 4.6 | SEM images of fibers after alkali treatment | 96 |
| Figure 4.7 | Force vs displacement for yarns in Portland and Geopolymer cement | 98 |
| Figure 4.8 | Photographic images of failure/rupture | 100 |
| Figure 4.9 | Four types of pores in woven fabric (a) planar way (b) on the graph paper | 101 |
| Figure 4.10 | Correlation of physical parameters from geometrical model with experimental results | 103 |
| Figure 4.11 | Load-Elongation curve of yarns | 104 |
| Figure 4.12 | Stress-strain curves for hybrid and non-hybrid fabrics in warp direction | 108 |
| Figure 4.13 | Stress-strain curves for hybrid and non-hybrid fabrics in weft direction | 109 |
| Figure 4.14 | Elastic Moduli of hybrid and non-hybrid fabrics | 110 |

| | | |
|--------------------|--|-----|
| Figure 4.15 | Prediction of tensile properties with WISETEX | 110 |
| Figure 4.16 | Correlation of tensile strength predicted by WISETEX and measured values | 111 |
| Figure 4.17 | Shear deformation of B/PET sample at different displacement levels | 113 |
| Figure 4.18 | Shear deformation of specimens at different displacement levels | 114 |
| Figure 4.19 | Comparison of shear angles between image analysis and experimental values | 117 |
| Figure 4.20 | Storage Moduli of different weaves | 119 |
| Figure 4.21 | $\tan \theta$ of different weaves | 120 |
| Figure 4.22 | Air permeability of various hybrid and non-hybrid woven structures | 122 |
| Figure 4.23 | Thermal conductivity VS fabric density | 123 |
| Figure 4.24 | Theoretical model and measured Thermal Conductivity | 124 |
| Figure 4.25 | Correlation of thermal conductivity from λ_{beta} , TC_i and theoretical model | 126 |
| Figure 4.26 | Correlation of thermal resistance from TC_i and λ_{beta} | 127 |
| Figure 4.27 | Thermal resistance from theoretical model and measured values | 127 |
| Figure 4.28 | Correlation of thermal resistance from λ_{beta} and TC_i vs Porosity | 129 |
| Figure 4.29 | Thermal Resistance vs Thickness | 130 |
| Figure 4.30 | Dependence of thermal resistance on thickness and porosity | 131 |
| Figure 4.31 | Dependence between volume resistance and surface resistance | 134 |
| Figure 4.32 | Volume resistance of all samples tested | 135 |
| Figure 4.33 | Volume resistance of (a) hybrid structures grouped according to the identical material composition, (b) hybrid structures grouped according to the identical weave pattern, (c) chosen basalt hybrid samples(d) non hybrid samples | 136 |
| Figure 4.34 | Sound absorption coefficient of all samples | 138 |
| Figure 4.35 | Effect of weave structure on sound absorption behavior of various hybrid fabrics | 140 |
| Figure 4.36 | Relationship between fabric porosity, airflow resistivity and NRC | 141 |
| Figure 4.37 | Dependence of acoustic impedance on elastic moduli and density of woven fabrics | 145 |
| Figure 4.38 | TGA curves for all hybrid and nonhybrid compositions | 146 |
| Figure 4.39 | TGA, DTG and DSC curves for different structures | 147 |
| Figure 4.40 | SEM images of hybrid fabrics after TGA | 148 |

Research Objectives

1. Research Objectives

The objectives of the study are:

A. To analyze the weavability problem during production of basalt hybrid fabrics

The purpose of this work is to study compatibility of basalt with other fibers in terms of weavability. The fibers in consideration are both thermoset and thermoplastic. Three types of weave structures were selected for the study i.e. plain, twill and matt weave. The structures produced were both hybrid and non-hybrid. During the sample production in weaving, behavior of each group was studied. With certain fibers there were too many problems in terms of weaving efficiency and end breakages. Fibers like polyester and polypropylene caused greater problems during weaving due to static charges associated with synthetics. The problems associated with breakages were more in starting of samples as different settings were required for different combination of fibers and variable weaves within the same combination of fibers. During the running of polyester, certain special treatments like special cutter adjustment and different settings which vary from the recommended ones were observed. A special cutter was developed for polypropylene as it is slippery in nature and normal cutter was unable to cut the yarn. For each combination of fibers monitoring, time study, breakages, efficiency and final settings were observed and noted. A special arrangement, during running of any combination of fibers was noted separately for future reference. Every weave and combination of fibers was allocated with separate time and special attention was given till the completion of each sample. All the record was maintained along with the working efficiency to keep up to date working of respective combinations.

B. To predict structural parameters and mechanical properties by using suitable geometrical/computational tools and verify the predictability

Several methods are employed for the analysis and mechanical modeling of textile structures. Different geometrical models/computational tools are used for modeling of the internal geometry and deformability of textile structures. Thread spacing and crimp are estimated by using geometrical models. Tensile properties of basalt hybrid and non-hybrid fabrics are predicted by computational tool and verified with experimental data.

C. To investigate the effect of weave and fiber composition on mechanical, thermal and functional properties in basalt based hybrid woven structures.

The fabrics are investigated for mechanical and thermal properties. Tensile and shear testing was carried out. Shear testing was done by a biased tensile testing method and results were correlated with image processing based evaluation. Thermal properties were also investigated. Complex comparison of basalt fiber as a new type of reinforcement vis-a-vis other reinforcing fibres was

made. For this reason basalt woven hybrid fabrics have been produced and the role of different reinforcing yarns in the structure and their properties and capabilities have been investigated. Polypropylene (PP), Polyester (PET) and jute yarns have been used in the hybrid fabrics besides basalt yarn, and the mechanical characteristics of the hybrid fabrics have been investigated as a function of weave and fiber composition by tensile testing and dynamic mechanical testing respectively. Electrical resistivity of various hybrid woven structures was investigated as a function of fiber type and weave structure.

D. Study of thermo-mechanical characteristics of basalt hybrid fabrics

Dynamic mechanical analysis for all non-hybrid and hybrid woven fabrics was performed on a DMA 40XT RMI equipment. The DMA test was executed in the temperature range of 27 to 100°C at a heating rate of 3°C/min. This test was performed according to EN ISO 6721-1. For each sample, five measurements were done. Dynamic mechanical analysis (DMA) yields information about the mechanical properties of a specimen placed, usually sinusoidal, oscillation as a function of time and temperature by subjecting it to a small, usually sinusoidal, oscillating force. It allows the measurement of two different moduli of the materials, a storage modulus (E') which is related to the ability of the material to return or store mechanical energy and a loss modulus (E'') which is related to the ability of the material to dissipate energy as a function of temperature. Ratio of loss modulus to storage modulus is given by $\tan(\delta)$. The effect of fiber composition and weave structure in hybrid woven fabrics was evaluated.

E. Study of acoustic properties of basalt hybrid fabrics

The acoustic impedance of a material is its most basic acoustic property. Impedance, defined as the ratio of the pressure to the volume displacement at a given surface in a sound-transmitting medium, is usually a frequency-dependent number. Acoustic property for all hybrid woven fabrics were measured by using two-microphone impedance tube according to ASTM E1050-08. The sound absorption coefficient (SAC) for the frequency range from 50-1600 Hz and 500- 6400 Hz was evaluated. It is correlated to the air resistivity of various hybrid woven structures. Effect of weave structure and porosity was studied in detail. Relationship between elastic moduli and sound is also analyzed.

F. Study of durability under accelerated aging conditions

The degradation of fiber due to the alkaline solution in the cement matrix seriously decreases the durability and may cause premature failure of the TRC. Calcium hydroxide, which is the primary cause of alkaline environment in cement is used to study the accelerated aging of basalt as well as other thermoset and thermoplastic fiber yarns. In this case, the high concentration of alkali is the main cause of fibers damage. Particularly, weight loss and reduction in mechanical properties could appear. In this work, the effect of accelerated ageing on the tensile properties of textile reinforcement materials was investigated with different variables e.g. time, pH and type of alkali (NaOH and $\text{Ca}(\text{OH})_2$).

G. Compatibility study of basalt and other yarns with cement

Further aim of the work is to investigate the effect of using different yarns on load bearing capacity in a cement matrix system. The interaction between the cement matrix and reinforcement is characterized by the bond behavior. It is very important that there is good adhesion between the reinforcing fibers and the concrete or cement matrix, otherwise debonding may take place. Bond strength may dominate the mechanical properties of fiber-reinforced concrete. Thus the pull out strength from a cement matrix was evaluated for basalt and other types of yarns.

Chapter 1- Introduction

1.1 General Introduction

The fast pace of technological advancement has always pushed engineering materials to their limits but in the last century the development of new materials is so fast as requirements for structures, automobiles etc. are changing rapidly. In the quest for ever more performance from existing materials, engineers have developed hybrid materials that in combination have characteristics superior to that of their individual constituents. Many of our modern technologies require material with unusual combination of properties that cannot be met by the conventional metal, ceramics and polymeric materials. This is especially true for materials that are needed for construction, transportation applications. Composites are emerging as realistic alternatives to the metal alloys in many applications like construction, automobiles, marine, aerospace applications, sports goods, etc. Composites can be defined as combination of dissimilar materials to perform task that neither of the constituent materials can perform alone, since hardly any material is used in its pure form today, have all-rounder properties. Composite materials have a long history of usage. The history of composites is as old as the history of mankind itself. The human body can be considered as a composite made of bones and flesh [1]. Composites are emerging as realistic alternatives to the metal alloys in many applications like automobiles, marine, aerospace applications, sports goods, etc.

The fiber/textile is an important constituent in Fiber/textile Reinforced composites. FRCs find applications in construction industries, decking, window and door frames, sports equipment such as bicycle frames, baseball bats, exercise equipment and so on. They are also suited for many automotive applications. The textile composites are composed of two materials i.e., a textile skeleton for reinforcement (called perform) and a binding adhesive (called matrix) material to keep the skeleton integrated into a specific shape. The output and the scope of application for reinforced fibers within polymeric composites have been gradually expanding all over the world. In comparison with conventional materials, fiber composites boast a number of advantages: corrosion resistance, chemical inertness, low factor of heat conductivity, high specific mechanical properties, small specific weight, high operating temperature, long wearing life, low cost of design installation. Fiber/textile reinforcements in composite material are generally used to improve the mechanical properties.

Materials selection has always involved a number of compromises for the engineering designer. Of course, the material's properties are extremely important, since the performance of the structure or component to be designed relies in the properties of the material used in its construction. However, properties come at a cost, and the engineer must balance cost factors in making a materials selection. The fiber generally occupies 30% - 70% of the matrix volume in the composites. The fibers can be chopped, woven, stitched, and braided. The most common fiber reinforcement in resin is glass fiber. There are other types of fibers for reinforcement such as carbon fiber, other plastic fibers.

Depending on the source, fibers are largely divided into two categories: natural and synthetic. A lot of work has been done by many researchers on composites containing natural and synthetic fibers [2-4]. But both these fibers have advantages and drawbacks. Synthetic fiber-reinforced thermoplastic composites have better mechanical properties than the natural fibers, like their high strength, better durability and moisture resistance properties [5] but they are not environmentally friendly.

Polypropylene (PP) and Polyester (PET) are the two major synthetic fibers mainly used in industry. Polyester is made from Terephthalic acid (PTA) and Ethylene Glycol. Polypropylene is a polyolefin made from a polypropylene monomer obtained from naphtha. PP is a popular fiber due to its properties like low density i.e lightest fiber, easy process ability, excellent orientation characteristics, superior tensile properties, good chemical resistance, hydrophobicity, resistance to micro-organisms and the relatively inexpensive cost of production. Polyester fibers have high tenacity and elastic modulus as well as low water absorption and minimal shrinkage in comparison with other fibers. While combustible at high temperatures, polyesters tend to shrink away from flames and self-extinguish upon ignition.

With low cost and high specific mechanical properties, natural fibers represent a good, renewable and biodegradable alternative to the most common synthetic reinforcement, i.e., glass fiber. Glass and carbon fibers are widely used for making composites. Environment-friendly and cost effective composites have recently received considerable attention among the scientists. The use of glass and carbon as reinforcements in composites is currently thought of attributable to environmental concern though they have possessed excellent mechanical, thermal properties and durability. In composites, use of natural fibers such as ramie, jute, sisal, hemp, bamboo, oil palm fibers, banana etc is increasing to act as reinforcement. Among these fibers, jute is of particular interest as production of jute is excessive in tropical countries and composites made of jute fibers have moderate flexural and tensile properties compared with other natural fibers. Several authors have studied the continuous jute fiber composites from different aspects, for example, mechanical properties [6–10], the effect of fiber treatments on mechanical properties [9–10], dynamic mechanical properties [11], physical properties [7], and processing and microstructures [11].

Concern for the environment, both in terms of limiting the use of finite resources and the need to manage waste disposal, has led to increasing pressure to recycle materials at the end of their useful life. As Fiber-reinforced polymer composites are widely applied in modern industry and many researches have been carried out to develop environmental fiber materials for the last decade. As a result, basalt fiber has taken notice of researchers as a new reinforcing fiber material [12]. Basalt fiber is extruded from melted basalt rock that consists mainly of Si and Al oxides. The tensile strength of single basalt fiber can be as high as carbon and also it has excellent thermal and chemical stability. Since its manufacturing process is simpler compared to that of glass fiber, basalt consumes less energy, and reduces environmental waste such as carbon dioxide through the manufacturing process [13]. Basalt is an environment friendly natural material. It is one type of high performance inorganic fiber which is made from natural basalt.

Basalt fiber is known as green industrial material and is colloquially known as the “21st-century nonpolluting green material”. Safe and abundant, basalt rock has long been known for its thermal properties, strength and durability. Basalt fibers are environmental friendly as its recycling is much more efficient than glass fibers. It is cheaper than carbon fibers, and exhibits a higher strength than glass [14-16]. It is inexpensive and has excellent properties such as corrosion resistance, minimal moisture absorption and the ability to withstand high temperatures, provide thermal insulation, and absorb sound. It is also a cost-effective and high-strength material that has been widely used in road construction, buildings and other applications that require reinforcement [15-20].

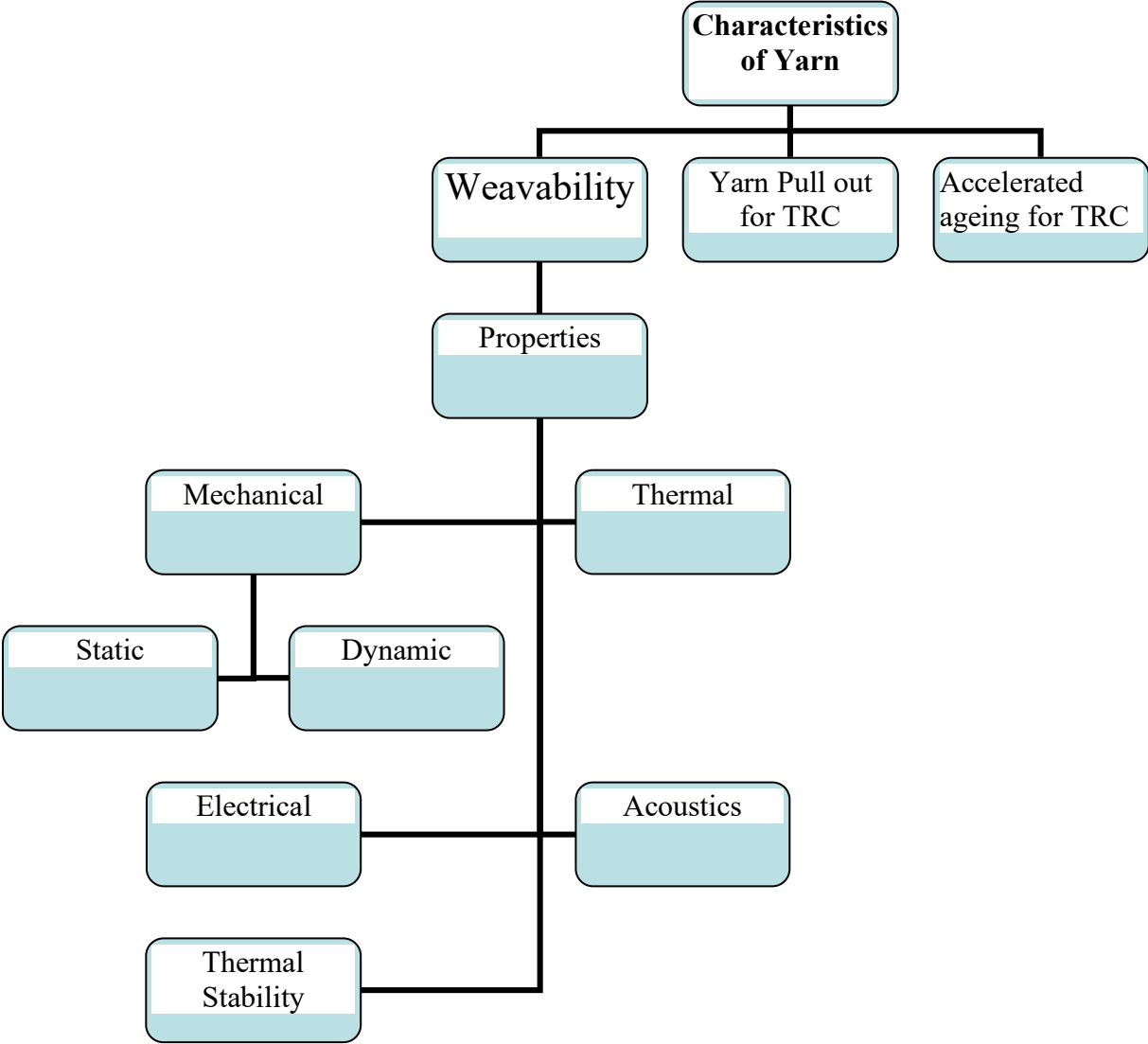
Without retaining a specific shape, the properties of a composite cannot be utilized [21-22]. Woven structure is characterized by orthogonal interlacing of at least two sets of yarns called warp and weft. Woven fabrics are used in various technical textile applications. In particular, woven fabric composites offer better dimensional stability over a large range of temperatures, they provide more balanced properties in the fabric plane and the interlacing of yarns provides higher out-of-plane strength, which can take up the secondary loads due to load path eccentricities, local buckling, better impact resistance and tolerance etc. compared to the common unidirectional laminated composites. Various patterns are used to weave two dimensional fabrics for technical textiles, out of which the most common designs are plain, rib, matt, twill and satin structures. Woven technical textiles are designed to meet the requirements of their end use. Their strength, thickness, extensibility, porosity and durability depend upon different factors such as the fabric weave, the thread density, raw materials and yarn linear density [23-24]. Recently, there has been growing interest in woven fabric composites. The use of woven fabric composites is increasing in the fields of aeronautics, automobile engineering, and military equipment.

Incorporation of several different types of fibers into a single matrix has led to the development of hybrid composites. Hybrid composite materials have extensive engineering application where strength to weight ratio, low cost and ease of fabrication are required. Hybrid composites provide combination of properties such as tensile modulus, compressive strength and impact strength which cannot be realized in standard composite materials. Hybrid composites give the privilege to create a material bearing desirable properties among the combination of fibers, that is more cost effective and one can mitigate the non-desirable properties from the combination. It can help to tailor the requirement for specific materials. In comparison with conventional composites, hybrid composites exhibit balanced strength and stiffness, balanced thermal distortion stability, fire resistant behavior, reduced weight and/or cost, improved fatigue resistance, reduced notch sensitivity, improved fracture toughness and impact resistance [25-26]. Hybrid composites are used in application areas where special properties are required in preferential directions.

The applications related to construction industry have a vital involvement of composite materials over the past decade due to their multifold advantages. Textile reinforced concrete (TRC) is an innovative high performance composite material consisting of textiles embedded in a fine-grained concrete matrix. Textile Reinforced/Fiber-reinforced composites are gaining popularity

within the civil construction sector. Applications like fiber-reinforced concrete, concrete retrofitting, concrete jacketing and internal and external reinforcement of composite concrete structures play an important role. Concrete (TRC) is rapidly replacing conventional materials due to its promising features.

1.2 The scope of this research



1.3 Dissertation Outline

The dissertation is divided into 5 Chapters.

| Chapter | Description |
|------------|---|
| Chapter 1. | - Introduction: General introduction about the topic of research. It contains details of the purpose and objectives of this research. |
| Chapter 2. | - State of the Art : A detailed study of previous literature and understanding of studies conducted and identify the limitations in past research. |
| Chapter 3. | - Experimental Materials and Methods: An overview about sample materials, formulae, scientific concepts, experimental and production methods used in this research. Elaborate explanation about methods and techniques used for production, characterization, and other experiments conducted. |
| Chapter 4. | - Results and Discussion: A detailed analysis of the results derived from various experiments. The results were tabulated and detailed statistical analysis was performed. Various interpretations were drawn from the analysis. |
| Chapter 5. | - Conclusion: This chapter contains the broad conclusions drawn from the result and analysis of the research. It also describes the future direction of this research. The outputs are in the form of scientific papers, book chapters and conference proceedings. |

Chapter 2 - State of the Art

2.1 General aspects of composites

The history of textiles can be traced back to the prehistoric times. "Multiphase materials have been known for millennia, recognition of this novel concept of combining together dissimilar materials during manufacture led to the identification of composites as a new class that was separate from the familiar metal, ceramics, and polymers"[21]. The human body can be considered as a composite made of bones and flesh. Wood is a natural composite of cellulose fibers in a matrix of lignin. Even from the early times, prehistoric man made and used composite materials. They made and used straw-reinforced clay for bricks in construction and structures as well as pottery. Most visible applications pave our roadways in the form of either steel and aggregate reinforced Portland cement or asphalt concrete. Reinforced concrete is another example of composite material. The steel and concrete retain their individual identities in the finished structure. However, because they work together, steel carries the tension loads and concrete carries the compression loads.

Now a days modern composites have evolved and adapted to use metal, ceramic, or polymer binders as matrices to reinforce a wide variety of fibers and particles of diverse materials from graphite to glass, from inorganic to organic. Over the last forty years, composite materials, plastics, and ceramics have been the dominant emerging materials [1,21]. Research into these materials is growing to advance modern technologies to capitalize on their particular properties and to maximize efficiency while reducing costs. For the last 30 years, the use of polymers and polymeric based composites in industries such as aerospace, automotive, and petroleum has exceeded that of all metals [21]. Composites are multifunctional materials consisting of two or more chemically distinct constituents, on a macro-scale, having a distinct interface separating them [26]. So the materials can be similar chemically but have boundaries between the different phases. The two materials have very distinguishable and disparate physical, as well as other morphological properties. An example of a composite that may easily go unnoticed despite its regular use in many beginning construction projects is plywood. Since plywood is composed of pieces of assorted lumber it combines the differing properties of all the lumbers for its strength, and the different wood pieces can easily be differentiated, and the borders of each piece can be identified as well. The basis of the renewed interest in composite research is that most physical, chemical, and processing-related properties can be enhanced by a suitable combination of materials [24].

Current applications of textiles have crossed many barriers and reached limits beyond expectations. Fields like sports and leisure, healthcare and wellness, energy generation and storage, electronics and IT, automotive and aerospace, just to give a few examples, are using hi-tech textile reinforced composite materials.

Recently the composites based on technical textiles can be found in many industrial applications as storage and transport structures (tanks, pipes, hoses, etc.), automotive industry, for car frames and other automobile parts (manifold, wheels), sport equipment industry is employing high

amounts of textile reinforced composites in the production of sporting goods and protective equipment (helmets, etc.). An interesting application is in building construction, as reinforcement of walls in order to develop strengthened structures with reduced thickness and subsequently low production costs [12,27].

Advantages of Textile Reinforced Composites (TRC)

Textile reinforced composites proved to be competitive materials due to certain advantages, in addition to their strength (given by the fiber/yarn structure) and ability to transmit strains (ensured by the polymeric matrix). These are:

- controlled anisotropy (due to textile reinforcement) - their structure can be designed so that fibers are oriented in preferential directions, depending on the maximum strain;
- textile reinforcements allow developing composites with a better strength-to-weight ratio in comparison with steel and other classic materials used for such applications;
- textiles maintain their integrity and behavior under extreme conditions: they are not susceptible to corrosion in outdoor applications, display dimensional stability under significant temperature gradient, are not sensitive to electromagnetic fields;
- these composites have an improved fatigue resistance.

Classification of composites

Composites, the wonder materials are becoming an essential part of today's society due to the advantages such as low weight, corrosion resistance, high fatigue strength, and faster assembly.

The textile composites are composed of two materials i.e., a textile skeleton for reinforcement (called **preform**) and a binding adhesive (called **matrix**) to keep the skeleton integrated into a specific shape. Without retaining a specific shape, the properties of a composite cannot be utilised.

On the basis of matrix phase, composites can be classified into metal matrix composites (MMCs), ceramic matrix composites (CMCs), and polymer matrix composites (PMCs) (Figure 2.1) [27]. The matrix material can be classified into metallic, polymeric and ceramic. Recently, the polymer matrix composites have been widely used for many applications like automotive parts, airplanes interior parts, household appliances and construction materials. The classifications according to types of reinforcement are particulate composites (composed of particles), fibrous composites (composed of fibers), and laminate composites (composed of laminates). Textile Fibrous composites can be further subdivided on the basis of natural/bio-fiber or synthetic fiber. Biofiber encompassing composites are referred to as bio-fiber composites. They can be again divided on the basis of matrix, that is, non-biodegradable matrix and biodegradable matrix. Bio-based composites made from natural/bio-fiber and biodegradable polymers are referred to as green composites. These can be further subdivided as hybrid composites and textile composites. Hybrid composites comprise of a combination of two or more types of fibers.

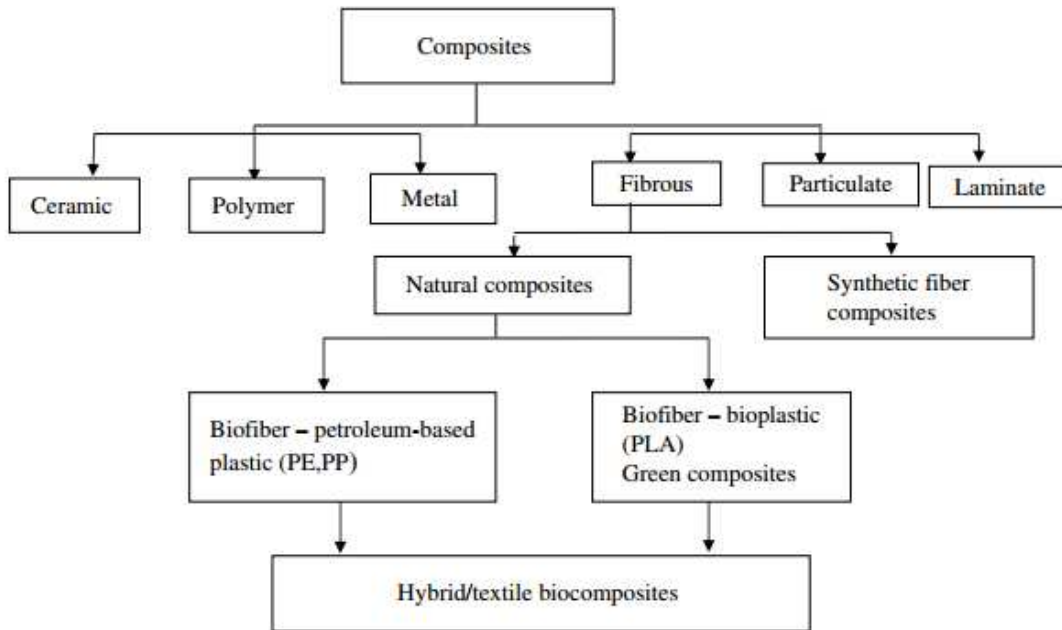


Figure 2.1: Classification of composites [27]

Hybrid composites

By mixing two or more types of fiber in a matrix to form a hybrid composite it may be possible to create a material possessing the combined advantages of the individual components and simultaneously mitigating their less desirable qualities. It should, in addition, be possible to tailor the properties of such materials to suit specific requirements. There are many situations in which, for example, a high modulus material is required but in which the catastrophic brittle failure usually associated with such a material would be unacceptable. The behavior of hybrid composites is a weighted sum of the individual components in which there is a more favorable balance between the inherent advantages and disadvantages. Also, using a hybrid composite that contains two or more types of fiber, the advantages of one type of fiber could complement with what is lacking in the other. As a consequence, a balance in cost and performance can be achieved through proper material design [28-29]. The concept of hybrid systems for improved material or structural performance is well-known in engineering design. The properties of a hybrid composite mainly depend upon the fiber content, length of individual fibers, orientation, extent of intermingling of fibers, fiber to matrix bonding and arrangement of both the types of fibers. The hybrid fibers in the composites can withstand higher load compared to single-fiber reinforcements in different direction based on the reinforcement, and the surrounding matrix keeps them in the desired location and orientation, acting as a higher load transfer medium between them.

There are several types of hybrid composites characterized as: (1) interply or tow-by-tow, in which tows of the two or more constituent types of fiber are mixed in a regular or random

manner; (2) sandwich hybrids, also known as core-shell, in which one material is sandwiched between two layers of another; (3) interply or laminated, where alternate layers of the two (or more) materials are stacked in a regular manner; (4) intimately mixed hybrids, where the constituent fibers are made to mix as randomly as possible so that no over-concentration of any one type is present in the material; (5) other kinds, such as those reinforced with ribs, pultruded wires, thin veils of fiber or combinations of the above. The concept of hybrid systems for improved material or structural performance is well-known in engineering design. However, it is the inspiration from nature's own materials that is recently motivating the path towards innovative material and structural designs [30-31]. The environmental issues have resulted in considerable interest in the development of new composite materials with addition of more than one reinforcement that are biodegradable resources, such as natural fibers as low-cost and environment-friendly alternative for synthetic fibers [32].

2.2 Classification of textile reinforcement

The reinforcement fibers themselves are unmanageable and are therefore usually arranged into sheets which can be handled, oriented on a mould, shaped and cut. The methods of binding the individual fibers together are varied and have significant impact on both the manufacture of the component and structural performance of the composite.

The reinforcing phase can either be fibrous or nonfibrous (particulates) in nature and if the fibers are derived from plants or some other living species, they are called natural fibers. These fibers can be extracted by many processes like mechanical decorticator, water retting, chemical retting etc. The fibers made from chemicals are called synthetic fibers and it may be glass, carbon, aramid, boron, ceramic fibers etc. The fibers obtained from natural compounds (cellulose, hemicellulose, lignin, pectin, wax etc.) are jute, flax, hemp, sisal, coir, banana, agave, snake grass fiber etc. [33-36]. Natural fibers produce composites that offer advantages like environmental friendliness, renewability of the fibers, good sound abatement capability and improved fuel efficiency. Despite the interest and environmental appeal of natural fibers, their use has been limited to non-bearing applications due to their lower strength and stiffness compared with synthetic fiber reinforced polymer composite. The stiffness and strength shortcomings of bio-composites can be overcome by structural configurations and better arrangement in a sense of placing fibers in specific locations for highest strength performance or using combination of fibers.

Considering the significant dimension of the textile material and its specific geometry [37], it is possible to define such structures as:

- Uni dimensional/directional (non-axial – roving yarns),
- Bi dimensional (monoaxial– chopped strand mats; non-axial – sheets; biaxial weave; triaxial – triaxial weave; multiaxial) and
- Tri dimensional (linear element – 3D solid braiding, multiple weave, triaxial and multiaxial 3D weave; plane element – laminates, beams, honeycombs).

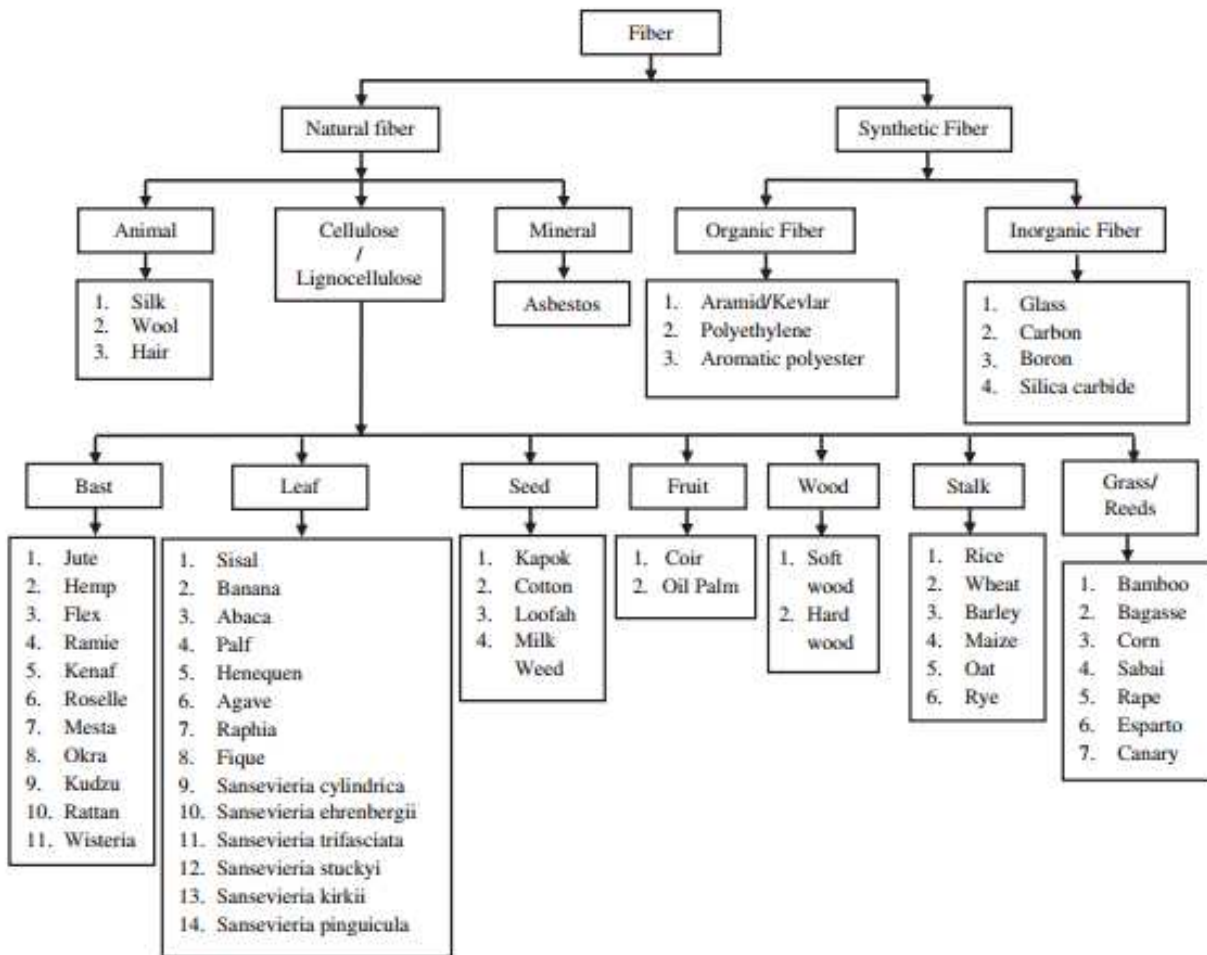


Figure 2.2: Classification of fibers [38]

Depending on their architecture [39], textile reinforcements can be assorted into 4 group as follows:

- Discrete, (discontinuous and uncontrolled orientation)
- Continuous, (linear orientation)
- With plane (planer orientation, entanglement)
- Special geometry,(3D orientation) as presented in Figure 2.3.

The textile component may be represented by short fibers, filaments or yarns, fabrics or complex structures, continuous or not, with (un)controlled orientation. In terms of technology, all specific processes from textile industries may be used to produce complex structures, but, due to their characteristics and the material geometry that results, they lead to different behavior and recommend materials for various applications. The main production processes employed in textile reinforcements are weaving, braiding, knitting and nonwovens production. Other

processes, such as filament winding and poltrusion, which process filaments, are also applied. The selection of a specific technological process takes into account its architectural capabilities, the material characteristics and behavior (dimensional stability, mechanical strength, drapability and formability etc.), as well as its suitability for the composite processing and application. The reinforcement fibers themselves are unmanageable and are therefore usually arranged into sheets which can be handled, oriented on a mould, shaped and cut. The methods of binding the individual fibers together are varied and have significant impact on both the manufacture of the component and structural performance of the composite. The fibers are bound in a variety of ways including weaving, stitching and knitting.

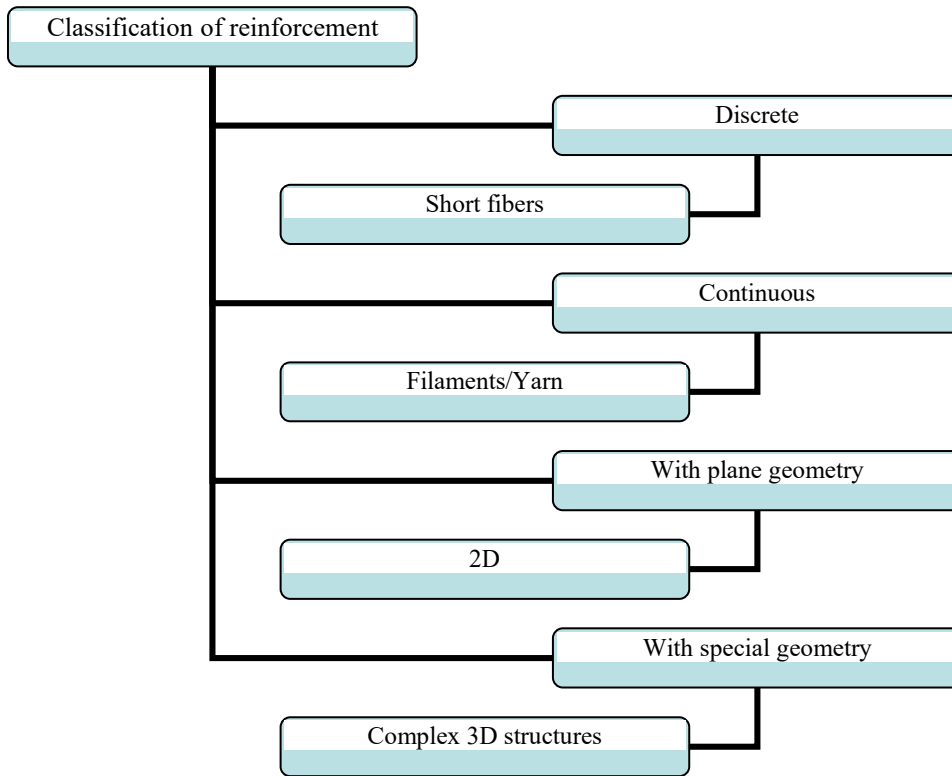


Figure 2.3: Classification of reinforcement according to their architecture [39].

2.2.1 Woven fabric

To mitigate the handling and forming difficulties associated with UD (uni-directional/dimensional) prepreg, reinforcing fibers are bunched together into warp and weft yarns or tows which are woven into a fabric. Woven fabric composites particularly offer better dimensional stability when they are exposed to a large range of temperatures. Woven fabric is one of the most widely used materials in structural applications [40]. Woven structures formulate an important part of technical textiles and their applications. Weave structure helps in providing better and balanced properties in plane of fabric area where as interlacement of yarns provide out of plane strength which results in take up of secondary load due to load path eccentricities, load

buckling, tolerance and better impact resistance in comparison with unidirectional laminated composites [41-45].

Woven structure is defined by orthogonal interlacement of at least two sets of yarns called warp and weft. The yarns which run horizontally or lengthwise are termed the warp, and the vertical yarns are referred to as the weft. The pattern in which the warp and weft yarns are interlaced is termed the weave.

The style of interlocking of the yarns determines the surface smoothness and formability of a fabric. The most common weave forms are plain, matt, twill and satin (Figure 2.4). Plain weaves have each warp yarn passing alternately under and over each weft yarn, in matt weave two or more yarns are passing alternately under and over groups of two or more weft, while twill weaves have two or more warp yarns alternately woven over and under two or more weft yarns in a regular repeated manner. Satin weaves are twill weaves modified to produce fewer intersections of warp and weft. The harness number indicates the number of yarns crossed and passed over or under, before the yarn repeats the pattern. Woven fabrics can also be classified depending upon the tightness and looseness of the interlacing yarns. In a closed-packing weave, the fabric is woven tightly, providing almost no gap between adjacent yarns, while in the case of open packing weaves, there are gaps between adjacent yarns, resulting in a loose weave. Woven fabrics are anisotropic, flexible, and with distinct viscoelastic properties. Hence, their mechanical characteristics depend upon complicated combinations of fiber bundles, yarn spacing's, stacking sequences, yarn sizes, fiber orientations, fiber architecture, and fiber volume fractions. Due to interlacing of fiber bundles, woven fabrics offer extra-high resistance to damage growth and exceptionally high values of the strain at failure in tension, compression, and impact loadings [38, 46]. They also possess good dimensional stability in the warp and weft directions, which results in a higher out-of-plane strength.

Considering that the woven fabric reinforced composite materials are not entirely homogeneous, large resin rich areas are formed by the interlacing of undulating warp and fill yarns. In the high performance fiber-polymer matrix system, the difference of damping is much larger than that of the stiffness. Large resin rich areas act as the built-in damper elements. Their distribution, depending on the architectures of the weave, determines the damping of the composite structure.

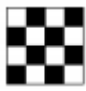
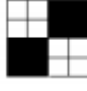
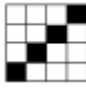
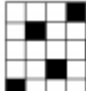
| | | | |
|---|---|---|---|
|  |  |  |  |
| Plain weave | Matt weave | Twill weave | Sateen Weave |

Figure 2.4: Woven structures [45].

2.3 Basalt fiber

The nature is continually providing varied resources for creating textile materials for various applications. Although many textile fibers in the nature are provided with the fibrous kind itself

it additionally offers raw materials that may be changed and formed into a filament in a way similar to the melt and solution spinning of other textile fibers. Basalt is an igneous rock, which is solidified volcanic lava. In recent years, basalt received attention as a replacement for asbestos fibers. Basalt has emerged as a contender in the fiber reinforcement of composites. Basalt fiber (BF) is capable to withstand very high temperature and can be used in high performance applications. Basalt fiber is new special reinforced fiber [47].

History

Basalt applications are well known from Roman age where this material was used in its natural form as a paving and building stone. The French Paul Dhé was the first with the idea to extrude fiber from basalt and he received U.S. patent in 1923. Around 1960, both the U.S. and the Soviet Union (USSR) began to investigate basalt fiber applications, particularly in military field. In the northwestern U.S., where large basalt formations are concentrated, Prof. R.V. Subramanian of Washington State University (Pullman) did a lot of research about its composition. Around 1970 U.S. glass companies imposed research strategies that favored glass fiber than basalt fiber. The result was a better glass fiber including successful development of S-2 glass fiber by Owens Corning. During the same time research in Eastern Europe was carried out by independent groups in Moscow, Prague and other locales, which was nationalized by the USSR's Defense Ministry concentrated in Kyiv, Ukraine, where technology was subsequently developed in closed institutes and factories. After the breakup of the Soviet Union in 1991, the results of Soviet research were declassified and made available for civil applications.

In present time several works are executed on development of modern continuous fibers from basalt stones. By industrial production of basalt fibers on the basis of new technologies their cost is equal and even less than cost of glass fiber. Today, basalt fiber research, production and most of marketing efforts are principally based in some of countries once part of the Soviet Union (Georgia, Ukraine, Russia) and in China [47-50].

Availability of basalt

Basalt fiber is obtained from natural Basalt which is dark colored, fine grained solidified volcanic rock. Basalt is a common term used for a variety of volcanic rocks. A hard, dense, inert rock found worldwide, basalt is an igneous rock i.e. it melts when heated like thermoplastic materials, which is solidified volcanic lava. Basalt originates from volcanic magma and flood volcanoes, a very hot fluid or semi fluid material under the earth's crust, solidified in the open air. Basalt flows cover about 70% of the earth's surface in which SiO_2 accounts for the main part, followed by Al_2O_3 , then Fe_2O_3 , FeO , CaO and MgO . For this reason, basalt rocks are classified according to the SiO_2 content as alkaline (up to 42% SiO_2), mildly acidic (43 to 46% SiO_2) and acidic basalts (over 46% SiO_2). Only acidic type basalts satisfy the conditions for fiber preparation. High silica contents are required to get glass network.

Basalt rock-beds with a thickness of as high as 200 meter have been found in the East Asian countries. Russia has unlimited basalt reserve. There are large deposits of these rocks in the Ural,

Kamchatka, Far East, Sakhalin, Kola Peninsula, Northwest Siberia and the Transcaucasia. Basalt formations in the Ukraine are particularly well suited to fiber processing. Basalt fibers have no toxic reaction with air or water, are non-combustible and explosion proof. When in contact with other chemicals, they have no reactions which may damage health or the environment [50-52].

Basalt can be suited for fire protective applications and so it can replace almost all applications of asbestos which possesses health hazards by damaging respiratory systems. It has been made label-free material in the US and Europe. Also, particles or fibrous fragments due to abrasion are too thick to be respirable but care in handling is recommended [53].

Production process

Basalt fibers are produced from basalt rock using single component raw material from the melt. No flux like boric oxide is added for processing. Glass and Basalt have different manufacturing processes despite the fact that both are inorganic. Glass fibers are produced from melted charge (composed of quartz sand, soda, limestone, fluxing agents, etc.). The fibers may be used, as per their requirement, as a filament or staple. Assembling a bundle of strands into one single strand makes roving of basalt. The basalt fibers which are produced can be converted into a suitable form for particular application like continuous basalt fiber, fabric, chopped fiber etc.

Typically basalt fibers are produced by two different technologies. The basalt fibers used as insulating materials in the construction and automotive industries are produced by so-called blowing technology with centrifugal cylinders (e.g. Junkers method). It is used for manufacturing cheap fibers with 60-100 mm length and 8-20 μm diameter. Continuous process is used for the production of basalt fiber just like glass. Quarried basalt rock is crushed, washed and loaded into a bin attached to feeders that transfers the material into melting baths in gas-heated furnaces. As basalt fiber is less complex, its processing is much easier than glass fiber. Glass is typically 50 percent silica and consists of boron oxide, aluminum and several other mineral materials that must be fed independently into a metering system before entering the furnace. Unlike glass, basalt fibers feature no secondary materials. The process requires a single feed line to carry crushed basalt rock into the melt furnace.

For more demanding applications, continuous fibers are prepared by spinneret technology from the melt spinning which can be processed by textile technologies similarly as traditional glass. These continuous fibers of 10-14 μm diameter can be obtained in the form of roving containing different numbers of elementary fibers.

From furnace, molten basalt, through feeder channel is fed and feeder window communicates with the recuperator. The feeder is given heat by waste gases of furnace and it has a window with a flange connected with slot-type bushing. The melt flows through electrically heated platinum/rhodium bushing with 200, 400, 800 or more holes. The fibers are drawn from the melt under hydrostatic pressure and subsequently cooled to get hardened filaments. Silane based sizing liquid is applied to impart strand lubricity, integrity and resin compatibility. These filament strands are collected together and forwarded to take up device for winding.

Short length basalt fibers can be produced directly from crushed basalt stones and the technology is very simple. The fibers are low cost, but they have relatively poor and uneven mechanical properties. Manufactured basalt fibers have a fineness of 9μ - 22μ (chopped fibers 10μ - 17μ) and 320 tex - 4800 tex for roving.

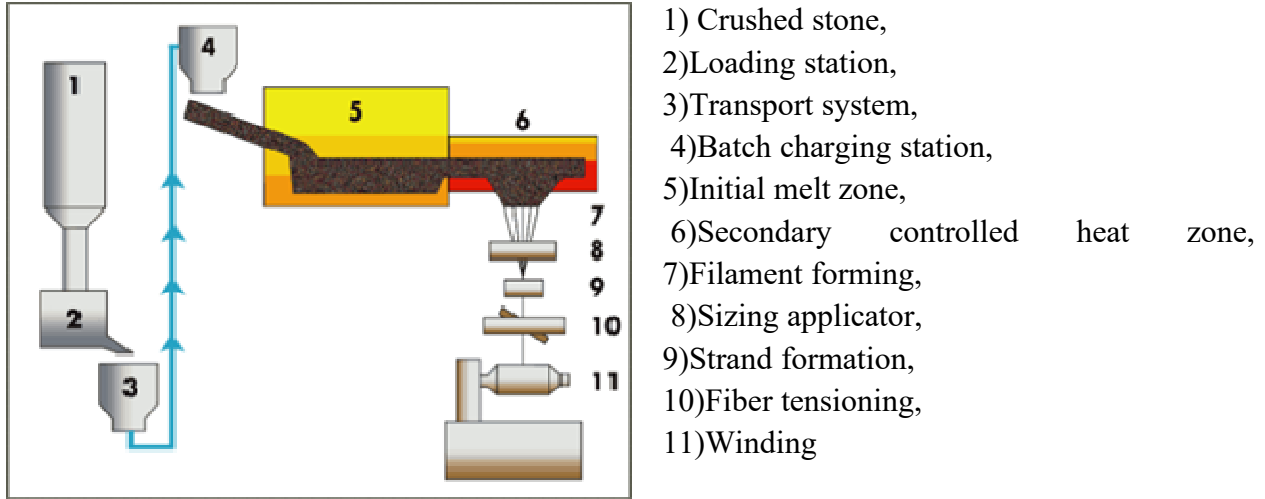


Figure 2.5: Basalt fiber spinning [54]

As basalt stone is of natural origin, basalt fiber manufacturers have no direct control over the purity and consistency of the raw basalt stone, as mineral level and chemical composition can differ from one location to other. In the production process of basalt fiber, temperature levels in the furnace, is of real importance as final mechanical properties of basalt fibrous materials have relevance with it. In fact it has been reliably determined that low variations in chemical composition of basalt rocks have a minor effect on the level of mechanical properties in continuous basalt fibers while the greatest effect comes from direct molding conditions of the fibers (drawing temperature and the period of melt homogenization). Chemical characteristics and uniformity of basalt query is very important for good fiber formation. The fiber dimension also has some effect on the final properties of fiber: as the filament diameter increases of 3-4 μ m, the strength value decreases from 2.8 to 1.8 GPA [47].

Properties

Growing environmental awareness throughout the world has triggered a paradigm shift towards designing materials compatible with the environment. Glass, Carbon, Kevlar and Boron fibers are being used as reinforcing materials in fiber-reinforced plastics, which have been widely accepted as materials for structural and nonstructural applications. However, these materials are resistant to biodegradation and can pose environmental problems. Glass fiber-reinforced composites are widely used to fabricate various applications in recent times but the aim to produce more environment friendly composites is leading to reduction in use of glass fiber [49,

50]. Basalt fiber has evolved as a replacement of glass fiber due to its environment friendliness. Basalt can be classified as a sustainable material because it is obtained from natural resource and during its production no chemical additives nor any solvents, pigments or other hazardous materials are added. It is known as green industrial material and when the basalt fibers in resin are recycled the same material is obtained again as natural basalt powder. The melting point is quite high i.e 1400 °C, which means that composite containing basalt is incinerated, the only product left in an un-molten basalt that can be used again [48-50]. During production of glass fiber some scarce components as (B₂O₃) are used and its recycling is not easy. Carbon fibers have very high cost. Basalt fiber is cheaper than carbon fibers, and exhibits a higher strength than glass [50]. Basalt based composites can replace steel (1kg of basalt reinforcement is equivalent to 9.6kg of steel) as lightweight concrete, which have comparable mechanical properties. As a result a lighter building is possible by using basalt fiber based bar instead of steel reinforcing bars. It also results in energy saving during production of basalt fiber which requires quite lower amount of fossil fuel as compared to steel. Reducing energy demands leads to lower emission of CO₂ in the atmosphere [47].

Table 2.1: Mechanical properties of structural materials.

| Material | Density (kg/m³) | Tensile strength (MPa) | Initial modulus (GPa) |
|------------------------------------|---------------------------------------|-----------------------------------|----------------------------------|
| Metal | | | |
| Steel | 7800 | 400 | 200 |
| Aluminum alloy | 2800 | 300 | 72 |
| titanium | 4500 | 350 | 115 |
| Wood | | | |
| Oak | 720 | 130 | 15 |
| Plastic | | | |
| Polyethylene | 960 | 20 | 0.5 |
| Vinyl plastic | 1400 | 60 | 3 |
| Glass reinforced plastic | | | |
| Unidirectional Glass-cloth-base | 2000 | 1600 | 56 |
| Laminate | 1900 | 500 | 30 |
| Randomly Oriented | 1400 | 100 | 8 |

Table 2.2: Mechanical properties of selected fibers [55].

| Fiber | Tenacity (N/tex) | Ultimate tensile strength (GPa) | Extension to break (%) | Initial modulus (GPa) | Density (Kg/m³) |
|---------------------------|-----------------------------|--|---------------------------------------|--------------------------------------|---------------------------------------|
| Natural | | | | | |
| Flax | 0.54 | 0.831 | 3 | 27.72 | 1540 |
| Hemp | 0.47 | 0.705 | 2.2 | 32.55 | 1500 |
| Jute | 0.31 | 0.465 | 1.8 | 25.8 | 1500 |
| Ramie | 0.59 | 0.885 | 3.7 | 21.9 | 1500 |
| Natural polymer | | | | | |
| Tenasco | 0.27 | 0.405 | 16.9 | 9 | 1500 |
| Fortisan | 0.59 | 0.885 | 6.4 | 24.15 | 1500 |
| Synthetic | | | | | |
| Nylon 6.6 HT | 0.66 | 0.752 | 16 | 5 | 1140 |
| Polyester HT | 0.56 | 0.778 | 7 | 18.35 | 1390 |
| Polypropylene | 0.65 | 0.591 | 17 | 6.46 | 910 |
| Para-aramid HM | 2 | 2.88 | 2.4 | 115.2 | 1440 |
| Carbon HM | 1.20 | 2.196 | 0.7-1.7 | 468.48 | 1830 |
| E-glass | 0.78 | 2 | 4 | 72.24 | 2580 |
| Basalt CBF | 0.7-0.9 | 1.8-2.5 | 3.1 | 80-93 | 2650 |
| PVA fibers | 0.7-1.23 | 0.91-1.60 | 7 | 8.45-22 | 1300 |
| SWCNTs | 10-41 | 13-53 | 16 | 1-5x10 ³ | 1300- 1400 |
| Metals | | | | | |
| Stainless steel fibers | 0.22-0.28 | 1.7-2.21 | 1.5-11 | 199 | 7900 |
| Steel | - | 0.34-2.1 | - | 210 | 7800 |
| Aluminum | - | 0.14-0.62 | - | 70 | 27007 |

Basalt fibers has attracted attention of users due to its excellent properties. Basalt fibers have better tensile strength than E- glass fibers, greater failure strain than carbon fibers as well as higher resistance to chemical attack, impact load and fire with less poisonous fumes. The superior properties of basalt fiber are: good range of thermal performance (−435 °F to 1760 °F), significant capability of heat and acoustic damping and outstanding vibration isolation, high tensile strength, high resistance to alkalis and acids, good electromagnetic properties, resistance to corrosion, resistance to radiation and UV light, ecological cleanliness, ease of handling and non-toxicity to the end user [56-57].

Basalt fiber is advantageous compared to carbon or glass from performance stand point. It is well-compatible with carbon fiber. The consequence is that high efficient hybrid materials can be manufactured by adding small (pre-determined) amount of carbon fibers to basalt fibers (e.g. basalt/carbon) [58-59]. The obtained thread, will have a small content of carbon fiber, which is expensive, so it will be cost effective. It will demonstrate considerably better elastic properties compared with basalt fiber. When used as (continuous) fibers, basalt can reinforce a new range of (plastic and concrete matrix) composites.

Table 2.3: Physical and mechanical properties [57-59]

| Properties | Basalt | E-glass | S2 -glass | Aramid | Carbon |
|---|-----------|-----------|-----------|-----------|-----------|
| Density (kg/m ³) | 2630-2800 | 2540-2570 | 2540 | 1450 | 1780 |
| Filament Diameter (μ) | 6-21 | 6-21 | 6-21 | 5-15 | 5-15 |
| Tensile strength of single filament (MPa) | 3000-4840 | 3100-3800 | 4020-4650 | 2900-3450 | 3500-6000 |
| Initial modulus (GPa) | 93-110 | 72.5-75.5 | 83-97 | 70-140 | 230-600 |
| Elongation at break (%) | 3.1-6 | 4.7 | 5.3 | 2.8-3.6 | 1.5-2.0 |
| Sound absorption coefficient(SAC) | 0.95-0.99 | 0.8-0.93 | | | |

The application temperature range of basalt fiber products are remarkably higher (-260°C to 700°C) when compared with glass (-60°C to 250°C). Basalt fibers can withstand higher temperatures of 1100°C-1200°C for hours without any physical damage. In construction industry, basalt can be used as rock wool due to its superior insulation properties.

Among various properties and characteristics, high resistance of basalt to alkali and acids is of wider importance. Basalt is relatively less stable in strong acids as compared to their behavior against alkalis; rather it can withstand alkaline medium as strong as pH of 13-14. They can retain up to 92% of their properties in 2 (N) NaOH and up to 75% of their properties in 2 (N) HCl acid and results in weight loss of only 5.0% and 2.2% respectively. When basalt is boiled with water, alkali or acid, its weight loss is significantly low that is why it is suitable to be used in concrete reinforcement materials in the form of bars [56]. The basalt fiber has low density e.g. 2800kg/m³ which is much lower than metal (steel) and closer to carbon and glass fibers while being cheaper than carbon fiber and having higher strength than glass fiber. Basalt can be used as low weight, low cost and tough material for composite reinforcement. Moisture regains and moisture content of basalt fibers is less than 1%. Basalt materials have strong resistance against the action of fungi and micro-organisms. It has hardness values between 5 to 9 on Mohr's scale resulting in better abrasion properties.

Applications

Wide range of possible applications result from the superior properties of basalt. It has excellent thermal, electrical and sound insulating properties. Basalt fiber is a possible polymer reinforcing material and can be applied in polymer matrix composites instead of glass fiber for many applications. The superior mechanical properties of fibers, the easy wetting of the filament surface and their recyclability make them particularly suitable for composites application. The

UV resistance, acid resistance, better alkali resistance and very low water absorption of fibers ensure excellent weatherability for basalt fiber reinforced composites.

Some possible applications of basalt fibers and basalt-based composites are: thermal and sound insulation/protection (e.g. basalt wool, engine insulation), industrial floors, heat and sound insulation for residential and industrial buildings, bullet proof vests, structural plastics, automotive parts, concrete reinforcement (constructions), insulating plastics etc. [59-66].

Flame resistance

Basalt fiber does not melt nor shrink in the flame and, when not mechanically stressed, keeps its geometrical integrity. Because of its thermal insulating properties it is already used as fire protection in the form of fabrics or tapes like fire-resistant curtains for hall partitioning and external emergency house protection in case of wild-fire, fire-blocking inter-liners for mass transportation seat covers. When coming to heat resistance, basalt is exceptionally suited to block fire. Basalt products resist the open flame. Basalt melts at 1450°C. A fabric made of basalt, with a Bunsen burner pointed at it (1100-1200°C) becomes red hot as a metal fabric would. This can last for hours [57]. For reference, an E-glass fabric of the same surface density gets pierced by the same flame in a matter of seconds.

Electrical resistance

The excellent thermal conductivity of basalt, combined with its equally high electrical resistivity and unique resistance to fire, has allowed basalt woven tapes to be selected for the construction of fire-proof electrical power cables. Basalt fibers are also incorporated into printed circuit boards, resulting in superior overall properties compared to conventional components made of fiber glass. It is also used in other electro technical applications such as extra fine resistant insulation for electrical cables and underground ducts [58].

High thermal insulation

Basalt fibers, at present, exhibit a resistance to temperature superior to E glass fibers. Chopped basalt fibers, non-woven basalt needled mats find their place in the automotive sector like construction of car and bike exhaust mufflers and in ovens. It can be used as frictional materials e.g car brake pads. In the automotive industry, Azdel Inc. (Southfield, Mich.), a 50/50 joint venture of GE Advanced Materials (Pittsfield, Mass.) and glass-fiber producer PPG Industries (Pittsburgh, Pa.), developed VolcaLite^R, a thermoplastic composite that combines thermoplastic resin polypropylene (PP) and long chopped basalt fiber. The company claims that the basalt/PP system offers acoustic absorption properties, low coefficient of thermal expansion (CTE), and a high strength-to-weight ratio, providing good ductility. It can be used for headliners, sunshades, trunk trims etc. [59]. They are used for the heat insulation of gas turbines, including in nuclear plant locations, as basalt is known to resist degradation caused by radiations, unlike glasses. It is also functional to very low temperatures. Useful applications are insulation of liquid nitrogen tanks and pipes.

Construction

Basalt fibers have very good hardness and thermal properties, and thus can have various application as construction materials like pipes, bars, fittings etc. Basalt based composite pipes can transport corrosive liquids and gases. The same equipment as for fiber glass pipes can be used for this. These pipes are reported to be several times stronger than glass-fiber pipes. Due to basalt's low thermal conductivity, deposition of salts and paraffin inside the pipes is also reduced. Other, structural basalt composite components (such as pipes and rods) are made from unidirectional basalt reinforcement. In combination with its high specific strength (9.6 times higher than steel), high resistance to aggressive media, and high electrical insulating properties, this results in specialty products such as insulators for high voltage power lines. As is well known, steel material tends to corrode if not protected adequately. There are many ways to limit the oxidation, using stainless steel or more expensive solution than simple steel - or bars obtained from glass fiber pultrusion. However this last solution is limited because of the lower resistance of the glass fiber in the alkaline environment associated with concrete. Using pultruded bars made with basalt fibers may be a right solution for this problem, given that basalt fibers are more resistant than glass fibers in the alkaline environment and, moreover they cannot corrode. Therefore, pultruded bars made with basalt fibers should insure good durability to the reinforced concrete, because they do not react in alkaline environments and with corrosive elements. Sudaglass (Houston, Texas) produces several products from basalt fiber, including concrete reinforcement rods. Pultruded from unidirectional basalt fiber, the rods are reportedly 89 percent lighter than steel reinforcement rods, have the same coefficient of thermal expansion as concrete and are less susceptible to degradation in an alkaline environment. The company claims that 1 ton of basalt rods can provide reinforcement equal to 4 tons of steel rods. Basalt fibers can also be used in machine building because of their good frictional, heat and chemical resistance. It can be also used for making products for sports activity like hockey sticks, tennis rackets, skis, snowboards, arrows etc. Mervin manufacturing is one of the companies who are dealing in basalt based composites for snowboard. The board was on exhibit first time in the Basaltex booth at the 2005 JEC Composites Show [62-66].

2.4 TRC (Textile reinforced concrete)

Composites, which are combinations of different materials leading to a new material, are often used in civil engineering. The reason is that the optimal plain material with regard to structural and economical performance does not often exist. Thus, it is necessary to combine the advantageous properties of single materials for instance load-bearing capacity, durability, weight and costs to eliminate mutually their drawbacks. The structural materials most often used in civil engineering are concrete and steel. Concrete is quite cheap and has relatively large compressive load-bearing capacity, but the tensile load-bearing capacity is very low. Thus, plain concrete is not applicable if significant tensile loading cannot be ruled out in advance, as it is the case in arch structures or short columns where predominantly compressive loading comes into picture.

In contrast, steel has relatively high tensile load-bearing capacity but it is quite expensive. A big advantage of embedding steel bars in concrete is due to the alkalinity of concrete, which automatically protects the steel from corrosion resulting from oxidation over long time periods. This protection is also referred to as passivation. Nevertheless, the alkalinity of concrete reduces successively due to chemical reactions with carbon dioxide. This process, also known as carbonation of the concrete, initiates at the surfaces and moves towards the inner parts of the concrete where it enables steel corrosion due to the lost passivation.

Conventional steel in combination with reinforcement of concrete is most common for construction despite some of the historical disadvantages of vulnerability to corrosion attack and durability. Various remedial methods have been applied to overcome the shortcomings of this building material, such as increasing the concrete cover, which, however, leads to an increased self-weight of the structure. In recent past, an attempt to improve sustainability of reinforced concrete came in the shape of development of Textile Reinforced Concrete (TRC), which is by providing non-corrosive textile materials as reinforcement with fine grained concrete matrix. It has evolved as a perfect alternative with excellent properties of thin and light weight structures along with corrosion resistance. Textile composites have certain other advantages too like high strength-to-weight ratio, ease of handling, drapability, speed of installation, and visual impact, reversibility etc. For the improvement of tensile and flexural strength of concrete material, textile reinforced concrete is used worldwide; it also adds structural integrity to the concrete beam. Textiles are used in concrete to control cracking due to plastic shrinkage and drying shrinkage. They also reduce the permeability of concrete and thus reduce bleeding of water. The concept of using fibers to improve the characteristics of construction materials is very old. Their use as reinforcement started since ancient times. Historically, horse hair was used in mortar and straw in mud bricks. Asbestos fibers were used in concrete in 1900. In the 1950s, fiber-reinforced concrete gained the interest due to evolution of the concept of composite materials. As soon as the health risks associated with asbestos were found, an urge to find a replacement for building materials was raised and generated. By the 1960s, materials for reinforcement of concrete were Glass, Steel and Synthetic fibers such as Polypropylene. Extensive research work is carried out to find out new fiber-reinforced concretes [1-2]. Variety of fibers were used to increase toughness and prevent cracking of cement. Sustainable, energy efficient and eco-friendly construction material is sought around the world. Sustainable, green construction material, natural fiber based reinforcement in a cement matrix is a feasible approach.

A cement is a binder, whereas concrete is the composite material resulting from the mixing and hardening of cement with water (or an alkaline solution in the case of geo polymer cement), and stone aggregates. Ordinary cement often called as Portland cement is a heterogeneous fine grained material but it has serious environmental concerns. Geo polymer cement (GPC) can be used in applications to fully or partially replace OPC with environmental and technical benefits, including an 80-90% reduction in CO₂ emissions and improved resistance to fire and aggressive chemicals [67-74].

The composites behavior between textile reinforcement and concrete matrix determines important properties of the textile reinforced concrete, such as durability and load bearing capacity/structural performance. Despite the fact that TRC based research has revealed many promising attributes, it has yet to reach its recognition due to a lack of available design tools, standards and long-term behavior. Although TRC has been extensively researched, the formalization of experimental methods and design standards is still in progress.

Textile reinforced concrete is a three-phase material consisting of textile reinforcement, concrete matrix and an interface. The force transferred from the brittle concrete matrix to the reinforcement is governed by the quality of the bond between the reinforcement and matrix. The safe introduction and transfer of the forces is required for the functionality of composite constructions. In fiber based composite materials, such as TRC, bond behavior between the yarn or roving and the cementitious matrix is a principal factor influencing the global structural behavior [74]. Yarns or rovings consist of multitudes of filaments which creates a complex heterogeneous structure. Pull-out tests is a common method applied to study the bond or pull-out behaviour of reinforcement embedded in a matrix.

A concrete structure should be designed, constructed and maintained to ensure durability over a required service life. The durability of a structure is important so that it can fulfil a safe functionality, while reducing costs, energy, extraction and production of new materials, maintenance, rehabilitation, replacement and deconstruction. To incorporate durability into design, the long-term performance of the applied building materials should be known or should be projectable using experiments. Durability is a broad term which consists of deteriorating processes such as chemical attack, fire resistance and many more effects. The durability performance pertaining to chemical attack on fibers should be investigated. The durability performance is most accurately measured in real-time though due to time constraints, accelerated aging are typically applied to predict the long-term performance of materials. In some research works, the effect of accelerated ageing on the tensile properties of textile reinforcement materials was investigated. The durability of TRC was characterized according to the influence of accelerated ageing based on alkali resistance on the structural performance of textile reinforcement. The hydration of cement is the reaction between the solid compounds and the liquid phase. Hydration of cement is a complex sequence of interactions occurring between water and chemical phases of the cement (viz., tricalcium silicate ($3\text{CaO}\cdot\text{SiO}_2$), dicalcium silicate ($2\text{CaO}\cdot\text{SiO}$), tricalcium aluminate ($3\text{CaO}\cdot\text{Al}_2\text{O}_3$) and tetra calcium aluminoferrite ($\text{Ca}_2(\text{Al,Fe})_2\text{O}_5$) [76]. Calcium hydroxide and calcium silicate hydrate are produced predominantly as hydrated cement products [72-74]. However, the cement hydration reaction equilibrium as well as nucleation and growth of the hydrated cement product may be disturbed by the presence of foreign substances like textile.

The degradation of fiber due to the alkaline pore solution in the cement matrix seriously decreases the durability and may cause premature failure of the concrete composite. Calcium hydroxide is the primary cause of alkaline environment in cement. In this case, the high concentration of alkali is the main cause of fibers damage. Particularly, weight loss and reduction

in mechanical properties could appear. In the technical literature different studies are present, but the reported results appear somewhat contrasting.

In the last decade, the research and development of all hybrid FRP (Fiber Reinforced Plastic) structures in civil engineering has progressed substantially in several countries [75]. The first all hybrid FRP bridge was constructed in Okinawa, Japan prefecture in 2001 (Ueda, 2005). This bridge is a two span continuous girder pedestrian bridge as shown in Fig. 2.6 which is located in the road-park of Ikei-Tairagawa road. All the structural elements have been made with Hybrid Fiber Reinforcement Plastics (GFRP & CFRP). The all HFRP solution was chosen for this bridge due to its heavily corrosive environment where the bridge is surrounded by the ocean.



Figure 2.6: Pedestrian Bridge in Okinawa, Japan made of Hybrid Composite [76]

2.5 Limitations

Many research work reported in literature mainly focused on glass, carbon and other fibers, but very little work is reported about use of Basalt fiber in hybrid fabrics. Also, very little work is done on hybrid woven fabrics, mainly focused on basalt and its weavability. Woven fabrics satisfy a wide range of needs and requirements and they are the main source of planar textile reinforcements. The physical and mechanical properties of these materials define the scope of their end use in a variety of applications. Therefore, it is crucial to have a better understanding of the parameters that influence the behavior of such hybrid woven materials. Information on usage of environment friendly material as basalt hybrid structure for composites, especially for TRC application is very limited. It is therefore necessary to study the effect of accelerated ageing on the tensile properties of textile reinforcement materials with different variables e.g. time, pH and type of alkali.

Prediction of properties using computational tools

The internal geometry of a textile reinforcement is an important factor of the reinforcement performance during composite manufacturing and in service life of the composite material. For the former, impregnation of the reinforcement is governed by its porosity (size, distribution and connectivity of pores). For the latter, load transfer from the matrix to the reinforcement is

governed by the fibre orientation, which plays a paramount role in the composite stiffness; stress-strain concentration loci, determining the composite strength. Several methods are employed for the analysis and mechanical modeling of textile structure. There is a long history of structural models for textile fabrics, starting with the semi-analytical truss models for plain weaves by Kawabata et al. and followed by a large number of extended models accounting for different mechanisms and using advanced techniques for efficient computation [77-87].

The mechanical modeling can be briefly classified as analytical and computational approaches, each having its own merits and demerits. Another important classification of the modeling aspects, which is based on the scale of models, is micromechanical, mesomechanical, and macromechanical modeling. The micromechanical modeling scale involves the study of orientation and mechanical properties of the constituent fibers. The mesomechanical modeling, on the other side, follows the concept of homogenization and evaluates the mechanical properties of a fabric unit cell, which in turn is used to calculate the effective material properties of the textile composite. Finally, the macromechanical modeling deals with predicting the mechanical properties of textile fabrics under complex deformations, assuming the fabric to be a continuous medium.

At the initial stage of modeling, by using the homogenization technique, the properties of yarns are calculated on the basis of their architecture (the number and orientation of fibers and yarn type) and the properties of fibers. The properties of yarns serve as the input for the second modeling stage, where the unit-cell properties of a woven fabric are determined with invoking the homogenization technique. Finally, at the third modeling stage, based on outcomes of the preceding stages, the mechanical performance of the whole structure under complex deformations is predicted.

Many researcher work on development of models [88-89] but the major drawback of these early models was their dependency on empirically obtained descriptions of the internal geometry of the textile. This means that the textile first has to be produced, and then measured, and that no predictions on the behaviour of yet non-existing textile composites can be made. In this way, the value of these 'predictive' models is rather limited. A step forward was achieved when models for the internal geometry of 2D- and 3D-weaves, initially developed for technical textiles the CETKA-model were applied to composite reinforcements [90-93]. This models are based on a minimum amount of topological data (weave style, inter-yarn distance) and yarn mechanical properties; it is a mechanical model, as it applies a yarn deformation energy minimization algorithm to predict the internal geometry of any 2D- and 3D-weave. Connecting this approach to the cell- or inclusion models of Gommers and Vandeurzen [88-89] resulted a more versatile way to calculate the homogenised properties of textile based composites. Since the year 1999, this approach has been systematically followed, extending the types of textiles to 2D and 3D woven two- and three-axial braided weft-knitted and non-crimp warp-knit stitched fabrics and laminates. The mechanical models not only generate the internal geometry of relaxed textiles, but also of textiles deformed in tension, compression and shear[93-96].

Mechanical Properties of textile materials

Experimental characterization of the mechanical properties of a woven reinforcement is an important issue to the better understanding of its behavior during the composite forming processes. It also provides data for numerical simulations that will allow predicting the feasibility of a part and improving the manufacturing processes.

Mechanical properties describe the resistance of material against external forces. The response of the textile material depends upon the material properties, type of loading and direction of loading. There are numerous factors which will affect the mechanical properties of a woven fabric. Firstly, there are fiber properties, and their molecular properties and structure. The raw material involved in the fabric formation is the yarn and structure is governed by threads per unit length/width of a fabric. The yarn properties are influenced by fiber properties and type of spinning whereas threads per unit length i.e. warp and weft thread density along with weave defines the fabric properties. Machine speed and conditions in weaving may be the other factors

The structural design of a textile fabric is largely dictated by its end-use application. It is a well-known fact that weave structure affects most of the mechanical properties of woven fabric. The dominant modes of woven fabric deformation involve in-plane redistribution and reorientation of fibres but they are not the only deformation modes.

Fabrics are highly anisotropic and the behavior in one direction is coupled to the behavior in the other in a nonlinear manner. Even under uniaxial loading, the response of a fabric is often nonlinear due to its woven structure and to nonlinearities in the material response [97-101]. In addition, many applications of fabric involve large rotations and deformations. Various deformation mechanisms, i.e. yarn stretch, un-crimping, crimp interchange, locking, trellising and yarn slip, and determine the mechanical response of a woven fabric. The ability of a fabric to be deformed by shearing distinguishes it from other thin sheet materials such as paper or plastic films. During shear deformation, the fabric experiences large angular variation between warp and fill yarns. In the process of tailoring a flat piece of fabric into a three-dimensional surface, shearing must occur. This ability of fabric to deform within its plane is important not only for tailoring but also for the handle of fabric [102-104]. This property enables fabric to undergo complex deformations and to conform to the shape of the body. Shear properties influence draping, flexibility and also the handle of fabric. It has application in technical textiles like inflatable structures made from woven fabrics used to seal conduits and large pipes with irregular shapes requires not only the typical material properties such as modulus of elasticity, axial strength, density, and Poisson's ratio, but also an estimation of the shear behavior to account for the drape-ability of the inflatable necessary to conform to the irregularities of the section to be sealed. Shear properties are important not only for standard fabrics but for textile reinforced composites preforming as well. It is necessary to study the inter/intra-ply shear behavior of fabric because of their wide application in production especially in the case of forming process. Shear is the main deformation mode during composite forming process [104] such as thermoforming.

The shear characteristics of fabrics have been analyzed in a number of ways ranging from mathematical models, which predict the material behavior based on fiber geometry and friction

coefficients, to mechanical testing, which directly measures a materials bulk resistance to shear deformation [105-106]. The shear mechanisms influence the draping and pliability of a fabric and determine the ability of the material to conform to a three dimensional surface .The ability of a fabric to conform to a double-curvature surface depends mainly on the in-plane shear behavior [107]. Because the fibers within a webbing are not continuous and are not connected along any two principle directions, the materials cannot be considered isotropic or homogeneous. These types of micro-materials can also display non-linear and unpredictable behavior under multiple stress states. Because of this, a theoretical analysis can become very complex or impossible and experimental determination of the material behavior becomes necessary. The shear properties of webbings will be dependent on the biaxial state of stress, which the material will be under. The material must be tested in a manner where the tensile and shear forces can be applied simultaneously.

Currently there are no standards regarding the shear testing of unidirectional or biaxial engineering fabrics. The two main tests for shear are the picture frame and bias extension tests. The picture frame test confines the fabric to pure shear loading and provides both shear force data and the inter-fibre 'locking' angle. This locking is usually defined at the onset of buckling (wrinkling) and fabrics can often reach angles of 40°-60° before this starts to occur.

An experimental methodology for determining the shear characteristics of woven webbings is proposed. Experimental methods are developed for testing the materials using the denominated "picture frame" designed to produce a shearing effect from an axial force. These frames allow the materials to be stressed biaxially prior to the shear testing to observe the shear performance under similar axial stress states, which will be seen in the material for specific applications. Testing yields load and displacement data, which can be used to determine the shear modulus as a function of the materials angular displacement

The mechanisms of shear are a function of weave pattern, friction coefficient, and pre-tensioning, and are roughly independent of the tensile strength of the individual fibers [107-110]. It may be considered that most of the theoretical works are concentrated on the shear behaviour of plain-woven fabrics.

The in-plane shear behavior of 2D fabric has been comparatively well investigated. Zhu et al. [111] carefully investigated the in-plane shear characterization of 2D fabric by experimental test, and found that the reduction of yarn was a key to wrinkling. Lomov et al. [112] presented shear tests of unbalanced 2/2 twill glass/PP fabric on picture frame in three different pretension states and studied the influence of tensile load in the yarn direction on the shear resistance for the fabric and the repeatability of the test method.

Lin et al. [113] established the finite element model based on the geometry of 2D fabric to simulate the in-plane shear deformation, the simulation results were identical with experiments.

Deformation kinematics

Picture frame test is an effective way for characterizing intra-ply shear property of fabrics. The picture frame test is preferred by many researchers for shear testing since it generates pure state of strain which can be imposed on the test specimen. Shearing is induced by restraining the textile reinforcement in a rhomboid deformation frame with fibers constrained to move parallel to the frame edges. A tensile force is applied at the crosshead mounting. The rig is jointed at each corner such that its sides can rotate and the interior angle between adjacent sides can change. The initially square frame thus becomes of rhomboid (or diamond) shape. Material inside the rig is subjected to pure shear deformation kinematics. The force required to deform the material is recorded at the crosshead mounting as a function of crosshead displacement.

The vertical actual fabric resistance force F_x measure in the testing machine is balanced by the fabric shear forces F_s , which is measured by relation:

$$F_s = \frac{F_x}{2 \cos \varphi} \quad (2.1)$$

Shear force (F_s) is determined by the axial force (F_x) frame length (L_{frame}), Fabric thickness (t) and the frame angle (φ). Meanwhile frame angle can be determined directly from cross head displacement/vertical displacement (D).

The shear force data can be normalized using the following equation:

$$F_{norm} = \frac{F_s L_{frame}}{L_{fabric}} \quad (2.2)$$

where $F_{normalized}$ is the shear force normalized according to the energy method, F_s is the shear force obtained from Eq. (3.2), L_{frame} is the side length of the frame and L_{fabric} is the side length of the fabric.

and fabric shear stress (τ) is given by relation :

$$\tau_{stress} = \frac{F_s}{L_{fabric} h} \quad (2.3)$$

Through trigonometric relations, the angle of the frame, φ is calculated

$$\varphi = \cos^{-1} \left[\frac{L\sqrt{2} + D}{2L} \right] \quad (2.4)$$

Shear angle (γ) can be obtained from measured frame angle by using the following equation:

$$\gamma = \frac{\pi}{2} - 2\varphi \quad (2.5)$$

Air permeability

Air permeability is one of the important factors on which thermal properties depend. Permeability is a feature, which represents the ease with which air/fluid moves through a porous medium. Many fabric functionalities like the performance of parachute and sailcloth, efficiency of filtration in industrial cloths, apparel comfort, flammability, thermal insulation efficiency, barrier fabric performance, and precision of the filter media depends on the resistance offered by the fabric to the passage of air and other fluids. Permeability is an important material property & its knowledge is required in various flow simulations while processing composites. This quantity is defined as the property of a porous material, which characterizes the ease with which a fluid is forced to flow through the material under an applied pressure gradient. Air permeability is one of the most important characteristics of woven fabrics [114-116].

Thermal conductivity & resistance of textile materials

In general, thermal properties of textiles include thermal conductivity and thermal resistance which are influenced by properties of textile materials such as fabric structure and density, material and properties of fibers, surface treatments, air permeability, temperature and humidity. Thermal conductivity is a physical property of fundamental importance. In general, Fourier's law of heat conduction is exploited for the measurement of thermal conductivity. Thermal conductivity λ ($\text{W}\cdot\text{m}^{-1}\text{K}^{-1}$) is an indicator of the ability of any material to conduct heat. Thermal conductivity is the quantity of heat transmitted through a unit thickness (h) in a direction normal to a surface of unit area (A), due to a unit temperature gradient (Δt) under steady state conditions, and when the heat transfer (Q) is dependent only on the temperature. Equation (2.6) is used to calculate the thermal conductivity of a fabric system.

$$\lambda = \frac{Q}{A \Delta t/h} \quad (2.6)$$

Thermal conductivity is a measure of the rate at which heat is transferred through unit area of the fabric across unit thickness under a specified temperature gradient. In short, thermal conductivity is an ability of any material to conduct heat. Higher values depict that heat will pass quickly whereas lower values indicate heat will pass slowly.

For a textile material which is composed of fibers and entrapped air, the thermal conductivity is a combination of the fiber and air thermal conductivity. The thermal conductivity of textile fabrics is based on the thermal conductivity of fibers, yarns and on the construction of fabrics that defines in terms of interlacements the major part of fabric porosity. Morton and Hearle have explained that thermal conductivity of fabric depends much more on the air entrapped within it than on fiber conductivity as thermal conductivity of air ($0.025 \text{ Wm}^{-1}\text{K}^{-1}$) is lower than that of

the fiber. On the other hand, the air immobilized in the fabric structure can also have significant influence on the fabric thermal behavior if it behaves as an insulating medium in the absence of convection.

Theoretical calculation of thermal conductivity

The fabric structure consists of binding points and air openings between binding points. If the fabric porosity is known, thermal conductivity of a fibrous bundle can be calculated. The thermal conductivity was calculated based on two phase model of porous systems [119]. The limit model is shown in Fig. 2.7.

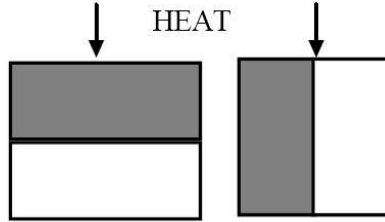


Figure 2.7: Limit arrangement of polymeric phase (gray) and air phase (white) in conductivity model.

The thermal conductivity of parallel arrangement λ_{hP} (higher limit) is equal to,

$$\lambda_{hP} = P \lambda_a + (1 - P) \lambda_f \quad (2.7)$$

For serial arrangements, thermal conductivity λ_{hS} (lower limit) is defined as,

$$\lambda_{hS} = \frac{\lambda_a \lambda_f}{P \lambda_f + (1 - P) \lambda_a} \quad (2.8)$$

Actual composition of a fibers and air phases can be presented by linear combination of parallel and series structures. The compromise is to compute the mean thermal conductivity of fibrous structure λ_h as arithmetic mean between upper and lower limit.

$$\lambda_h = \frac{\lambda_{hP} + \lambda_{hS}}{2} \quad (2.9)$$

Materials with low thermal conductivity are used as thermal insulators. Thermal resistance is the opposition to flow of heat energy. Thermal resistance 'R' (Km^2W^{-1}) is defined as the difference of the temperature across a unit area of the material of unit thickness (h) when a unit of heat energy flows through it in a unit of time.

$$R = \frac{h}{\lambda} \quad (2.10)$$

Thermal resistance is directly proportional to the thickness (h) and inversely proportional to the thermal conductivity (λ).

Functionality is the most important feature as the fabric needs to meet the handling requisition of environmental factors and structural requirements as per application. Textile materials have found a range of applications in the field of thermal insulation. Different types of fabrics in combination with various coatings and treatments are being studied to understand and improve the effectiveness of thermal insulators. In recent times, a wide range of textile materials has been used for technical usages such as building insulation, automobiles, aircraft and industrial process equipment. Reduction of heat loss and acquisition via surface coating is one of the most efficient methods for reducing energy consumption in buildings. Since the heat loss and acquisition via surface coatings comprises over 40% of the building cooling and heating overload, its reduction could be effective in the aspect of energy reduction. Using materials with low thermal conductivity during the design and construction of buildings will ensure that the insulation of surface coatings is an effective method of reducing cooling and heating overload, as well as energy consumption [117-118]. In principle, the thermal conductivity of an insulator can be measured by placing a thin sample of an unknown material between two plates—one heated and the other cooled—and measuring the electrical power required to attain a temperature gradient across a sample of known thickness. The testing methods for determination of thermal properties of any material can be divided into two major groups: steady-state and transient-state methods. The main difference between these two methods is that steady-state requires the specimen to reach a stable test temperature. This is time consuming. Transient-state methods perform a measurement during the process of heating up or cooling down. Measurements can be done quickly. Different methods have been used in the determination of the thermal properties of fabrics are described by many workers are divided into four method [119-120]. The first is *cooling method* in which a hot body is surrounded by a fabric whose outer surface is exposed to the air, and the rate of cooling of the body is determined. Second is *disc method*, where the fabric is held between two metal plates at different temperatures, and the rate of flow of heat is measured, third is *Measurement of propagation of waves (heat pulses)*, It is an extension of the rate of the cooling method. In this technique, multiple waves of temperature gradients are passed through the sample and the damping of the wave is used to calculate the heat flux through the sample [121] and fourth is *constant temperature method*, where the fabric is wrapped around a hot body and the energy required to maintain the body at a constant temperature is found. In practice, the measurement of the rate of heat flow in a particular direction is difficult as the heater, even when supplied with a known amount of power, all the power coming from the heater does not automatically go into the sample, and the sample does not necessarily experience one-dimensional heat flow with parallel heat flux vectors through it. Dissipates its heat in all

directions. Most successful heat transport measuring instruments are: Togmeter (BS 4745, 1971), guarded hot plate (ASTM D 1518-85, 1990), Alambeta instrument (SENSOR, 1990) and Thermal conductivity analyzer (TCI) [120-123].

Electrical properties of textile materials

For a long time, different textile materials have been used as insulators. Insulating materials are used to isolate components of an electrical system from each other and from ground, as well as to provide mechanical support for the components. From the ancient age, the conductive wire was wrapped with cotton or silk yarns for insulation. It is of interest to know that the first material to insulate the conducting thread was silk used by Stephen Grey in 1729[124]. Since then, different textile materials have been used as insulating purpose [125-127]. Textile materials can be used as insulator where heat is generated during current flow through wire in high voltage. It can be used in case of high voltage phenomenon where high current passes through conductor. Specially designed textile material can also be used as gloves, jackets (apron) for electrical work or as floor covering in the room where high voltage electrical appliances are kept. Electrical properties of textiles are judged in terms of surface resistivity [Ω] and volume resistivity [$\Omega \cdot \text{cm}$]. Resistivity is a feature of the raw material. It is known the electrical resistivity of a material is an intrinsic physical property, independent of the particular size or shape of the sample.

Volume resistivity ρ_v [$\Omega \cdot \text{cm}$] was calculated from the following relation:

$$\rho_v = R_v \frac{S}{h} \quad (2.11)$$

where, R_v [Ω] is volume resistance reading, h is thickness of the fabric [cm], and S is the surface area of the electrodes [cm^2].

Surface resistivity is measured by applying a voltage potential between two electrodes of specified configuration that are in contact with the same side of a material under test. Surface resistivity ρ_s [Ω] was calculated from relation:

$$\rho_s = R_s \frac{2\pi}{\ln \frac{R_2}{R_1}} \quad (2.12)$$

where R_s [Ω] is the surface resistance reading, R_1 is the outer radius of the center electrode [m], and R_2 is the inner radius of the outer ring electrode [m].

In order to keep the environment free from pollution, the use of biodegradable and environmental friendly material is important and hence it has attracted the interest in natural materials. In the past glass fiber (E glass or electrical glass) was used as insulator. It was particularly well suited to applications in which radio-signal transparency was desired, such as aircraft radomes, antennae and computer circuit boards. It used the nature scare component boric oxide (B_2O_3) and also it is not environmental friendly [47]. Basalt fiber is able to replace glass

fiber in many fields. Basalt fiber was one type of high performance inorganic fibers which were made from natural basalt. It is environmentally friendly material in all aspects. Basalt fiber is known as green industrial material. It has wide range of applications due to their superior characteristics. They have excellent thermal, electrical and acoustic insulation. It has much higher heat insulating values. They do not conduct electricity; no field is induced when exposed to RF radiation, transparent to RF and Microwave radiation. Volume resistance of basalt fiber is almost equal to ones of glass fibers. So, switch from glass to basalt does not change radar transparency of construction. It has also high electrical properties make it perfect for printed circuit boards, delicate electric cables and underground wires [128].

Table 2.4: Electrical properties Basalt vs. Glass [47].

| Properties | Basalt | E-glass |
|--|--------------------|--------------------|
| Specific volume electrical resistance ($\Omega \cdot m$) | 1×10^{12} | 1×10^{11} |
| tangent Loss angle frequency(1 MHz) | 0.005 | 0.0047 |
| Relative dielectric permeability (1MHz) | 2.2 | 2.3 |

Jute fiber is an abundant natural biodegradable fiber. Traditionally, jute fiber was used for the manufacture of carpet backing, ropes, canvas and sackings et al. Recently, the demand of natural biodegradable and eco-friendly fiber has risen worldwide due to the improving of people's living standards and demand for environmental protection. In recent years, jute is becoming increasingly used in technical applications like for composites etc. Its electrical resistance is (10^7 ohm-cm). Dry jute exhibits high electrical resistance but electrical resistance drops down at a very high rate with the absorption of moisture. The dielectric constant of jute at a frequency of 2 kHz is 1.8 in dry jute, 2.4 at 65% RH and 3.6 at 100% RH [130].

Thermoplastic polymers are traditionally used as electrically insulating materials. Polyester fibers belong to the group of thermoplastic fibers. They are characterized by relatively high values of thermal resistance factors. The high specific heat value (1200-1350 J/kg/K) results good thermal insulation of polyester and polyester fibers are distinguished by very good electric properties, and are poor conductors of direct current. Their resistivity is within the range of $10^{14} \Omega \cdot cm$. Dielectric constant at 1MHz is 3.0. They are already used in dry and wet laid nonwovens made from polyester fibers and some inorganic fibers for various insulation and industrial applications [129-130]. Nowadays, polypropylene-based materials are frequently used in the textile, building industries and as well as electrical application, due to their significant advantages such as low cost, lightweight, flexibility, low values of dielectric properties, thermal and chemical stability, recyclability, etc. Polypropylene, are largely non-polar and hydrophobic. There is no dipole in the polymer because of symmetry. Furthermore both bonding and non-bonding electrons are tightly held and displaced little by external fields. These materials exhibit very little dielectric polarization,

and as a result dielectric constant is low. So don't conduct electricity. Their electrical resistivity is higher than range of 10^{15} Ω .cm .The dielectric constant of PP at a frequency of 1 kHz is 2.3.Polypropylene, offer superior protection for sensitive electronic components and serve as a barrier to prevent consumers and service workers from experiencing electric shock [131].

Acoustic properties of textile materials

Today worldwide much importance is given to the acoustical environment. Noise control and its principle play an important role in creating an acoustical eco-friendly pleasing surroundings. This can be achieved when the intensity of sound is controlled to a level that is acoustically eco-friendly comfort atmosphere by converting the sound energy into thermal energy using different types of acoustic materials. Most industrial noise producers like compressor, heavy machines (or) equipment's, textile machineries and vehicles need some type of acoustical absorbing materials to reduce the human difficulties. The mechanism for reducing sound depends on where the sound comes from. If it is generated within a room then sound is *absorbed*. If it is airborne, it is originating from outside then to keep sound out it is necessary to *insulate* the space. And if it transmitted through the structure then the structure needs to be *isolated* from the source of vibration. Cellular and porous solids can be good absorbing media and they can help isolation. But they are not very good at insulation against sound.

Fibrous, porous and other kinds of materials have been widely used as sound absorptive materials. These porous textile materials with air inside the pores act as absorbing or damping medium. Damping refers to the capacity of the material to dissipate energy. Thicker materials generally show greater damping. Porous materials can greatly improve sound absorption, especially, if the material contains open pores like channels. Sound enters through the channels and converts to heat as it moves through the material, thus efficiently dampening the sound.

The acoustic phenomenon and its consequences in environments, such as work place and residential homes, have gained paramount importance. The acoustic characteristics of a room or an auditorium can be controlled by covering the walls, ceiling and floor with materials having suitable acoustic absorptive characteristics .The use of various types of textiles in mass residential building units has emphasized this importance. While extensive research in the field of acoustic properties of nonwoven fabrics has been extensively undertaken, in the case of other types of textiles, namely woven and knitted fabrics, very limited research has been conducted. Prior to the present research, other researchers, such as Aso and Kinoshita [132-134] had investigated the relationship between the flow resistance and the absorption characteristics of cotton fabrics. In these researches the effects of thickness, weight and fabric cover have been investigated. In another research work the absorption properties of fiber assemblies was studied and the importance of porosity and total surface area of the fiber assembly as pivotal factors was emphasized. Na et al. [135] studied the sound absorption coefficient of micro-fiber made fabrics via the reverberation method. It was found that these fabrics, with the exception of mesh structures, absorb the complete range of the sound frequencies better than fabrics made of conventional fibers. Other studies in this field have rather focused on the absorption mechanism

and methods of sound absorption measurement. Lee and Joo [136] examined the sound absorption coefficient of recycled polyester nonwovens. The relationships between acoustic absorption property and nonwoven parameters, such as fiber and web properties were established.

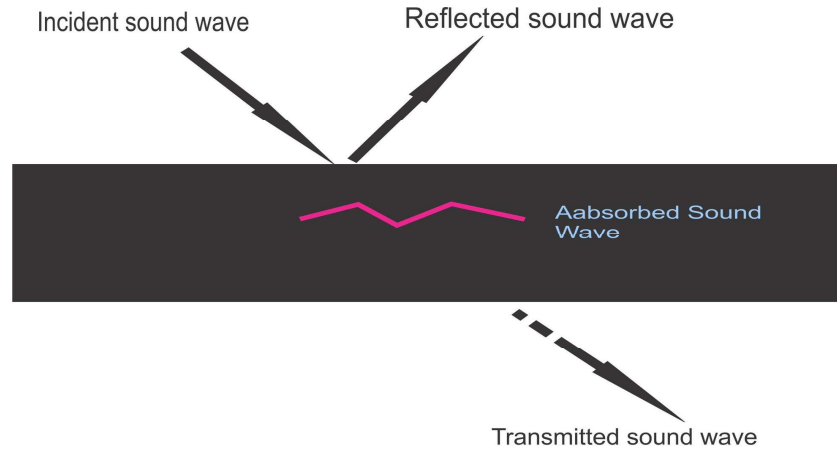


Figure 2.8: Acoustic characteristics of textile materials.

Acoustic absorption is the transformation of sound energy to thermal energy due to friction between the moving air particles and the material itself. Textile materials (porous materials) that reduce the acoustic energy while the sound wave passes through are referred to as acoustic absorbing textile materials. When the sound wave falls on a textile material, some amount of the sound will be reflected, some amount will be transmitted through and some will be absorbed by the material. The reflection, transmission and absorption of sound are influenced by the type of fiber and structural characteristics of the product. The incident sound wave while entering the air passages of the material, the frictional resistance to flow is induced by the fiber inside and kinetic energy of the flow in and out of the passage is converted to thermal energy.

Engineers always seek new materials and arrangements to enhance the sound absorption techniques. Currently, sound absorption materials commercially available for acoustic treatment consist of glass, mineral or synthetic fibers. A study on sound absorption characteristics of rock wool and glass fiber [132] indicated that these fibers behave alike. However, when the issues of safety, insulation, environment and health are considered, they pose interference to human health and surroundings. Thus, environmentally friendly materials of high flame resistance and high insulation as well as good sound absorption properties are needed.

The air flow resistance can yield good absorption regardless of the thickness of the fabrics. Air Flow Resistivity, is calculated as follows:

$$r = \frac{\Delta p}{v h} \quad (2.13)$$

Where, r - air flow resistivity ($\text{Pa}\cdot\text{s}\cdot\text{m}^{-2}$)

Δp - Pressure difference in Pascal,

v -linear air flow velocity in m/s
h- Thickness in meters

The influence of the structural characteristics on acoustical and sound resistance of the developed fabric samples are measured and interpreted. Based on results, the effect of fabric structural parameters on the sound absorption coefficient was established. In this work NRC of the samples were also obtained

Relationship between tensile moduli and sound propagation

Specific acoustic impedance is measures of the opposition that a system presents to the acoustic flow resulting of an acoustic pressure applied to the system. The SI unit of acoustic impedance is the pascal second per cubic meter ($\text{Pa}\cdot\text{s}/\text{m}^3$). Specific acoustic impedance (Z) (characteristic impedance, wave impedance) is the opposition of a medium to wave propagation, and it depends on the medium properties and the type of wave propagating through the medium. Concerning the interaction between sound and materials ,one common magnitude that is generally mentioned as realted to properties of materials that affect sound transmission is the acoustic impedance (Z) of a material, defined as the product of its density(ρ) and accoustic velocity(v)

$$Z = \rho v \quad (2.14)$$

Since acoustic velocity or speed of sound propagation through a certain material medium is generally defined as:

$$V = \sqrt{E/\rho} \quad (2.15)$$

Then the accoustic impedance can be redefined as Specific acoustic impedance

$$Z = \sqrt{E\rho} \quad (2.16)$$

Where E is moduli in N/m^2 and (ρ) is density of the medium in kg/m^3

Above equation summarizes the direct relation of acoustic impedance with two essential properties of material through which sound wave travels which are inertial and elastic properties. These properties are considered as under:

Elastic properties are the characteristics of a material which enables it to bear stresses and retain its original condition when subjected to force application or stress. Under observation of microscope, elastic materials possess atoms or molecules bonded by strong forces of attraction among them. When a material is subjected to force application, its stronger attractive forces help it to retain its shape and prevent from getting deformed. The designed sequence of binding forces describes material as rigid material (the one with high elastic modulus) to flexible materials

(ones with low elastic modulus).

Inertial properties can be described as property of material to resist against a change in its state of motion. The density of material is the magnitude related to its inertia. Under microscopic examination, density of a material is related with mass of particles forming it and their packing. The designed sequence depicts density of solid materials in relation with inertia or mass of particles considering volume to be equal. This illustrates that particles with greater inertia are less affected by interaction among neighboring particles.

Acoustic impedance is therefore a magnitude that plays a relevant role in determining sound transmission at the boundary between two materials/mediums which have different acoustic impedance. Very elastic materials and dense are usually good for sound reflector to attenuate the sound propagates in air. Elastic materials and steel frames can transmit vibrations throughout the building. Not good for isolation. Impact noise is transmitted directly into the structure/fabric of a building, here low modulus materials can be useful. Sound absorber should have less elasticity. In isotropic materials, the elastic constants are the same for all directions within the material. However, most materials are anisotropic and the elastic constants differ with each direction. The elastic constants for the longitudinal direction are different than those for the transverse directions.

Chapter 3 - Experimental Materials and Methods

3.1 Materials

Fibers and yarns/tows

Basalt is a fiber originated from rocks and having excellent thermal resistance. Polypropylene is a thermoplastic polymer and can be made by polymerizing propylene molecules. It is a by-product of oil refining processes. It is a low-cost polymer with versatile applications. It has the lowest density among all synthetic fibers. PP possesses several useful properties like high heat distortion temperature, transparency, flame resistance, dimensional stability and high impact strength which widen its application. Polyester is also thermoplastic polymer and it most commonly refers to polyethylene terephthalate (PET). It has high flame resistance and elasticity. Polyester is the most versatile, most cost effective and most widely used fiber in various applications. Natural fibers are gaining importance in recent years for green composite applications. Jute is a long, soft, shiny vegetable fiber that can be spun into coarse, strong threads. It is one of the most affordable natural fibers and is second only to cotton in amount of production in the whole world. It falls into the bast fiber category. It is 100% bio-degradable, recyclable and thus environmentally friendly. It is a thermoset polymeric fiber. The idea of current research was to use these common polymeric fibers in the weft and warp along with basalt warp/weft so as to create hybrid woven structures and to further investigate the compatibility with cement in composite manufacturing. The polyester and jute yarns used in our study were available commercially. Polypropylene yarn was taken from company Synthetic (Pakistan). The basalt yarn was used as received from company Kamenny Vek (KV) (Russia). The details of fibers and yarns are given in Table 3.1.

Table 3.1: Properties of fibers and yarns used

| Properties | Basalt | Polyester | Polypropylene | Jute |
|------------------------------|--------|-----------|---------------|-------|
| Diameter of fibers (micron) | 12 | 22 | 34 | 18 |
| No. of filaments | 890 | 900 | 300 | ----- |
| Linear density of yarn (Tex) | 295 | 250 | 292 | 296 |
| TPM (Twists/m) | 20 | 24 | 30 | 180 |
| Tensile strength (N) | 92.75 | 57.44 | 88.91 | 41.43 |
| Tensile elongation (%) | 1.29 | 12.27 | 12.55 | 1.39 |
| Tenacity (N/tex) | 0.315 | 0.305 | 0.23 | 0.139 |
| Initial modulus (MPa) | 9,378 | 1069 | 721 | 3,741 |

Cement and geopolymer for compatibility study

A commercial ordinary portland cement (OPC) was used and green cement (GEOPOLYMER BAUCIS L110) produced by České lupkové závody, a.s was taken.

Alkali for accelerated aging study

The chemicals used for accelerated aging treatment are analytical grade NaOH (sodium hydroxide, Lach:ner.s.r.o, Czech Republic) and $\text{Ca}(\text{OH})_2$ (Calcium hydroxide LACHMEMA.N.P.Brno, Czech Republic).

3.2 Methods

3.2.1 Preparation of samples on CCI sample loom

The fabric samples produced are:

1. Plain weave, B/PP, B/PET and B/J,
2. Matt weave, B/PP, B/PET and B/J,
3. Twill weave, B/PP, B/PET and B/J.

Pure non-hybrid fabrics were also made for the comparison purposes. All fabric samples were made on the CCI sample loom with the same thread density for all fabrics approx. 12 threads/cm in warp and 8 threads/cm in weft. Basalt is a new material for the industry. There is no standard available for settings to run such a yarn, as is the case with some of the other materials like cotton, polyester or blends of both for instance runs extensively across the industry. The advantage of commonly used fibers is that, there is always a reference of settings available from where one can start the initial running and then fine tuning can be done, which was not the case with basalt. The cutters were changed and special double cutters were applied to cut which helped in smooth and proper cutting of yarn without much of the problems.



(a) CCI Sample loom

(b) Industrial trial on Picanol rapier loom

Figure 3.1: CCI sample loom and commercial rapier loom for running the fabric samples.

Study of basalt yarn weavability with PET, PP and jute

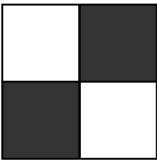
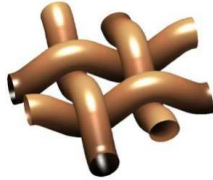
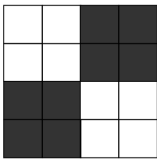
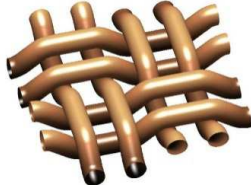
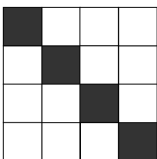
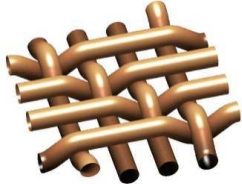
The weaving trials were first undertaken on CCI sample loom before weavability on commercial rapier loom so as to identify the efficiency of using basalt with other thermoplastic and thermoset yarns. The details are shown in Table 3.2.

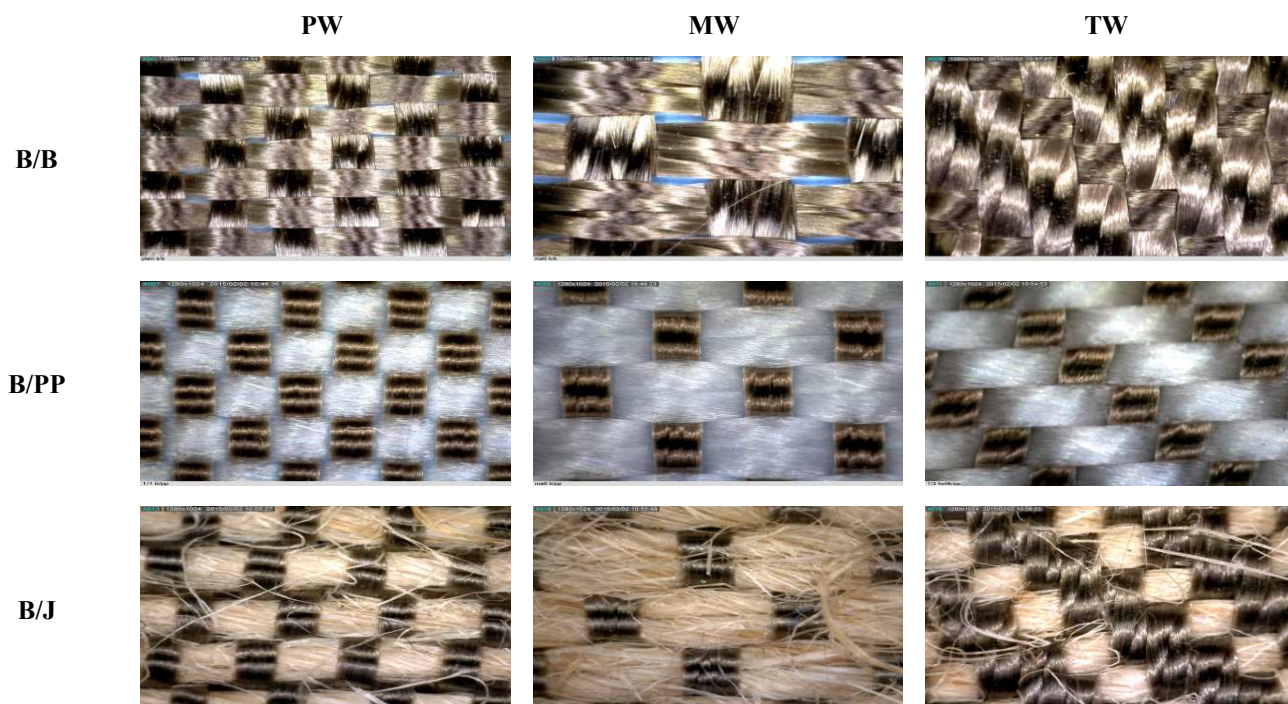
Table 3.2: Production parameters for CCI sample loom.

| Sl. No. | Weave | Machine speed (rpm) | Warp breakages (/hour) | Weft breakages (/hour) | Total sample time (hour) | Time for setting (hour) | Time for fault mending (hour) | Running time (hour) | Running Efficiency (%) |
|---------|---------------------|---------------------|------------------------|------------------------|--------------------------|-------------------------|-------------------------------|---------------------|------------------------|
| 1 | B/B 1/1 plain | 40 | 13 | 7 | 2.5 | 0.8 | 0.47 | 1.23 | 49.2 |
| 2 | B/B 2/2 matt | 40 | 7 | 5 | 2 | 0.5 | 0.3 | 1.2 | 60 |
| 3 | B/B 1/3 twill | 40 | 6 | 5 | 2 | 0.5 | 0.25 | 1.25 | 62.5 |
| 4 | B/PP 1/1 plain | 40 | 13 | 6 | 2.2 | 0.7 | 0.47 | 1.03 | 46.8 |
| 5 | B/PP 2/2 matt | 40 | 10 | 5 | 2.2 | 0.5 | 0.43 | 1.27 | 57.7 |
| 6 | B/PP 1/3 twill | 40 | 6 | 5 | 2.2 | 0.5 | 0.33 | 1.37 | 62.3 |
| 7 | B/PET 1/1 plain | 35 | 13 | 14 | 2.2 | 0.9 | 0.55 | 0.75 | 34.1 |
| 8 | B PET 2/2 matt | 35 | 10 | 10 | 2.3 | 0.85 | 0.5 | 0.95 | 41.3 |
| 9 | B/PET 1/3 twill | 35 | 9 | 11 | 2.3 | 0.8 | 0.5 | 1 | 43.5 |
| 10 | B/Jute 1/1 plain | 30 | 13 | 22 | 3 | 1.4 | 0.97 | 0.63 | 21.0 |
| 11 | B/Jute 2/2 matt | 30 | 11 | 17 | 2.8 | 1.22 | 0.87 | 0.71 | 25.4 |
| 12 | B/Jute 1/3 twill | 30 | 10 | 17 | 2.8 | 1.2 | 0.81 | 0.79 | 28.2 |
| 13 | PP/PP 1/1 plain | 40 | 10 | 6 | 2.5 | 0.8 | 0.35 | 1.35 | 54 |
| 14 | PP/PP 2/2 matt | 40 | 7 | 5 | 2 | 0.5 | 0.28 | 1.22 | 61 |
| 15 | PP/PP 1/3 twill | 40 | 6 | 5 | 2 | 0.5 | 0.22 | 1.28 | 64 |
| 16 | PP/B 1/1 plain | 40 | 8 | 5 | 2.2 | 0.7 | 0.33 | 1.17 | 53.2 |
| 17 | PP/B 2/2 matt | 40 | 6 | 4 | 2.2 | 0.5 | 0.3 | 1.4 | 63.6 |
| 18 | PP/B 1/3 | 40 | 6 | 4 | 2.2 | 0.5 | 0.28 | 1.42 | 64.5 |
| 19 | PET/PET 1/1 plain | 30 | 12 | 14 | 2.5 | 1 | 0.8 | 0.7 | 28 |
| 20 | PET/PET 2/2 matt | 30 | 10 | 10 | 2.4 | 0.9 | 0.78 | 0.72 | 30 |
| 21 | PET/PET 1/3 twill | 30 | 9 | 11 | 2.5 | 0.9 | 0.8 | 0.8 | 32.0 |
| 22 | PET/B 1/1 plain | 35 | 12 | 7 | 2.7 | 0.9 | 0.85 | 0.95 | 35.2 |
| 23 | PET/B 2/2 matt | 35 | 10 | 6 | 2.6 | 0.85 | 0.78 | 0.97 | 37.3 |
| 24 | PET/B 1/3 twill | 35 | 9 | 5 | 2.6 | 0.83 | 0.77 | 1 | 38.5 |
| 25 | Jute/Jute 1/1 plain | 25 | 19 | 22 | 3 | 1.5 | 1.1 | 0.4 | 13.3 |
| 26 | Jute/Jute 2/2 matt | 25 | 17 | 17 | 2.9 | 1.4 | 0.99 | 0.51 | 17.6 |
| 27 | Jute/Jute 1/3 twill | 25 | 17 | 17 | 2.8 | 1.3 | 0.95 | 0.55 | 19.6 |

Weave indicates the pattern of interlacement between warp and weft yarns. The schematic representation of different weaves is shown in Table 3.3. The ‘fill’ indicates that the longitudinal yarn or end is passing over the transverse yarn or pick. The ‘empty’ signifies that the pick is passing over the end. The scheme of sample preparation is shown in Fig 3.2.

Table 3.3: Fabric structure developed

| Sr # | Textile weave | Complete repeat | Schematic diagram |
|------|----------------------|---|---|
| 1. | Plain weave (PW) |  |  |
| 2. | 2/2 Matt weave (MW) |  |  |
| 3. | 1/3 Twill weave (TW) |  |  |



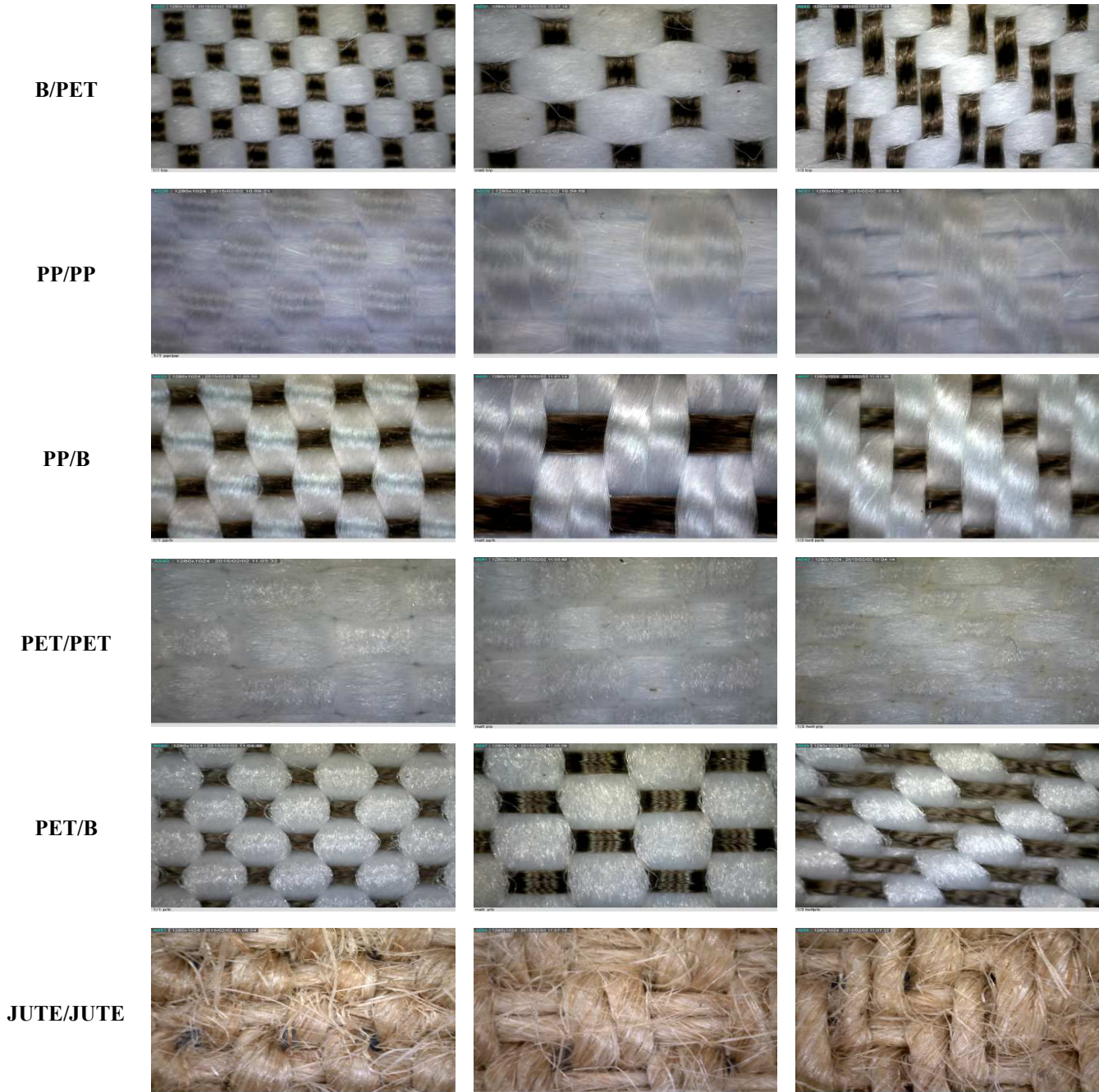


Figure 3.2: Photographs (Dinolite) of the structures developed with magnification 1280 x1024

3.2.2 Characterization of the raw materials

Energy-dispersive X-ray analysis of basalt fiber

Elemental detection via electron dot-mapping was conducted using energy dispersive X-ray (EDAX) analysis on the scanning electron microscope (SEM; VEGA TESCAN 3SBH) for basalt fiber so as to ascertain the chemical composition.

ATR–FTIR analysis of cements

FTIR stands for Fourier Transform Infra-Red, the preferred method of infrared spectroscopy. In infrared spectroscopy, IR radiation is passed through a sample. Some of the infrared radiation is absorbed by the sample and some of it is passed through (transmitted). The resulting spectrum represents the molecular absorption and transmission, creating a molecular fingerprint of the sample. Like a fingerprint no two unique molecular structures produce the same infrared spectrum. This makes infrared spectroscopy useful for several types of analysis.

Attenuated total reflection (ATR) infrared spectroscopy (Nicolet iZ10, Thermo Fisher Scientific Corporation) was used in order to understand the chemical structure of the cement. Transmission method was used with 16 scans for a background, 16 scans for a sample and the spectral range was 4000 -7500 cm^{-1} with a resolution of 4/ cm . Commercial Ordinary Portland Cement (OPC) and Geo Polymer Cement (GPC) were used and subjected to chemical analysis.

Inductively coupled plasma (ICP-OES) of cements

Inductively Coupled Plasma (ICP) analytical techniques can quantitatively measure the elemental content of a material from the ppt to the wt% range. Quantitative chemical analysis may be performed by one or more complimentary techniques, commonly including spark optical emission spectroscopy (Spark OES), inductively coupled plasma spectroscopy optical emission spectroscopy (ICP OES), x-ray fluorescence spectroscopy (XRF) etc. [137].

ICP-OES is a powerful technique for fast analysis. It is a trace-level, elemental analysis technique that uses the emission spectra of a sample to identify, and quantify the elements present. The concentration of metals in cement samples were determined by the inductively coupled plasma-optical emission spectrometer. Optical emission spectroscopy is done on Perkin Elmer optima 2100 DV. In this work, ICP analysis was used for cement prepared by direct suspension of the powder in dilute acid medium.

The aim of this investigation was to develop a rapid method of quality control for such raw materials. The results showed that this technique is sensitive enough for each element of interest and no serious interferences were detected after a detailed inter-element interference study.

3.2.3 Testing methods for fabrics

Physical properties

Projection microscope was used for taking SEM images of fiber cross-section. The fabrics used in the study were preconditioned in a conditioning room at standard atmospheric conditions ($20 \pm 2^\circ\text{C}$, $65 \pm 2\%$ RH) for 24 h.

Yarn number was measured according to ASTM D 1059-01.16. Measurements were taken from 10 warp samples and 10 filling samples for each fabric.

Yarn twist was measured according to ASTM D 1423-99.17. Measurements were taken from 25 warp samples and 25 filling samples for each fabric.

Fabric thickness was measured according to ASTM D 1777-96.13. Measurements were taken at 10 randomly selected areas.

Mass per unit area (weight) was measured according to ASTM D 3776-96.14. 5 measurements

were taken for all samples.

Number of yarns per unit distance, was measured according to ASTM D 3775-03.15. Measurements were taken at five randomly selected areas. All the fabric samples were tested for their ends and picks per centimeter value using pick counting glass.

Fabric cover % was calculated using the following expression;

$$\text{Fabric cover \%} = [d_1 n_1 + d_2 n_2 - d_1 d_2 n_1 n_2] \times 100 \quad (3.1)$$

Where, d_1 and d_2 are the warp and weft yarn diameter (cm), respectively, and n_1 and n_2 are ends per centimeter and picks per centimeter values, respectively.

Estimation of thread spacing and crimp by using geometrical models

The relationship between thread spacing in warp and weft direction is estimated by using geometrical models for plain, twill and matt weave. The weave factors as shown in table 3.4 are considered. It is a number that accounts for the number of interlacements of warp and weft in a given repeat.

Table 3.4 Weave factors for various weaves

| Weave | No. of warps/repeat | No. of warp interlacements | No. of wefts/repeat | No. of weft interlacements | Warp weave factor | Weft weave factor |
|-----------|---------------------|----------------------------|---------------------|----------------------------|-------------------|-------------------|
| 1/1 Plain | 2 | 2 | 2 | 2 | 1 | 1 |
| 1/3 Twill | 4 | 2 | 4 | 2 | 2 | 2 |
| 2/2 Matt | 4 | 2 | 4 | 2 | 2 | 2 |

A simplified algorithm is used to solve fabric geometrical model equations and relationships between useful fabric parameters such as thread spacing and crimp. Such relationships help in guiding the direction for moderating fabric parameters. Soft computing was used to provide a platform to manoeuvre crimp in warp and weft over a wide range with only three fabric parameters; yarn tex, modular length of warp and modular length of weft yarn. Soft computing has enabled solutions by interaction of crimp interchange and crimp balance equations. This exercise offers several solutions for fabric engineering by varying the above three parameters.

Mechanical properties

Static mechanical properties

Tensile test

Tensile tests apply forces directly on the material sample, by using clamps to securely grip two opposite ends of the sample and then pulling the ends away from each other. As the force is slowly increased the stress on the material gradually increases and the sample elongates until it reaches its maximum strain level and the material breaks.

Tensile properties of yarns used were measured according to standard CSNENISO 2062. For each sample, 20 measurements were done.

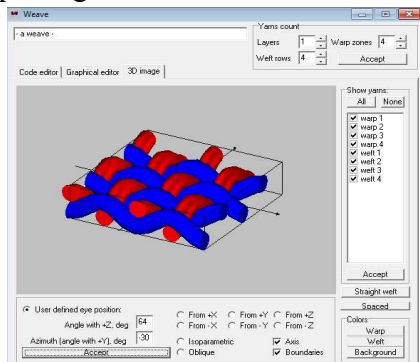
Tensile properties of all fabric samples in warp and weft direction were measured on a TIRA 2300 (LaborTech s.r.o., Opava, Czech Republic) universal testing machine. The tensile testing speed was 100 mm/min. This test was performed according to EN ISO 13934-1. The specimen size for tensile testing was 20 cm x 5 cm as per standard. All tensile tests were performed at room temperature. For each sample, 20 measurements were done.



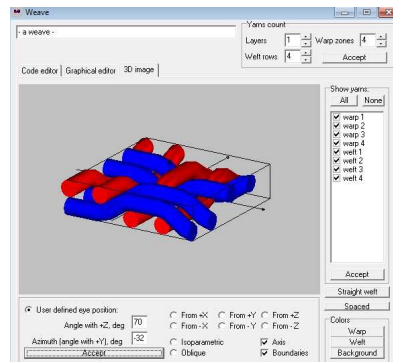
Figure 3.3: TIRA tester for tensile properties.

Prediction of tensile properties using Wisetex

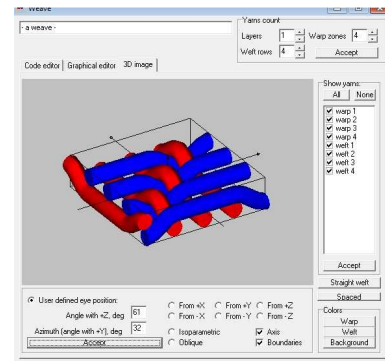
WiseTex is a computational tool for modeling of the internal geometry and deformability of textile structures. Internal geometry of textiles take full advantage of the hierarchical principle of textile modelling. The simulation algorithm extensively uses the minimum energy principle, calculating the equilibrium of yarn interactions. The models cover wide range of textile structures, either relaxed or after compression, shear or tensile deformation. S.V. Lomov et al. who developed a model for the internal geometry of 2D- and 3D-weaves (the CETKA-model [138-139], based on a minimum number of topological data (weave style, inter-yarn distance) and yarn mechanical properties. The model is a mechanical model, as it applies a yarn deformation energy minimization algorithm to predict the internal geometry of any 2D- and 3D-weave. The mechanical models not only generate the internal geometry of relaxed textiles, but also of textiles deformed in tension, compression and shear. The models are implemented in the software package *WiseTex*.



(a) 3D geometry PW



(b) 3D geometry MW



(c) 3D geometry TW

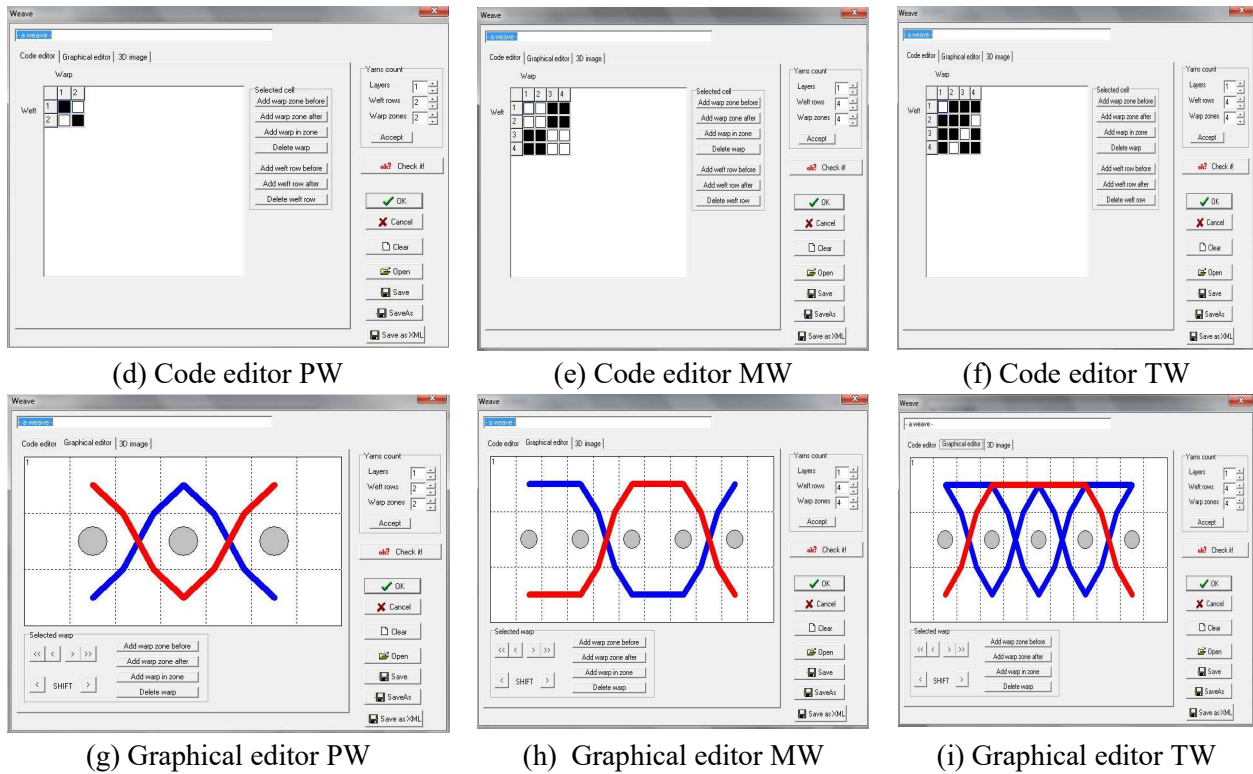


Figure 3.4: Weave structure (a-c) 3D image, (d-f) code editor and (g-i) graphical editor.

In this work, investigation of tensile deformation is done by the modelling tool applied to all fabrics. The geometry of a woven structure in the relaxed state is determined by the equilibrium of forces of the warp/weft interaction, caused by the necessity to accommodate the topology of contacts between yarns in a weave. Bending of yarns necessary to maintain this topology creates transversal forces in yarns intersections. The latter leads to yarn compression and flattening and, in case of non-symmetry of a contact conditions, to local deflection (resisted by friction between yarns) of yarns from ideal straight directions (prescribed by tension of warp and weft on a loom). In the relaxed state there is no tension of yarns; the weaving process does not imply twisting of yarns. Therefore, the following fabric parameters should be known.

1. Weave structure is coded by the method proposed either in code editor, graphical editor or 3D image. The data consist of the number of weft layers L and rows N_{We} , the number of warp zones N_{Wa} (a warp zone consists of warp yarns situated in the z -direction one above the other) and warp yarns in a zone N_{Wazi} , and the intersection codes.
2. Tightness of a fabric: A density of yarns placement in a fabric is characterized by ends and picks count P_{Wa} , P_{We} and yarn spacing
3. Warp and weft parameters - The warp and weft parameters e.g. linear densities, yarn cross-section dimensions in the free state, coefficient of friction between yarns, the law of yarn compression or some evaluation of compressed yarn dimensions in the fabric should be provided.

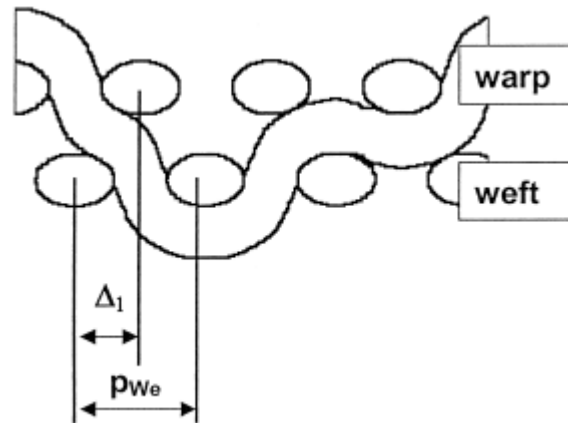


Figure 3.5: Fabric parameters: yarn spacing [138].

The model calculates equilibrium between tensile forces, compression and bending resistance of the yarns, the yarn crimp and sums up the yarn tensions to calculate the force applied to the fabric to achieve the given deformation.

Shear test

In this work, a picture frame was used to analyze the in-plane shear behavior of all fabric samples. Shear properties of all fabrics were measured on tensile testing machine by picture frame method under small angular displacements (15 degrees), however jamming of the fibers and wrinkling of the material, which occurred at large angular displacements would not have been observable. It is an effective way for characterizing in-plane shear property of fabrics. Testing yields load and displacement data, which can be used to determine the shear modulus as a function of the materials angular displacement.

The frame is extended diagonally along opposing corners using simple tensile testing equipment as shown in Figure 3.6. Shear test was performed on TIRA (LaborTech s.r.o., Opava, Czech Republic) with a crosshead speed of 10 mm/min. The nonlinear behavior of shear force versus shear angle and the deformation mechanism were analyzed. Load–displacement(axial force–displacement curves of intra-ply shear tests are analyzed. For each sample type, 10 measurements were taken.

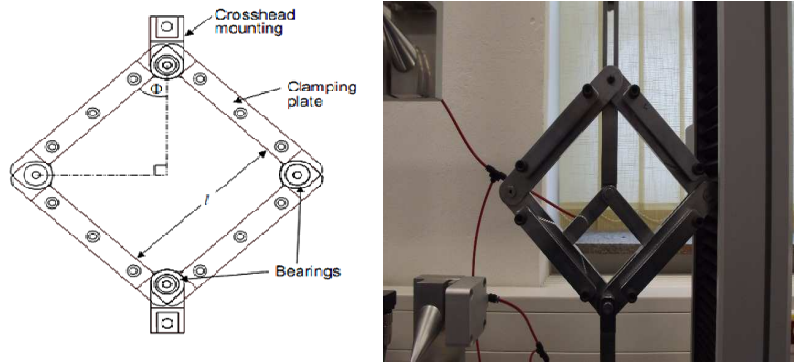


Figure 3.6: Picture frame fixture design.

Description of the test method/Working of picture frame.

In Fig. 3.6, picture of picture frame fixture for shear testing is given. A square frame with side length L equal to 200 mm was used. Slippage between the specimen and the grips was avoided by using four bars, which clamped the specimen. The apparatus has four legs which are hinged to form a picture frame. Further, there is a rod which runs across one of the diagonal of the frame. It should be noted that this rod is not in the plane of the frame but runs behind the frame. The lower end of the rod is hinged with the common hinge of the two legs meeting in that corner. The other opposite corner hinge is resting in the slot provided in the rod. The slot is about 6 cm long for maximum deformation of frame. Further, at the lower end the rod is again hinged to individual legs of the frame. The lower end of the rod is fixed in crossheads of the loading machine. Fabric conforms to its final geometry mostly by yarn rotation, i.e., shearing between weft and wrap yarns, denoted as the shear angle γ . γ is commonly assigned as zero (0) at the initial stage when weft and wrap yarns are perpendicular to each other. By adjusting the distance between the upper and lower crossheads, the angles between the arms of fixture reach 90° . The distance can be set as the original reference value, i.e., the zero displacement position, in computer, so that later on, all the experiments can automatically begin from this zero point. Also, the force can be set to zero at this position. This shear angle will be used as a common parameter for comparison. Thus, when the load is applied through the upper end of the rod, it pushes these two legs apart and deforms the frame. These two legs in turn push their adjacent legs making their common hinge to slide in the slot of the rod. The plate deforms into a diamond shape. After clamping, the specimen between two parallel plates and using heavy duty bolts,

In the picture frame shear test, the fabric is bolted to a stiff four bar linkage system/clamping plates/heavy duty bolts and has diamond knurled surface for better gripping. The force needed to deform the fixture must be measured accurately to determine the actual force required in shearing the fabric. The empty frame is tested under the same condition to find the frictional effects between bearings and slots, After several trials of this test, the average value of load at each displacement point is calculated. This is to record the load-displacement behavior of the empty fixture under the same condition as in the real shear experiment. Thus the frictional effect is considered and eliminated during sample testing. To eliminate the error caused by the weight

and inertia of the fixture, the net load obtained was subtracted from the machine-recorded load when the fabric is being deformed in the picture frame. Then this resultant load is considered and accounted as an actual load. The fabrics for shear tests were prepared according to the size of the picture frame. Samples were prepared under dry conditions at ambient air temperatures. In order to prevent the pressures from imposing on test fabric by the fixture during the large deformation, the central area of shear deformation was 100 mm X 100 mm, and the four corner parts were cut off (Figure 3.7) in order to avoid edge buckling. These frames allow the materials to be stressed biaxial prior to the shear testing to observe the shear performance under similar axial stress states, which will be seen in the material for specific applications. The specimens were aligned carefully within the bars of the picture frame, eliminating any slackness in the material but applying no significant pre-stress. A tensile load is applied (vertically), which also causes a horizontal compressive force because of the linkage system. As a result, a state of shear (at 45° to loading directions) is created in the test fabric. Shear angle was calculated by Equation 2.5.

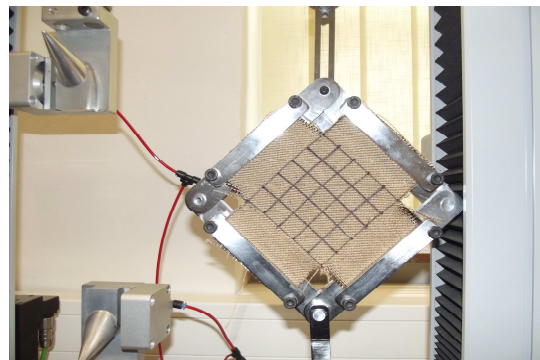


Figure 3.7: Clamping of sample in fixture.

Image analysis using MATLAB for determination of shear angle

The next step is to enhance and process the images, which was done using the MATLAB software on a computer. Image analysis can aid in the determination of the shear angle and displacement at any particular point on the surface of fabric specimen. The complete displacement of the specimens during loading process was obtained by image analysis methods. The images were captured at certain regular interval of time using digital camera. A special program was developed in MATLAB 7.10 (R 2010a) using Hough's transform to find the angle between the lines on the specimens. This image was analyzed to obtain shear angle and displacement of the specimen during the test. The image file string is examined and then the appropriate image reading function is called by MATLAB `imread`. As the images taken were colored, the images were converted to grayscale and then normalized to a matrix of values ranging from zero to one. This matrix is returned by the function in the variable `I`. Grid pattern was applied on the specimen surface before the test and used as the reference points of image analysis. Around 16 points (25 square cells (4cm^2 each) with 90° angle at 4 points) can be chosen on a 100 mm x 100 mm specimen for image analysis to determine the displacements and shear angles at the chosen points. First, by manually choosing the points on a reference image, the X

and Y coordinates of each point can be determined in pixel as shown in Figure 3.8. The difference of X and Y coordinates of each chosen point between the reference image and the image chosen for analysis represents the displacements in X and Y directions.

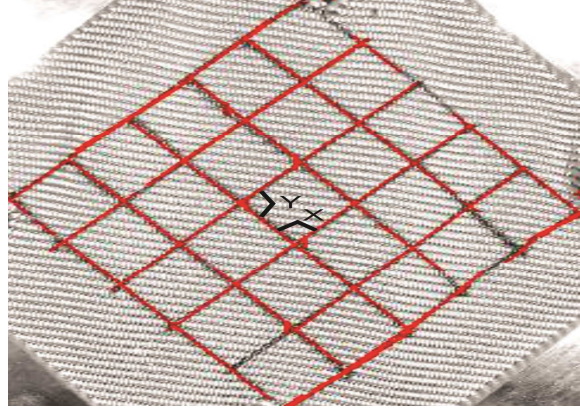


Figure 3.8. Determination of shear angle using image analysis.

Figure 3.8 shows the main idea of Hough transform applied to find the shear angle in image analysis technique. The Hough transform is widely used in image analysis, computer vision and digital image processing to find shapes in a binary digital image. This approach is preferred when the objective is to find lines or curves in an image. The parameter ρ represents the distance between line and origin, θ is the angle of the vector from origin to this point. In Figure 3.8, the X, Y angle is presented on gray image for better understanding in sample and shear angle is calculated using this information. Figure 3.8 shows the points where the lines intersect giving the distance and angle. This distance and angle indicate the line which bisects the points being tested at each 5 mm displacement in every 30 seconds interval. It helps researchers to understand more about detections of angles using houghs transform. In Fig 3.9, the points in Hough's histogram are clearly shown.

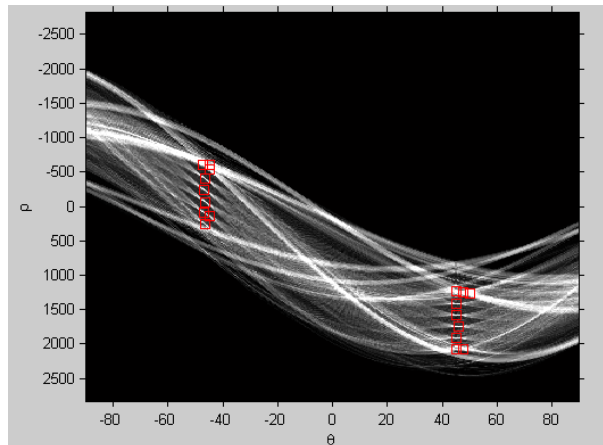


Figure 3.9: Detected lines and points in Hough's histogram.

Dynamic mechanical properties

DMA facilitates in material selection for specific end-use applications. The task of evaluating new materials and projecting their performance for specific applications is a challenging one for engineers and designers. Forced vibration (non-resonant) variable frequency apparatus applies a constant amplitude (stress or deformation amplitude). The storage and loss moduli are then measured as function of temperature using dynamic mechanical analysis (DMA). Tensile mode is ideal for investigating thin specimens, such as films/fibers, thin materials in the low-to-medium modulus range. The sample is clamped at its ends with sufficient pretension applied to avoid sample buckling and to keep the sample under tension during the whole experiment. The sample is clamped into a frame of measurement head and is heated by the furnace. The sample in the furnace is subjected to stress from the force generator via probe. To make the strain amplitude constant, the stress is applied as the sinusoidal force. This frequency is one of the measurement conditions. The deformation amount generated by the sinusoidal force is detected. Viscoelastic values such as elasticity and viscosity are calculated from the applied stress and the strain is plotted as a function of temperature or time. The DMA was performed on a DMA 40XT RMI equipment. The samples were tested using tensile mode at a frequency of 1 Hz in temperature scan mode. The DMA test was executed in the temperature range of 27 to 100°C at a heating rate of 3°C/min. This test was performed according to EN ISO 6721-1. All of the samples were investigated only in the warp direction. For each sample, five measurements were done.

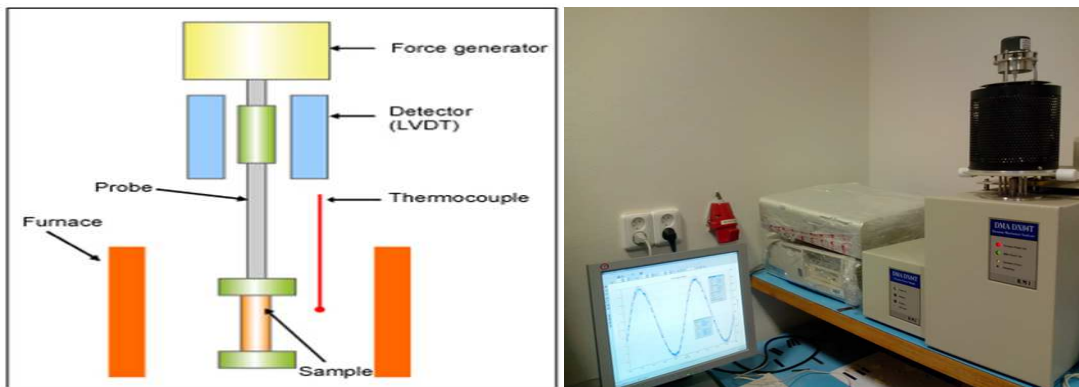


Figure 3.10: Schematic diagram of the experimental set up of DMA

Transmission and thermal properties

Air Permeability

All the samples were conditioned in standard atmospheric temperature of about $20^{\circ} \pm 2^{\circ}\text{C}$ and $65 \pm 2\%$ relative humidity for 24 h before subjecting to testing. The Air permeability of the samples were analyzed by using the air Permeability Tester, FX 3300 air permeability tester 111 according to standard ISO 9237(1995). The measurement was performed at a constant drop of 200 Pa (20 cm² test area) in the standard atmosphere. The air permeability is described as the rate of air flow passing perpendicularly through a known area, under a prescribed air pressure

differential between the two surfaces of a material. The principle of FX 3300 air permeability tester 111 depends on the measurement of air flow passing through the fabric at a certain pressure gradient. In this instrument any part of the fabric can be placed between the sensing circular clamps (discs) without the garment destruction. As the fabric is fixed firmly on its circumference (to prevent the air from escaping), the fabric dimensions do not play any role. There is also enough space between the clamps and the instrument frame, which allows the measurement on large samples. The averages of 20 measurements for each sample were taken, and mean values of the thermal properties were calculated. To confirm repeatability, measurements were performed thrice at an interval of 30 days for all the samples. The precision of the instrument was measured up to two decimal places for the same fabric that was tested in similar conditions and the accuracy was approximately 14%. Tests were performed according to standard ISO 9237 (1995) for each sample.

Thermal conductivity and resistance

Measurement of the thermal insulation properties of the fabrics was done by means of Alambeta according to ISO EN31092 standard. This method belongs to the 'plate methods', the acting principle of which relies on the convection of heat emitted by the hot upper plate in one direction through the sample being examined to the cold bottom plate adjoined to the sample. The instrument directly measures the stationary heat flow density (by measuring the electric power at the known area of the plates), the temperature difference between the upper and bottom fabric surface, and the fabric thickness. The device calculates the real thermal resistance for all fabric dimensions. The values of thermal conductivity, thermal resistance and fabric thickness under a 200 Pa contact pressure were determined.

Measurement of thermal properties of fabrics are also done by TCi according to the standard test method EN 61326-2-4:2006. TCI developed by C-Therm is a device for conveniently measuring the thermal conductivity of a small sample by using the MTPS (modified transient plane source) method. The principle of the apparatus (TCi) is based on conductors in series with respect to the direction of heat flow. The ratio of the temperature drop across the conductors is equal to the ratio of their thermal resistance. Thus, if the temperature drop across a material of known thermal resistance (standard resistance) and across a test specimen in series is measured, the thermal resistance of the test specimen can be evaluated. Contrary to other devices, TCi can measure the thermal conductivity of materials in the states of solid, liquid, powder, and mixed. In addition, it can measure thermal conductivity using only one side. The TCi consists of a sensor, power control device, and computer software. A spiral-type heating source is located at the center of the sensor, and heat is generated at the center. The heat that has been generated enters the material through the sensor during which a voltage decrease occurs rapidly at the heating source, and the thermal conductivity is calculated through the voltage decrease data. The thermal properties of the sample material are inversely proportional to the rate of increase in the sensor voltage. The thermal conductivity is calculated through the voltage drop data. The tests of thermal properties were repeated five times and for air permeability was repeated 10 times. The

means and SD of data were calculated for all tests.

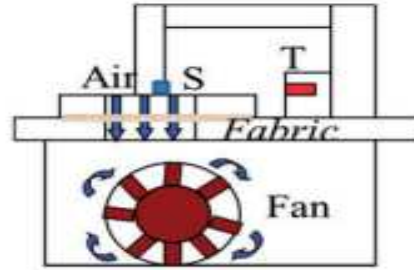


Figure 3.11: Schematic diagram of the experimental set up to measure air permeability [116]

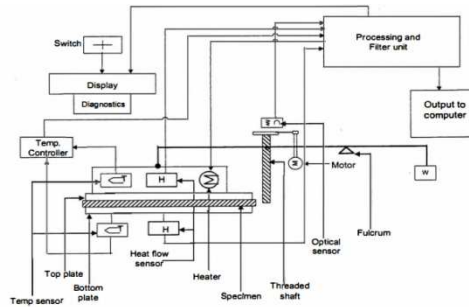


Figure 3.12: Schematic diagram of the experimental set up to measure thermal properties [115]

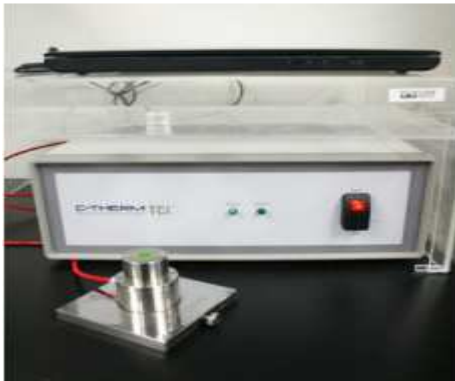


Figure 3.13: Schematic diagram of the experimental set up to measure thermal properties [117]

Electrical properties

Electrical resistivity (also known as resistivity, specific electrical resistance or volume resistivity) is an intrinsic property that quantifies how strongly a given material opposes the flow of electric current. A low resistivity indicates a material that readily allows the movement of electric charge. Electrical resistance measurement was done on a measuring device (ohmmeter) 4339B High Resistance Meter. The electrical volume and surface resistivity of the samples tested were measured according to the standard ASTM D257-07, at temperature 22.3°C and relative

humidity 40.7%. Measurement results were recorded out after 60 s from the moment of placing the electrodes on the textile sample. Voltage value was maintained at 100V. Volume resistivity is measured by applying a voltage potential across opposite sides of the sample and measuring the resultant current through the sample [130]. Resistivity was measured by Equations 2.11 & 2.12.

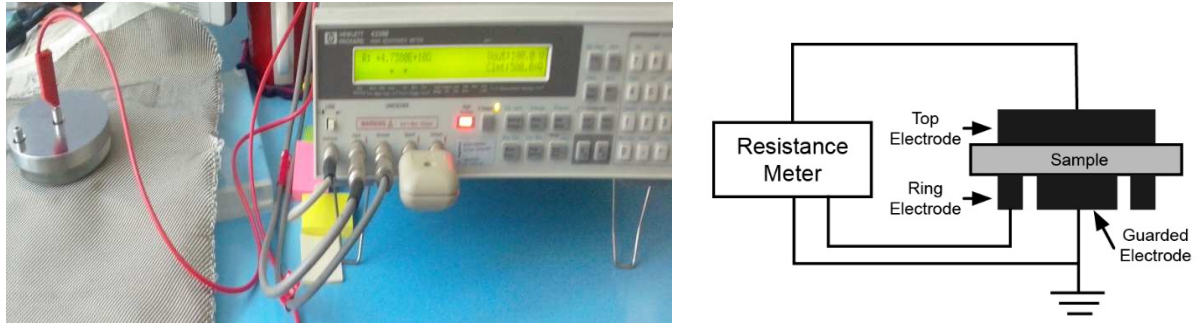


Figure 3.14 (a) Resistivity measurement system and (b) schematic diagram of an experimental set-up to measure electrical resistance

Acoustic properties

The amount of research conducted on sound absorption properties of woven fabrics in comparison to nonwoven and spacer textile fabrics is very limited. This work deals with the study of the acoustic characteristics of woven fabrics in relation to fabric structural parameters and air flow resistivity.

Sound absorption mechanisms

Generally, the following four phenomena can be held responsible for absorption of sound by woven fabrics:

- (1) Internal visco-thermal dissipative effects. These are mainly dominated by visco-inertial effects due to the negligible thickness of fabric.
- (2) Flow distortion effects generated on both sides of the fabric.
- (3) Acoustic resonance in the cavity at the back of sample. This influences fabric response to normal incidence plane wave.
- (4) Bending vibrations of the fabric.

In order to achieve the objectives of the research, sound absorption coefficient of hybrid woven fabric samples was determined. The various measurement technique used to measure sound absorption are Reverberant Field Methods, Impedance Tube Methods, Steady State Methods etc. In this work, the sound absorption of all fabrics samples were calculated using two terms, namely sound absorption coefficient (SAC) and noise reduction coefficient (NRC) using impedance tube method. SAC is the measure of sound absorbed by the samples for each and every frequency and overall sound absorption of different materials can be compared through NRC. It is defined as the arithmetic average of SAC at four different frequencies, namely 250 Hz,

500 Hz, 1000 Hz and 2000 Hz [135]. SAC varies from zero (0) to one (1). Sound absorption performance is a function of frequency and is performed generally with the increase in frequency. The performance of all fabrics samples were analyzed for acoustic absorption.. The acoustic impedance of a material is its most basic acoustic property. Impedance, defined as the ratio of the pressure to the volume displacement at a given surface in a sound-transmitting medium, is usually a frequency-dependent number. In this research, the impedance tube method was used to determine the normal incident sound absorption coefficient, SAC (α). Acoustic property was measured by using two-microphone impedance tube according to ASTM E1050-08. It uses plane sound waves that strike the material straight and so the sound absorption coefficient is called normal incidence sound absorption coefficient, SAC. Since in this method a sound wave strikes the material perpendicularly, the measured sound absorption coefficient is known as the normal incidence sound absorption coefficient. The following measurement methods are divided according to the size of evaluated samples. The device is used to determine the sound absorption coefficient, SAC (α) of circular samples with a diameter of 100 mm for the frequency range from 50-1600 Hz and 29mm for the determination of sound absorption coefficient, SAC (α) of circular samples for the frequency range of 500-6400Hz. In the impedance tube method, sound waves are confined within the tube. Thus, the size of the test sample needs only to be large enough just to cover the small circular cross-section area of the impedance tube. Thus the method avoids the need to fabricate large test sample with lateral dimensions several times the acoustic wavelength. The lower working frequency is due to the accuracy of the signal processing equipment. The upper working frequency has been chosen to avoid the occurrence of non-plane wave mode propagation. This method is based on the evaluation of the sound absorptive properties of materials at normal incidence sound waves. Standard test method for impedance and absorption of acoustic materials using a tube with two microphones and a digital frequency analysis system was used. In this method, the samples are fastened to one end of tube, and the loud speaker that can emit sound waves of well-defined frequencies is attached to the other end of the tube. The emitted waves travel through the tube and are reflected back from the sample. The reflected waves are received by the microphone. The received waves by the microphone are pictorially shown on the screen.

The calibration procedure uses a special calibration specimen and the correction is valid for all successive measurements. This procedure is performed once and after calibration the microphones remain in place. The signal amplitude has to be at least 10 dB higher than the background noise at all frequencies of interest, as measured at the chosen microphone locations. During a test, any frequency having a response value 60 dB lower than the maximum frequency response value has to be rejected. 20 measurements were repeated for each sample. The variability was restricted to 95% confidence interval. For comparison among fabrics mid frequency range is used i.e 250-2000 Hz. Typically, perforated materials only absorb the mid-frequency range unless special care is taken in designing the facing to be as acoustically transparent as possible.

Calculation of NRC (Noise reduction coefficient)

Usually when materials are used as acoustic barriers the index denoting the acoustic property of the barrier is known as sound absorption coefficient. Another index is known as noise reduction coefficient or NRC which is the arithmetic average of absorption coefficients at frequencies of 250, 500, 1000, 2000 and 4000 Hz. In this work NRC of the samples were also obtained. The "Noise Reduction Coefficient" (NRC) is a measure of how much sound is absorbed by a particular material, and is derived from the measured Sound Absorption Coefficients. The NRC was determined using the following formula:

$$NRC = \frac{\alpha_{250\text{Hz}} + \alpha_{500\text{Hz}} + \alpha_{1000\text{Hz}} + \alpha_{2000\text{Hz}}}{4} \quad (3.2)$$

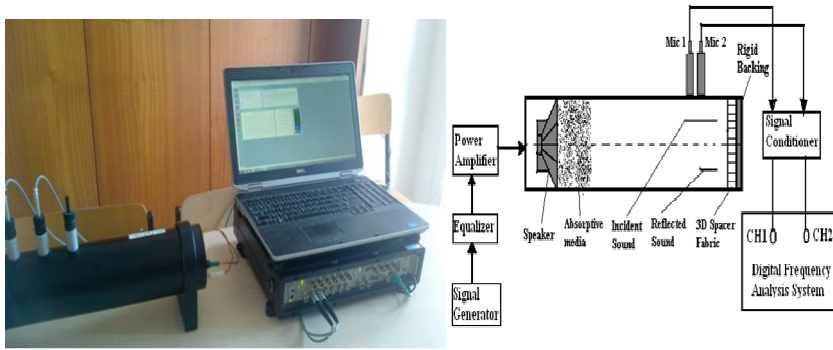


Figure 3.15: (a) Impedance tube method and (b) schematic diagram of an experimental set-up.

In this work acoustical characteristics of hybrid woven fabrics including sound absorption coefficient and factors affecting sound absorption coefficient via the impedance tube method are determined. The sound absorption coefficient of woven fabrics is significantly lower than that of nonwoven textiles. Despite this fact, woven fabrics are preferred in end-uses, where nonwoven textiles cannot be used due to both technical and economic reasons. The factors that chiefly determine a materials sound absorption property are its fibre type, fibre size, material thickness, density, porosity and air flow resistance. Among these factors, the air flow resistance is the major contributing parameter in various materials. Flow resistance has been used as an important parameter in theoretical equations by many researchers. It is therefore important to consider the flow resistance of an acoustic sample, which is calculated by Equation 2.13. Correlation between acoustic impedance and modulus was calculated by Equation 2.16.

Thermal stability

Thermal properties of materials also indicate the physical response of materials to the application of heat and resultant change in temperature in response to the applied heat. Physical impact of temperature on materials is reversible in case of short term application where as it is non reversible in long term application as it associates with the chemical changes. The long term effects at elevated temperature are aging/degradation resulting in affecting the mechanical, physical and chemical properties. Thermal analysis includes a group of analytical methods in

which the properties of a substance or a polymeric material are measured as a function of temperature. The thermal behavior of hybrid and non-hybrid woven fabrics were studied under thermogravimetric analysis (TGA). The thermogravimetric analysis was performed on Mettler Toledo in air from 30°C to 600°C at heating rate of 10°C/min. For each sample, decomposition temperatures and the maximum rates of decomposition were determined. Melting points were determined by Stuart SMP3. It is an easy and accurate visual way to determine melting points of different substances. Results were verified by DSC. The differential scanning calorimetry was performed on DSC 6 Perkin Elmer instrument from 30°C to 300°C at heating rate of 10°C/min.

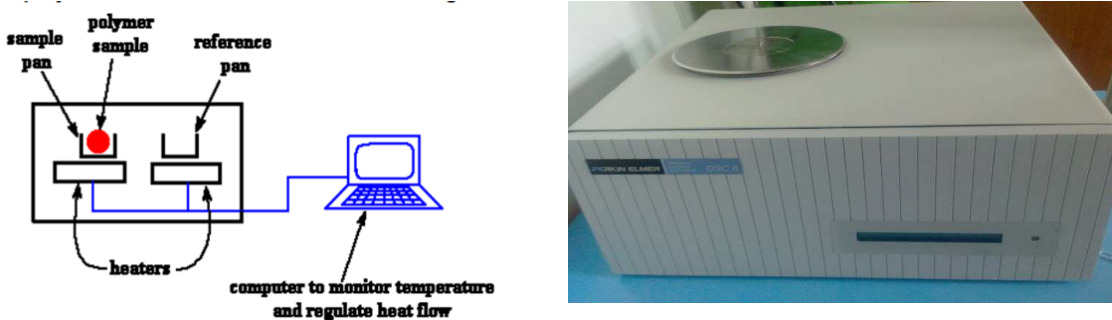


Figure 3.16: Schematic diagram Perkin Elmer Differential Scanning Calorimeter DSC6.

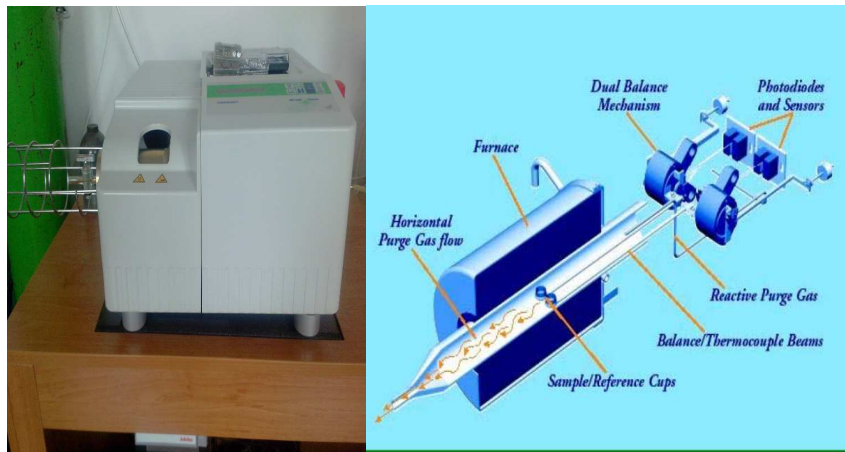


Figure 3.17: Mettler Toledo TGA/SDTA851.

3.3 Characterization of load bearing capacity and durability of yarns in cement composites

Preparation of cement matrix

The OPC pastes were prepared by mixing the cement with distilled water. The water to cement ratio (w/c) of 0.4 was maintained. The samples were thoroughly mixed using glass rod for ten minutes and then allowed to hydrate in air-tight plastic containers. Preparation of geopolymer(GPC) mixture is typically used with 5 parts by weight of GPC cement and 4 parts by weight of alkali (NaOH) as recommended by supplier.

Yarn pull out test

At present, no standard test setup to investigate the pull-out behavior of TRC is available; as such, relevant experimental work from literature was revealed to help establish an experimental setup. Direct pull-out tests are included in this research to characterize the complex pull-out behavior of a textile structure embedded in a concrete matrix with a particular focus on basalt, PP, PET and jute based TRC. More specifically, the pull-out of a single yarn from the textile woven fabrics was carried out which resulted in a representative smeared pull-out behavior of the yarn embedded woven structure

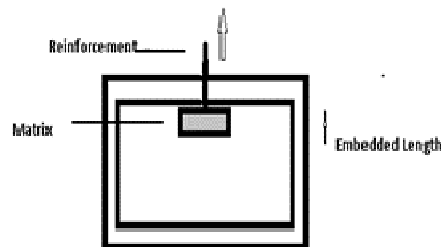
The pull-out test primarily gives information on the compatibility/interfacial behavior between the yarns selected for the reinforcement and the cement matrix. From this test, estimates can be derived for the failure behavior, and thus for the durability and load bearing capacity. The pull-out tests encompassed the evaluation of both pull-out and rupture of the textile material as failure modes.

So strand/yarn in cement test, is used to quantitatively analyze this test. The yarn specimens were embedded into cement slab of 40x40x10 mm. The yarn is precisely placed in the center of the specimen. The yarn lengths have to be set so as to ensure protruding ends, for mounting in a tensile tester. It is important to protect the protruding yarn ends from the exposure to avoid strength losses. The specimens were demolded after 48 h and then dried again for 48 h at room temperature. Five specimens were produced for each yarn in order to obtain a representative trend of the pull-out behavior.

The yarn was pulled out from the cement by *TIRA 2300 (LaborTech s.r.o., Opava, Czech Republic) universal testing machine* at the rate of 2.0 mm/min. The experimental setup developed to conduct the pull-out tests is illustrated in Fig. 3.18. In the standard pull-out test, load applied to the yarn end is recorded as a function of the displacement of other end with respect to a “stationary” point in the cement block, usually at the substrate or grips holding the matrix. The test was conducted according to force control such that the load was applied by a pneumatic jack on top of the rigid frame structure. The force-displacement curves and the peak pull-out forces were recorded.



(a) TIRA tester



(b) Experimental set up

Figure 3.18: Pull out test method

Accelerated aging in alkaline solution

The action of aqueous sodium hydroxide and calcium hydroxide solutions 10 g/L (w/V) on basalt, PET, PP and jute yarns were investigated under a variety of conditions of pH and time. For this purpose, loss in weight (W), breaking load, % elongation to break and scanning electron micrographs of the yarn surfaces were studied. Tensile tests were conducted on specimens before and after ageing treatment, given that the materials could be tested based on their level of degradation. Furthermore, the interpretation of the experimental results involved the documentation of visual observations before and after testing. To measure weight loss properties, the specimens were weighed by a digital balance to a precision of $\pm 0.1\%$. Then the dried specimens were fully immersed into alkali solutions for 1 week and 2 week at room temperature. The samples were then reweighed after drying. 2 m length of each yarn, were immersed in three separate tight plastic cylindrical containers in order to avoid any evaporative loss, containing NaOH (98% concentrated) and $\text{Ca}(\text{OH})_2$ (96% concentrated) with 10, 11 and 12 pH in separate containers at room temperature. The specimens have to be straight during all the test and the solution level is marked on the container, in order to monitor possible evaporation. Once removed from the alkaline solution, the test specimens were treated with acetic acid (100 mL) to neutralize the remaining hydroxide and rinsed in distilled water to remove any alkali sticking to the surface and visually examining prior to commencing tensile testing. These yarns were dried in oven for 30 min and finally air-dried for 24 hours before further use. NaOH is a strong alkali and used for checking accelerated ageing effect more rapidly.

Scanning Electron Microscope (SEM) for characterizing surface degradation

SEM was used for morphological analysis and for investigating the surface degradation of alkali treated samples. SEM images were prepared with different magnifications ranging from 2.5 KX to 50 KX. The microstructures of yarns were prepared on a Vegas-Tescan Scanning Electron Microscope (SEM) with accelerating voltage of 20 kV. The surfaces of the samples were coated with gold by means of a plasma sputtering apparatus prior to SEM investigation. SEM provides detailed high resolution images of the samples by a focused electron beam across the surface and detecting secondary or backscattered electron signal. It provides images with magnifications up to $\sim \times 50,000$ allowing sub-micron-scale features to be seen i.e. well beyond the range of optical microscopes. It is useful for characterization of particulates and defects in the material and examination of grain structure and segregation effects in the fabric structure.

Tensile measurement to evaluate loss of mechanical properties

Textile materials are exposed to an alkaline environment in the cement matrix, which makes them susceptible to damage. A comparison of the measured breaking strength to the breaking strength of undamaged yarns allows an assessment of the selected reinforcement. Tensile properties of all alkali treated and control samples were measured on a TIRA 2300 (LaborTech s.r.o., Opava, Czech Republic) universal testing machine according to standard ASTM E 2098-00.

3.4 Statistical analysis with ANOVA

All the measurements were made under standard atmospheric conditions. The means and standard deviations (SD) of data were calculated for all the tests. The upper and lower (\pm) 95% confidence interval of the mean is specified for the values in the figures. The tested data were statistically analyzed using data analysis software ORIGIN LAB (origin pro 8), MATLAB & Minitab statistical package. The one-sample t-confidence interval and test procedures are used to make inferences about population parameters i.e. population mean based on data from a random sample and is also used for hypothesis testing for population mean. Use one-sample t-procedures when you do not know the standard deviation of the population. One-sample t-procedures, your sample should also be distributed. The results were evaluated statistically according to two-way variance analysis (ANOVA), and the factors were the 'fibre type' and 'weave pattern'. The mean values were compared with each other according to the Student-Newman-Keuls (SNK) Test by using a statistical package program separately for every test. $P < 0.05$ was regarded as statistically significant. The Minitab statistical package was used to execute the statistical analysis. All test results were statistically assessed at significance level, p-value, $0.05 \leq p\text{-value} \leq 0.01$. If the p-value is smaller than or equals 0.05, the effect of weave structure and fiber type are considered to be significant.

Chapter 4 - Results & Discussion

4.1 Weavability study for basalt yarns

4.1.1 Production of hybrid and non-hybrid fabrics

Basalt is a relatively new material for the weaving industry. There is no established setting available to run such a yarn. In the case with some of the other materials like cotton, polyester or blends of both for instance runs extensively across the industry. The advantage of extensively used fibers are that, there is always a reference of settings available from where one can start the initial running and then fine tuning can be done, which was not the case with basalt. Basalt is a relatively stronger yarn as compared to others used in this work, and thus it was difficult to handle weft insertion. Once initial settings for basalt were optimized, it was successful in running compared to all the other yarns.


Weavability of basalt warp with basalt weft

The first sample produced was in the basalt non--hybrid type, where basalt was used in both warp and weft. Plain weave was the weave selected for the sample. The back rest setting did not affect basalt yarn with the running on machine, rather it helped in making clear warp shed line. The shed height and shed angle were adjusted so that it forms a clear shed and does not create any kind of problem in weft insertion. The sample running took some time before the final settings were made. It caused some wastage of yarn too but ultimately the setting was finalized, it was a smooth and clear running till the completion of one sample.

2/2 matt weave is a weave that requires less tightness of bottom shed line as compared to plain weave. Rest of all the settings was same except the change in back rest height. This was done in order to make the bottom shed line just a little less tight compared to plain weave. As plain weave was the first weave in the line, the tension and other settings were known and they were kept same for the matt weave.

The third combination of basalt warp and weft, was made with 1/3 twill weave. The initial problem with this weave was, most of the yarns were in the bottom shed at the time of weft insertion which was creating a problem with frequent end breakages. The tension was reduced as a first step but yarn shed was becoming slack with the decrease in tension to the level where breakage stopped. The aim for running of a yarn with successful results is to have minimum possible alterations with the change of weave, so that a standard result can be achieved. In this case lower back rest position helped in making the bottom shed line slightly slack which helped in finally controlling the warp breakages. The loom parameters are mentioned in Table 4.1 for different weave combinations.

Table 4.1: Machine settings for basalt/basalt

| | | 1/1 plain | 2/2 matt | 1/3 twill |
|-------------------------|---|---|-------------|--------------|
| | |  | | |
| Back rest position (mm) | | 7 | 6 | 5 |
| Machine Speed (RPM) | | 300 | 300 | 300 |
| Warp tension (kN) | | 4 | 3.5 | 3 |
| Frame height (mm) | 1 | 100 | 100 | 100 |
| | 2 | 102 | 101 | 101 |
| | 3 | 104 | 102 | 102 |
| | 4 | 106 | 103 | 103 |
| Shed angle (degrees) | | 30 | 28 | 28 |

Weavability of basalt warp with polypropylene weft

To start with the running of PP yarns, the machine settings were the same as basalt/basalt plain weave. The back rest was raised, in order to make the bottom shed tighter rather than increasing tension. This was successful with no warp or weft breakage at all. It was open to the maximum angle for clear weft insertion.

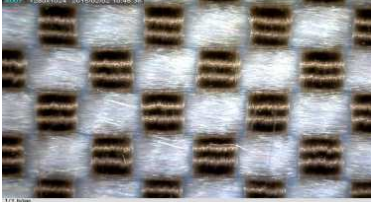
With 2/2 matt weave, same settings were kept as for plain weave. The only problem was the necessity of slightly loose bottom shed line as compared to plain weave. The back rest position was lowered by 1cm which resulted in lower tension on bottom shed line. This low tensioned bottom shed line helps in performing better for matt weave, because in this case two sets of yarns move at the same time in opposite directions.

1/3 twill has majority (75%) of threads in the bottom shed when the weft insertion takes place; it is therefore the requirement for the shed to be less tight in the bottom line. The sample was run with same settings as matt weave but it resulted in frequent warp breakages in the process, a lower tension resulted in the entanglement of warp yarns as was the case experienced with basalt/basalt combination. Thus the tension was maintained at the same level as the other two combinations of basalt/polypropylene and the position of back rest was lowered by 2cm as compared to matt weave. It resulted in a smooth running of the whole sample and no further issue was found during the running.

One problem that was associated with all three above mentioned weaves was the cutting of weft yarn before the new pick insertion. Polypropylene is a slippery yarn and normal cutter does not cut it properly. The cutter angle was changed in order to solve the problem. An early cutting was started so that longer time was available to cut the yarn also use of special cutters helped in smooth and proper cutting of yarn without much of the problems.

The machine settings for plain, matt and twill weaves with basalt warp and polypropylene weft are given in Table 4.2.

Table 4.2: Machine settings for basalt/PP.

|  | | 1/1 plain | 2/2 matt | 1/3 twill |
|---|---|--------------|-------------|--------------|
| Back rest position (mm) | | 7 | 6 | 5 |
| Machine Speed (RPM) | | 300 | 300 | 300 |
| Warp tension (kN) | | 4 | 3.5 | 3 |
| Frame height (mm) | 1 | 100 | 100 | 100 |
| | 2 | 102 | 101 | 101 |
| | 3 | 104 | 102 | 102 |
| | 4 | 106 | 103 | 103 |
| Shed angle (degrees) | | 30 | 28 | 28 |

Weavability of basalt warp with polyester weft

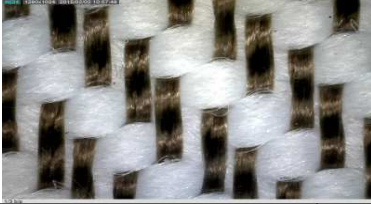
The difference in running of polyester to that of polypropylene is due to less compact structure of PET yarn as compared to that of PP and this would mean a low tensioned shed line. To start with the running, the warp tension was reduced by moving the back rest down, in order to have minimum contact surface of yarn. The shed angle was increased to give more space for insertion of a bulkier PET yarn. This was successful with no filling breakages. The problem associated was cutting of this yarn which was very difficult to handle even with the special cutter. Therefore, two cutters were used at the same time to cut the yarn. No weft breakage took place with this.

With 2/2 matt weave, similar settings were kept as for plain weave, the only problem that occurred was the cutting of polyester yarn. The shed was kept open enough and tension was less so there was less chance of pick to entangle with the warp shed. The same cutter combination that was used with plain weave was a successful one.

1/3 twill has majority of threads in the bottom shed when the weft insertion takes place; it is therefore the requirement for the shed to be low tensioned in the bottom shed. The machine settings for the plain weave were such that shed was wide open to have space for the polyester weft insertion with ease, no difference in setting was done in this case, which resulted in a smooth running of the whole sample and no further issue was caused during the running.

The machine settings for plain, matt and twill weaves with basalt warp and polyester weft are given in Table 4.3.

Table 4.3: Machine settings for basalt/polyester.

|  | | 1/1 plain | 2/2 matt | 1/3 twill |
|---|-----|-------------------------|-------------|--------------|
| | | Back rest position (mm) | 6 | 6 |
| Machine Speed (RPM) | 275 | 275 | 275 | |
| Warp tension (kN) | 3.5 | 3.5 | 3.5 | |
| Frame height (mm) | 1 | 98 | 98 | 98 |
| | 2 | 100 | 100 | 100 |
| | 3 | 102 | 102 | 102 |
| | 4 | 104 | 104 | 104 |
| Shed angle (degrees) | 30 | 30 | 30 | |

Weavability of basalt warp with jute weft

This was the most challenging task for weft insertion. For plain weave; the original settings for basalt warp did not work with jute weft yarn. There were so many protruding fibers with jute that forced to change the settings for clear shed. With increased tension to the shed, jute fibers were flying in the shed. Therefore minimum possible tension was applied to the warp sheet, and then the back rest was raised and adjusted in order to make a tight and straight shed as much as possible. Weft yarn from jute was still creating problems to be inserted into the sheds and was probably the toughest due to hairiness in yarn. The settings for 2/2 matt and 1/3 twill did not change much. Jute is easier to cut, there was no issue with the cutter, but the machine settings were the ones which were done with most dense qualities in industry where it was necessary to avoid the entanglement of warp sheet as well as entanglement of weft yarn with the warp sheet. The trick for weaving jute is, to make a small shed which is open enough in order to avoid contact with weft yarn. This could be achieved due to superior property of basalt warp in contrast to running jute warp with jute weft.

Weavability of polypropylene warp with basalt weft

Plain weave was selected for the first sample with same settings as basalt warp. The PP warp was able to sustain the tension quite well due to its strength and even a moderate tension helped in formation of clear warp shed line. The consideration was that, no untwisting of yarn takes place during weft insertion. The settings for 2/2 matt and 1/3 twill weaves were also similar as basalt warp. The settings are mentioned in Table 4.5.

Table 4.4: Machine settings for basalt/jute.



|  | | 1/1 plain | 2/2 matt | 1/3 twill |
|---|---|--------------|-------------|--------------|
| Back rest position (mm) | | 6 | 6 | 6 |
| Machine Speed (RPM) | | 275 | 275 | 275 |
| Warp tension (kN) | | 2.5 | 2.5 | 2.5 |
| Frame height (mm) | 1 | 104 | 104 | 104 |
| | 2 | 101 | 101 | 101 |
| | 3 | 103 | 103 | 103 |
| | 4 | 100 | 100 | 100 |
| Shed angle (degrees) | | 32 | 32 | 32 |

Table 4.5: Machine settings for polypropylene/basalt.


|  | | 1/1 plain | 2/2 matt | 1/3 twill |
|---|---|--------------|-------------|--------------|
| Back rest position (mm) | | 7 | 6 | 5 |
| Machine Speed (RPM) | | 300 | 300 | 300 |
| Warp tension (kN) | | 4 | 3.5 | 3 |
| Frame height (mm) | 1 | 100 | 100 | 100 |
| | 2 | 102 | 101 | 101 |
| | 3 | 104 | 102 | 102 |
| | 4 | 106 | 103 | 103 |
| Shed angle (degrees) | | 30 | 28 | 28 |

Weavability of polyester warp with basalt weft

As polyester was a bulkier yarn, a higher shed angle was necessary. The angle of shed formation was increased for a smooth weft insertion reducing chance of contact of weft yarn with the warp line. Normal combination of cutters for this sample was suitable. For 2/2 matt weave the shed was a little tighter for running of this bulkier yarn effectively. The sample was completed

without much of the problem once the minor adjustments were done. For 1/3 twill similar tension level was maintained. The settings are given in Table 4.6.

Table 4.6: Machine settings for polyester/basalt.

|  | | 1/1 plain | 2/2 matt | 1/3 twill |
|---|---|-------------------------|-------------|--------------|
| | | Back rest position (mm) | 6 | 5 |
| Machine Speed (RPM) | | 250 | 250 | 250 |
| Warp tension (kN) | | 3 | 3 | 3 |
| Frame height (mm) | 1 | 100 | 100 | 100 |
| | 2 | 105 | 105 | 105 |
| | 3 | 98 | 98 | 98 |
| | 4 | 103 | 103 | 103 |
| Shed angle (degrees) | | 30 | 30 | 30 |

Weaving of non-basalt fabrics

Propylene/polypropylene

Polypropylene is a synthetic filament yarn and it is sufficiently strong. It was an interesting proposition to use polypropylene as it needs some effort to start with. Once it is done with all the settings, it gives almost no warp breakages over a longer period of time. The important considerations were:

- This raw material is used on commercial scale in the industry, it is not required to be sized due to its strength but vegetable oil is applied to the yarn which helps in enabling the protruding fibers to settle down in case it is needed. During the production of this sample, it was desired to start it as early as beam is ready because of its tendency to stick with each other due to static charges.
- It is a strong yarn so at some points it was difficult to handle when it comes to weft insertion.
- During the start of a sample, there was a problem with shed settings which was observed in general.

Once initial settings of polypropylene were made, it was successful in running without creating much of the problems. The settings are given in Table 4.5.

Polyester/polyester

Polyester is also a synthetic filament yarn. This raw material is used on commercial level in the industry; it is not required to be sized due to its strength. There is a problem of static charges

with polyester, when a sample was stored overnight; leading to huge pill formation due to protruding fibers attracting each other. The settings were similar as PP yarn weaving. Details of settings are given in Table 4.7.

Table 4.7: Machine settings for PP/PP.



|  | | 1/1 plain | 2/2 matt | 1/3 twill |
|---|---|--------------|-------------|--------------|
| Back rest position (mm) | | 6 | 5 | 5 |
| Machine Speed (RPM) | | 300 | 300 | 300 |
| Warp tension (kN) | | 4 | 3.5 | 3 |
| Frame height (mm) | 1 | 100 | 100 | 100 |
| | 2 | 102 | 101 | 101 |
| | 3 | 104 | 102 | 102 |
| | 4 | 106 | 103 | 103 |
| Shed angle (degrees) | | 30 | 28 | 28 |

Table 4.8: Machine settings for PET/PET.

|  | | 1/1 plain | 2/2 matt | 1/3 twill |
|---|---|--------------|-------------|--------------|
| Back rest position (mm) | | 5 | 5 | 5 |
| Machine Speed (RPM) | | 250 | 250 | 250 |
| Warp tension (kN) | | 3 | 3 | 3 |
| Frame height (mm) | 1 | 100 | 100 | 100 |
| | 2 | 100 | 100 | 100 |
| | 3 | 95 | 95 | 95 |
| | 4 | 95 | 95 | 95 |
| Shed angle (degrees) | | 30 | 30 | 30 |

Jute/Jute


Jute is the most difficult yarn to weave among all the fibers under investigation. The options that can be tried before running of jute in warp can be either application of size liquor or wax. Jute yarn strand has a real abrasive nature, most of the fibers are protruding from the yarn surface and

they are very hard to control. The features of jute which cause it to be most difficult to handle are, stiffness of yarn, abrasive nature of yarn, tendency of strand of fibers to open when put under tension and minimum residual elongation when used for weaving which makes it most difficult when the tension is applied on yarn.

- It was not possible to apply size liquor to the cone of jute as the liquor is normally applied to yarn in the form of warp sheet.
- The second option for jute running in warp was application of wax, which stays on the strand of yarn on slow speeds but with higher speed the wax just drops off from the strand of yarn.
- Another way for the running of jute was to maintain higher humidity level; however, yarns started to stick together. Another problem associated with the moisture is, jute absorbs moisture so rapidly that it starts losing its strength.
- Jute yarns were run on a moderate speed. The problems associated with change of tension and nature of shed were sticking of yarns together in the shed line, which was causing pill formation and cuts in the surface of the fabric which were never desired.

For the matt weave, a special drawing in of sample was done and machine started working smoothly. For 1/3 twill weave, skip draft was used with a lowered position of back rest. By moving dropper box to the front, an open and tight shed was formed. Details of settings are given in Table 4.9.

Table 4.9: Machine settings for jute/jute.

|  | | 1/1 plain | 2/2 matt | 1/3 twill |
|---|---|-------------------------|-------------|--------------|
| | | Back rest position (mm) | 5 | 5 |
| Machine Speed (RPM) | | 150 | 150 | 150 |
| Warp tension (kN) | | 2 | 2 | 2 |
| Frame height (mm) | 1 | 95 | 92 | 94 |
| | 2 | 95 | 96 | 94 |
| | 3 | 90 | 90 | 88 |
| | 4 | 90 | 88 | 88 |
| Shed angle (degrees) | | 30 | 30 | 30 |

The weavability efficiency of all the samples is summarized in Table 4.10.

Table 4.10: Weavability efficiency of all hybrid and non-hybrid combinations

| Sample No. | Weave | Machine speed (rpm) | Warp breakage (/hour) | Weft breakage (/hour) | Running time (hours) | Efficiency (%) |
|------------|---------------------|---------------------|-----------------------|-----------------------|----------------------|----------------|
| 1. | B/B1/1 plain | 300 | 17 | 18 | 3 | 68 |
| 2. | B/B 2/2 matt | 300 | 15 | 16 | 3 | 70 |
| 3. | B/B1/3 twill | 300 | 14 | 15 | 3 | 73 |
| 4. | B/PP1/1 plain | 300 | 17 | 19 | 3 | 66 |
| 5. | B/PP 2/2 matt | 300 | 15 | 17 | 3 | 69.5 |
| 6. | B/PP 1/3 twill | 300 | 15 | 16 | 3 | 70 |
| 7. | B/PET 1/1 plain | 275 | 16 | 20 | 3 | 64 |
| 8. | B/PET 2/2 matt | 275 | 15 | 17 | 3 | 69 |
| 9. | B/PET 1/3 twill | 275 | 15 | 17 | 3 | 69 |
| 10. | B/Jute 1/1 plain | 275 | 17 | 25 | 3 | 56 |
| 11. | B/Jute 2/2 matt | 275 | 16 | 23 | 3 | 58 |
| 12. | B/Jute 1/3 twill | 275 | 16 | 22 | 3 | 61 |
| 13. | PP/PP 1/1 plain | 300 | 18 | 20 | 3 | 62 |
| 14. | PP/PP 2/2 matt | 300 | 16 | 18 | 3 | 69 |
| 15. | PP/PP 1/3 twill | 300 | 15 | 16 | 3 | 71 |
| 16. | PP/B 1/1 plain | 300 | 18 | 19 | 3 | 65 |
| 17. | PP/B 2/2 matt | 300 | 16 | 17 | 3 | 69 |
| 18. | PP/B 1/3 twill | 300 | 15 | 15 | 3 | 71 |
| 19. | PET/PET 1/1 plain | 250 | 3 | 18 | 20 | 60 |
| 20. | PET/PET 2/2 matt | 250 | 3 | 17 | 17 | 67 |
| 21. | PET/PET 1/3 twill | 250 | 3 | 16 | 17 | 67 |
| 22. | PET/B 1/1 plain | 250 | 3 | 18 | 19 | 65 |
| 23. | PET/B 2/2 matt | 250 | 3 | 16 | 17 | 69 |
| 24. | PET/B 1/3 twill | 250 | 3 | 15 | 15 | 71 |
| 25. | Jute/Jute 1/1 plain | 150 | 3 | 26 | 32 | 38 |
| 26. | Jute/Jute 2/2 matt | 150 | 3 | 24 | 30 | 40 |
| 27. | Jute/Jute 1/3 twill | 150 | 3 | 25 | 30 | 40 |

The results of weavability efficiency was analyzed with the help of MINITAB® statistical software package (MINITAB, State College, PA; <http://www.minitab.com/en-US/default.aspx>). The output of analysis of variance (ANOVA) is given in Table 4.11. The ANOVA results show that there is significant difference (p value of less than 0.05 at α level = 0.05) in weave and yarn material.

Table 4.11: Analysis of variance output for Efficiency

| Source | DF | Adj SS | Adj MS | F-value | P-Value |
|------------|----|---------|---------|---------|---------|
| Regression | 9 | 2412.72 | 268.080 | 128.58 | 0.00 |
| Float | 1 | 133.39 | 133.389 | 63.98 | 0.000 |
| Materials | 8 | 2279.33 | 284.917 | 136.65 | 0.000 |
| Error | 17 | 35.44 | 2.085 | | |
| Total | 26 | 2448.17 | | | |

S 1.44394 R-sq 98.55% R-sq(adj) 97.79% R-sq(pred) 96.36%

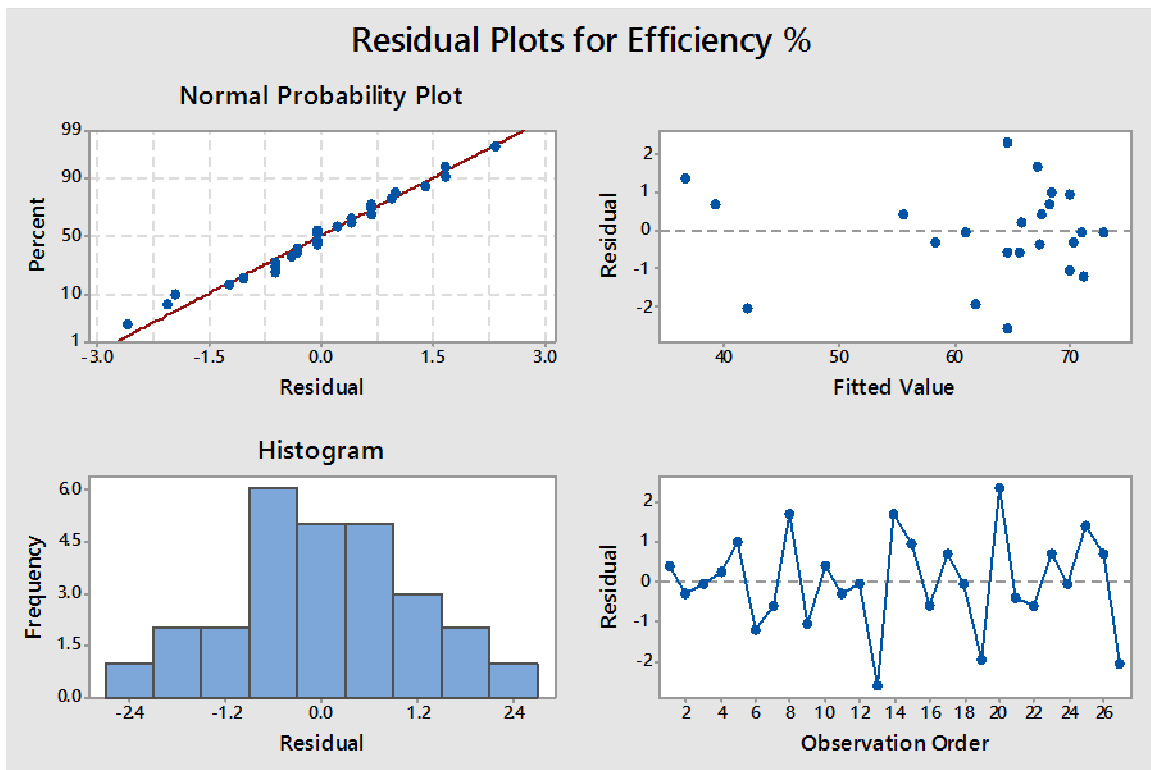


Figure 4.1: Residual Plots for Efficiency %

For the Efficiency data, the histogram does not follow a normal curve. Evaluate the normal probability plot to assess whether the residuals are normal. For the Efficiency data, the residuals appear to follow a straight line. No evidence of nonnormality, skewness, outliers, or unidentified variables exists. For the Efficiency data, the residuals appear to be randomly scattered around zero. No evidence of nonconstant variance, missing terms, outliers, or influential point's exists.

For the Efficiency data, the residuals appear to be randomly scattered about zero. No evidence exists that the error terms are correlated with one another.

4.2 Characterization of fiber and cement raw materials

Energy-Dispersive X-Ray Analysis of Basalt

Table 4.12 shows the summary of elements detected in energy-dispersive X-ray (EDAX) analysis. Spectral analysis detected number of elements in basalt. Presence of silica (Si) (24.58 wt%) and oxygen (O) (32.98 wt%) was found to be dominant as compared to other elements.

Table 4.12: Elemental composition of basalt.

| Element | Wt% |
|---------|--------|
| C | 12.37 |
| O | 32.98 |
| Na | 1.64 |
| Mg | 2.16 |
| Al | 8.69 |
| Si | 24.58 |
| K | 1.34 |
| Ca | 6.03 |
| Ti | 0.81 |
| Fe | 9.40 |
| Total: | 100.00 |

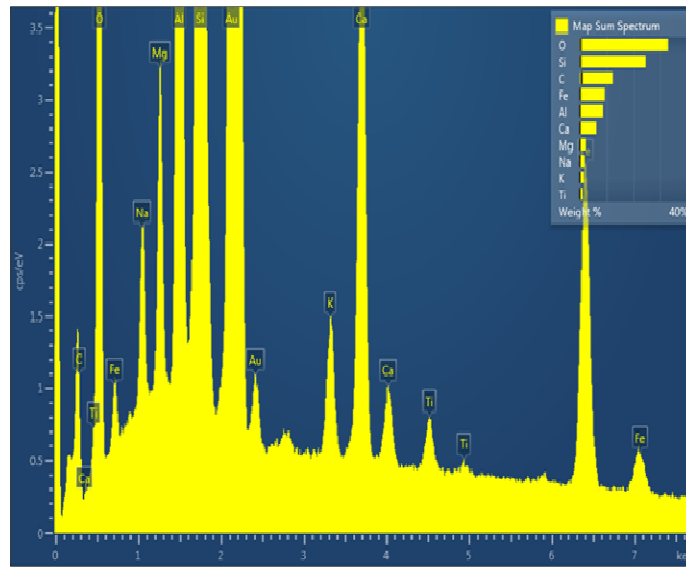


Figure 4.2: Energy-Dispersive X-Ray Analysis of Basalt

FTIR of OPC & GPC

Cement contains several chemical components with functional groups, such as Si-O, SO₄, H₂O, OH, Al-O and CO₃, which are infrared active.

The FTIR spectrum of the anhydrous OPC Fig. 4.3(a) shows peaks at 1616 cm⁻¹ which correspond to stretching and bending modes of water absorbed. The carbonates (CaCO₃) peak at 1421 cm⁻¹ and 878 cm⁻¹ are observed due to the reactions of atmospheric CO₂ with calcium hydroxide. The triplet bands appearing at wave number 1151-1092 cm⁻¹ are due to ν₃ modes of -SO₄⁻². The vibration modes are often denoted by ν₁ (systematic stretch), ν₂(bending), ν₃(asymmetric stretch). The strong band at 917cm⁻¹ is due to Si-O asymmetric stretching vibration of C₃S and/or C₂S (Tricalcium silicate (3CaO.SiO₂)/Dicalcium silicate 2CaO.SiO₂). The band assignments are in good agreement with those reported in the previous studies.

Figure 4.2(b) shows the FTIR-spectra of GPC. The stretching vibration of O-C-O was still detected in each of the GPC samples at 1424cm⁻¹ which was attributed to the carbonation

reaction. The carbonation process occurred because an excessive amount of Na was available from the alkaline activator solution where it reacted with CO₂ from the atmosphere. These bands are connected with the presence of CaCO₃ and Na₂CO₃. The band attributed to asymmetric stretching vibration of Si-O-Si and Al-O-Si around area 1011–1027 cm⁻¹ indicated the formation of aluminosilicate gel. Besides that, symmetric stretching vibrations Si-O-Si were located at 778–798 cm⁻¹. At 583–721 cm⁻¹, symmetric stretching vibrations of Si-O-Si and Al-O-Si were identified. In the meantime, the bending vibrations of Si-O-Si and O-Si-O were found at area 467–479 cm⁻¹.

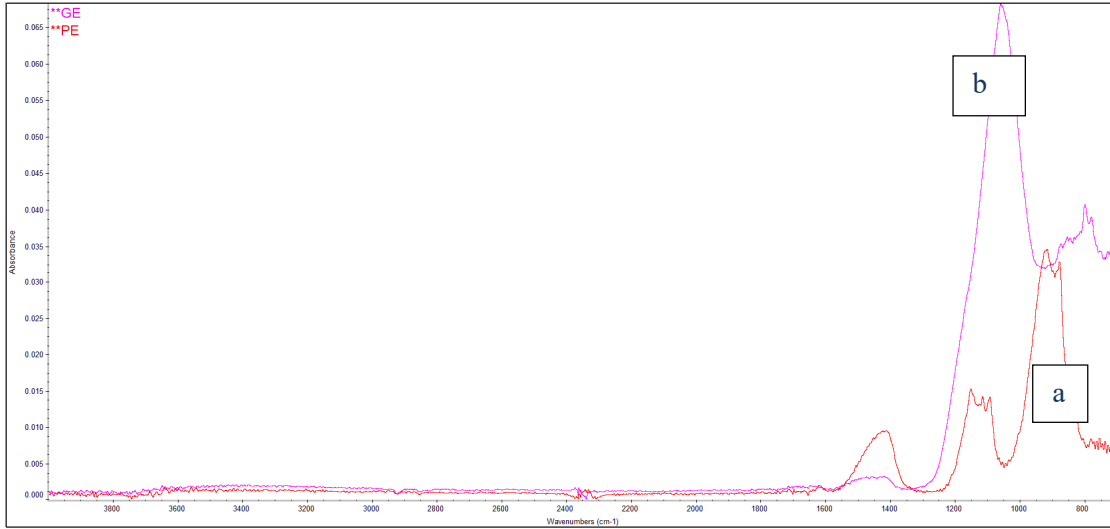


Figure 4.3: FTIR spectra of used cement materials (a) OPC, (b) GPC.

Inductively coupled plasma (ICP-OES) analysis of cement

The conventional chemical analysis of cements generally involves tedious procedures for sample preparation. In this study, the concentrations of elements in cement samples were determined by ICP-OES method. This method is designed to determine the composition of a wide variety of materials, with excellent sensitivity (Measurement uncertainty of less than 1% relative). The results are shown in Table 4.13, and are in good agreement with certified values, except for Si. Probably this result is related to their more pronounced refractory behavior. It is known that Si is used in cement mainly as the tri- and di-calcium silicate phase and requires additional power to obtain proper atomization and excitation.

Table 4.13: Metal contents (concentration) of used cements.

| Components | GPC | OPC |
|------------|-------|-------|
| | mg/kg | mg/kg |
| Be | 3.41 | 1.11 |
| Cu | 20.1 | 172 |
| Cr | 117 | 75.4 |

| | | |
|----|--------|--------|
| Ni | 52.9 | 45.4 |
| Pb | 32.7 | 73.2 |
| Fe | 3595 | 16777 |
| Mg | 19957 | 10178 |
| Ca | 91329 | 415569 |
| Na | 3432 | 2042 |
| Mn | 1744 | 525 |
| Al | 79410 | 23497 |
| B | 270681 | 170867 |
| Ti | 3514 | 1586 |
| V | 90.1 | 39.5 |
| Zn | 40.8 | 274 |
| Sr | 199 | 773 |
| Ba | 345 | 341 |
| K | 5567 | 7882 |

4.3 Accelerated aging in alkaline solution

The degradation of fiber due to the alkaline pore solution in the cement matrix seriously decreases the durability and may cause premature failure of the concrete composite. Calcium hydroxide is the primary cause of alkaline environment in cement. In this case, the high concentration of alkali ions is the main cause of fiber damage. Particularly, weight loss and reduction in mechanical properties could appear. In the technical literature different studies are present, but the reported results appear somewhat contrasting. After a careful scientific research, accelerated aging tests were made to evaluate the weight loss and the loss of mechanical properties of basalt, PP, PET and Jute fibers, in order to quantify their performance limits. 5 samples for each category were tested and their averages is reported.

Visual observations

The external appearance of the yarns specimens was examined pre- and post-alkali treatment, for comparison of color, surface degradation and change in shape. In Basalt yarn, no significant visible change of color or surface texture were observed after 7 days of immersion in pH=10, pH=11 and pH=12 of two types of alkali namely NaOH and CaOH₂. The Jute samples degradation was marked by color change. These samples lost a great deal of stiffness to the point that they broke prior to removal from the solution. For those exposed to pH 12, the observed degradation was similar to the pH 11 samples, yet these could be further tested in tension. The PP and PET specimens also lost a significant amount of physical stiffness. Effect of sodium hydroxide is stronger in all samples as compared to calcium hydroxide.

Weight loss %

The specimen's weight was measured both before and after the aging in order to evaluate weight loss. The percentage weight loss was calculated using the following formula:

$$WL\% = \left(\frac{W_1 - W_2}{W_1} \right) 100 \quad (4.1)$$

Where W_1 is the weight of the original sample and W_2 is the weight of the alkali immersed sample. The calculated weight loss are given in Table 4.14.

Table 4.14: % Weight loss.

| Reinforcement Type | Weight loss [%] (1 week) | | | | | | Weight loss [%] (2 week) | | | | | |
|--------------------|--------------------------|-------|-------|---------------------|-------|-------|--------------------------|-------|-------|----------------------|-------|-------|
| | NaOH | | | Ca(OH) ₂ | | | NaOH | | | Ca (OH) ₂ | | |
| | pH 10 | pH 11 | pH 12 | pH 10 | pH 11 | pH 12 | pH 10 | pH 11 | pH 12 | pH 10 | pH 11 | pH 12 |
| B | 0.4 | 0.8 | 1.0 | 0.3 | 0.5 | 0.7 | 1.0 | 1.1 | 1.5 | 0.8 | 1.0 | 1.2 |
| PP | 1.4 | 1.6 | 1.7 | 0.9 | 1.0 | 1.1 | 1.8 | 2.0 | 2.4 | 1.5 | 1.8 | 2.0 |
| PET | 2.8 | 3.2 | 3.5 | 2.0 | 2.5 | 3.0 | 3.5 | 4.0 | 5.1 | 3.0 | 3.5 | 4.2 |
| J | 4.7 | 6.2 | 7.2 | 4.1 | 5.0 | 5.2 | 7.0 | 9.5 | 14 | 5.5 | 7.0 | 8.5 |

These results reflect the conditions for a range of pH and duration of alkali treatment in aqueous sodium hydroxide and calcium hydroxide solution. The weight loss increases with increasing treatment time, pH and use of stronger alkali (NaOH). The weight loss of basalt fiber is minimum as it is least affected by alkali followed by PP fiber.

Tensile test of alkali treated yarns

After the aging in alkali solution, tensile tests were made in order to evaluate the maximum load F_{max} and the ultimate tensile elongation % of all the yarns before and after the aging, comparing the values obtained from controlled sample. ASTM E 2098-00 standard test method was used for this test. Results are given in Table 4.15 & 4.16.

Table 4.15: Mean tensile strength after 1 week of alkali treatment.

| Reinforcement | Load (N) | | | | | | Elongation (%) | | | | | |
|---------------|----------|-------|-------|---------------------|-------|-------|----------------|------|------|----------------------|------|------|
| | NaOH | | | Ca(OH) ₂ | | | NaOH | | | Ca (OH) ₂ | | |
| | pH10 | pH11 | pH12 | pH10 | pH11 | pH12 | pH10 | pH11 | pH12 | pH10 | pH11 | pH12 |
| B | 82.94 | 78.22 | 75.00 | 85.5 | 82.36 | 80.23 | 1.27 | 1.23 | 0.64 | 1.28 | 1.2 | 1.2 |
| PP | 80.25 | 75.55 | 70.33 | 82.7 | 77.33 | 70.99 | 10.55 | 10 | 9.8 | 11 | 10.5 | 10 |
| PET | 50.91 | 47.88 | 42.75 | 52.8 | 48.97 | 43.88 | 10.92 | 9.3 | 8.1 | 10.9 | 9.8 | 8.8 |
| J | 36.44 | 32.22 | 27.23 | 38.2 | 35.21 | 30.97 | 1.28 | 1.2 | 1.15 | 1.19 | 1.1 | 1.0 |

Table 4.16: Mean tensile strength after 2 week of alkali treatment.

| Reinforcement | Load (N) | | | | | | Elongation (%) | | | | | |
|---------------|----------|-------|-------|---------------------|-------|-------|----------------|------|------|----------------------|------|------|
| | NaOH | | | Ca(OH) ₂ | | | NaOH | | | Ca (OH) ₂ | | |
| | pH 10 | pH 11 | pH12 | pH10 | pH11 | pH12 | pH10 | pH11 | pH12 | pH10 | pH11 | pH12 |
| B | 60.33 | 52.37 | 48 | 75.2 | 69.8 | 62.3 | 0.72 | 0.59 | 0.46 | 1.1 | 0.94 | 0.88 |
| PP | 65.23 | 60.0 | 58.36 | 72.5 | 68.3 | 62.3 | 9.8 | 9.4 | 8.8 | 10.5 | 10.2 | 10 |
| PET | 38.99 | 32.49 | 29.0 | 42.99 | 35.8 | 29.66 | 9.6 | 8.8 | 8.0 | 9.9 | 9.5 | 8.0 |
| J | 27.55 | 22.59 | 15.33 | 30.0 | 26.77 | 22.74 | 1.12 | 1.08 | 1.04 | 1.15 | 1.12 | 1.06 |

The graphical representation of strength loss is given in Fig. 4.4 & 4.5.

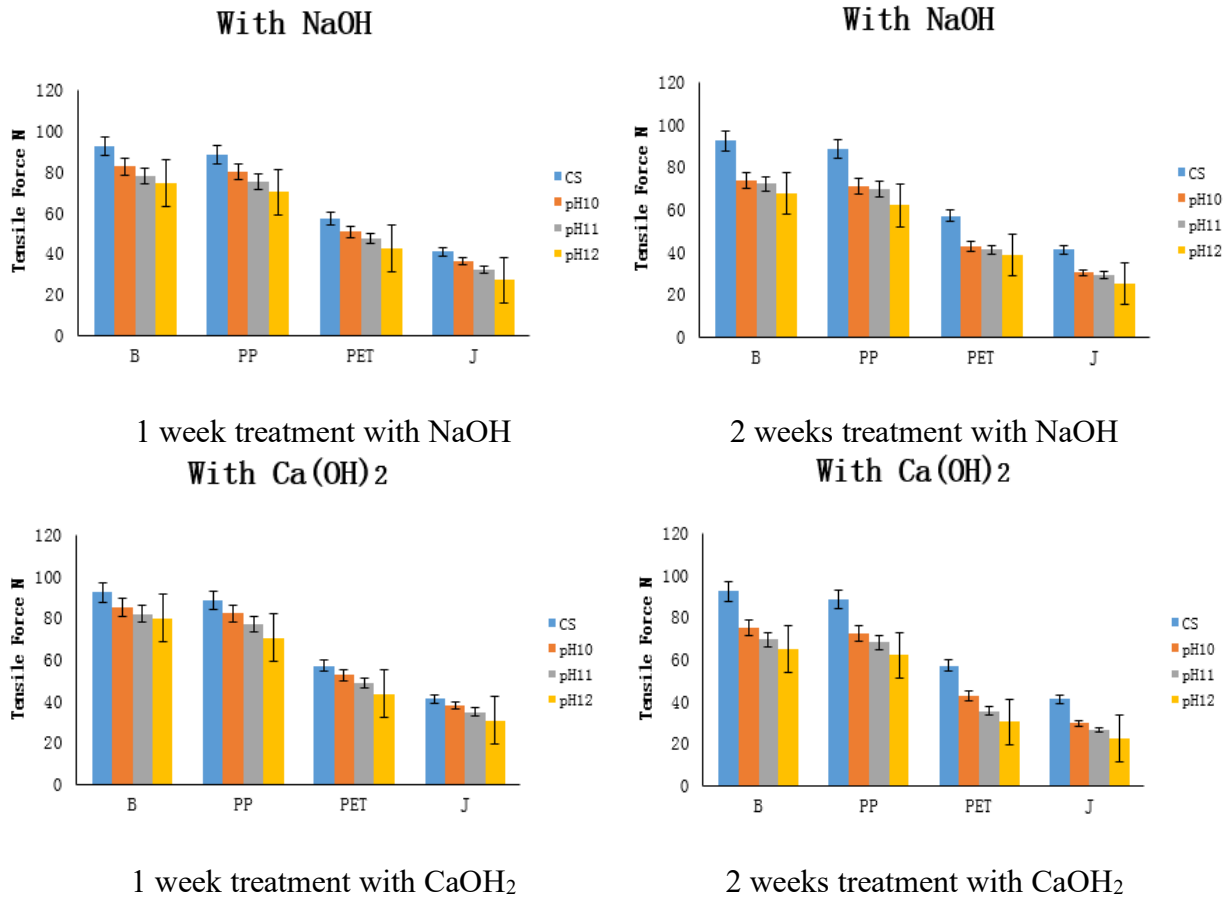
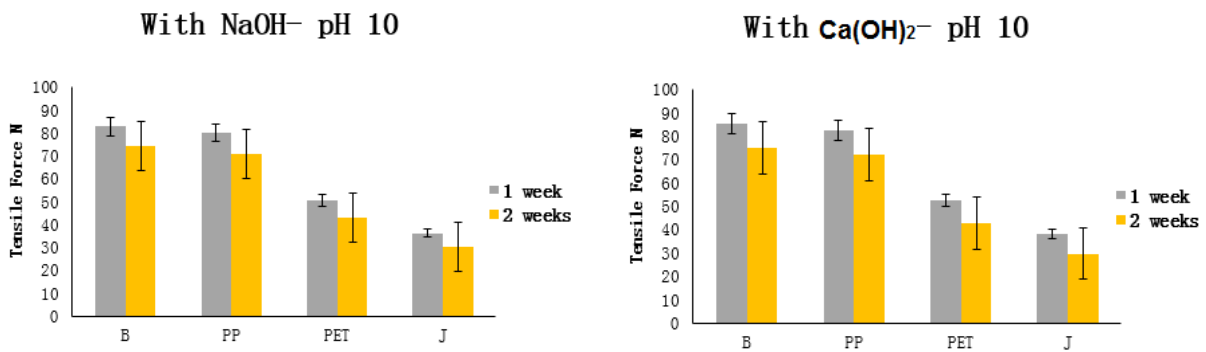


Figure 4.4: Effect of pH on degradation of yarn after alkali treatment.



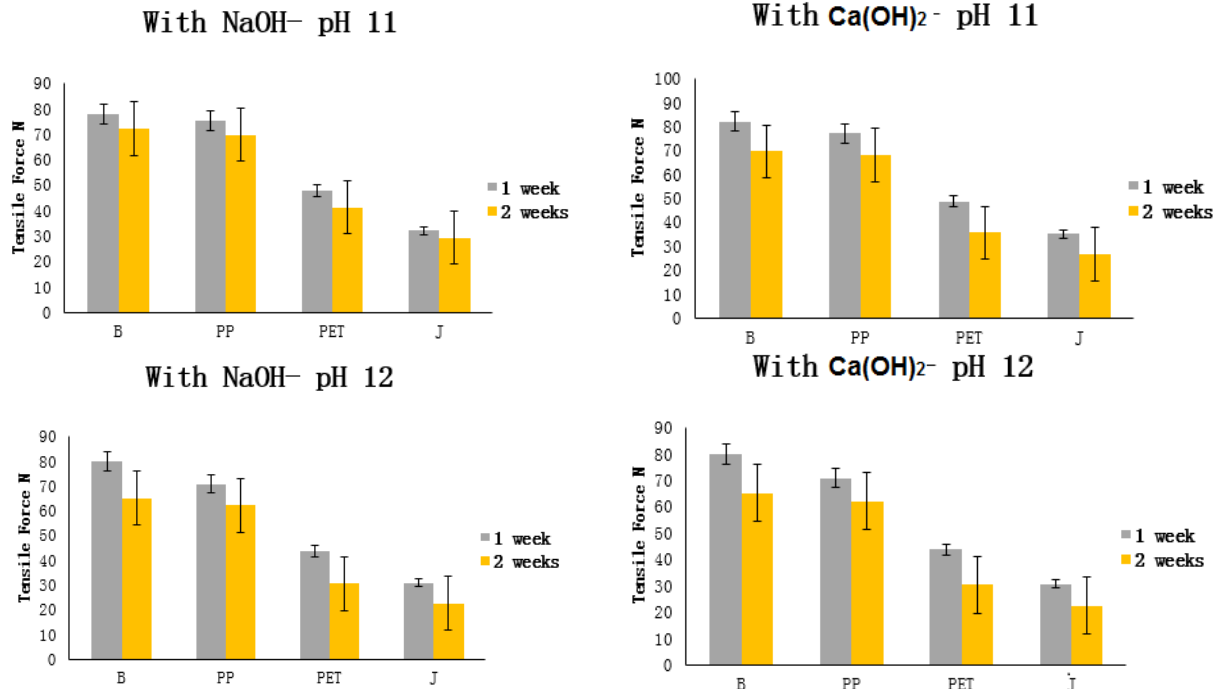


Figure 4.5: Effect of time on degradation of yarn after alkali treatment.

The tensile test results for the controlled samples are compared to the alkali treated samples in terms of applied maximum load versus elongation %. It can be noticed that ultimate tensile strain decreases in all the fiber types along with decrease in F_{max} . Reduction in mechanical properties in basalt yarn is minimum. The percentage reduction is maximum 30% after 14 days of accelerated ageing as compared to other yarns especially jute yarn where % reduction is more than 38 %.

Basalt yarn mechanical properties are decreased probably due to the crystallographic structure of basalt, which is made by olivine (single tetrahedron), pyroxenes (linear chain) and plagioclase (tetrahedral space structure). In fact, alkaline aggressive environment can break some bonds of the linear tetrahedral chain of pyroxenes, so that a strength reduction can be seen. Moreover, Fe can react with O_2 , causing the formation of reaction products (oxides), which can reduce strength not changing the weight. Besides, some cations of the solution (Na^+ , K^+ , Ca^{2+} , Mg^{2+} , Fe^{2+} , Fe^{3+} , Al^{3+}) could freely bind to fibers silicate structures. For example, Na^+ can substitute Ca^{2+} in the same position of the network because these two atoms have comparable dimensions. The cations exchange could affect the network of basalt, varying its mechanical and chemical properties, but not varying the weight.

Jute is a ligno-cellulosic fiber with hemicellulose (22-24%), α - cellulose (58-60%) and lignin (12-14%) as the main constituents with other minor constituents as well. Among the three main organic components, hemicellulose and lignin are amorphous with relatively low polymerization degree, so they have a higher hydrolysis rate and solubility in alkaline medium than cellulose, which is the main reason for the degradation. The alkaline pore water dissolves the lignin and hemicellulose of fiber, which are sensitive to $Ca(OH)_2$ and high alkalinity causes hydrolysis of cellulose molecules, which leads to degradation of molecular chains and then a reduction in

degree of polymerization and lower tensile strength. The crystallization of lime in the lumen of the fibers and middle lamellae leads to a decrease in the technical fiber flexibility and strength and relatively lower durability of jute fiber in cement matrix.

After treatment, semicrystalline and amorphous portions in the fibers, such as hemicellulose, lignin and other alkali-soluble fraction, were preferentially removed.

The alkali treatment produced a drop in both tensile strength and Young's modulus of the fibers. This was attributed to the damage induced in the cell walls and the excessive extraction of lignin and hemicellulose, which play a cementing role in the structure of the fibers. Alkali treatment leads to destruction of the total structure, first by removing the cementing material, and it splits the fiber into finer filaments. Any lingo cellulosic material is composed of multicellular fiber. Each unit cell of fiber consists of small cellulose microfibrils, which are surrounded and cemented together with lignin and hemicellulose. The treatment produced fibrillation, i.e. splitting of the microfibrils that compound the technical fiber. This process leads to diameter lowering and higher dispersion in strength values. SEM images showed that some of the fibers were split, had ramifications and presented a tape form rather than cylindrical.

Although PET can offer good mechanical properties and is suitable for some applications; however it is susceptible to hydrolysis under strong alkaline conditions, when hydroxyl anion attacks the electron deficient carbonyl carbon atom of the ester group (The polar C=O bond provides an active site for chemical reaction) and, in turn, results with a scission of the bond in the polymer chain. PET can also be susceptible to heightened degradation where there is concrete or cement present. The PET material loses its weight when the polymer chains break down and dissolve in the alkaline bath. The attack of highly ionized aqueous sodium hydroxide is limited essentially to the surface of the PET material as the nonpolar PET disfavors diffusion of ionic bodies inside the polymer phase. Thus the diameter of PET filaments decreases with the loss of polymer on the surface. However, the molecular weight and tenacity of the slimmed filaments remain essentially unchanged.

Polypropylene can be considered as inert to acid and alkali attack. Polypropylene fibers have a high resistance to acids and alkalis in all concentrations, and up to comparatively high temperatures. Although PP has not very good bond with the cement matrix, this fiber is considered as attractive for the reinforcement of cement matrices, because of their high resistance to the alkaline environment of cement matrix and of low cost.

SEM morphology analysis

The time-dependent degradation of fiber surface is additionally investigated using an electron-microscope.

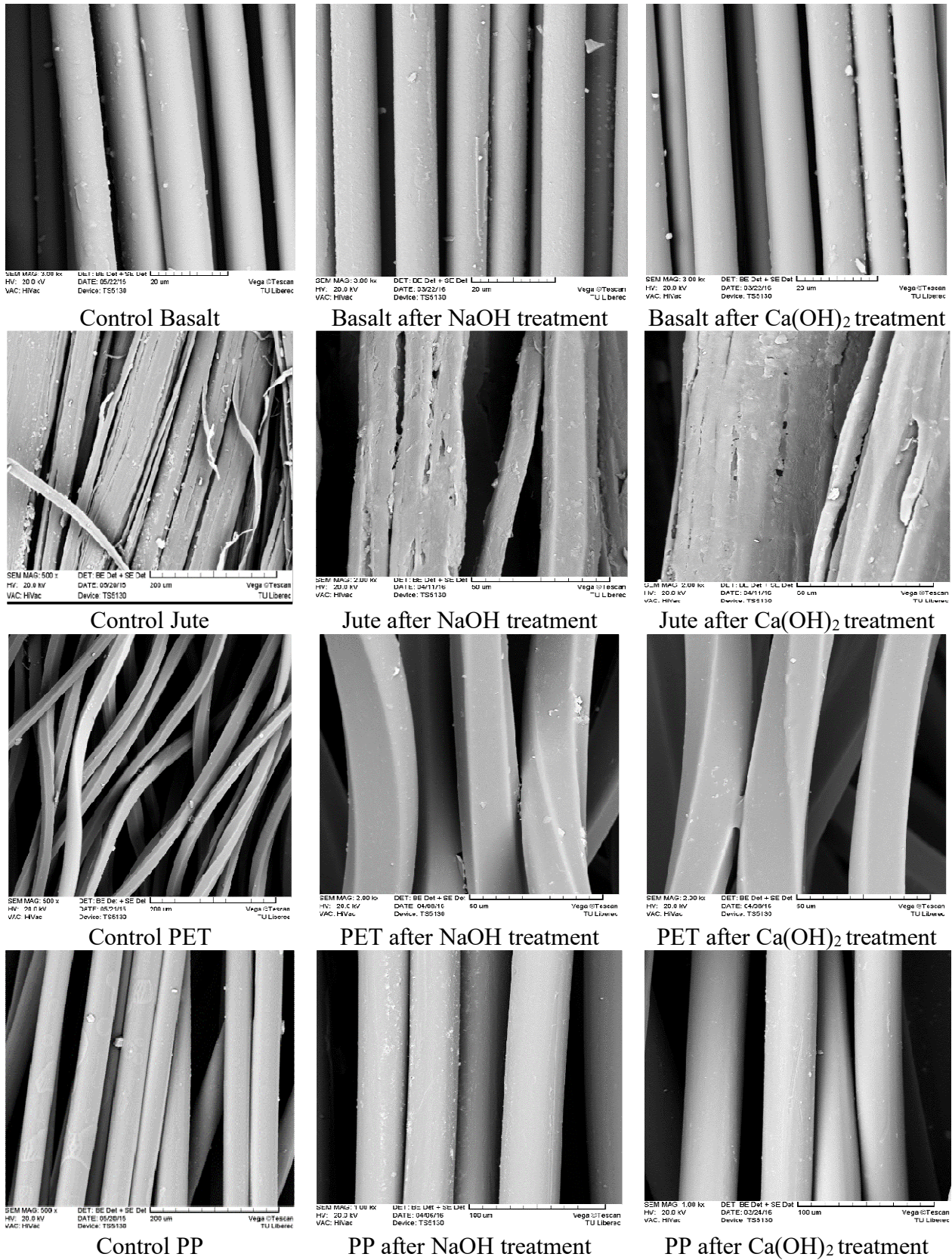


Figure 4.6: SEM images of fibers after alkali treatment.

Surface morphology of fiber samples was analyzed by using a scanning electron microscope. The microstructure of yarn surfaces indicated that the jute fiber encountered the most severe alkali attack and precipitation of hydration products in the cement matrix. Fibrillation and diameter reduction is evident in the jute fiber. Fig. 4.5 also shows the damage in the cell walls and a rougher fiber surface. Also, the collapse of fiber lumen can be seen. This is responsible for the decrease in capillary pressure and therefore decreases in permeability.

On the contrary, the controlled jute fiber (Fig. 4.5) shows open lumens. Besides, SEM images showed the presence of diffused micro-cracks on fiber surface and evidenced a variation in surface morphology before and after aging.

4.4 Yarn pull out test from cement matrix

The interaction between the concrete matrix and reinforcement is characterized by the bond behavior. It is very important that there is good adhesion between the reinforcing fibers and the concrete or cement matrix, otherwise debonding may take place. If bond strength at the interface between the fiber and the matrix is too high, the reinforcement ruptures after the first crack initiates. On the other hand, the reinforcement is easily pulled out if the bond strength is too low. Bond strength may dominate the mechanical properties of fiber-reinforced concrete. Pull out test is most general test for this purpose. This test is useful to get information about the load transfer behavior between matrix and reinforcement. The pull-out tests characterize both pull-out and rupture of the textile yarn as failure modes. The breaking point does not designate the definitive breaking point of the yarn in itself, but rather the location of crack initiation.

The force/displacement curves for all yarns are shown in Fig. 4.6. It consists of three parts corresponding to the three stages of a pull-out test. The three different bonding areas are clearly visible. In the case of pull-out failure, the pre-peak bond behavior is governed by adhesive bond (increasing area) which is followed by the destruction of the adhesive bond occurring due to debonding of the yarn from the matrix through interfacial crack propagation. Lastly, the remaining pull-out force i.e. ‘tail’ force is based on friction i.e. frictional interaction between the fiber and the matrix. From these curves, the average maximum force and the respective average crack-opening displacement, i.e. total slip, were calculated.

The traditional way to characterize the quality of interfacial bonding is calculating the apparent interfacial shear strength (apparent IFSS, τ_{app}), according to the definition.

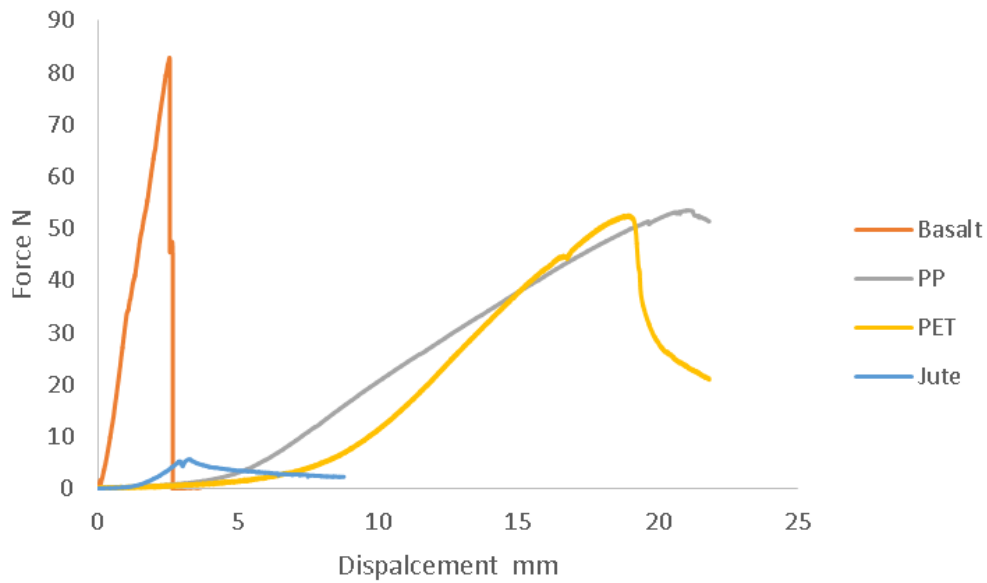
$$\tau_{app} = F_{max}/(\pi d l_e) n \quad (4.2)$$

where d is the fiber diameter, l_e is the embedded length and n is no. of filaments/fibers

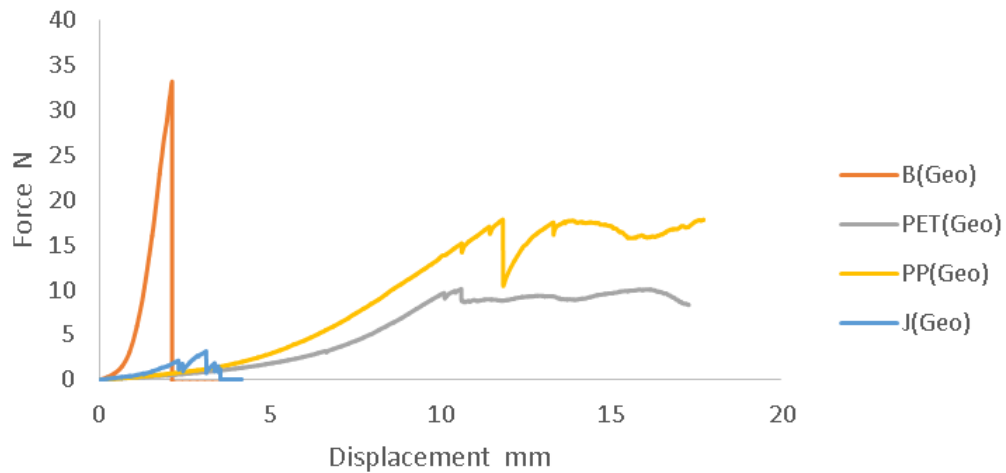
The τ_{app} values calculated from Eq. 4.2 usually suffice to distinguish between ‘‘good’’ and ‘‘poor’’ bond strength and to estimate the efficiency of matrix and fiber surface interfacial bonding.

Table 4.17: Apparent interfacial shear strength (τ_{app}) for different fibers in cement.

| Reinforcement type | app τ_{app} | |
|--------------------|------------------|-------|
| | OPC | GPC |
| B | 1.769 | 0.709 |
| PP | 0.872 | 0.222 |
| PET | 0.663 | 0.169 |
| JUTE | 0.091 | 0.051 |



(a)



(b)

Figure 4.7: Force vs displacement for yarns in Portland and Geopolymer cement.

In case of basalt, very small slippage (displacement) is observed (can be visible in pictures) as they have good adhesion with cement matrix. Maximum stress recorded as tensile stress of yarn is highest in case of basalt yarn. Similar situation is observed in case of jute yarn, but in this case Force recorded is much lower as jute yarn has overall lower strength value.

In case of PP and PET, adhesion is not good and it can be viewed by high slippage/displacement/deformation. Such large displacement prior to material failure are crucial with regard to structural safety as well as energy dissipation, in particular in the case of dynamic loading. However, the fact that high strength levels can be only reached at high deformations means that for the service state, where only small deformations are acceptable, and the design load-bearing capacity of TRC must be considerably lower than its tensile strength. Moreover, relatively wide cracks observed at high deformations are undesirable.

It can be seen that performance of highly twisted yarn e.g. PP is higher than less twisted PET yarn. This can be explained on the basic of mechanical anchoring which is the result of waviness. Also if density of crimped yarn increased effect is more prominent. The experimental findings are given in Table 4.18.

Table 4.18: Experimental findings of the pull out study.

| Reinforcement type | Max force (N) | | Crack opening displacement at max force (mm) | | Failure mechanism |
|--------------------|---------------|-------|--|------|-------------------|
| | OPC | GPC | OPC | GPC | |
| B | 82.90 | 33.24 | 2.56 | 1.46 | Telescopic |
| PP | 53.54 | 17.87 | 21.19 | 9.30 | Pull out |
| PET | 52.61 | 10.14 | 10.84 | 7.28 | Pull out |
| JUTE | 5.68 | 3.21 | 2.30 | 4.24 | Rupture |

Photographic investigation in Fig 4.7 shows that overall, the force is transmitted by adhesion and friction between the reinforcement and the concrete. The load transfer between the filaments enclosed in the yarn/roving will however occur either based on adhesion or friction depending on the quality of the bond. The bond quality differs across the depth of yarn/roving which causes a complex failure mechanism involving the partial rupture and pull-out of singular filaments. The failure mechanism denoted as *pull-out*, was often observed to be a telescopic failure (i.e. partial rupture and pull-out) a common failure phenomenon.

**Reinforcement
type**

Portland (OPC)

Cement type

Geopolymer (GPC)

Basalt



PP



PET



Jute



Figure 4.8: Photographic images of failure/rupture.

4.5 Testing of fabric samples

4.5.1 Physical properties

The details of fabric cover %, areal density, thickness have been presented in Table 4.19. All the basic fabric structural parameters e.g. the real warp and weft density, mass per square meter, porosity and fabric thickness, were measured according to standardized procedures. The fabric thickness was obtained using Thickness Meter (Mesdan Lab). For each sample, 20 measurements were done and the mean and standard deviation were calculated.

The volume porosity of the hybrid composition is calculated based on ratio of the component fibers. With regards to fabrics the inter-yarn, inter and intra-fiber spaces contribute to the total porosity in woven structures. Inter-yarn porosity (macro porosity) is more important but if fabrics are made of different fibers, inter-fiber space (micro porosity) also plays a major role.

Volume porosity can be calculated from fabric and fiber densities respectively, but the weaves influence the shape and dimension of pores. The weave determines the interlacement pattern which ultimately affects the nature of pores and fabric volume porosity. Backer classified the pore structure occurring in textile fabric depending on the weave, into four basic categories as shown in Fig. 4.8 assuming that the planes perpendicular to the fabric surfaces and bisecting any two adjacent warp and filling yarns are used to form a unit cell. For Type 1, the four yarns of a unit cell alternate from top to bottom surface of the cloth and vice versa. One warp and one filling alternate for Type 2. No alteration of yarns is visible for Type 3. For Type 4, either two warp yarns or two filling yarns alternate from top to bottom surface and vice versa.

At least two or three types of pores will be there in most of fabric constructions. The fabric having the plain weave construction consists entirely of Type 1 pore structure. Pore volume and shape of two fabrics woven with identical yarn diameter and yarn spacing will vary depending on the manner of interlacing of the threads. The pore walls are not flat and their cross-section changes with the fabric thickness with respect to the type of pores, type of yarns and their characteristics.

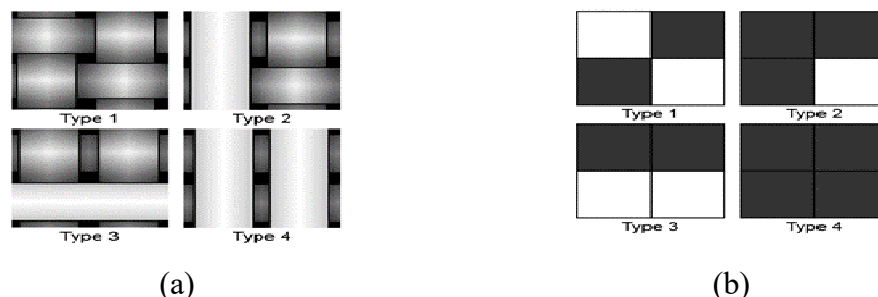


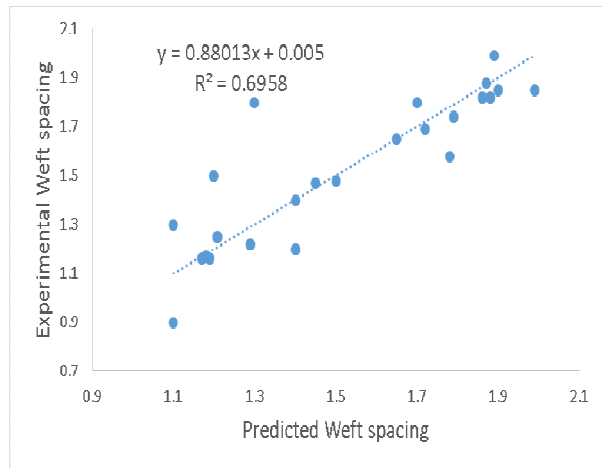
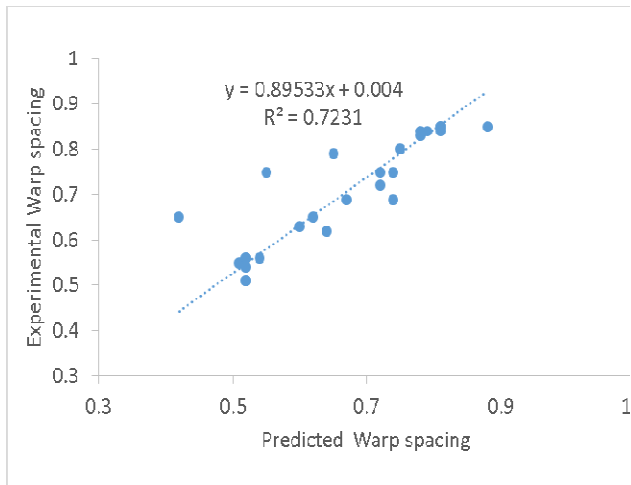
Figure 4.9: Four types of pores in woven fabric (a) planar way (b) on the graph paper.

Table 4.19: Physical parameters of fabrics.

| Sample code | Structures | Areal Density (g/m ²) | Thickness (mm) | Cover factor | Porosity |
|-------------|---------------|-----------------------------------|----------------|--------------|----------|
| S1. | B/B PW | 552.24 | 0.76 | 24.50 | 0.63 |
| S2 | B/B MW | 609.86 | 0.80 | 24.40 | 0.67 |
| S3. | B/B TW | 644.78 | 0.86 | 24.23 | 0.67 |
| S4. | PP/PP PW | 530.00 | 1.54 | 24.29 | 0.65 |
| S5. | PP/PP MW | 711.22 | 2.18 | 24.84 | 0.69 |
| S6. | PP/PP TW | 690.00 | 2.42 | 24.48 | 0.70 |
| S7. | PET/PET PW | 602.00 | 1.89 | 23.78 | 0.67 |
| S8. | PET/PET MW | 640.00 | 2.07 | 24.25 | 0.64 |
| S9. | PET/PET TW | 620.00 | 2.10 | 23.41 | 0.65 |
| S10. | Jute/ Jute PW | 685.23 | 2.12 | 23.67 | 0.66 |
| S11. | Jute/ Jute MW | 683.00 | 2.16 | 23.45 | 0.71 |
| S12. | Jute/ Jute TW | 646.00 | 2.23 | 23.45 | 0.72 |
| S13. | B/PP PW | 562.12 | 0.76 | 24.70 | 0.62 |
| S14. | B/PP MW | 571.89 | 1.15 | 24.60 | 0.64 |
| S15. | B/PP TW | 695.97 | 1.23 | 24.37 | 0.68 |
| S16. | B/PET PW | 512.32 | 0.85 | 20.62 | 0.62 |
| S17. | B/PET MW | 500.00 | 1.80 | 20.62 | 0.69 |
| S18. | B/PET TW | 536.21 | 1.87 | 20.96 | 0.72 |
| S19. | B/Jute PW | 532.12 | 1.02 | 20.66 | 0.77 |
| S20. | B/Jute MW | 533.00 | 1.49 | 21.38 | 0.78 |
| S21. | B/Jute TW | 698.00 | 1.80 | 25.07 | 0.78 |
| S22 | PP/B PW | 595.28 | 1.32 | 23.84 | 0.63 |
| S23. | PP/B MW | 593.93 | 1.42 | 23.31 | 0.63 |
| S24. | PP/B TW | 560.03 | 1.52 | 23.31 | 0.67 |
| S25. | PET/B PW | 700.32 | 1.40 | 23.75 | 0.77 |
| S26. | PET/B MW | 539.35 | 1.06 | 22.31 | 0.79 |
| S27. | PET/B TW | 702.93 | 1.95 | 23.97 | 0.80 |

Estimation of thread spacing and crimp based on geometrical model

The warp and weft thread spacings as well as crimps were estimated using geometrical models as stated in methodology section. The experimentally measured values are correlated with estimations. Results are shown in Figure 4.10.

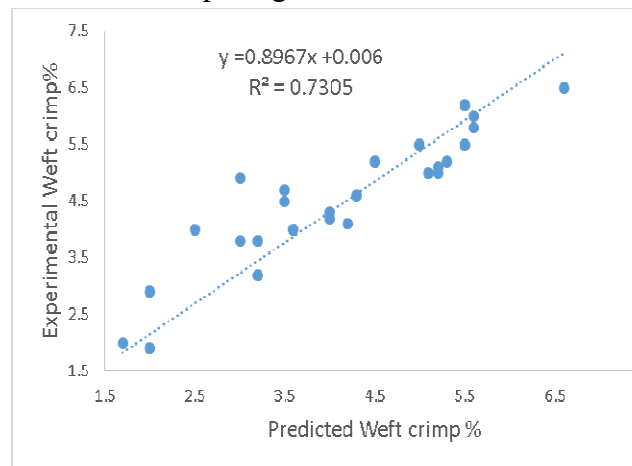
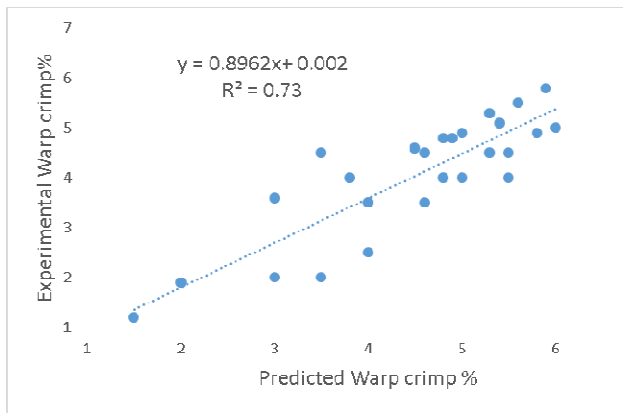


| Equation $y = a + b \cdot x$ | Value | t-test Significance "Yes" or "No" | Adj. R- Square | F-test Significance "Yes" or "No" |
|---------------------------------|--------------|--|-------------------|--|
| Intercept | 0.004 | Yes | 0.72 | Yes |
| Slope | 0.89 | Yes | | |

| Equation $y = a + b \cdot x$ | Value | t-test Significance "Yes" or "No" | Adj. R- Square | F-test Significance "Yes" or "No" |
|---------------------------------|--------------|--|-------------------|--|
| Intercept | 0.005 | Yes | 0.69 | Yes |
| Slope | 0.88 | Yes | | |

Warp thread spacing estimated and measured

Weft thread spacing estimated and measured



| Equation $y = a + b \cdot x$ | Value | t-test Significance "Yes" or "No" | Adj. R- Square | F-test Significance "Yes" or "No" |
|---------------------------------|--------------|--|-------------------|--|
| Intercept | 0.002 | Yes | 0.73 | Yes |
| Slope | 0.89 | Yes | | |

| Equation $y = a + b \cdot x$ | Value | t-test Significance "Yes" or "No" | Adj. R- Square | F-test Significance "Yes" or "No" |
|---------------------------------|--------------|--|-------------------|--|
| Intercept | 0.006 | Yes | 0.73 | Yes |
| Slope | 0.89 | Yes | | |

Warp crimp estimated and measured

Weft crimp estimated and measured

Figure 4.10: Correlation of physical parameters from geometrical model with experimental results

4.5.2 Static mechanical properties

The knowledge of tensile properties is very important for development of a fabric for specific end use; strength and elongation are two of most important properties that are required for the performance as per end use. Their study involves many difficulties due to a great degree of bulkiness in the fabric structure and strain variation during deformation. Every woven fabric is made of large number of threads, each thread having even a larger number of fibers; any slight deformation of the fabric will subsequently give rise to a chain of complex movements of the latter components. This is very complicated, since both fibers and yarns behave in a non-Hookean way during deformation. At the beginning of loading, extension occurs in amorphous parts, where primary and secondary bonds are extended and are shear loaded. During this stage if the external force is removed, most of the extension/elongation will be recovered and the material shows elastic response. If further load is applied, long chains of molecules are rearranged as a result of disconnection of secondary bonds resulting in plastic deformation. The re-arrangements of the reciprocal position of molecules give material better possibility to resist additional loading. If the loading continuous, a final break will occur.

Tensile properties of yarns

The tensile properties are very important in terms of making a decision about end use of the material. The tensile behavior of fabrics is closely related to the inter-fiber friction effect, the ease of crimp removal and load-extension properties of the yarns themselves. Thus tensile properties (i.e. tensile force and tensile elongation) of all yarns used were measured and for a better comparison, breaking tenacity of yarns are presented in Figure 4.11. The tensile test for each type of yarn was repeated 30 times and their average was taken. It was established that Basalt yarn is the strongest and Jute has the lowest breaking tenacity among the yarns under investigation.

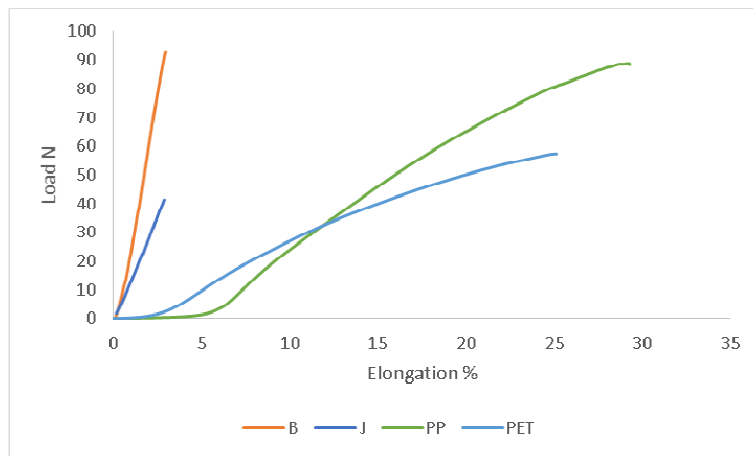


Figure 4.11: Load –Elongation curve of yarns

Tensile properties of basalt hybrid fabrics

The tensile properties of woven fabrics has many complexities as fabric is anisotropic in nature and has initial modulus which changes with strain. Anisotropy is a characteristic of most fabrics, especially woven; the impact of the direction of loading on tensile properties can be enormous and is frequently examined.

The tensile behavior of woven fabrics is known to be affected by its sett and construction. In this study, tensile properties of hybrid and non- hybrid woven fabrics were characterized by fabric breaking load and elongation. Tensile properties of all fabrics were measured in both warp and weft direction. Measurement of tensile stress–strain properties is the most common mechanical measurement on fabrics. It is used to determine the behavior of a sample while under an axial stretching load. The results of all measurements are shown in Table 4.20.

Effect of fiber type on tensile properties of basalt hybrid fabrics

In warp direction, B/B has highest tensile modulus as basalt is strongest yarn and jute has lowest. With the use of basalt in warp/weft, stress/strain behavior changes a lot. Tensile/Initial moduli of all fabrics increased with the hybridization with basalt. When basalt yarn is introduced, the tensile modulus of hybrid fabric sharply increases to 50 % for B/PP, 40% for B/PET and 70% for B/J respectively. In addition, strain decreases dramatically as basalt yarn is introduced, which suggests that the toughness of hybrid fabric began to decline. It was found out that the extensibility of yarns in weft direction influences the tensile force in warp direction. Increased modulus in warp direction is observed with fabrics having PP and PET in weft and the lowest warp way modulus is obtained for plain jute fabrics which involve weakest yarns. In hybrid structures B/PP has highest modulus in warp direction. As Polypropylene yarn has higher strength than polyester the results are evident. It is quite clear that effect of yarn tensile properties have significant influence on fabric behavior. With the use of PET in weft direction modulus in warp direction increase for all weaves. The hybridization of basalt in warp direction improves moduli more as compared to use of basalt in weft direction.

Table 4.20: Mechanical properties of fabrics.

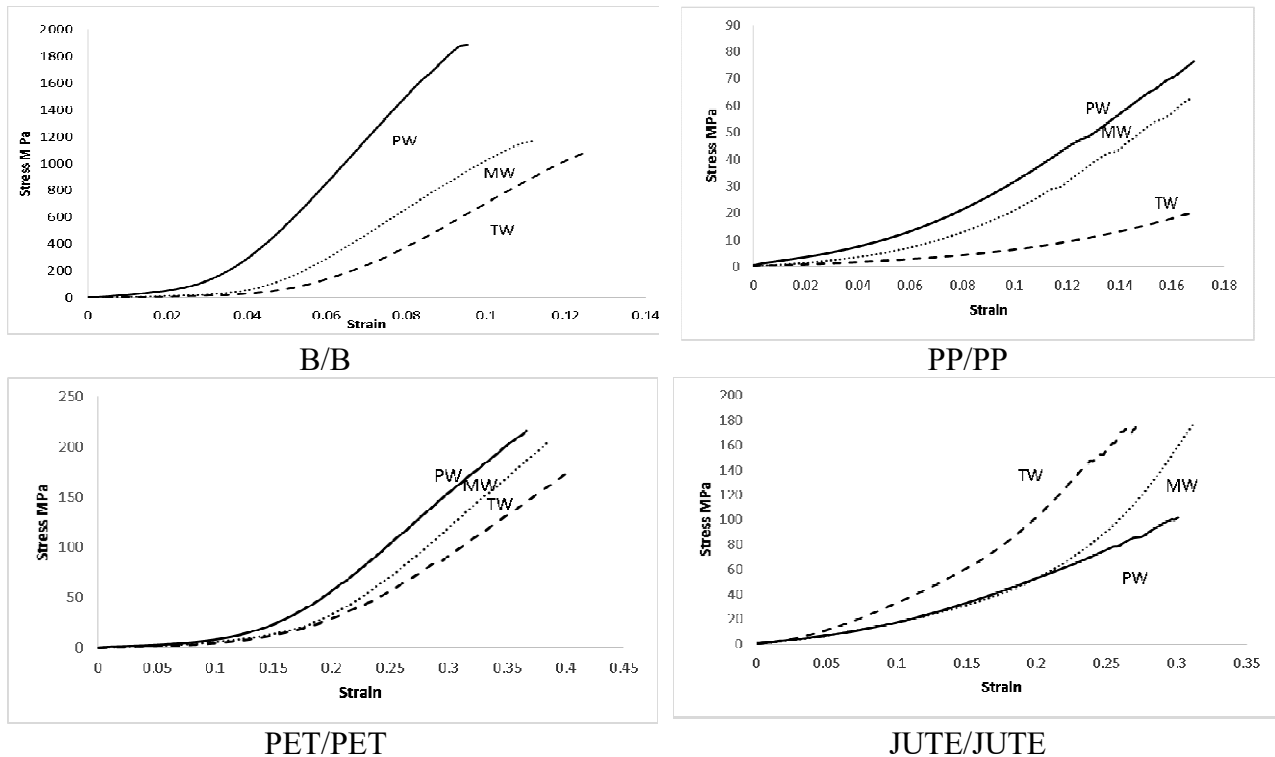
| Sample code | Structures | Stress (MPa) | Strain | Initial modulus warp (MPa) | Stress (MPa) | Strain | Initial modulus weft MPa) | Shear rigidity G (MPa) |
|-------------|--------------|--------------|---------|----------------------------|--------------|--------|---------------------------|------------------------|
| S1. | B/B PW | 1403.482 | 0.0435 | 3839.7 | 1154.923 | 0.0387 | 3912.9 | 0.005 |
| S2. | B/B MW | 1165.291 | 0.0558 | 2289.39 | 522.99 | 0.0319 | 2046.93 | 0.038 |
| S3. | B/B TW | 1055.212 | 0.0648 | 2157.25 | 843.5945 | 0.0492 | 1875.23 | 0.028 |
| S4. | PP/PP PW | 311.7578 | 0.2308 | 129.9 | 225.1836 | 0.1295 | 306.53 | 0.095 |
| S5. | PP/PP MW | 258.1218 | 0.196 | 127.88 | 150.3892 | 0.0795 | 293.1 | 0.076 |
| S6. | PP/PP TW | 240.0066 | 0.2844 | 91.16 | 216.4202 | 0.104 | 280.04 | 0.064 |
| S7. | PET/PET PW | 281.2843 | 0.2004 | 156.4 | 244.8727 | 0.203 | 191.7 | 0.211 |
| S8. | PET/PET MW | 236.5101 | 0.213 | 138.31 | 188.8245 | 0.1685 | 179.64 | 0.205 |
| S9. | PET/PET/TW | 230.2057 | 0.279 | 117.48 | 213.3865 | 0.1936 | 175.25 | 0.178 |
| S10. | Jute/Jute PW | 101.949 | 0.15935 | 77.41 | 153.7207 | 0.0423 | 369.95 | 0.095 |

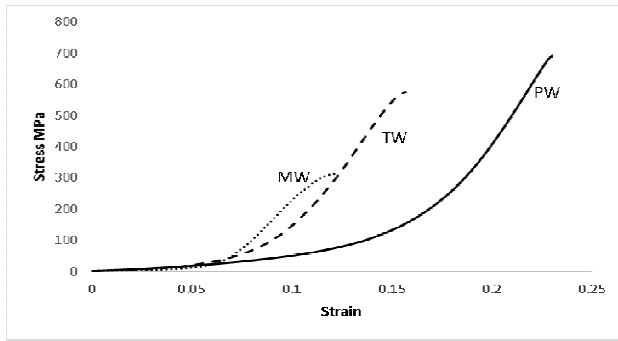
| | | | | | | | | |
|------|---------------|----------|---------|--------|----------|--------|---------|-------|
| S11. | Jute/Jute MW | 180.7494 | 0.14935 | 100.25 | 124.8776 | 0.036 | 347.83 | 0.093 |
| S12. | Jute/ Jute TW | 169.8772 | 0.134 | 114.68 | 165.2143 | 0.0416 | 335.34 | 0.093 |
| S13. | B/PP PW | 691.8423 | 0.1152 | 602.95 | 821.4353 | 0.0634 | 760.06 | 0.399 |
| S14. | B/PP MW | 312.1837 | 0.0604 | 985.26 | 555.1334 | 0.1154 | 451.55 | 0.355 |
| S15. | B/PP TW | 575.0361 | 0.0786 | 916.8 | 442.6213 | 0.1162 | 399.38 | 0.309 |
| S16. | B/PET PW | 520.3608 | 0.0592 | 443.27 | 522.2689 | 0.3063 | 312.05 | 0.120 |
| S17. | B/PET MW | 277.7597 | 0.039 | 545.6 | 412.0756 | 0.3512 | 214.35 | 0.069 |
| S18. | B/PET TW | 454.1116 | 0.0442 | 511.66 | 389.1398 | 0.3313 | 186.87 | 0.056 |
| S19. | B/Jute PW | 535.0833 | 0.113 | 256.52 | 192.9011 | 0.0245 | 926 | 0.372 |
| S20. | B/Jute MW | 247.1936 | 0.0892 | 467.75 | 290.4344 | 0.0406 | 838.48 | 0.320 |
| S21. | B/Jute TW | 469.0942 | 0.1217 | 466.1 | 170.7475 | 0.0546 | 478.44 | 0.250 |
| S22. | PP/B PW | 407.6736 | 0.2153 | 204.46 | 163.3242 | 0.0195 | 1359.98 | 0.176 |
| S23. | PP/B MW | 395.1777 | 0.13865 | 180.58 | 172.9343 | 0.0205 | 1100.73 | 0.169 |
| S24. | PP/B TW | 360.2388 | 0.1544 | 170.09 | 128.5157 | 0.0267 | 877.98 | 0.148 |
| S25. | PET/B PW | 520.043 | 0.4554 | 180 | 202.9197 | 0.0252 | 1024.18 | 0.958 |
| S26. | PET/B MW | 365.4254 | 0.29855 | 177.16 | 225.5169 | 0.0683 | 1008.13 | 0.353 |
| S27. | PET/B TW | 389.9997 | 0.3621 | 148.96 | 157.1115 | 0.0337 | 695.24 | 0.428 |

Effect of weave structure on tensile properties of basalt hybrid fabrics

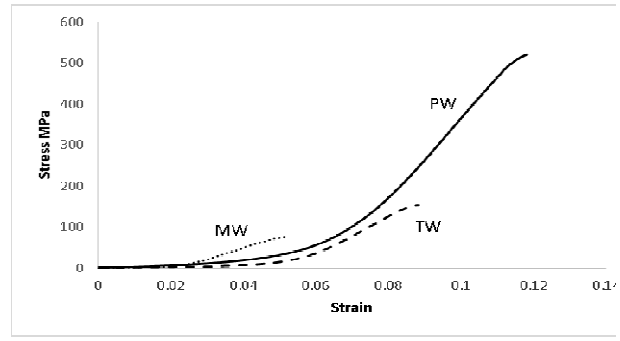
The tensile behavior of fabrics is closely related to the inter-fiber friction effect, the ease of crimp removal and load-extension properties of the yarns themselves. Extensibility refers to the degree with which a fabric will increase in length under tension. Different weaves have different degree of extensibility. The amount of crimp within the fabric construction plays a role in determining the extensibility of a fabric. Crimp is defined as the waviness or distortion of a yarn due to the interlacings within the weave. The higher the number of interlacing per unit area the greater the crimp. In general, the longer the floats within the construction the less extensible the fabric will be. A comparative account of the effect of weave structure on tensile properties of various hybrid and non-hybrid fabrics is also shown in Fig. 4.12-4.13. It is also established that the type of weave has a great influence on the tensile modulus of fabrics in warp direction. It is obvious that in non- hybrid structures, plain weave has highest value followed by matt and twill. The highest level of stress and elastic modulus is observed in plain weave because of the maximum number of interlacing points in a given area and therefore the highest degree of crimp, resulting in higher friction between yarns. So they can absorb more energy. In jute fabrics twill has highest modulus followed by matt which have longer floats compared to plain weave. B/J has highest tensile moduli as Jute is a staple yarn with protruding fibers, there is higher contact surface area with basalt warp which results in higher level of inter yarn friction and resistance to tensile deformation. For B/J, matt weave has highest strength followed by twill and plain weaves respectively. As jute is staple yarn so due to cohesive entanglement of surface hairs, matt weave has highest strength followed by twill which have longer floats compared to plain weave. In hybrid fabrics when basalt is used in warp, the highest tensile modulus is obtained in matt weave (groups of yarns have woven together), due to its cohesiveness and because grouping of yarn pairs leads to increase in contact area which subsequently increases friction between warp and weft. Plain weave has lower modulus, as basalt is a brittle yarn and during weaving, a lot of weaving stresses acted on it causing fiber rupture. During tensile test, breaking elongation of

warp yarn is lower as the yarn is already extended during weaving process. This results in lower residual strain. The differences in the same weave depend considerably on the material used in weft. Plain weave has the maximum number of interlacing points, which is twice as high as that of other weaves and, as a result, stress and strain is higher. Also, warp crimp is the highest in plain weave, which influences tensile elongation. A lower tensile elongation/strain is typical of the fabrics woven in basket/matt weave. However, matt weave has relatively higher load bearing capacity. Maximum stress level in matt weave is lower because of excessive frictional restraint which results in catastrophic failure at break. It was also found out that different properties of yarns have direct influence on the tensile elongation of fabrics in warp direction. When basalt is used in warp direction, tensile elongation values are lower as basalt is brittle yarn with low elongation. In B/J fabrics initial modulus is measured after decrimping zone. No further straightening of yarns is possible which leads to jamming of structure restricting further elongation. When using basalt in weft direction, modulus is not affected much as compared to non-hybrid fabrics. Among all structures plain weave has highest moduli followed by matt and twill. B/Jute has highest tensile moduli when basalt is used in warp as Jute is a staple yarn with protruding fibers. There is higher contact surface area with basalt warp which results in higher level of inter yarn friction and resistance to tensile deformation. By using basalt in warp direction, fabrics tensile strength increased. B/PP has highest value followed by B/PET and B/Jute respectively. Moduli of PP/B and PET/B is quite higher in weft direction due inherently lower extensibility of basalt yarns.

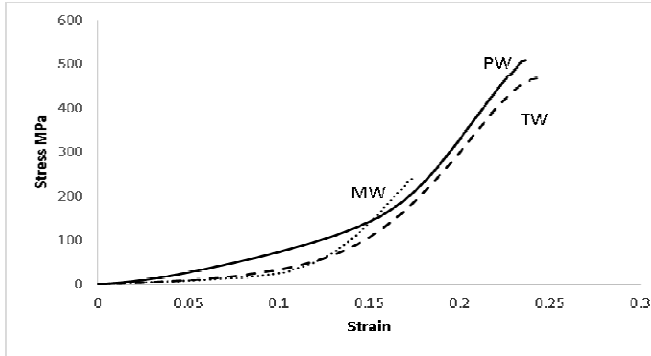




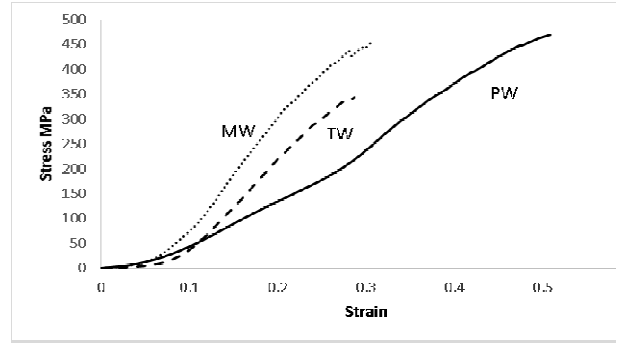
B/PP



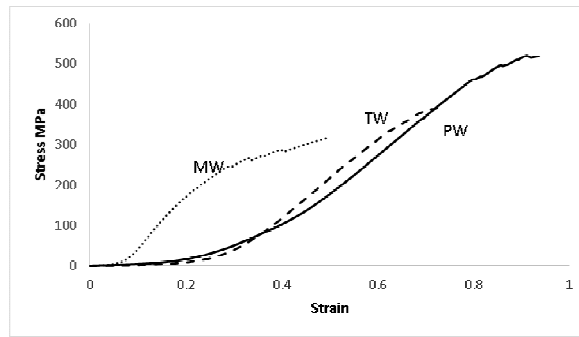
B/PET



B/J

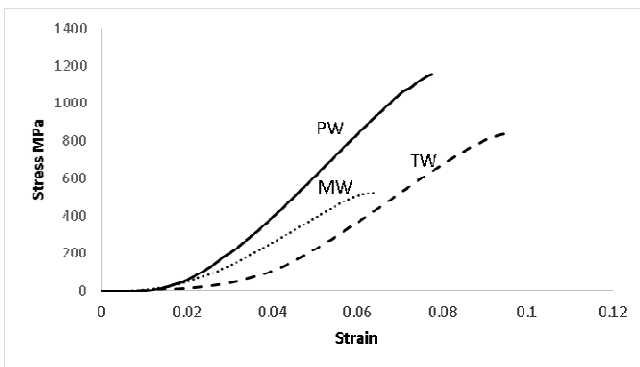


PP/B

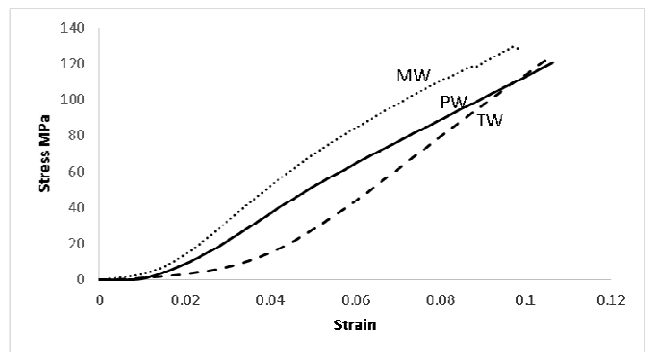


PET/B

Figure 4.12: Stress-strain curves for hybrid and non-hybrid fabrics in warp direction.



B/B



PP/PP

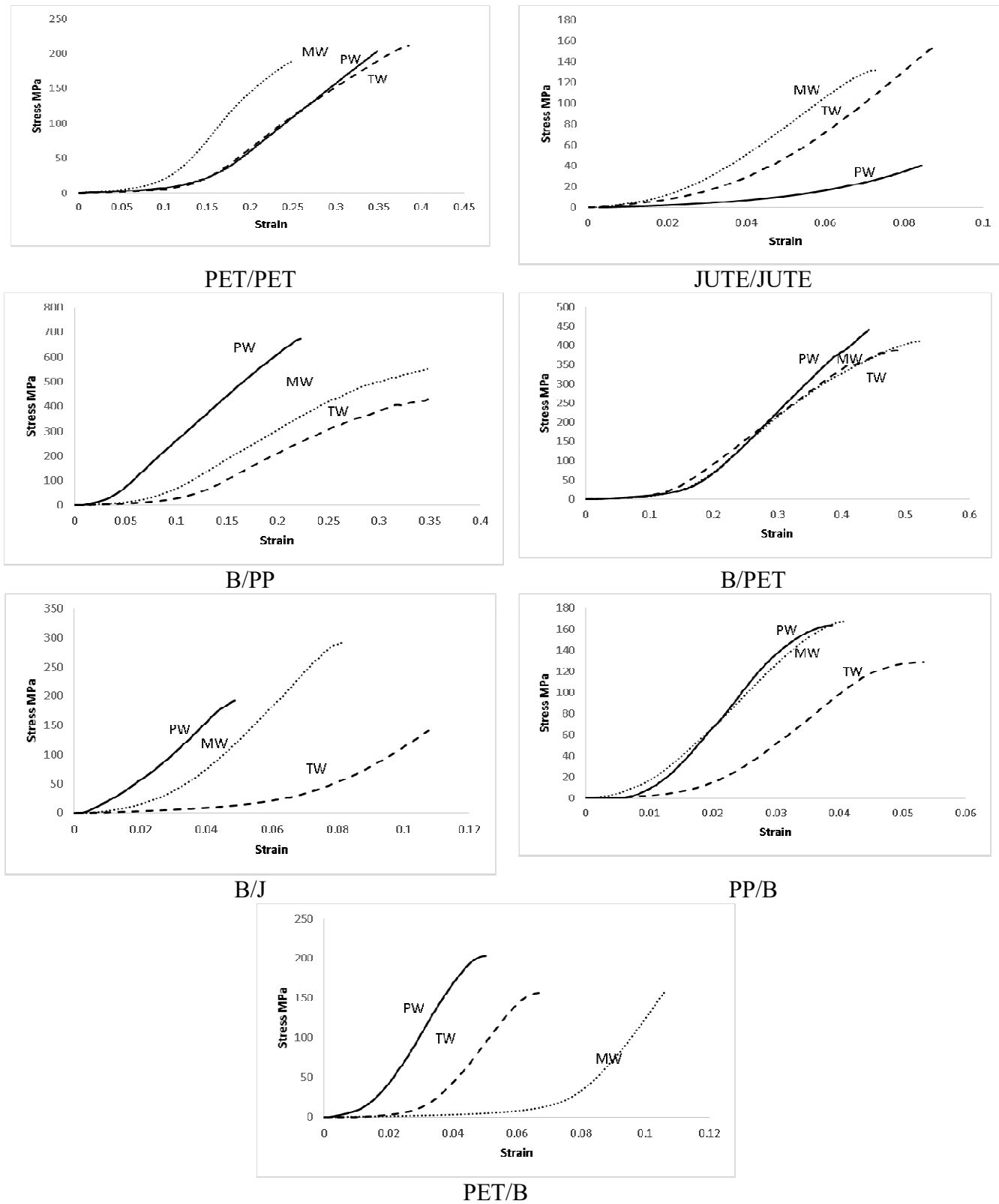


Figure 4.13: Stress-strain curves for hybrid and non-hybrid fabrics in weft direction.

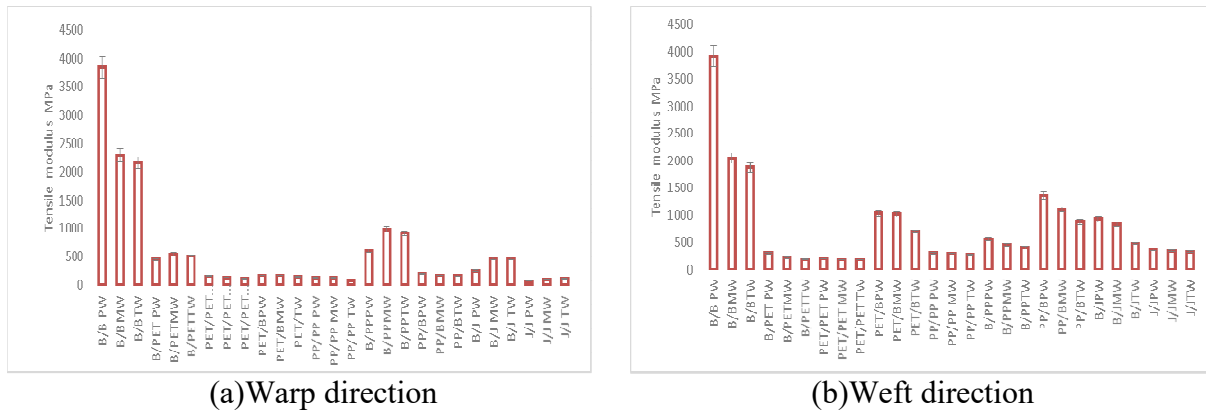


Figure 4.14: Initial moduli of hybrid and non-hybrid fabrics.

Prediction of tensile properties using Wisetex

Several models can be used for creation of fabric simulations and prediction of mechanical properties. The models are implemented in WiseTex software. Calculations for uniaxial tension in warp direction and weft direction are done.

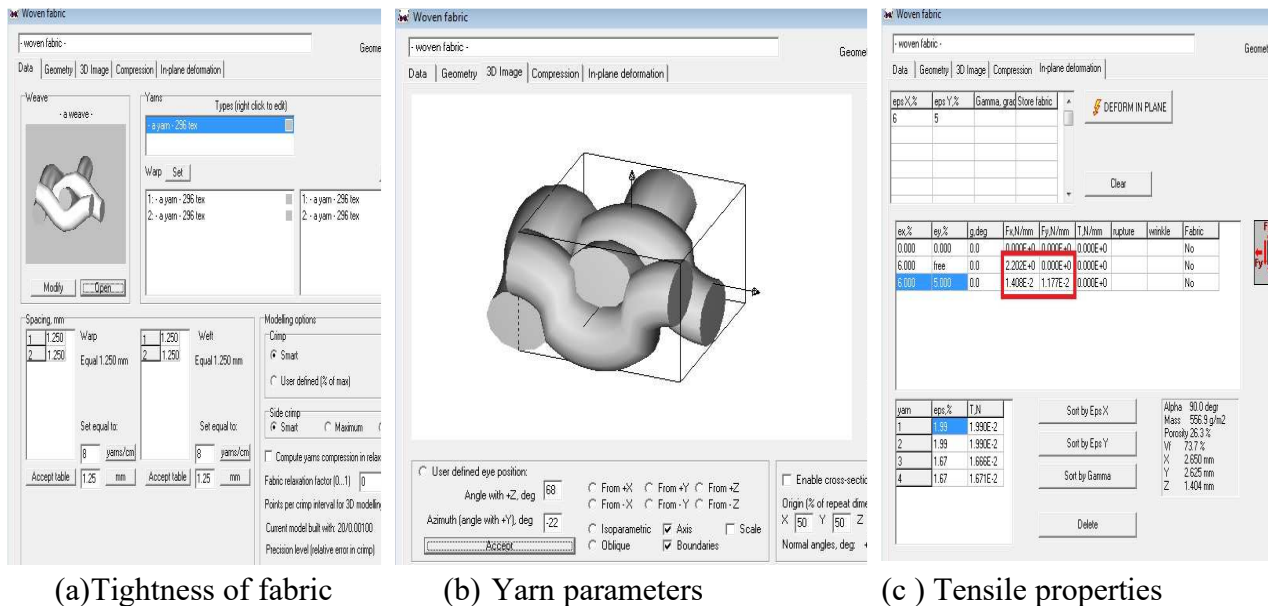
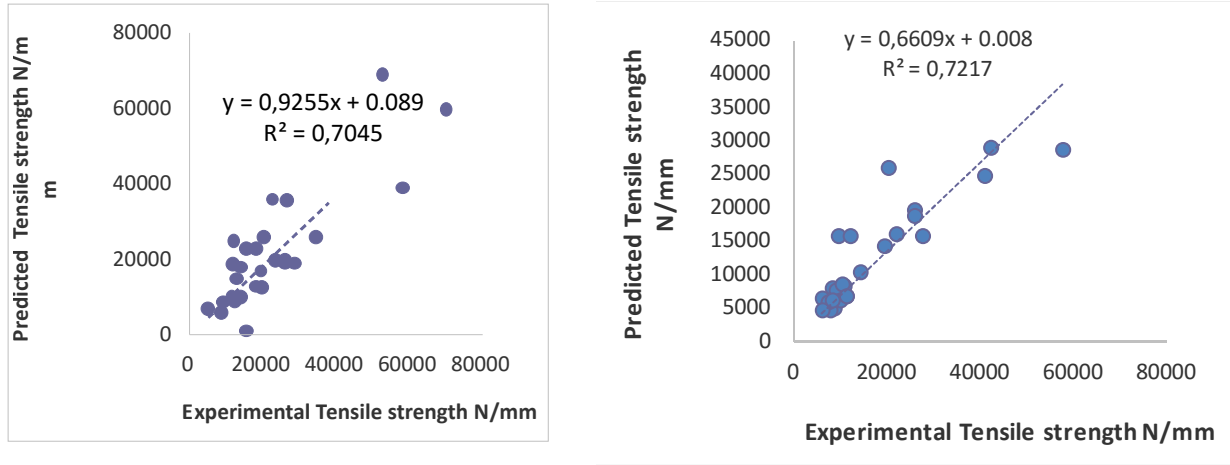


Figure 4.15: Prediction of tensile properties with WISETEX.

The calculated values are compared with the measured tensile properties. The results of the simulations have been compared with the experimental observations, resulting in a reasonable agreement between them. The comparison with experiments validates the models for fabric tensile properties. Its correlation is only 70% as new kind of material was used for development of hybrid fabrics in this work. The most important factors of the uncertainty of these data are (1)

approximate nature of the model, which does not consider details of the contact between the yarns and (2) numerical difficulties of convergence for very low compression and tension stiffness of the yarns in the initial stage of deformation.



(a) warp

(b) weft

| Equation $y = a + b \cdot x$ | Value | t-test Significance "Yes" or "No" | Adj. R- Square | F-test Significance "Yes" or "No" |
|---------------------------------|-------|--|-------------------|--|
| Intercept | 0.089 | Yes | 0.704 | Yes |
| Slope | 0.925 | Yes | | |

(a)

| Equation $y = a + b \cdot x$ | Value | t-test Significance "Yes" or "No" | Adj. R- Square | F-test Significance "Yes" or "No" |
|---------------------------------|-------|--|-------------------|--|
| Intercept | 0.008 | Yes | 0.72 | Yes |
| Slope | 0.661 | Yes | | |

(b)

Figure 4.16: Correlation of tensile strength predicted by WISETEX and measured values.

Shear properties of basalt hybrid woven fabrics

The structural design of a textile fabric is largely dictated by its end-use application. It is a well-known fact that weave structure affects most of the mechanical properties of woven fabric. Fabrics are highly anisotropic and the behavior in one direction is coupled to the behavior in the other in a nonlinear manner. Even under uniaxial loading, the response of a fabric is often nonlinear due to its woven structure and due to nonlinearities in the material response. In addition, many applications of fabric involve large rotations and deformations. Various deformation mechanisms e.g. yarn stretch, un-crimping, crimp interchange, locking, trellising and yarn slip etc. determine the mechanical response of a woven fabric. The ability of a fabric to be deformed by shearing distinguishes it from other thin sheet materials such as paper or plastic films. During shear deformation, the fabric experiences large angular variation between warp and weft yarns. In the process of deforming a flat piece of fabric into a three-dimensional surface, shearing must occur. This ability of fabric to deform within its plane is important not only for tailoring but also for the molding of fabric reinforced composites. This property enables fabric to undergo complex deformations and to conform to the shape of the final object. Shear properties

influence draping, flexibility and also the deformability. It is necessary to study the inter/intra-ply shear behavior of fabric because of their wide application in production especially in the case of forming process. Based on the deformed configuration of the fixture, shear angle is calculated. A vertical displacement of 40 mm, which corresponds to a shear angle of around 50° was found to be the maximum displacement but the buckling occurs after 20 mm displacement with shear angle range of $20\text{-}30^\circ$.

The picture frame test method is verified for the fabrics under consideration. Fig. 4.17 shows the array of images for a fabric specimen captured during the loading process at each 5mm displacement for every 30 seconds. In the beginning, (Figure 4.17a), there is no shearing. Subsequently the shear deformation resistance is mainly from the friction between the yarns before reaching the limiting locking angle. The limiting locking angle is the ultimate shear deformation observed by means of local wrinkling/buckling. As the shear stress increases, however, a critical stage is reached where the fabric starts to deform out of its plane, buckling as a result. Under smaller angular displacements, the deformation of the material is too small to overcome the friction between the yarns. As such, the material acts as a rigid body and the slope representing the shear modulus is large. Between 2.5 and 6 degrees of angular displacement, there is yarn slippage at the intersection and elastic bending resulting in the flattening of the curve. For woven fabrics there exists a shear locking angle. When the shear locking angle is reached the threads are physically jammed up, and with no in plane preload, buckling occurs. At angles above 13 degrees, there is jamming and wrinkling within the material requiring larger shear stresses to produce the displacements. B/B plain weave shows highest initial modulus as compared to matt and twill weave. In plain weave more interlacement between warp and weft yarns results in more friction, more resistant to slippage. Dissimilar yarn based fabrics have less cohesive forces. In matt weave, it has longer float on both sides so it exhibits more resistant to angular slippage in a biased direction. In B/PET, spacing between adjacent yarns is high, less chance of inter-yarn cohesion so less resistance to slippage. In matt weave, due to yarn floats on both faces of fabric, it is more resistant to slippage. Polyester yarn is bulky, relatively high specific surface friction and thus cohesion between weft yarns dominates the frictional resistance. In B/J, as jute is a spun yarn, there is surface hairiness and cohesion of yarn is enhanced. All these yarn surface behavior plays vital role in deciding the shear resistance and shear rigidity of basalt hybrid woven fabrics. Among structures where basalt is used in weft, plain weave has highest initial modulus and high shear resistance followed by matt and twill which is predominantly due to higher interlacement between warp and weft.

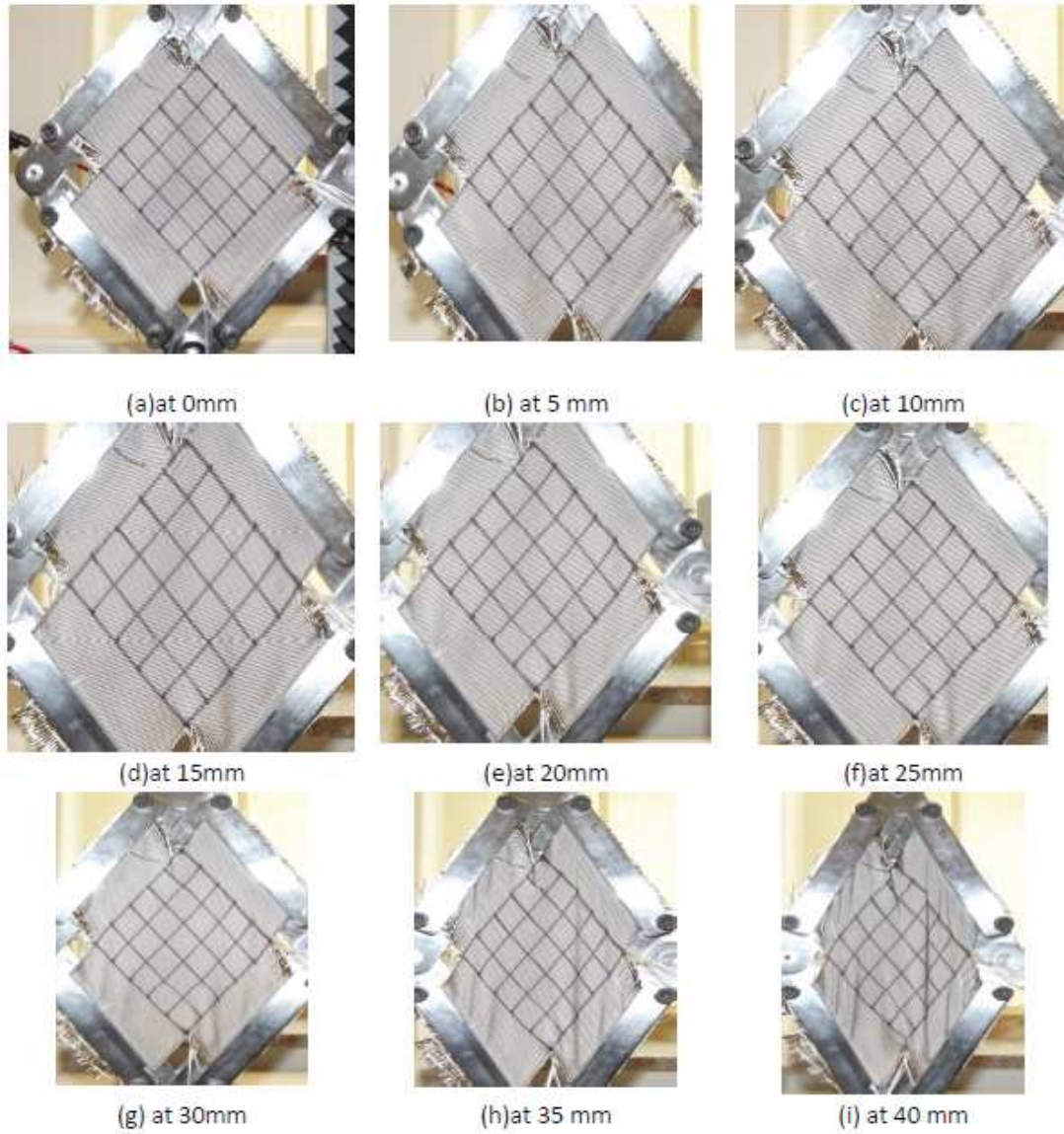
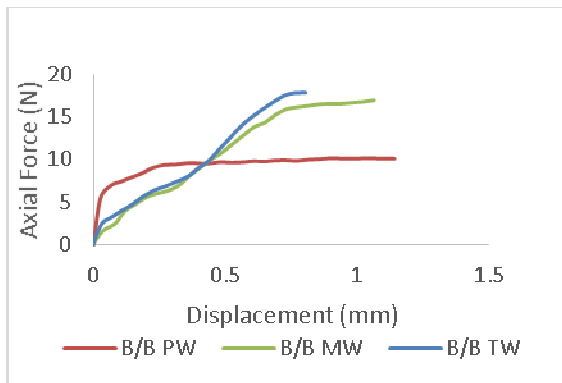
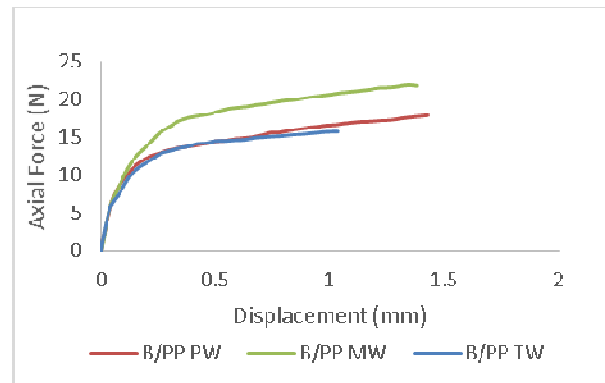


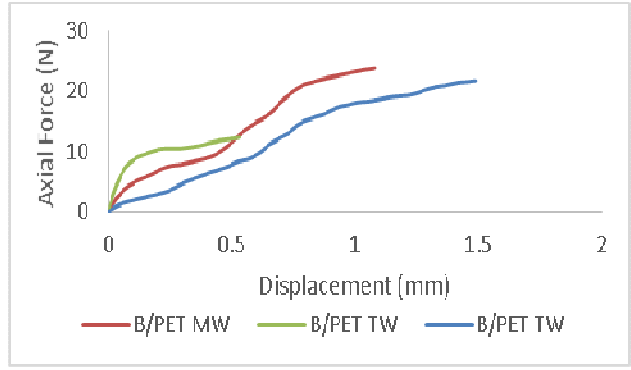
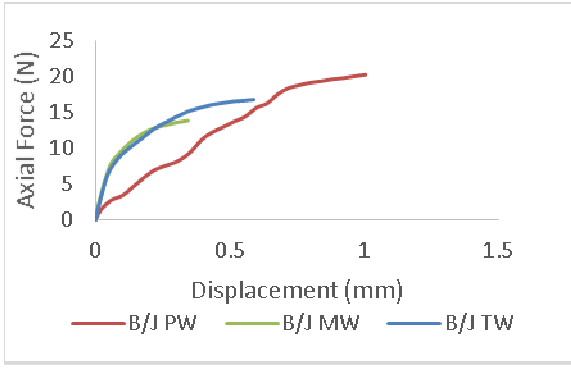
Figure 4.17: Shear deformation of B/PET sample at different displacement levels.



(a)

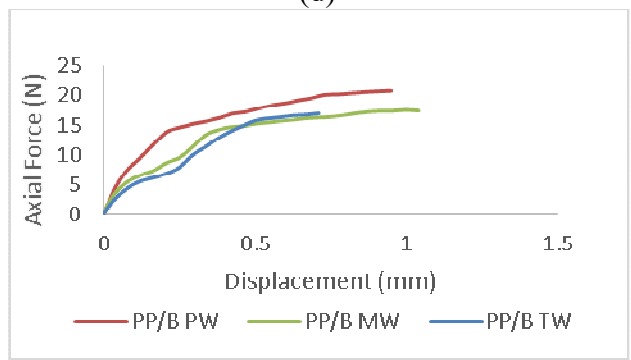
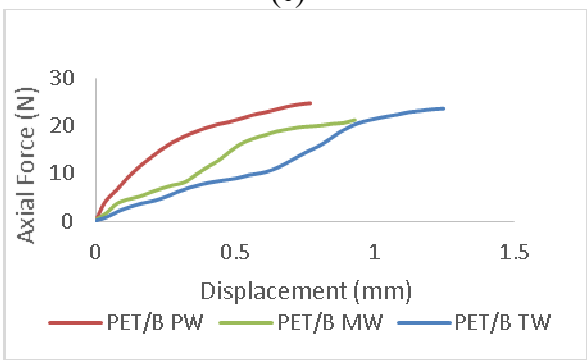


(b)



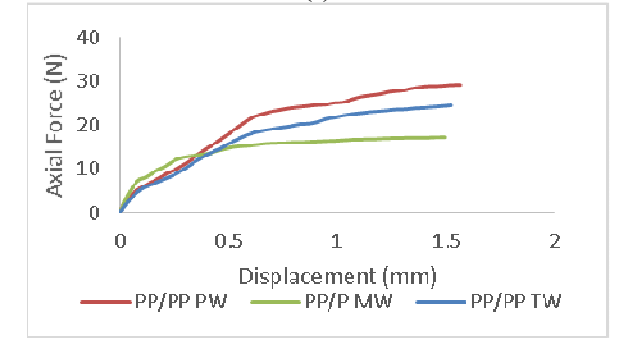
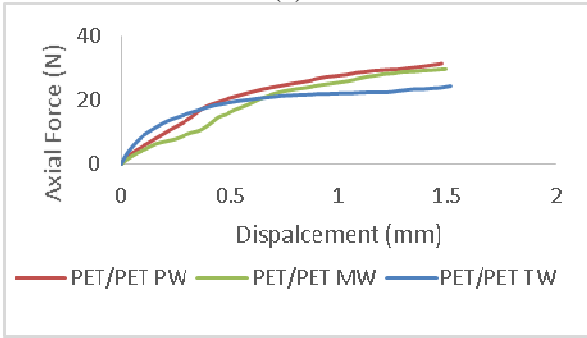
(c)

(d)



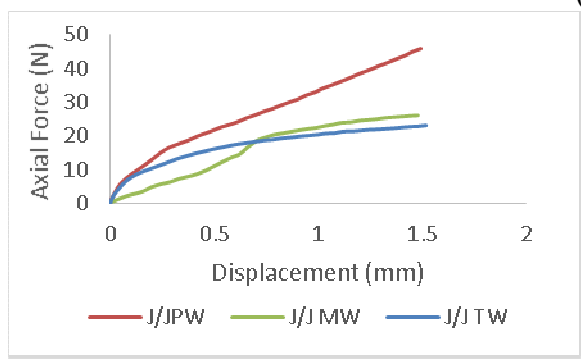
(e)

(f)



(g)

(h)



(i)

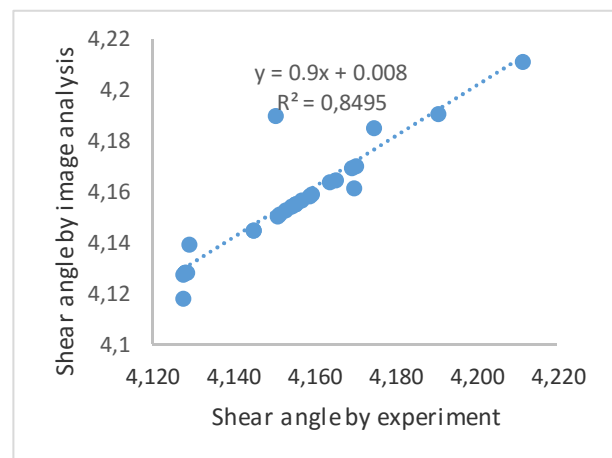
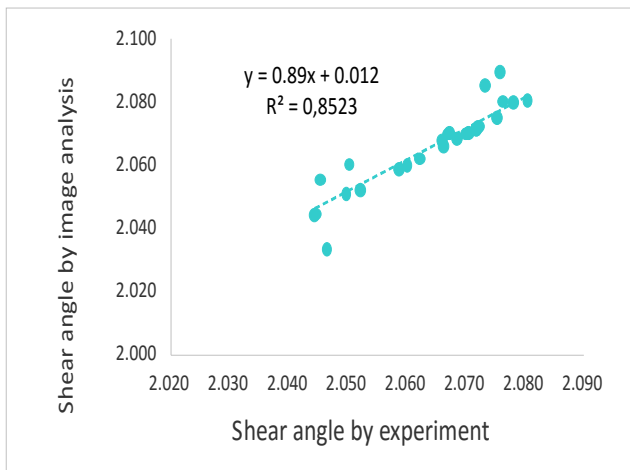
Figure 4.18: Shear deformation of specimens at different displacement levels.

Determination of shear angle using image analysis method

Fig. 4.17 shows the image of a fabric specimen captured during the loading process without displacement. This image was analyzed to obtain shear angle and displacement of the specimen during the test. The image file string is examined and then the appropriate image reading function is called by MATLAB `imread`. The image is then converted to a gray image and then normalized to a matrix of values ranging from zero to one. This matrix is returned by the function in the variable `I`. Image analysis can aid in the determination of the shear angle and displacement at any particular point on the surface of fabric specimen. Grid pattern was applied on the specimen surface before the test and used as the reference points of image analysis. Around 16 points (25 square cells (4cm² each) with 90° angle at 4 points) can be chosen on a 100 mm x 100 mm specimen for image analysis to determine the displacements and shear angles at the chosen points. First, by manually choosing the points on a reference image, the X and Y coordinates of each point can be determined in pixel. The difference of X and Y coordinates of each chosen point between the reference image and the image chosen for analysis represents the displacements in X and Y directions respectively.

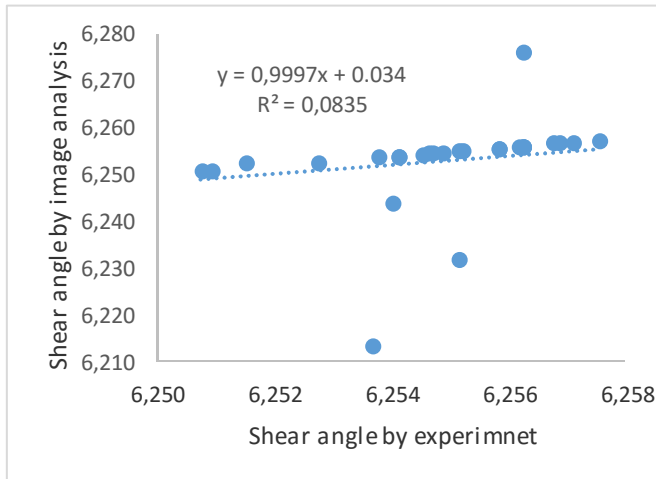
Correlation between experimental and image analysis based results

The shear angles are calculated by considering sample length and it is further used for calculation of shear force. The differences between image analysis and calculated shear angle using sample length at the chosen points are relatively small. Less than 8% CV was obtained in all measurements. It does not show any significant difference until pre-buckling (upto 20 mm displacement) but significant difference is observed after 20 mm displacement. It is also believed that during image processing in MATLAB, detection of X and Y coordinates on the image is not accurate due to wrinkling in the central zone of samples. Fig 4.19 shows the comparison of shear angles between all samples at different displacement levels using image analysis and results from experimental measurements.



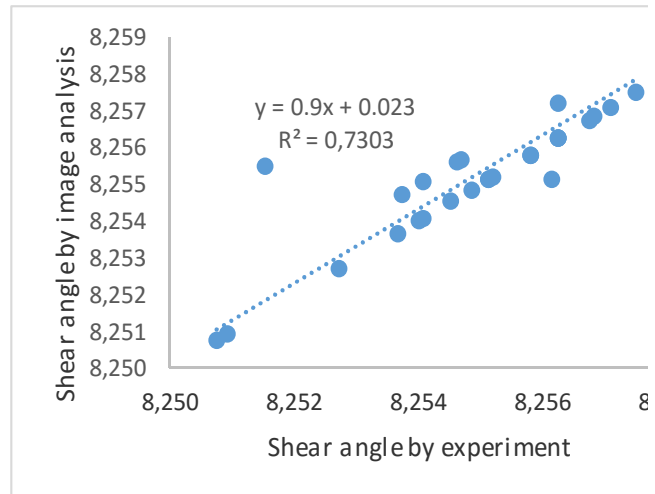
| Equation $y = a + b*x$ | Value | t-test Significance "Yes" or "No" | Adj. R- Square | F-test Significance "Yes" or "No" |
|---------------------------|--------------|--|-------------------|--|
| Intercept | 0.012 | Yes | 0.85 | Yes |
| Slope | 0.89 | Yes | | |

(a) 5mm displacement



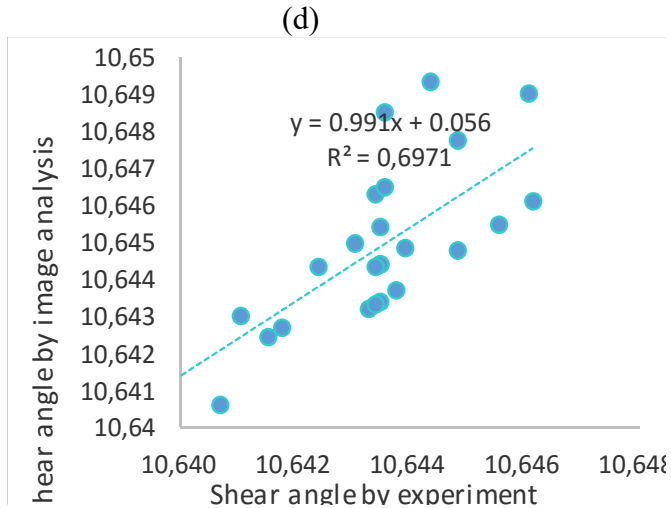
| Equation $y = a + b*x$ | Value | t-test Significance "Yes" or "No" | Adj. R- Square | F-test Significance "Yes" or "No" |
|---------------------------|--------------|--|-------------------|--|
| Intercept | 0.008 | Yes | 0.849 | Yes |
| Slope | 0.9 | Yes | | |

(b) 10mm displacement



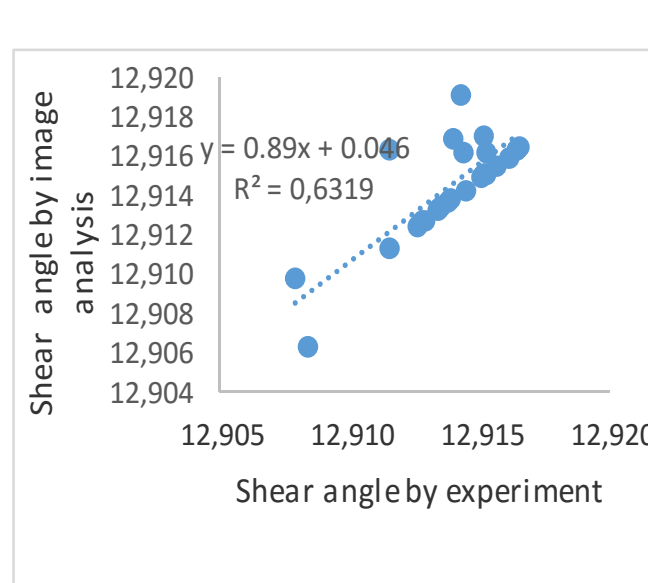
| Equation $y = a + b*x$ | Value | t-test Significance "Yes" or "No" | Adj. R- Square | F-test Significance "Yes" or "No" |
|---------------------------|--------------|--|-------------------|--|
| Intercept | 0.034 | Yes | 0.835 | Yes |
| Slope | 0.99 | Yes | | |

(c) 15mm displacement



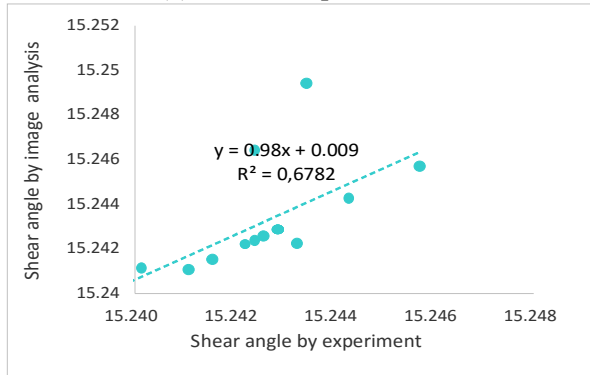
| Equation $y = a + b*x$ | Value | t-test Significance "Yes" or "No" | Adj. R- Square | F-test Significance "Yes" or "No" |
|---------------------------|--------------|--|-------------------|--|
| Intercept | 0.023 | Yes | 0.73 | Yes |
| Slope | 0.9 | Yes | | |

(d) 20 mm displacement



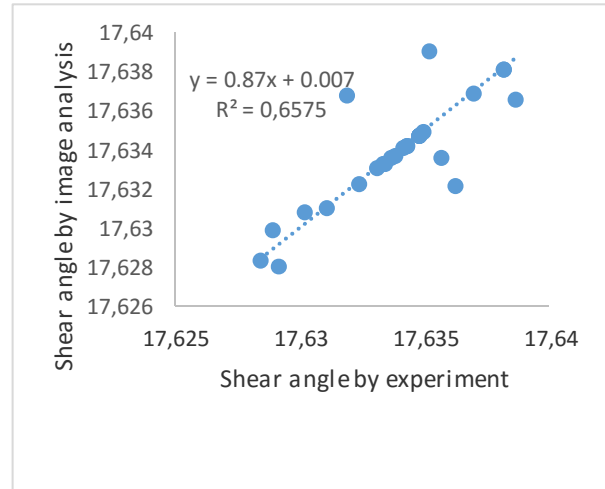
| Equation $y = a + b \cdot x$ | Value | t-test Significance "Yes" or "No" | Adj. R- Square | F-test Significance "Yes" or "No" |
|---------------------------------|--------------|--|-------------------|--|
| Intercept | 0.056 | Yes | 0.697 | Yes |
| Slope | 0.99 | Yes | | |

(e) 25mm displacement



| Equation $y = a + b \cdot x$ | Value | t-test Significance "Yes" or "No" | Adj. R- Square | F-test Significance "Yes" or "No" |
|---------------------------------|--------------|--|-------------------|--|
| Intercept | 0.046 | Yes | 0.632 | Yes |
| Slope | 0.89 | Yes | | |

(f) 30 mm displacement



| Equation $y = a + b \cdot x$ | Value | t-test Significance "Yes" or "No" | Adj. R- Square | F-test Significance "Yes" or "No" |
|---------------------------------|--------------|--|-------------------|--|
| Intercept | 0.009 | Yes | 0.678 | Yes |
| Slope | 0.98 | Yes | | |

(g) 35 mm displacement

| Equation $y = a + b \cdot x$ | Value | t-test Significance "Yes" or "No" | Adj. R- Square | F-test Significance "Yes" or "No" |
|---------------------------------|--------------|--|-------------------|--|
| Intercept | 0.007 | Yes | 0.657 | Yes |
| Slope | 0.87 | Yes | | |

(h) 40mm displacement

Figure 4.19: Comparison of shear angles between image analysis and experimental values.

4.5.3 Dynamic mechanical properties

The mechanical properties of fibers depend on their molecular structure, where macromolecules can be arranged in crystalline (specific arrangements of molecules) or amorphous (coincidental arrangements of molecules) structure. The macromolecules are oriented mostly along the fiber axis and are connected to each other with intermolecular bonds. When a force is applied, the macromolecular structure starts changing. The rate of molecular rearrangement depends on the load level and on the mobility of the macromolecules, which again is governed by the physical and chemical structure and arrangement of the molecules (i.e., side group, bonding, etc.). Temperature also accelerates the rearrangement of the macromolecules as a result of increasing mobility, coupled with a higher free volume. The dynamic mechanical analysis (DMA) is mostly employed for investigating the structures and viscoelastic behavior of polymeric materials for figuring out their relevant stiffness and damping characteristics for various applications. It has considerable practical significance when determined over a range of temperature and frequencies. Classical DMA outputs are storage modulus (E'), loss modulus (E'') and mechanical damping

factor ($\tan \delta$). The storage modulus represents the stiffness of a viscoelastic material and is proportional to how much energy a material can absorb, whereas the loss modulus shows how much energy (heat) the material releases. The mechanical damping factor or internal friction in a viscoelastic system can be utilized to show the impact resistance of the material. A higher $\tan \theta$ value is indicative of a material that has a higher, non-elastic strain component, while a lower value indicates one that is more elastic.

Storage modulus, loss modulus, and $\tan \delta$ are described as a function of temperature in Figs 4.20 and 4.21. All the hybrid fabrics exhibited higher storage modulus (higher stiffness) than the non-hybrid fabrics. Tensile strength of the fabrics showed the same behaviour. At each temperature, hybrid fabrics exhibit higher modulus than the non-hybrids. Storage modulus of hybrid fabrics increased significantly with the incorporation of basalt yarn especially when it is used in warp direction. This condition is primarily attributed to the increase in the stiffness of the structure due to the nature of basalt fiber that allows more stress to bear. As seen from the figure, there is a decreasing trend in the storage modulus (decrease in stiffness) over the entire experimental temperature range. B/B structures are least effected by the temperature as compared to other materials due to the stable property of basalt(inorganic) fiber over wide range of temperatures. Thermoplastic polymers are semi crystalline, so they have high degree of orientation which strongly affects their mechanical properties. At low temperatures, the molecules are so immobile that they are unable to resonate with the oscillatory loads and therefore remain stiff. The macromolecular segments cannot change shape, especially through rotation about C–C bonds, and so the molecular entanglements act as rigid crosslinks. At elevated temperatures, the molecular segments become readily mobile and have no difficulty resonating with the load. When the timescale of molecular motion coincides with that of mechanical deformation, each oscillation is converted into the maximum-possible internal friction and non-elastic deformation. The entanglements more or less remain firmly in place, but may occasionally slip and become disentangled. The loss modulus, which is a measure of this dissipated energy, also reaches a maximum.

In PET structures, below the glass transition temperature (T_g) modulus decrease is not significant. It is important to mention that modulus in the glassy state is determined primarily by the strength of the intermolecular forces and the way the polymer chains is packed. At higher temperatures, mobility increases and the molecules lose their packing arrangement. Near the glass transition, the storage modulus drops significantly. All chain segments cannot store more energy for a given deformation than a rubbery segment which is free to move. Thus, every time a stressed frozen segment becomes free to move, excess energy is dissipated and consequently there is an abrupt fall near the glass transition region.

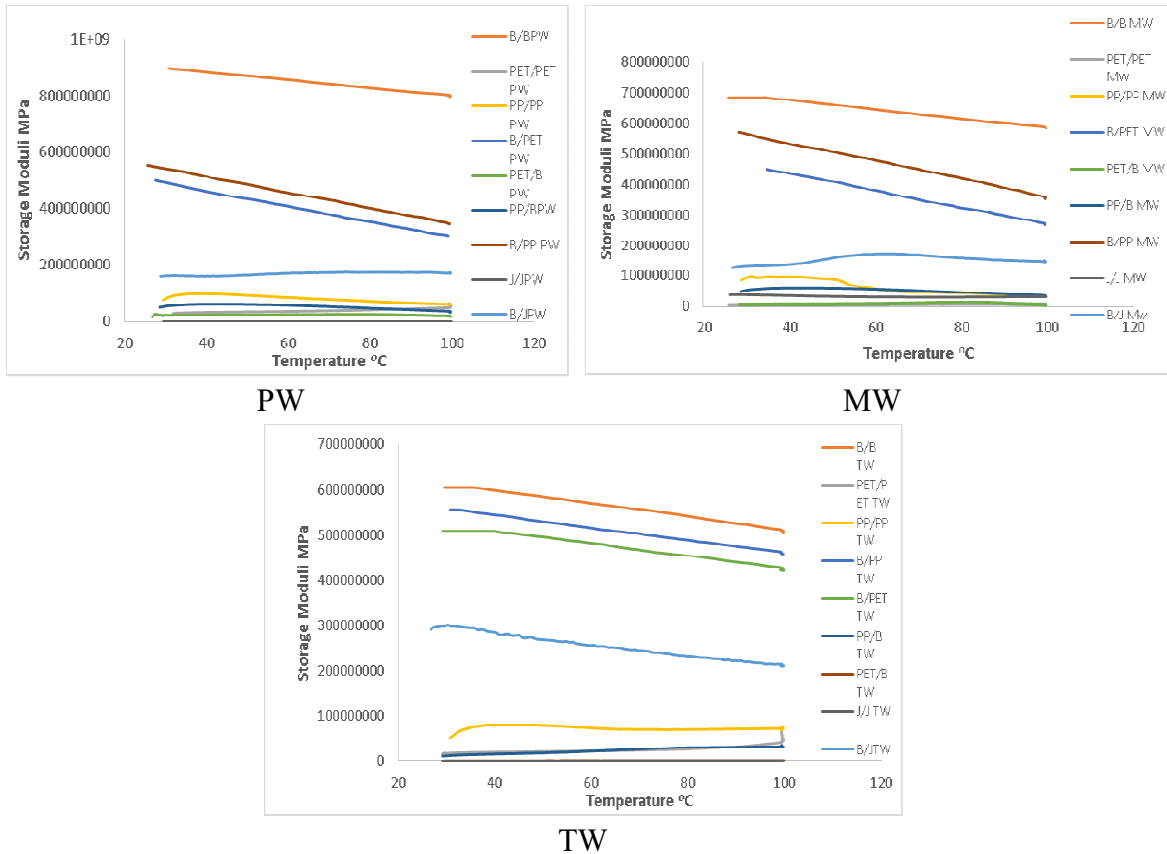


Figure.4.20: Storage moduli of different weaves.

The loss tangent or $\tan \delta$ is a ratio of the loss modulus to the storage modulus and is measured as the mechanical loss or damping factor. The damping properties of the material act to balance between the elastic and viscous phases in a polymeric structure. Material with higher $\tan \delta$ suggests that more heat was produced and more deformation could not be recovered when external force was removed. In nature, $\tan \delta$ is the response of inner frictional forces. The variation of $\tan \delta$ of non-hybrid and the hybrid fabrics as a function of temperature is presented in Figure 4.21. It can be observed that there was a decreasing trend in the loss tangent over the temperature range. This can be justified by the restriction of the motion of polymer chains resulting from the incorporation of rigid fibers. In this case, the incorporation of basalt fibers for hybrid fabrics, which act as barriers to the mobility of polymer chain, led to a lower degree of molecular motion and consequently lower damping characteristics. Matt weave structure shows lower value of $\tan \delta$ showing fabrics have better impact resistance under elevated temperatures.

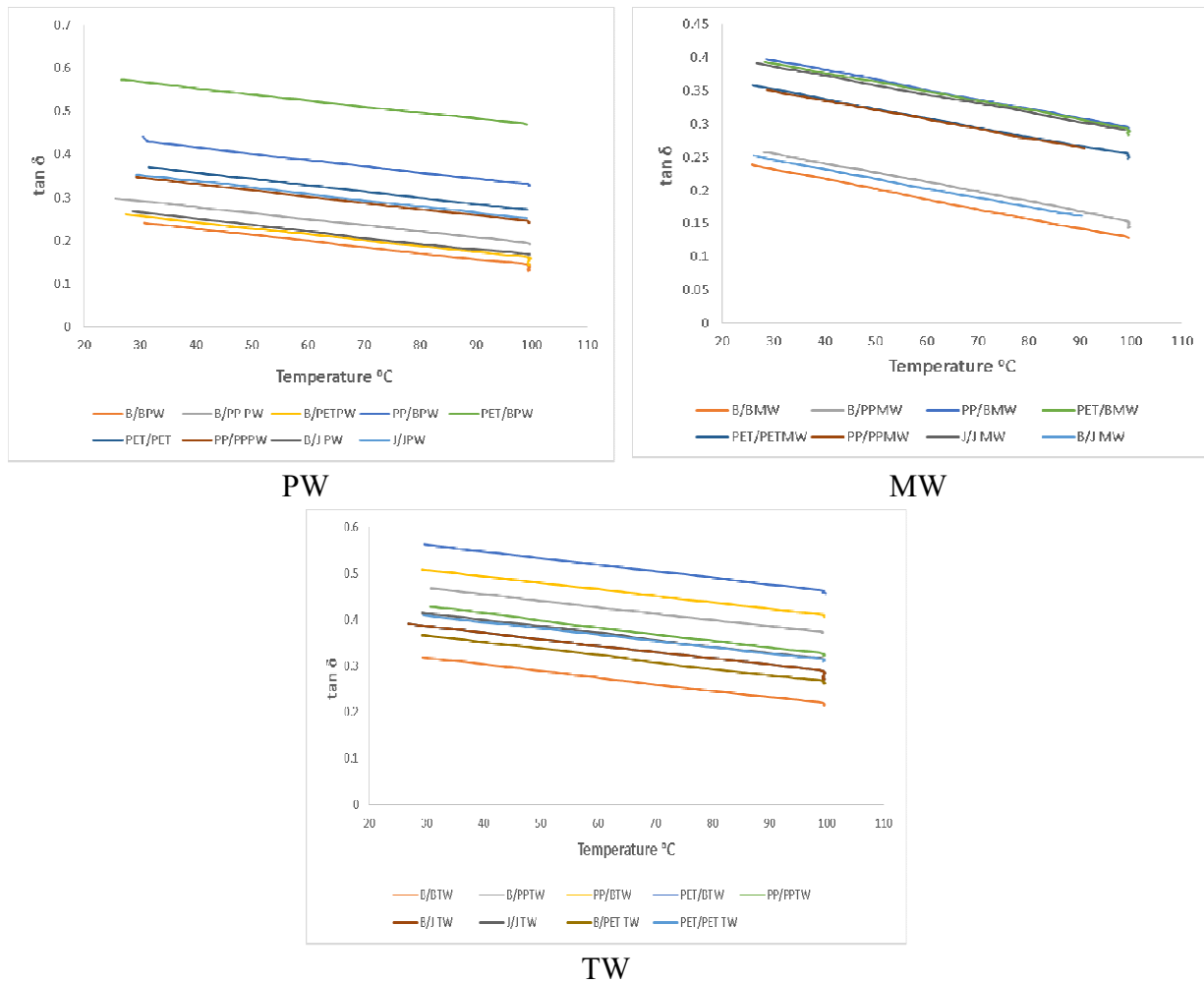


Figure 4.21: $\tan \delta$ of different weaves.

4.5.4 Thermal and transmission related properties

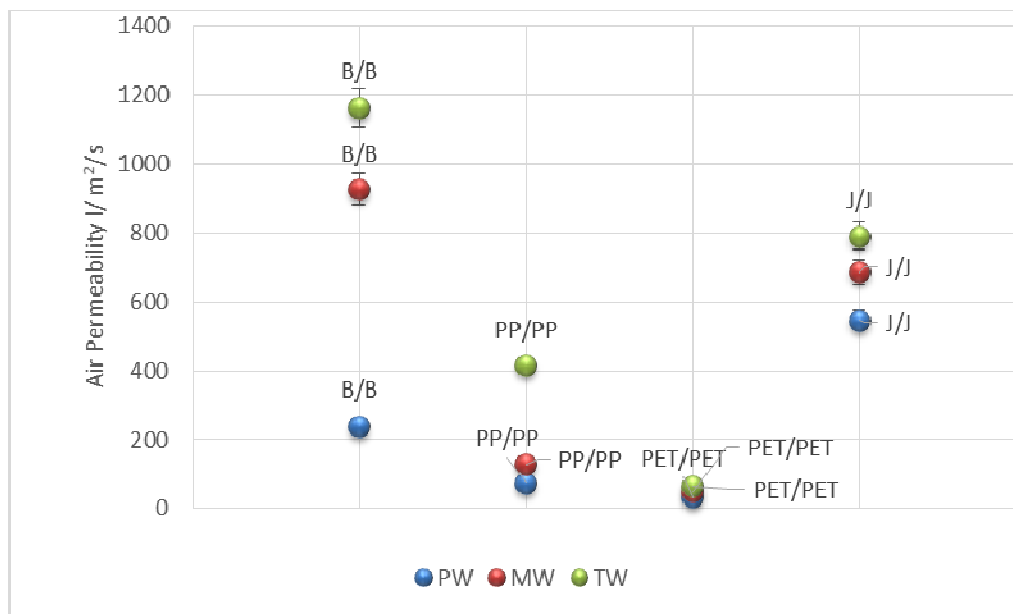
Air permeability

Air permeability is one of the important property of woven fabrics. In general, thermal properties of textiles including thermal conductivity and thermal resistance, are influenced by fabric structure, density, material and properties of fibers, surface treatments, air permeability, temperature, and humidity. Generally, air permeability depends on the material of constitutive yarns and structural parameters (type of weave, type of yarn (spun or filament), yarn size (linear density), twist factor in the yarn, thread density (ends and picks), and crimp%, and thickness of the fabric. Denting also affect air permeability. In most cases, structural parameters are far more important. Porosity plays the crucial role among them. Studies on the structural factors influencing the air permeability of fabrics assume that airflow takes place in the spaces between yarns. Therefore the inter-yarn pore is an important parameter influencing the openness of the fabric structure. It is not necessary that fabric with high porosity must have high air permeability especially for thicker structures as air permeability depends on shape and diameters of pores as

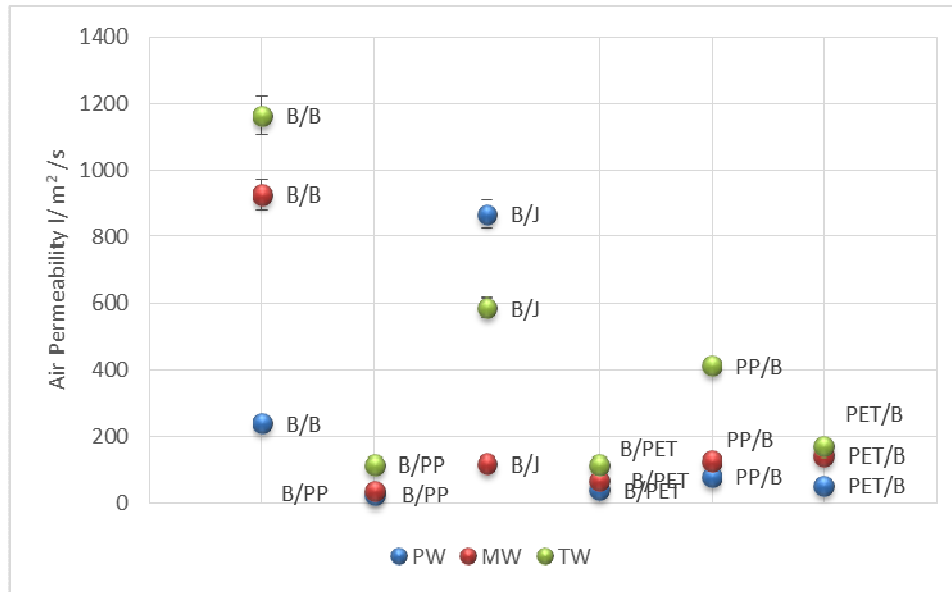
well. During transport of air through the woven fabrics, part of the energy of air is used to overcome the friction of the fluid on the fabric and the rest to surmount the inertia forces. So when the size of pores decreases, the fluid friction on the fabric decreases. Among non-hybrid structures as shown in Fig. 4.22, B/B has highest value of air permeability, because of open structure resulting from smaller yarn diameter due to higher density of fibers. It is followed by jute/jute combination. jute/jute has lower permeability than B/B due to hairy structure of yarn which blocks the inter yarn spaces. Among all the non-hybrid structures, twill has highest porosity, followed by matt and plain respectively.

Among non- hybrid fabrics, the bigger differences observed between the air permeability values of the plain and twill fabrics are due to differences in their characteristic covering properties. For equivalent weaving parameters, twill fabric has a lower fabric density and thus higher porosity, resulting in a looser structure because of lower number of yarn intersections compared to the plain fabrics. Thus the twill fabrics are much more permeable to air than the plain fabrics.

Among most hybrid woven structures, 1/3 twill woven fabrics show highest air permeability with the exception of B/J twill fabric due to higher cohesiveness of yarns resulting from surface hairiness. Twill weave has lower number of cross-over points and longer yarn floats as compared to other weaves. It is noted that most of the air flow takes place through the gaps between warps and wefts due to the nature of air, i.e air always finds its easiest way to flow.



(a) Non hybrid



(b) Hybrid

Figure. 4.22: Air permeability of various hybrid and non-hybrid woven structures.

The B/J plain woven fabric has highest permeability due to highest fractional porosity which is attributed to jute which is a staple yarn, having more irregularities in fiber structure as well as yarn structure so more inter-fiber porosity and inter-yarn porosity. Twill has higher value of air permeability compared to matt weave due to less interlacement, more number of pores in its weave structure.

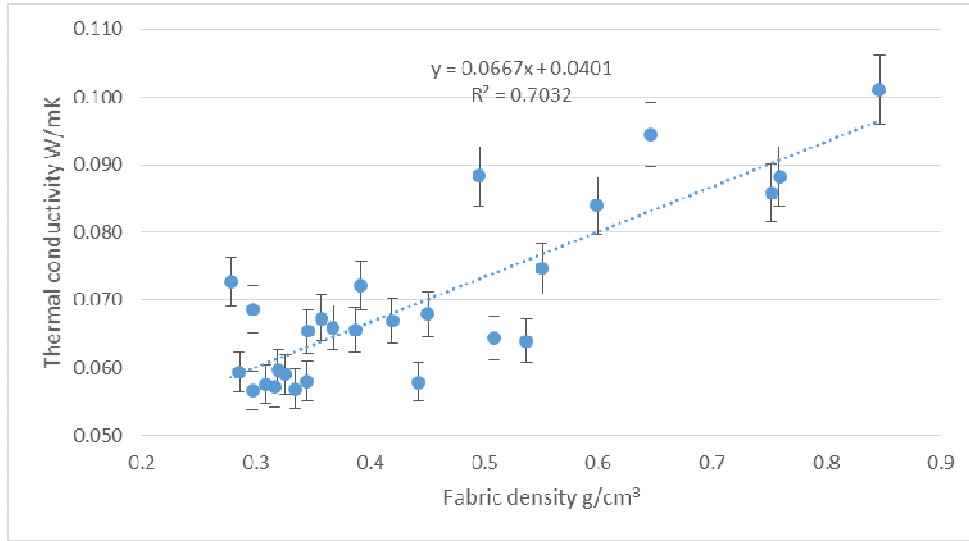
Among all hybrid structures, highest air permeability is observed in B/J structures that is because of higher yarn porosity in jute, while in other structures i.e B/PP, PP/B, B/PET and PET/B lower air permeability is observed because of compact structure in filament yarns. The PP yarn is relatively bulkier among the filament yarns and it results in a better cover of the fabric, therefore less permeable to air, which is also investigated by other researchers.

From this analysis it was found that samples woven in twill weave have nearly 5- 25% higher air permeability compared to plain structures for the same sett (thread density) of the woven fabrics. This is due to the fact that pores in plain weave (pore type No.1) are the least influenced by denting and allow the lowest air permeability. Plain weave fabrics also have the most stable structure due to the highest number of interlacing points of warp and weft and that prevents yarns from grouping. Matt weaves have two equal floats in both sides of fabric which helps in its grouping and ultimately results in moderate size of pores. Twill weaves have a lower number of interlacing points and larger floats of threads, which tend to group together resulting in a bigger size of pore between groups of adhering yarn floats and consequently in a higher air permeability.

Thermal properties

Thermal conductivity of textile fibers is generally dependent on their chemical composition, porosity and moisture content. In all structures fabric density has significant effect on thermal

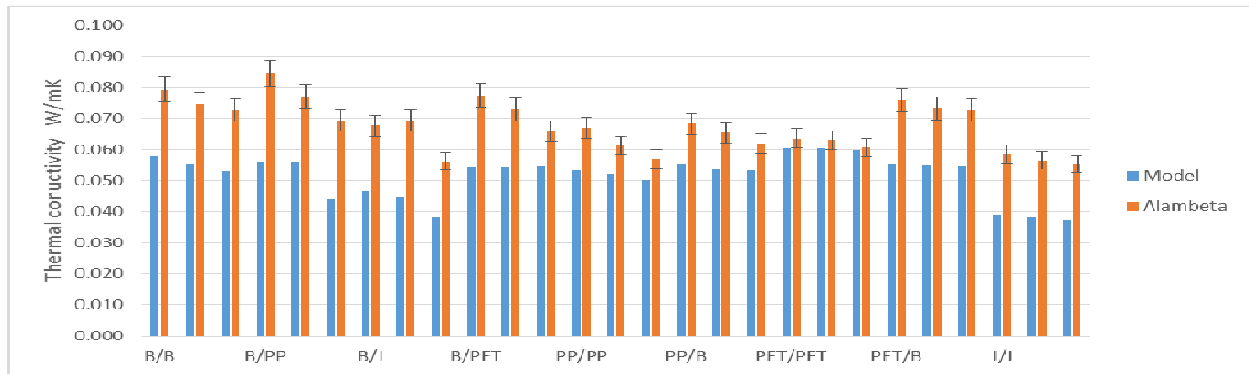
conductivity. As fabric density increases thermal conductivity also increases.



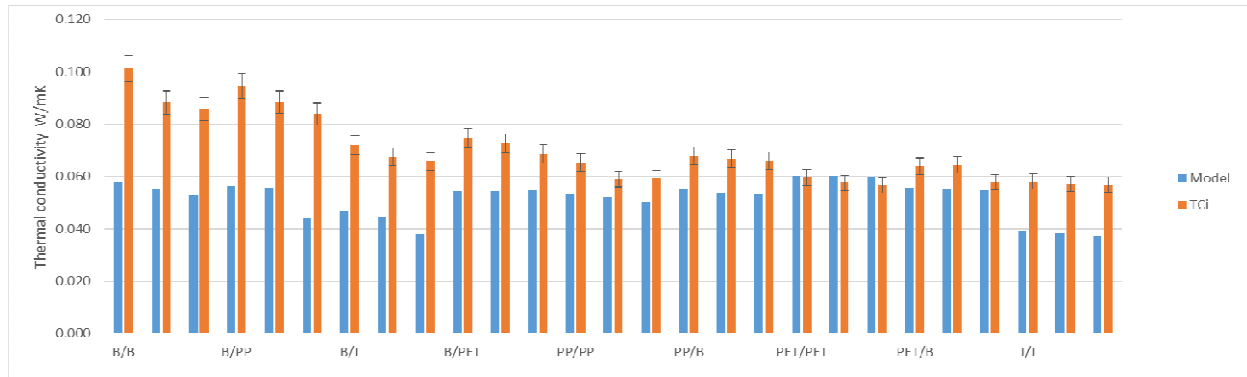
| Equation $y = a + b*x$ | Value | t-test Significance “Yes” or “No” | Adj. R-Square | F-test Significance “Yes” or “No” |
|---------------------------|--------|---|---------------|---|
| Intercept | 0.0401 | Yes | 0.7032 | Yes |
| Slope | 0.0667 | Yes | | |

Figure 4.23: Thermal conductivity VS fabric density.

The thermal conductivity was calculated using the theoretical model explained in equations 2.7, 2.8 and 2.9.



(a) Alambeta

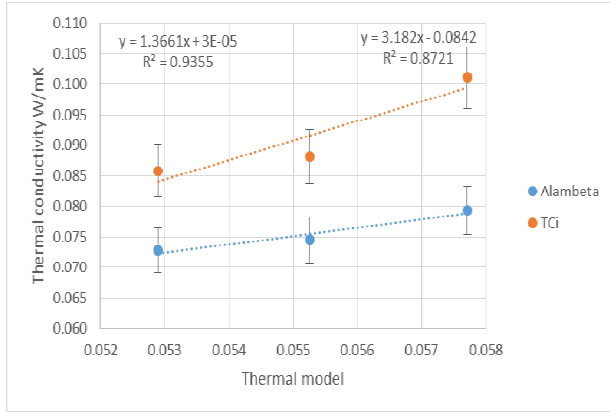


(b) TCI

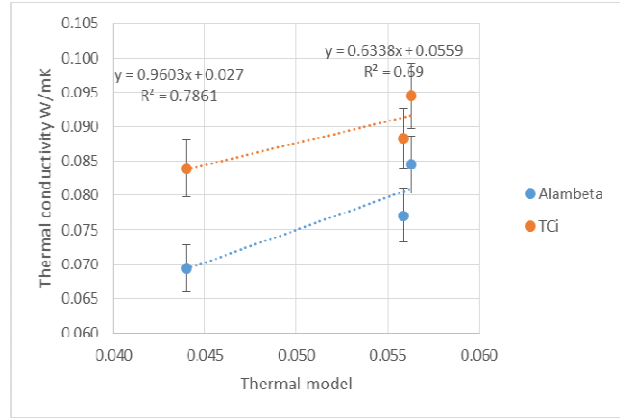
Figure 4.24: Theoretical model and measured thermal conductivity.

Among all structures as shown in Fig. 4.24, plain weave has highest thermal conductivity due to maximum interlacement and thus increase in fabric density. The fabric with a twill pattern has lower number of cross over points, longer yarn floats and, as a result, lower yarn crimps than the fabric with a plain pattern for the same warp and weft densities. This results in a looser and more open structure in twill fabrics. Consequently, as also mentioned in literature, the thermal conductivity values of the plain fabrics are higher than corresponding values of the twill fabrics. Among all structures, thermal conductivity of 100% basalt fabric is highest followed by structures having PP and PET yarns. Although basalt fiber has low value of thermal conductivity but in case of fibrous structures e.g. yarns and woven fabrics, thermal properties are greatly influenced by the porosity which is around 65-85%. Basalt yarn has a compact structure and thus less porosity than PET and PP structures. Between PET and PP structures, the later has higher packing density and thus higher thermal conductivity. Thermal conductivity of hybrid structures are increasing by adding basalt yarn due to the reason mentioned above.

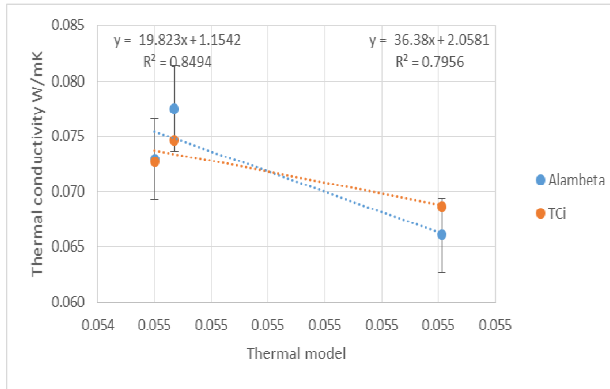
The parallel/series structure gives a firsthand prediction and gives reasonable prediction accuracy for practical application due to its simplicity as shown in Fig. 4.25. From theoretically calculated indicators of thermal conductivity, it is clear that the measured values with device Alambeta are most similar to theoretical values of samples.



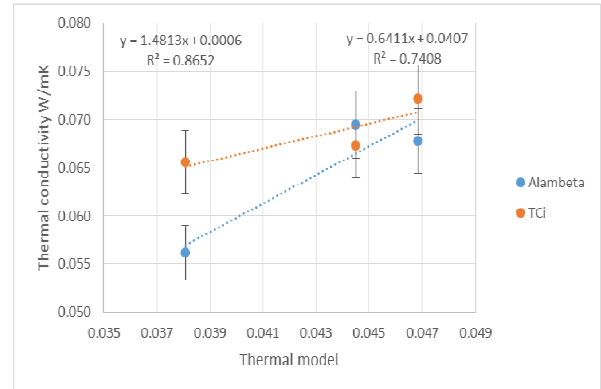
B/B



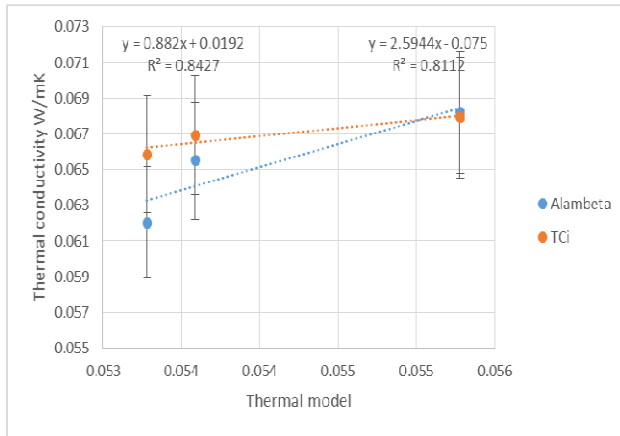
B/PP



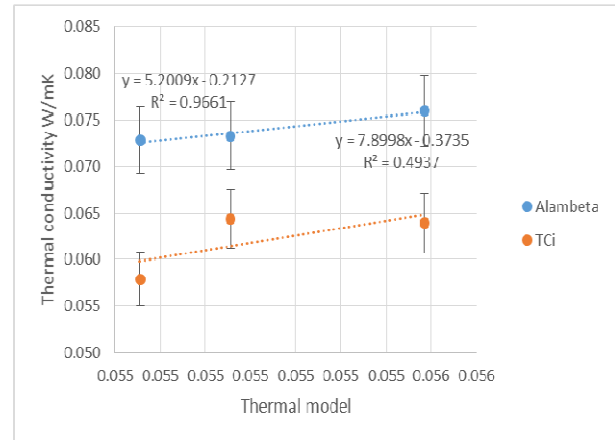
B/PET



B/Jute



PP/B



PET/B

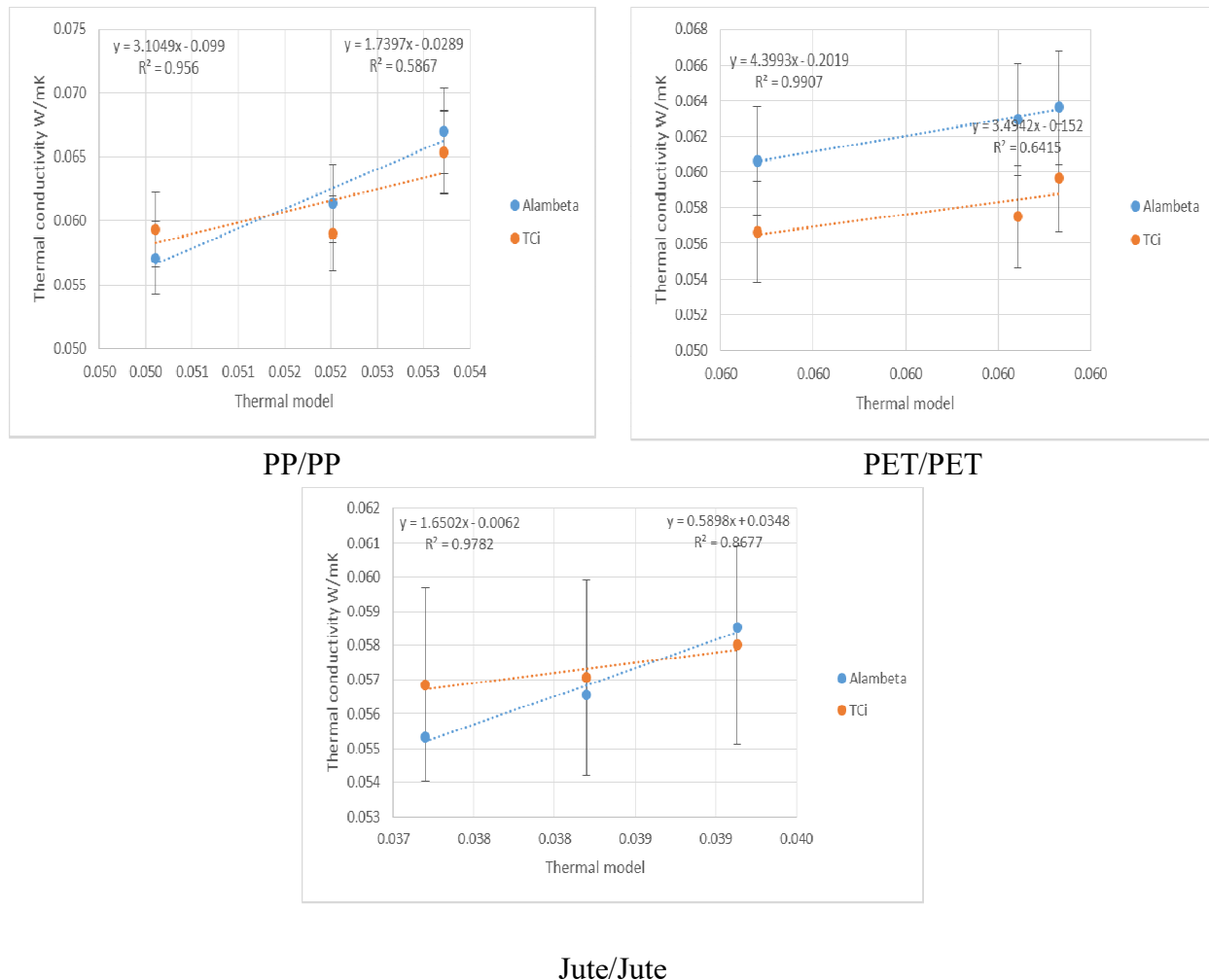


Figure 4.25: Correlation of thermal conductivity from Alambeta, TCi and theoretical model.

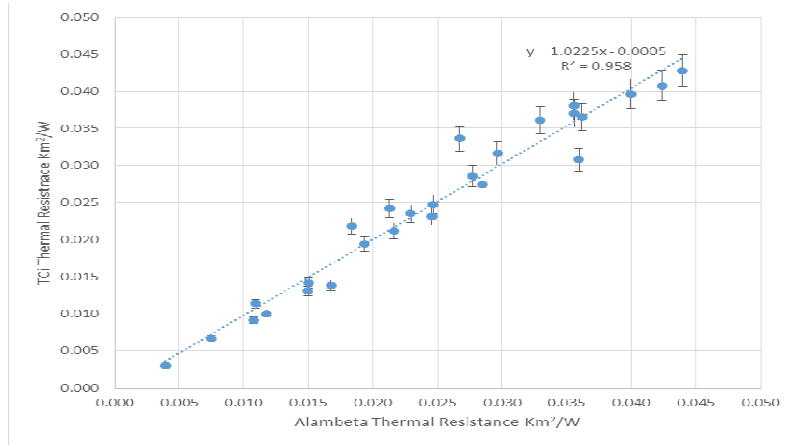
Thermal resistance

Thermal insulation properties are mainly dependent on thermal resistance properties. All thermal properties e.g. intra-fiber (chemical composition, fines, cross-section of component fibers), inter-fiber (yarn structure and properties) and inter-yarn (fabric physical and structural characteristics) are taken into account. Any textile material will offer some resistance against the transmission of heat because of the air traps within the individual fibers (intra fiber porosity) and also between fibers (inter fiber porosity). Higher the thermal resistance value, lower will be the heat loss.

Correlation of thermal resistance calculated from TCi and alambeta measurements

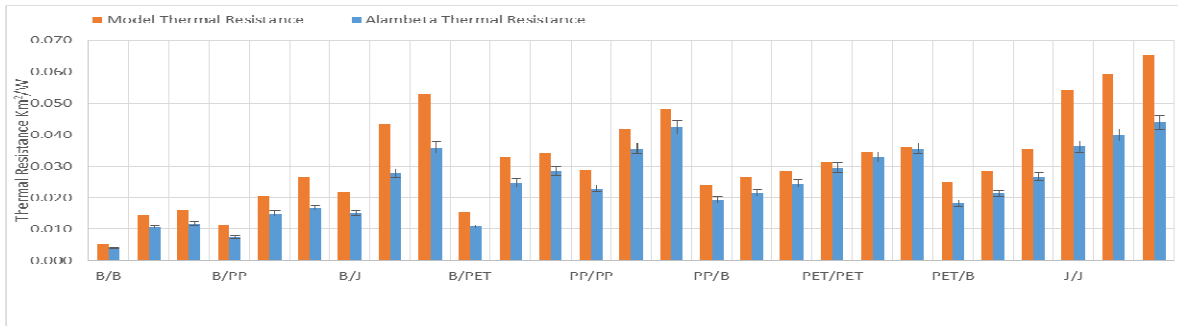
The measurements from TCi and alambeta instrument are correlated based on thermal conductivity and thermal resistance. The correlation of the two instruments for thermal resistance is shown in Fig. 4.26. The thermal resistance of both the instruments are correlated well with R² = 0.95. A relationship between theoretical calculations and actual measurements of thermal resistance by Alambeta and TCi is shown in Fig. 4.27(a&b). It has given reasonable prediction

accuracy for practical applications.

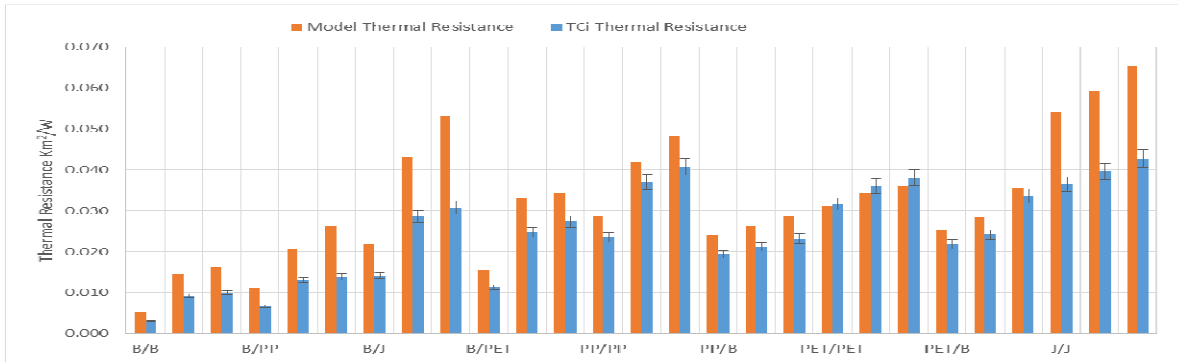


| Equation $y = a + b \cdot x$ | Value | t-test Significance “Yes” or “No” | Adj. R-Square | F-test Significance “Yes” or “No” |
|---------------------------------|--------|---|---------------|---|
| Intercept | 0.0005 | Yes | 0.958 | Yes |
| Slope | 1.0225 | Yes | | |

Figure 4.26: Correlation of thermal resistance from TCI and Alambeta

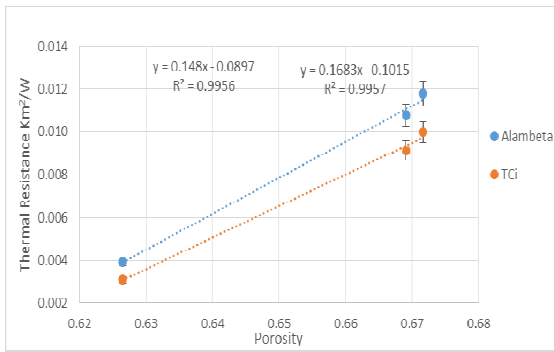


(a) Alambeta

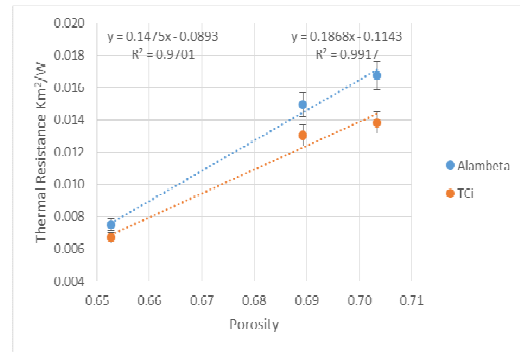


(b) TCI

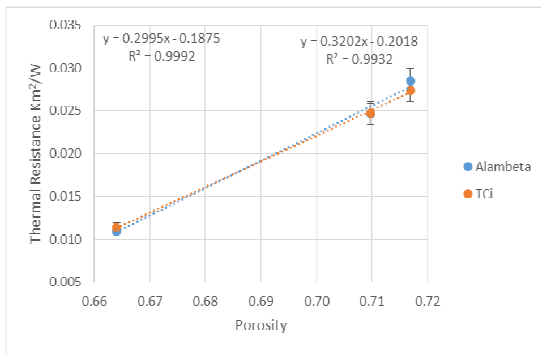
Figure 4.27: Thermal resistance from theoretical model and measured values.



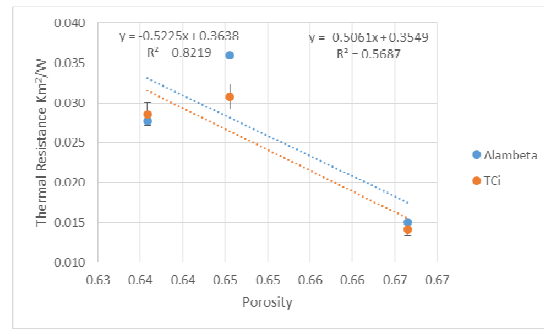
B/B



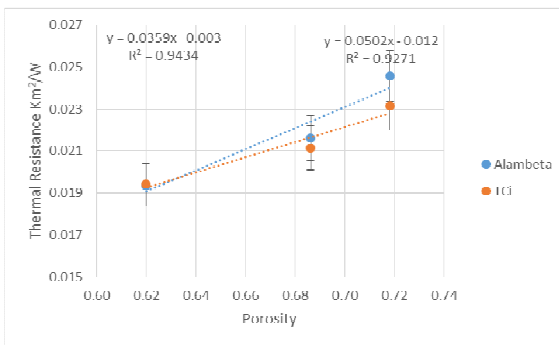
B/PP



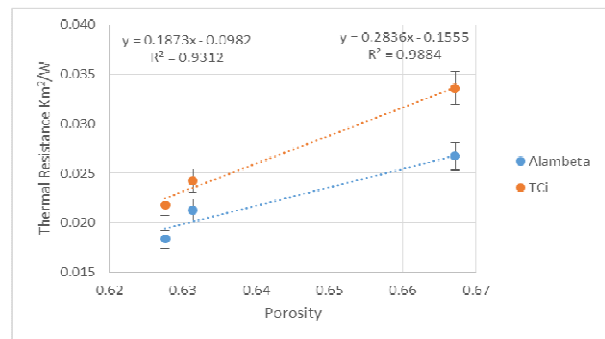
B/PET



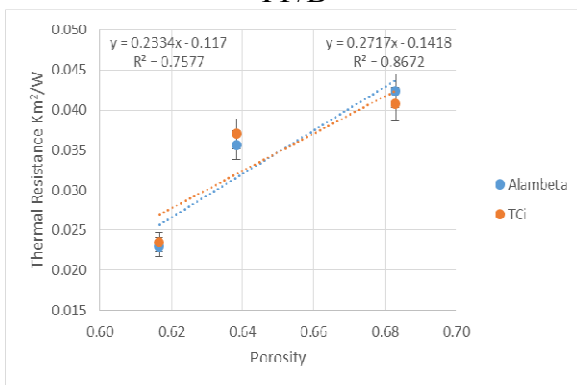
B/Jute



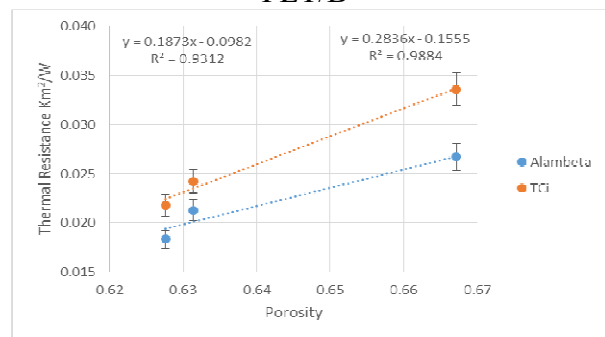
PP/B



PET/B



PP/PP



PET/PET

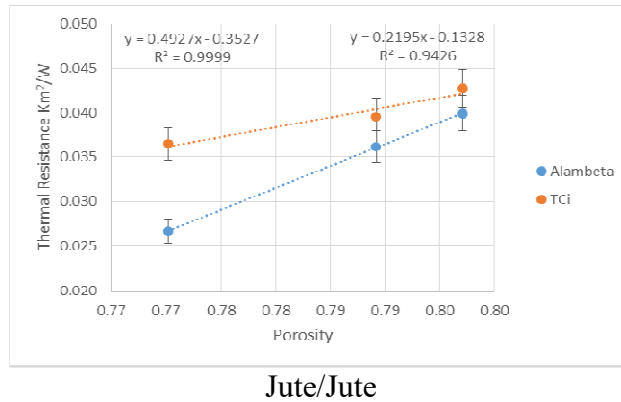
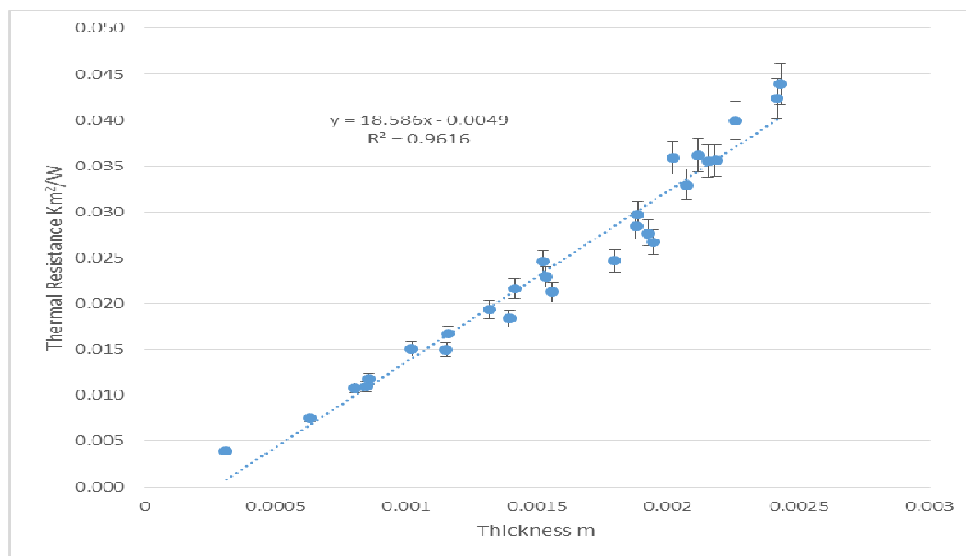


Figure 4.28: Correlation of thermal resistance from alambeta and TCi vs porosity.

Correlation between results from alambeta and TCi with porosity is significant as shown in Fig. 4.28. Among all structures, jute based fabrics have higher thermal resistance values because of inter fiber micro pores and inter yarn (macro porosity). Jute fiber has empty lumens in the cells, this hollow nature may increase intra fiber porosity. Also natural fibers have smaller diameter so by decreasing the diameter, the number of fibers increases for same linear density of yarn and thus increases the total volume of air pockets within the yarn and fabric structure. Secondly, as because it is a staple yarn, it has more hairiness on the surface and thus increases content of air pores in the fabric. Physical clogging of air will lead to increase in thermal insulation. With the addition of basalt fiber, thermal resistance of hybrid fabrics decreased. In all hybrid structures using basalt in warp, B/Jute has highest thermal resistance due to the reason explained above. Similar results are obtained by many researchers for increasing jute % in knitted structures. Higher level of hairiness results in more physical clogging of air which leads to increased thermal insulation. B/PET has second highest value of thermal resistance as the PET yarn is more bulky and has less twist so it has higher thermal resistance value than PP.



| Equation $y = a + b*x$ | Value | t-test Significance “Yes” or “No” | Adj. R-Square | F-test Significance “Yes” or “No” |
|---------------------------|--------|---|---------------|---|
| Intercept | 0.0049 | Yes | 0.96 | Yes |
| Slope | 18.586 | Yes | | |

Figure 4.29: Thermal resistance vs thickness.

Among all hybrid structures where basalt is used in warp, twill weaves have highest resistance followed by Matt and Plain respectively, although this effect is not significant in case of B/PP and B/PET. Twill weaves have a lower number of interlacing points and larger floats of threads, which tend to group together, there is lower yarn crimp, so more loser/bulky structure leading to clogging of higher volume of air. The overall thickness of fabric is also higher for twill fabric consequently giving higher thermal resistance. Matt weaves have two equal floats in both warp and weft direction of fabric which help in yarn grouping resulting moderate size of pores. In matt structure, due to floating of yarn on both surfaces, clogging of air occurs.

Among all weave structures, plain has minimum thermal resistance because of structural compactness and only one types of macro-pores in their structure. Plain woven fabrics also have more dense structure due to the highest number of interlacing points of warp and weft and that prevents yarns from grouping.

It is stated by many research workers that thermal resistance of fabric largely depends on the fabric thickness. They have used different levels of pressure in their experiments and measured conductivity. In the case of fabrics made of the same fibers, the thermal resistance depends mainly on fabric thickness and is directly proportional to it. The fabrics investigated in the present work are characterized by different thicknesses depending on the weave and different fiber composition. The thermal resistance is also strongly correlated with thickness in the present study as is shown in Fig. 4.29.

A surface plot provides a three-dimensional view of how the factors affect the response. Minitab plots the values for the x- and y-factors (predictors) on the x- and y-axes, while a continuous surface represents the values for the z-factor (response). Minitab uses interpolation to create the surface area between the data points. A contour plot provides a two-dimensional view in which the settings that produce the same response are shown as contour lines of constant responses. For a more complete interpretation, use a surface plot with a contour plot.

As it is obvious from one axis of graph, thickness has a direct relation with thermal resistance. As thickness increase, thermal resistance increase. As porosity increase, thermal resistance also increases. For the thermal resistance, the 3D surface plot shows that the highest thermal resistance values were found near an average thickness of 0.0025 m and average porosity of 0.80. For the thermal resistance data, the contour plot shows that the highest thermal resistance values were found near an average thickness of 0.0025 m and average porosity of 0.80.

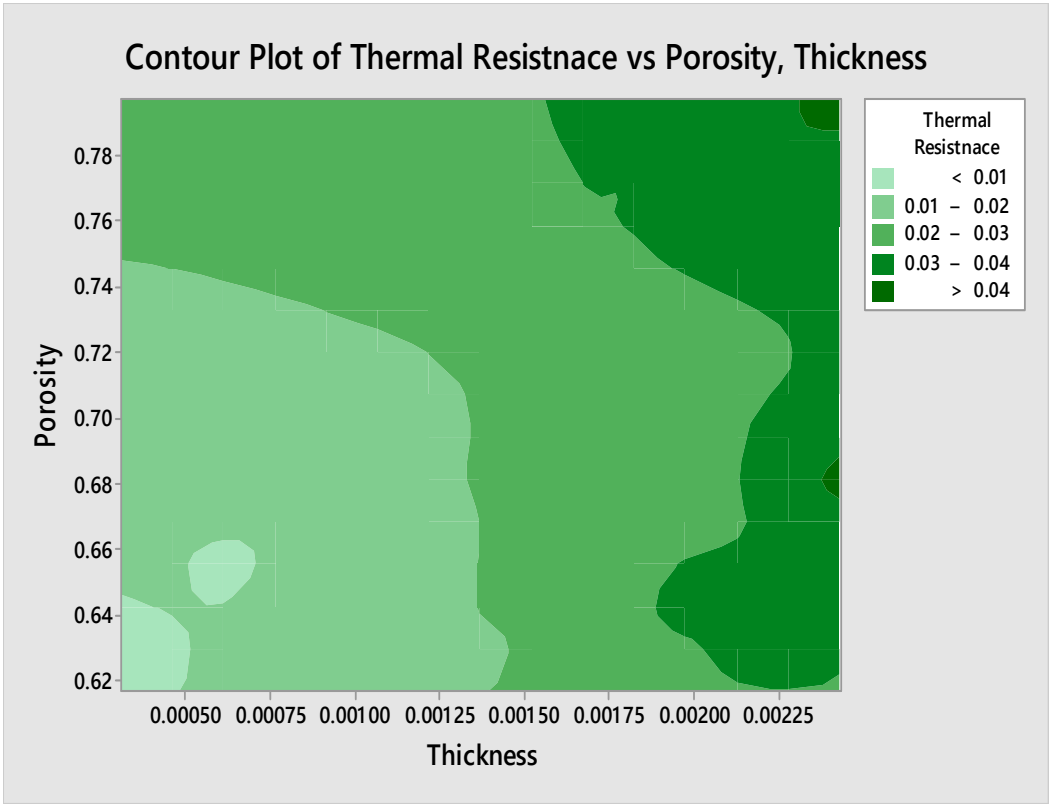
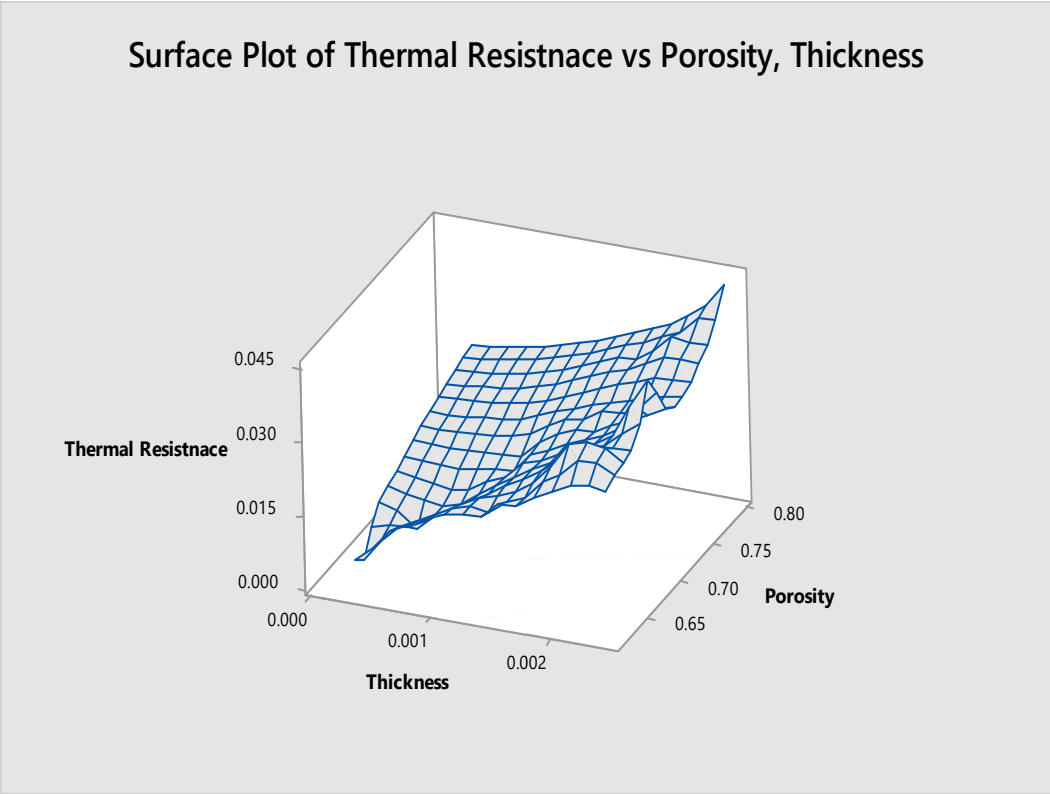


Figure 4.30: Dependence of thermal resistance on thickness and porosity.

Various thermal and transmission related properties for hybrid and non-hybrid fabrics are summarized in Table 4.21.

Table 4.21: Thermal and transmission properties of hybrid and non-hybrid fabrics.

| Sr. No. | Structures | Air permeability (l/m ² /s) | Thermal Conductivity by Alambeta (W/mK) | Thermal Conductivity by TCi (W/mK) | Thermal Resistance by Alameta Km ² /W | Thermal Resistance by TCi Km ² /W |
|---------|--------------|--|---|------------------------------------|--|--|
| S1. | B/B PW | 208.00 | 0.079 | 0.101 | 0.004 | 0.003 |
| S2. | B/B MW | 851.13 | 0.075 | 0.088 | 0.011 | 0.009 |
| S3. | B/B TW | 878.89 | 0.073 | 0.086 | 0.012 | 0.010 |
| S4. | PP/PP PW | 74.76 | 0.067 | 0.065 | 0.023 | 0.024 |
| S5. | PP/PP MW | 128.00 | 0.061 | 0.059 | 0.036 | 0.037 |
| S6. | PP/PP TW | 414.22 | 0.057 | 0.059 | 0.042 | 0.041 |
| S7. | PET/PET PW | 34.59 | 0.064 | 0.060 | 0.030 | 0.032 |
| S8. | PET/PET MW | 49.36 | 0.063 | 0.057 | 0.033 | 0.036 |
| S9. | PET/PET/TW | 64.94 | 0.061 | 0.057 | 0.036 | 0.038 |
| S10. | Jute/Jute PW | 546.44 | 0.059 | 0.058 | 0.036 | 0.037 |
| S11. | Jute/Jute MW | 685.44 | 0.057 | 0.057 | 0.040 | 0.040 |
| S12. | Jute/Jute TW | 789.80 | 0.055 | 0.057 | 0.044 | 0.043 |
| S13. | B/PP PW | 57.99 | 0.084 | 0.095 | 0.008 | 0.007 |
| S14. | B/PP MW | 89.82 | 0.077 | 0.088 | 0.015 | 0.013 |
| S15. | B/PP TW | 118.13 | 0.069 | 0.084 | 0.017 | 0.014 |
| S16. | B/PET PW | 40.53 | 0.078 | 0.075 | 0.011 | 0.011 |
| S17. | B/PET MW | 69.84 | 0.073 | 0.073 | 0.025 | 0.025 |
| S18. | B/PET TW | 116.00 | 0.066 | 0.069 | 0.028 | 0.027 |
| S19. | B/Jute PW | 867.22 | 0.068 | 0.072 | 0.015 | 0.014 |
| S20. | B/Jute MW | 320.80 | 0.069 | 0.067 | 0.028 | 0.029 |
| S21. | B/Jute TW | 586.00 | 0.056 | 0.066 | 0.036 | 0.031 |
| S22. | PP/B PW | 82.28 | 0.068 | 0.068 | 0.019 | 0.019 |
| S23. | PP/B MW | 128.00 | 0.066 | 0.067 | 0.022 | 0.021 |
| S24. | PP/B TW | 414.22 | 0.062 | 0.066 | 0.025 | 0.023 |
| S25. | PET/B PW | 54.22 | 0.076 | 0.064 | 0.018 | 0.022 |
| S26. | PET/B MW | 145.75 | 0.073 | 0.064 | 0.021 | 0.024 |
| S27. | PET/B TW | 172.55 | 0.073 | 0.058 | 0.027 | 0.034 |

4.5.5 Electrical properties

In Table 4.22, the average values of volume and surface resistance, volume and surface resistivities, fractional porosity, no. of pores, cover factor etc. are given. All the discussion is based on the results of measured volume resistance as it gives more accurate value of electrical resistance of fabric, because of different interlacing structure related to the thickness of the fabrics.

Table 4.22: Calculated porosity and measured resistance of samples.

| Sample No. | Structure | Fractional porosity [%] | No. of pores/cm ² | Cover factor % | R_s [Ω] | ρ_s [Ω .cm] | R_v [Ω] | ρ_v [Ω .cm] |
|------------|-------------------|-------------------------|------------------------------|----------------|--------------------|--------------------------|--------------------|--------------------------|
| S1. | B/B (Plain) | 0.63 | 88.34 | 81.80 | 2.13E+11 | 2.13E+12 | 1.31E+11 | 8.36E+13 |
| S2. | B/B (Matt) | 0.67 | 92.94 | 75.61 | 2.62E+11 | 2.62E+12 | 1.64E+11 | 4.06E+13 |
| S3. | B/B (Twill) | 0.67 | 88.34 | 75.77 | 1.81E+11 | 1.81E+12 | 1.54E+11 | 3.59E+13 |
| S4. | PP/PP (Plain) | 0.65 | 80.86 | 75.71 | 1.26E+10 | 1.25E+11 | 1.21E+10 | 1.57E+12 |
| S5. | PP/PP (Matt) | 0.69 | 94.44 | 75.16 | 1.29E+10 | 1.29E+11 | 1.90E+10 | 1.73E+12 |
| S6. | PP/PP (Twill) | 0.70 | 85.42 | 75.52 | 1.55E+10 | 1.55E+11 | 1.38E+10 | 1.14E+12 |
| S7. | PET/PET (Plain) | 0.67 | 88.34 | 76.22 | 1.45E+10 | 1.44E+11 | 7.28E+09 | 7.70E+11 |
| S8. | PET/PET (Matt) | 0.64 | 100.03 | 75.75 | 1.59E+10 | 1.59E+11 | 1.33E+10 | 1.28E+12 |
| S9. | PET/PET (Twill) | 0.65 | 85.40 | 76.59 | 1.75E+10 | 1.75E+11 | 8.48E+09 | 8.65E+11 |
| S10. | Jute/Jute (Plain) | 0.66 | 91.17 | 76.33 | 1.29E+11 | 1.29E+12 | 8.49E+10 | 8.00E+12 |
| S11. | Jute/Jute (Matt) | 0.71 | 86.77 | 76.54 | 1.07E+11 | 1.07E+12 | 7.74E+10 | 7.16E+12 |
| S12. | Jute/Jute (Twill) | 0.72 | 86.76 | 76.55 | 7.44E+10 | 7.43E+11 | 4.78E+10 | 4.94E+12 |
| S13. | B/PP (Plain) | 0.62 | 92.94 | 79.30 | 8.23E+11 | 8.22E+12 | 3.10E+10 | 9.76E+12 |
| S14. | B/PP (Matt) | 0.64 | 106.29 | 78.31 | 1.58E+11 | 1.58E+12 | 1.16E+11 | 2.01E+13 |
| S15. | B/PP (Twill) | 0.68 | 92.94 | 75.63 | 7.61E+10 | 7.60E+11 | 6.21E+10 | 1.07E+13 |
| S16. | B/PET (Plain) | 0.62 | 92.94 | 79.38 | 2.32E+10 | 2.32E+11 | 1.32E+10 | 3.11E+12 |
| S17. | B/PET (Matt) | 0.69 | 93.10 | 79.37 | 2.07E+10 | 2.07E+11 | 1.35E+10 | 1.50E+12 |
| S18. | B/PET (Twill) | 0.72 | 97.63 | 79.09 | 1.60E+10 | 1.59E+11 | 1.33E+10 | 1.79E+12 |
| S19. | B/Jute (Plain) | 0.77 | 88.33 | 79.34 | 2.00E+11 | 2.00E+12 | 7.30E+10 | 1.43E+13 |
| S20. | B/Jute (Matt) | 0.78 | 97.67 | 78.62 | 1.53E+11 | 1.52E+12 | 7.77E+10 | 1.04E+13 |
| S21. | B/Jute (Twill) | 0.78 | 106.94 | 74.93 | 1.99E+11 | 1.99E+12 | 1.32E+11 | 1.47E+13 |
| S22. | PP/B (Plain) | 0.63 | 83.69 | 76.16 | 1.78E+11 | 1.77E+12 | 5.04E+10 | 7.62E+12 |
| S23. | PP/B (Matt) | 0.63 | 82.58 | 76.68 | 7.51E+10 | 7.50E+11 | 4.77E+10 | 6.72E+12 |
| S24. | PP/B (Twill) | 0.67 | 82.46 | 76.69 | 4.47E+10 | 4.47E+11 | 3.69E+10 | 4.83E+12 |
| S25. | PET/B (Plain) | 0.77 | 94.38 | 76.03 | 1.82E+10 | 1.82E+11 | 1.22E+10 | 1.61E+12 |
| S26. | PET/B (Matt) | 0.79 | 89.85 | 77.69 | 1.62E+10 | 1.61E+11 | 1.18E+10 | 1.95E+12 |
| S27. | PET/B (Twill) | 0.80 | 89.85 | 76.24 | 8.92E+09 | 8.91E+10 | 1.18E+10 | 1.21E+12 |

Because the samples do not contain any additional surface modification, surface resistance (which indirectly describes ability to conduct an electric current on the surface) should not be significantly different as compared to the volume resistance (which indirectly describes ability to conduct an electric current through the bulk of the material) and in addition there should be a relation between these two characteristics. Dependence between volume and surface resistance is shown in Fig. 4.31 (logarithmic scale for both axes is used). Volume resistance is increasing with increasing surface resistance and this relation can be approximated by power function. The solid line in this graph corresponds to the power regression model with parameters obtained by the minimizing sum of squared errors. Corresponding coefficient of determination $R^2 = 0.73$ indicates the good quality of fit. As in surface resistance, only surface pores are considered, so it does not give accurate results and also if hybrid structure with unbalance float is used, this effect can be more irregular. Therefore, for further investigation only volume resistance was used.

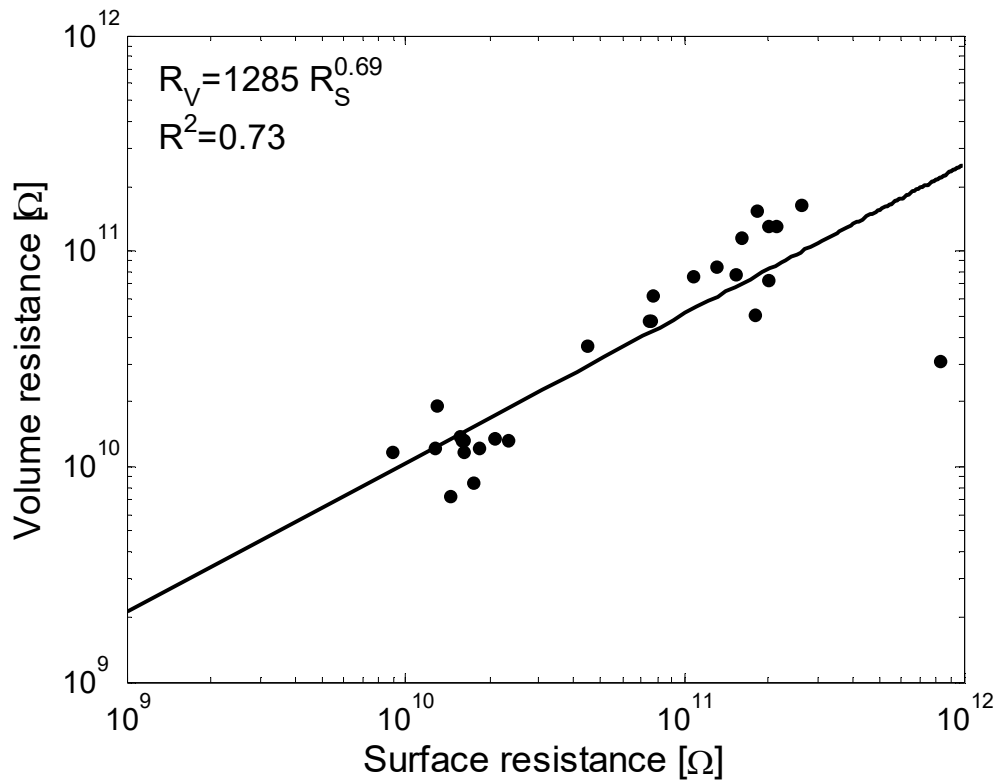


Figure 4.31: Dependence between volume resistance and surface resistance.

Figure 4.32 shows overall electrical resistances (mean values and 95 % confidence intervals) of all samples under investigation. It is visible that the highest electrical resistance is shown by 100 % basalt samples with twill and matt structures. There is no statistically significant difference between electrical resistances of twill and matt weave of B/B samples. On the other hand, statistically significant difference can be observed between samples with different material composition having the same weave pattern.

The electrical resistance values of the fabrics are mainly determined by the presence of air in the interstices i.e between the binding points of woven fabric. Air is a bad conductor of electricity showing resistivity at 20 °C ranging from $1.3E+16$ to $3.3E+16$. Plain and basket weaves belong to a group of similar weaves but the floating of yarns is different by direction: in plain weave – no floating takes place, in basket weave – two floating of each yarn in both directions and in twill woven samples there is floating over three consecutive yarns. The investigated samples differ with respect to the type of pores formed between the interlacing points, as shown in Table 4.19. It is evident that plain weaves have only one type of pore (Pore 1) while matt weaves have three types of pores (25 % of Pore 1, 50 % of Pore 3 and 25 % of Pore 4) and twill weaves have also three types of pores (25 % of Pore 1, 50 % of Pore 2 and 25 % of Pore 4).

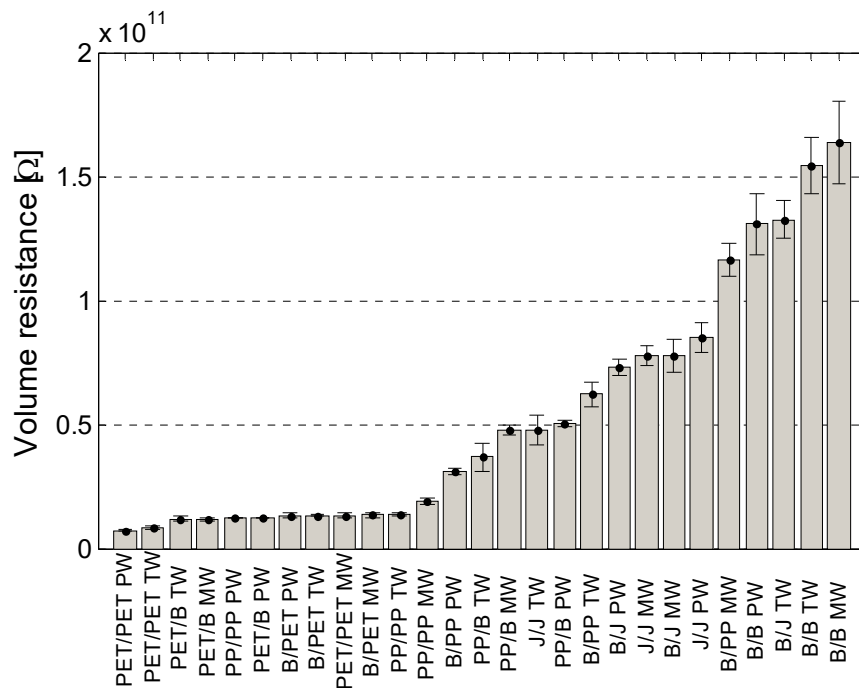
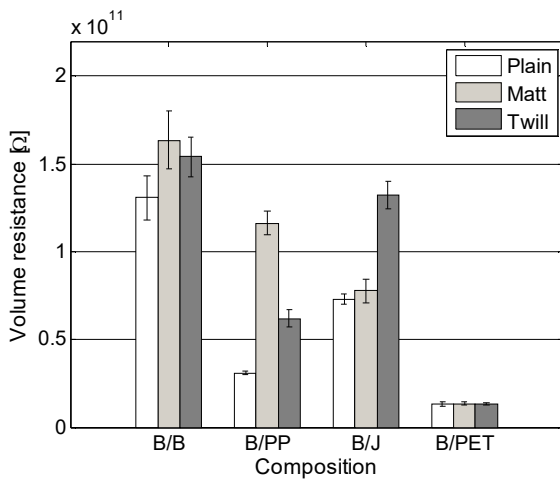


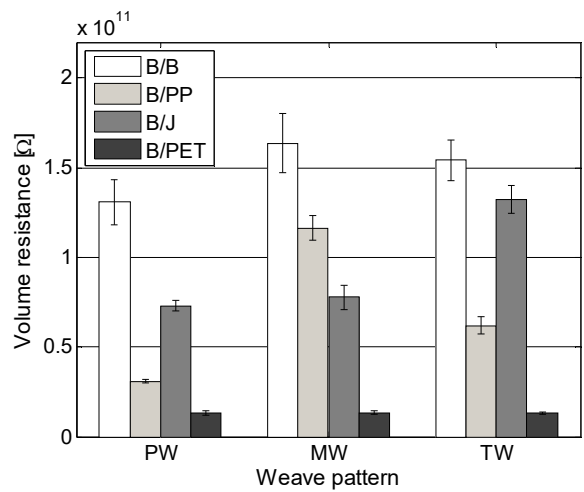
Figure 4.32: Volume resistance of all samples tested.

This effect is also visible from Figure 4.33(a), in which mean values and 95% confidence intervals of sample resistances are grouped according to the identical material composition. Based on exploratory data analysis it can be summarized that structure (weave pattern) has statistically significant effect on the resulting resistance especially for samples where one of the component is basalt and the second component is either basalt, polypropylene, polyester or jute. Plain woven structure has the lowest resistance which is in agreement with the pore analysis described above. The weave structure has negligible effect for B/PET samples. Figure 4.33(b) shows bar diagram for mean values together with 95 % confidence intervals for sample resistances grouped according to the identical weave pattern (structure). It was confirmed that material composition of warp and weft has statistically significant effect on resulting electrical resistance for all sample groups, whereas the highest resistance is observed in B/B samples and lowest resistance in B/PET samples.

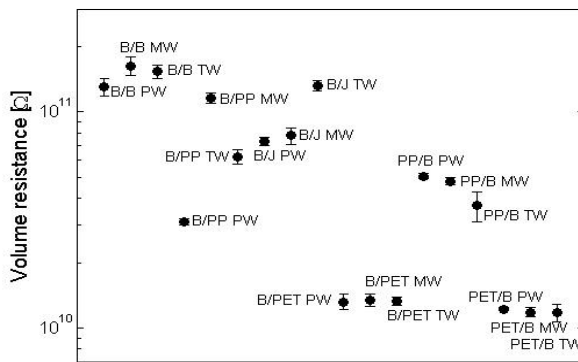
It can be seen (in Figure 4.33(c)) that on comparison of hybrid structures (when basalt is used in warp), it is quite clear that it has higher electrical resistance in all weaves. In all compositions, plain weave has lowest electrical resistance due to only one type of pores in it. Plain weave has relatively lower porosity parameters i.e. less number of pores and lower portion of open area as compared to matt and twill weaves. The 100% basalt plain woven fabric shows relatively lower electrical resistance because of smaller thickness, as thickness depends on yarn diameter or yarn fineness. Both matt and twill weaves have higher thickness because of longer floats. Matt weave shows highest number of pores and % open area, thus more air can be entrapped in the structure and offer more resistance to electric current.



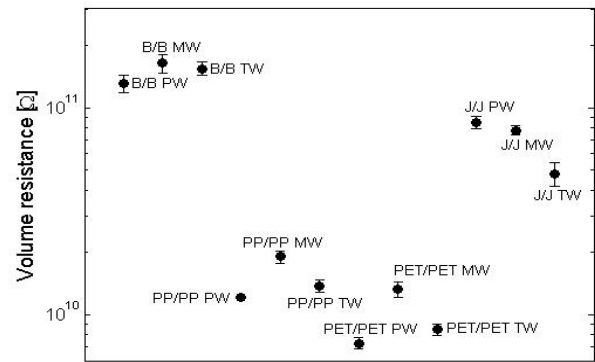
(a)



(b)



(c)



(d)

Figure 4.33: Volume resistance of (a) hybrid structures grouped according to the identical material composition, (b) hybrid structures grouped according to the identical weave pattern, (c) chosen basalt hybrid samples(d) non hybrid samples

It can also be observed that in all the hybrid structures, highest electrical resistance is in B/Jute structures. Although jute material has lower electrical resistivity than polypropylene and polyester, the synthetic fibers (PET & PP) tend to generate static electricity and thus exhibit lower resistance. Electrical properties are influenced by the size of electrostatic charge that is directly related to the size of the electrical resistance and thermal resistance of textile fabrics. Static electricity is the collection of electrically charged particles on the surface of a material; various materials have a tendency of either giving up electrons and becoming positive (+) in charge or attracting electrons or becoming negative (-) in charge. Some materials cause or create more static electricity than others. Static electricity can be generated on insulating materials surface by the following ways: charging by electrostatic induction, charging by friction, charging by ionizing radiation etc. The high resistivity of polymers allows large electrostatic charges to accumulate. *Antistatic* formulations of polymers have much reduced resistivity so that

electrostatic charge may be dissipated by leakage currents. Polyester is very sensitive to static electricity and this is may be major reason of its low value in all hybrid and non-hybrid structures. Jute is staple yarn and highly twisted while in other structures i.e. B/PP, PP/B, B/PET and PET/B the constituent yarns have lower amount of twist which leads to inherent yarn flatness, the fibers in the yarn spread out in the fabric resulting in smaller inter yarn pores.

Among hybrid structures where basalt is used in weft, plain weave shows maximum resistance, this may be due to increase in number of pores and % of open area as both PP and PET are filament yarns with very light twist and thus they become more flattened in twill weave due to relatively longer yarn floats.

It is also observed that among non-hybrid structures, B/B composition has highest electrical resistance followed by Jute/Jute. Although material engineering theory predicts that basalt and jute based materials should exhibit lower electrical resistivity than polyester and polypropylene, the deviation in electrical behavior may be due to static electricity generated on synthetic materials and relatively higher amount of twist in basalt as well as jute yarns. Among the different woven structures investigated, matt weave shows highest electrical resistance followed by twill weave except in Jute/Jute compositions. This may be because jute is a staple spun yarn having lot of hairiness on the surface, thus a higher level of porosity resulting in enhanced electrical resistance.

4.5.6 Acoustic properties

Researchers always seek new materials and arrangements to enhance the sound absorption efficiency. This work is based on previous studies on use of textiles as noise control elements. The factors that mainly determine a materials sound absorption property are its fiber type, fiber dimensions, material thickness, density, porosity and air flow resistance. Reports show that the use of nonwoven materials for noise reduction is based on inbuilt advantages such as porous fibrous structure, light weight, bulky in nature, economically low price and their versatility. They are more suitable for automotive and building industries and they can also absorb sound in order to decrease sound pollution in the environment. Currently, sound absorption materials commercially available for acoustic treatment consist of glass, mineral or synthetic fibers. A study on sound absorption characteristics of rock wool and glass fiber indicated that these fibers behave alike. A composite structure with a combination of perforated panel, rubber particle, porous material, polyurethane foam and glass wool were found to demonstrate significant sound attenuation. However, when the issue of safety, insulation, environment and health are considered, they pose interference to human health and surroundings. Thus, environmentally friendly materials of high flame resistance and high insulation as well as good sound absorption properties are needed.

From Fig. 4.34, it can be observed that, with the increase of frequency, the sound absorption coefficient (SAC) of all the samples increases. As is known that with the increase of frequencies, larger is the sound energy which accelerates the air vibration inside fabrics and creates the opportunities of friction between air and pore walls. This process causes sound energies to be converted into heat energies and gradually diminishes the sound effect. This is indicated as an

increase in SAC.

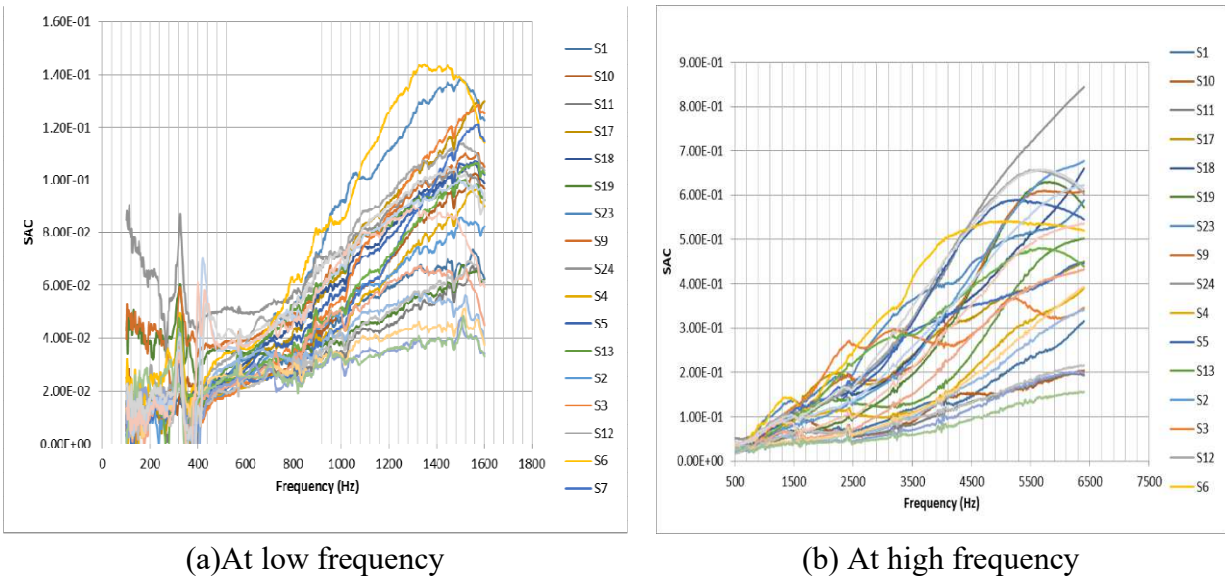


Figure 4.34: Sound absorption coefficient of all samples.

It can be seen that fabrics with polyester fiber have better SAC. The reason for better SAC of polyester fabrics may be finer fibers which results in higher number of fibers per unit weight of the material. This leads to higher total fiber surface area, and greater possibilities for a sound wave to interact with the fibers and ultimately dissipate inside the structure. 100% Jute and Basalt fabric shows lower SAC values in both frequency ranges. With the use of basalt fiber for hybrid structures SAC improves for all fabrics.

Porosity is one of the most important parameters which affect sound absorption. This effect can be explained in terms of the friction between the air inside the material (within pores, between fibers) and the solid walls of the material. Moreover when sound propagates within a porous material, it is reflected many times because there are several air-solid-air interfaces. Due to friction and to the multiple reflections within the pores, part of the energy associated with sound is transferred to the solid skeleton of the material, by making its particles vibrate, and therefore, it is dissipated.

As stated earlier, the viscous resistance of air in the porous material has an important influence on the sound absorption mechanism. Flow resistance has been used as an important parameter in theoretical estimations by many researchers. It is therefore important to consider the flow resistance of an acoustic sample.

Typically, perforated materials only absorb the mid-frequency range unless special care is taken in designing the facing to be as acoustically transparent as possible. Smaller denier yields more fibers per unit mass of the material; when the total fiber surface area increases, the possibilities frictional flow resistance of sound wave increases. Normal sound absorption coefficient was measured experimentally using the impedance tube for all samples having different grades of

porosity, pore size and pore opening. Static flow resistance could also measure acoustical performance. The parameters affecting airflow resistivity and noise reduction coefficient (NRC) are shown in Table 4.23.

Table 4.23: NRC and others parameters

| Sample No. | Structure | Porosity | Air flow Resistivity Pa s/m ² | Noise reduction coefficient NRC |
|------------|-------------------|----------|--|---------------------------------|
| S1. | B/B (Plain) | 0.63 | 3081854.043 | 0.032 |
| S2. | B/B (Matt) | 0.67 | 292267.5505 | 0.041 |
| S3. | B/B (Twill) | 0.67 | 265221.7724 | 0.037 |
| S4. | PP/PP (Plain) | 0.65 | 1741754.395 | 0.030 |
| S5. | PP/PP (Matt) | 0.69 | 715430.4029 | 0.039 |
| S6. | PP/PP (Twill) | 0.70 | 199683.709 | 0.033 |
| S7. | PET/PET (Plain) | 0.67 | 3066023.035 | 0.055 |
| S8. | PET/PET (Matt) | 0.64 | 1953844.908 | 0.066 |
| S9. | PET/PET (Twill) | 0.65 | 1428528.858 | 0.058 |
| S10. | Jute/Jute (Plain) | 0.66 | 172807.0901 | 0.028 |
| S11. | Jute/Jute (Matt) | 0.71 | 129107.6903 | 0.034 |
| S12. | Jute/Jute (Twill) | 0.72 | 104123.6289 | 0.029 |
| S13. | B/PP (Plain) | 0.62 | 5439858.825 | 0.045 |
| S14. | B/PP (Matt) | 0.64 | 1929528.226 | 0.079 |
| S15. | B/PP (Twill) | 0.68 | 1457075.467 | 0.054 |
| S16. | B/PET (Plain) | 0.62 | 5819123.035 | 0.054 |
| S17. | B/PET (Matt) | 0.69 | 1592776.11 | 0.077 |
| S18. | B/PET (Twill) | 0.72 | 917094.6442 | 0.059 |
| S19. | B/Jute (Plain) | 0.77 | 225878.5382 | 0.046 |
| S20. | B/Jute (Matt) | 0.78 | 323865.6605 | 0.061 |
| S21. | B/Jute (Twill) | 0.78 | 168958.8754 | 0.056 |
| S22. | PP/B (Plain) | 0.63 | 1841457.845 | 0.035 |
| S23. | PP/B (Matt) | 0.63 | 1103460.452 | 0.062 |
| S24. | PP/B (Twill) | 0.67 | 316821.0028 | 0.052 |
| S25. | PET/B (Plain) | 0.77 | 2644212.018 | 0.060 |
| S26. | PET/B (Matt) | 0.79 | 879623.5211 | 0.087 |
| S27. | PET/B (Twill) | 0.80 | 595624.01 | 0.074 |

The static flow resistance determines that, as the pore size opening is increased then static flow resistance decreases. Elastic materials and steel frames can transmit vibrations throughout the building and are not good for sound insulation. The maximum sound absorption for all samples occurs at a frequency of 1000 Hz.

Fig. 4.35 depicts the effect of weave structure on sound absorption behavior of various hybrid fabrics.

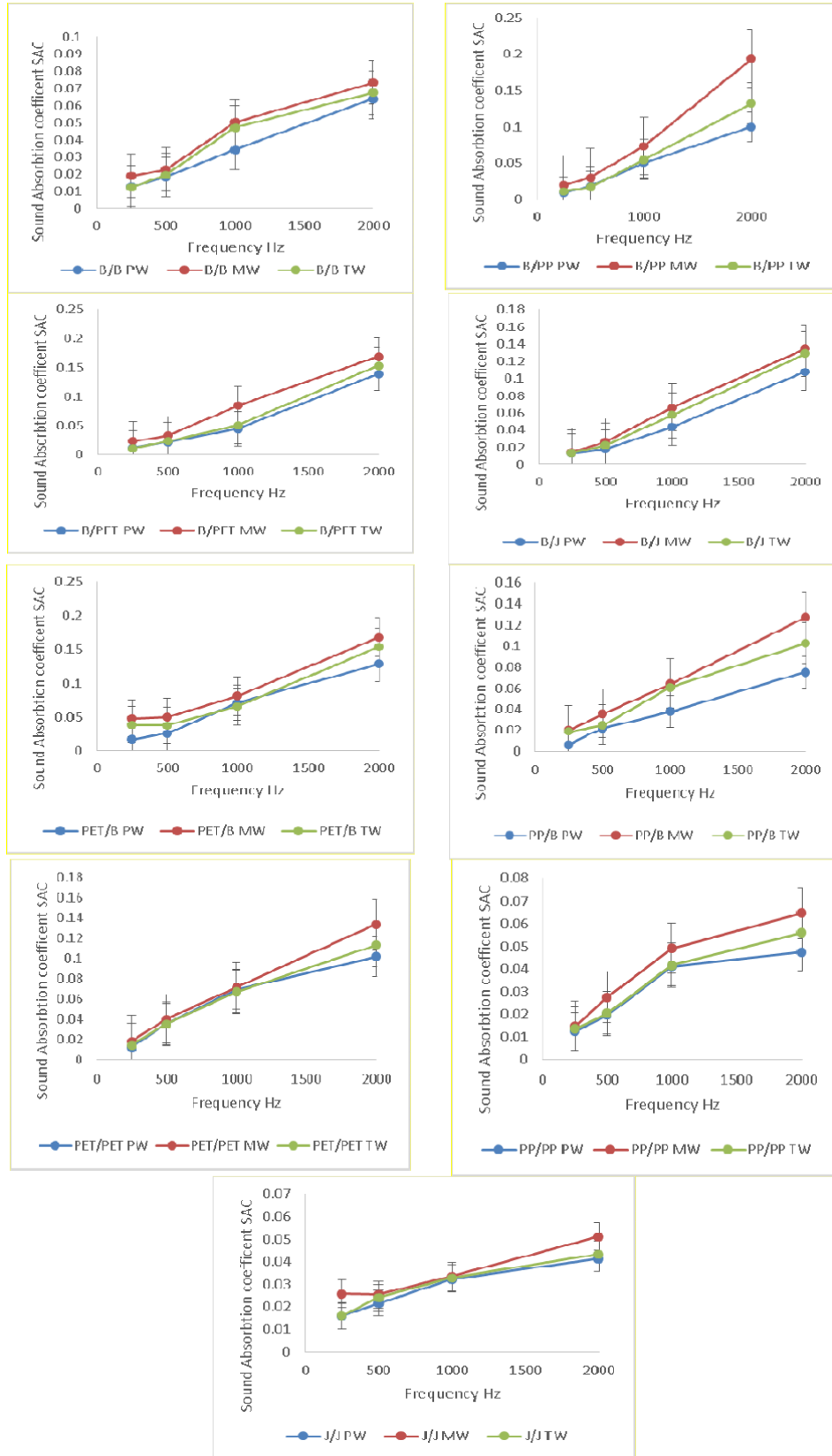


Figure 4.35: Effect of weave structure on sound absorption behavior of various hybrid fabrics.

A relationship between fabric porosity, airflow resistivity and NRC is shown in Fig. 4.36.

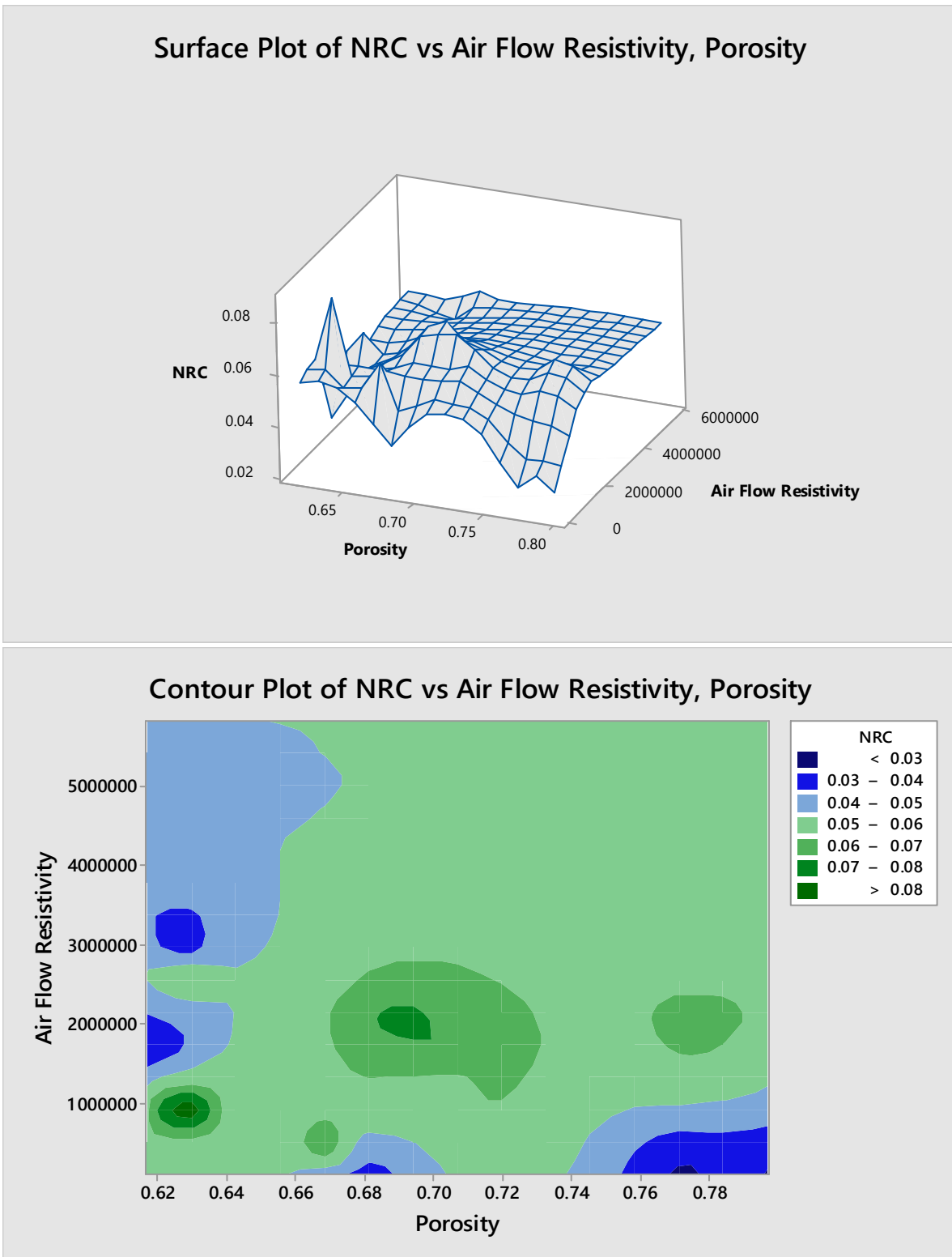


Figure 4.36: Relationship between fabric porosity, airflow resistivity and NRC.

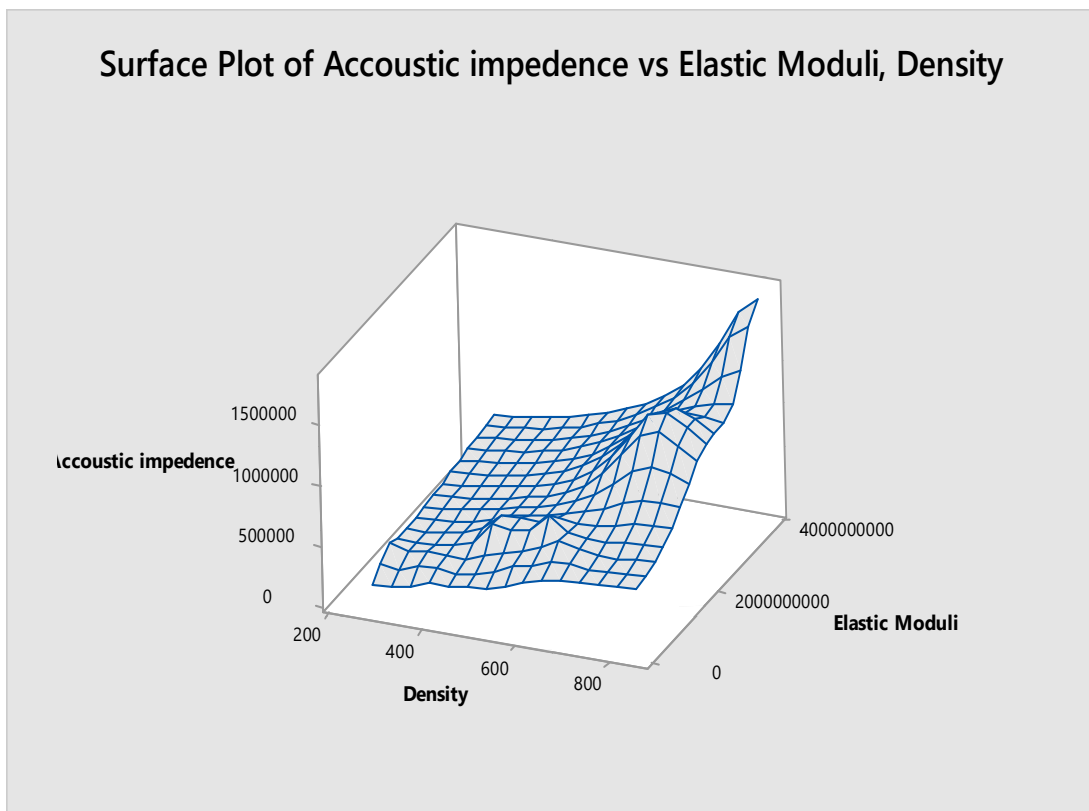
This phenomenon can be justified by considering that, upon reaching the fabric surface depending on fabric characteristics, the incident sound wave is partially absorbed, transmitted or reflected. Yarn intersection points in the fabric act as frictional elements that resist sound wave propagation through the fabric. Fabric internal tortuosity causes sound wave amplitude to decrease. This in turn leads to conversion of sound energy into heat. Plain weave has maximum number of intersection points. The maximum and minimum NRC values were obtained for plain and non-plain (matt and twill) fabrics. This is due to different interlacing of yarn in these weave types. The plain weave has the greatest number of yarn inter-sections, which results in increases in weight and density of this fabric. Additionally, shorter free float length causes less air to be entrapped within the thread spaces in the fabric. Thus, the NAC of the fabric against sound waves is decreased. Therefore, absorption occurs due to energy loss as the sound wave passes through the fabric and the frictional resistances offered by the fibers and entrapped air in the fabric is overcome. Accordingly, the severe crimping of the yarns in the plain weave offers more resistance to sound waves. The length of free float of the yarns in twill and matt fabric is an additional contributing factor in absorption of large proportion of the incident sound wave by the fabric. The increase in yarn twist results in increases in yarn compactness. This in turn reduces both fabric cover and the amount of voids in the yarns, thus the observed reduction in fabric NRC/SAC.

It can be seen that fabrics with polyester fiber have better NRC. The reason for better NRC of polyester fabrics may be finer fibers which results in higher number of fibers per unit weight of the material. This leads to higher total fiber surface area, and greater possibilities for a sound wave to interact with the fibers and ultimately dissipate inside the structure. Finer fibers yields more fibers per unit mass of the material; when the total fiber surface area increases, the possibilities of sound wave frictional flow resistance increases. Additionally, PET yarn is bulkier yarn and also it has less twist. The increase in yarn twist results in increases in yarn compactness. This in turn reduces both fabric cover and the amount of voids in the yarns, thus the observed reduction in fabric NRC/SAC. 100% Basalt fabric shows lowest NRC values in both frequencies. By hybridization with basalt, the noise reduction coefficient increases as the combination of dissimilar yarns results in higher crimp of individual yarns and more porosity in the structure.

Matt weave structures have highest value of NRC due to more porosity. This phenomenon can be justified by considering that, upon reaching the fabric surface depending on fabric characteristics, the incident sound wave is partially absorbed, transmitted or reflected. Yarn intersection points in the fabric act as frictional elements that resist sound wave propagation through the fabric. Fabric internal tortuosity causes sound wave amplitude to decrease. This in turn leads to conversion of sound energy into heat. Matt weave has more number of pores as compared to plain weave. Thus, the NRC of the fabric against sound waves is increased. Therefore, absorption occurs due to energy loss as the sound wave passes through the fabric and the frictional resistances offered by the fibers and entrapped air in the fabric is overcome.

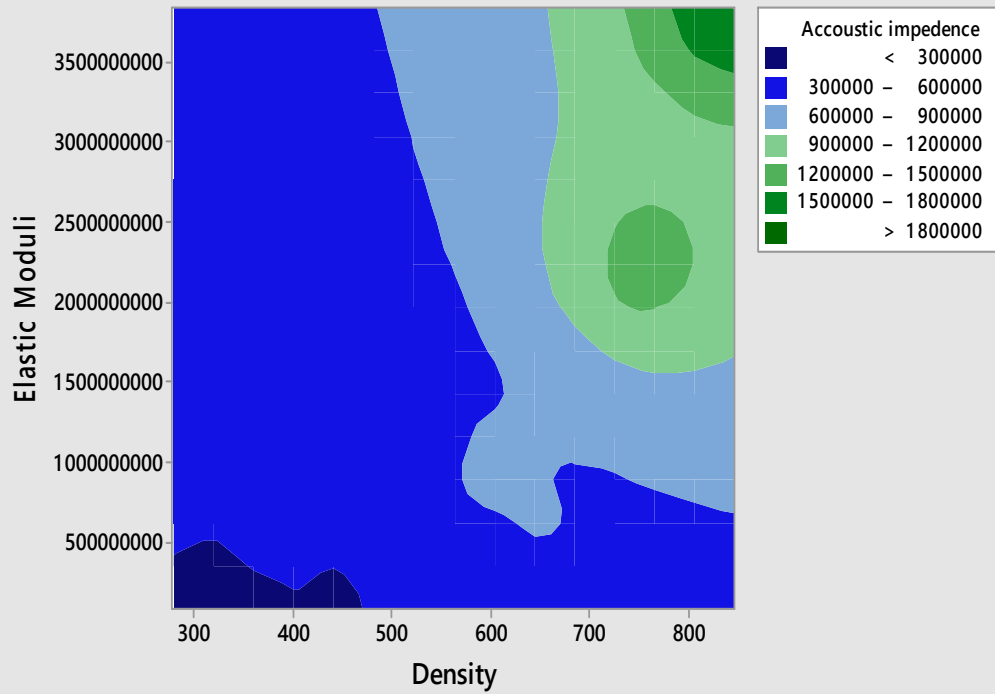
Specific acoustic impedance

Porous materials are usually good sound absorber but bad sound reflector. Specific acoustic impedance serves as an index to explain how efficiently energy sound can be transferred from one medium to another. The specific impedance of a medium is “opposing the propagation of a plane sound wave”. Specific acoustic impedance depends on elastic moduli of materials with linear relationship between them. As elastic modulus of material increases, impedance value increases i. e material can be good sound reflector, but not good sound absorber. As it is obvious from one axis of graph, density has an indirect relation with acoustic impedance. As density increase acoustic impedance start decreasing, but this effect is not pounced as compared to elastic moduli, which have significant effect on acoustic impedance .As elastic moduli increases, acoustic impedance increase. Dependence of specific acoustic impedance on elastic moduli and density of woven fabrics is shown in Figure 4.37.



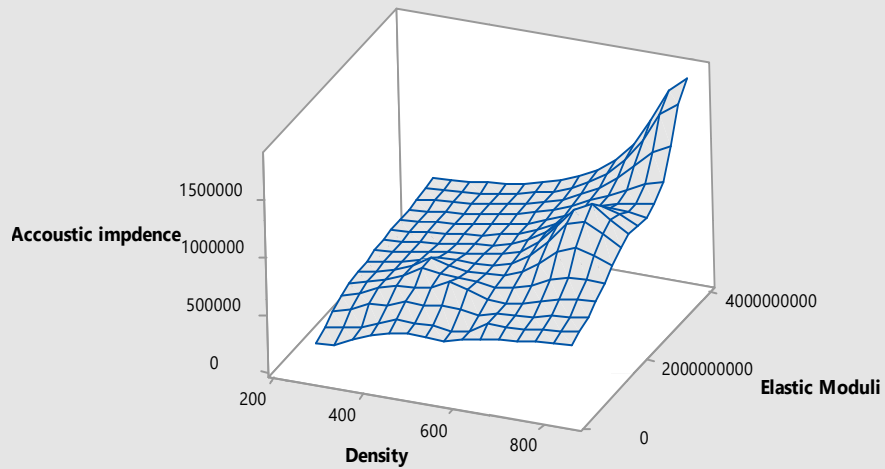
Warp way

Contour Plot of Accoustic impedance vs Elastic Moduli, Density

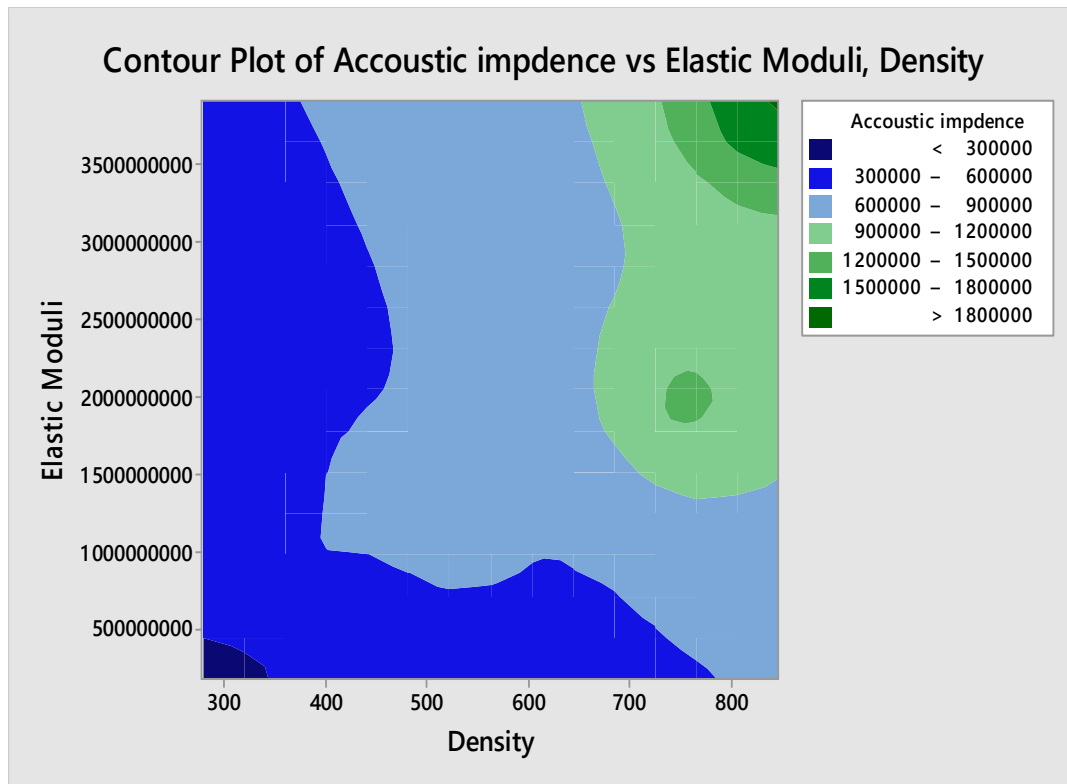


Warp way

Surface Plot of Accoustic impedance vs Elastic Moduli, Density



Weft way



Weft way

Figure 4.37: Dependence of specific acoustic impedance on elastic moduli and density of woven fabrics.

This effect can be explained in terms of the friction between the air inside the material (within pores, between fibers) and the solid walls of the material. Moreover when sound propagates within a porous material, it is reflected many times because there are several air-solid-air interfaces. Due to friction and to the multiple reflections within the pores, part of the energy associated with sound is transferred to the solid skeleton of the material, by making its particles vibrate, and therefore, it is dissipated.

4.5.7 Thermal Stability

Degradation of polymers is a physiochemical process (i.e may involve physical or chemical processes). The thermal degradation behavior is extremely important for understanding flammability behavior of materials. Thermo gravimetric analysis provides a method for the determination of mass change in the material as a function of temperature in controlled atmosphere. To evaluate the thermal stability of fabrics, the TGA analysis was carried out and pursued by presenting comparative analysis between different types of fabrics as shown in Fig. 4.38.

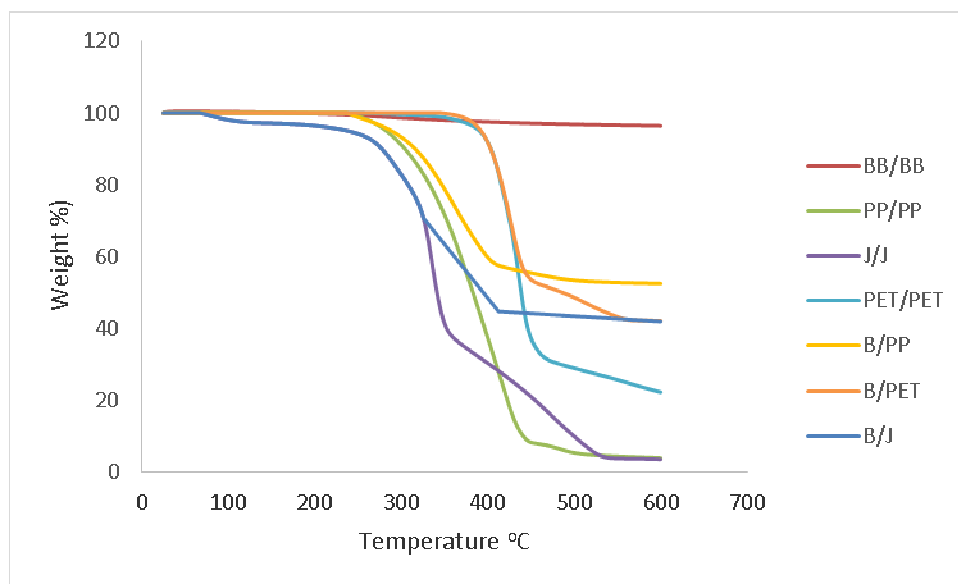


Figure 4.38: TGA curves for all hybrid and nonhybrid compositions.

For the 100 % basalt samples (B/B), it can be observed there are stages of weight loss in TGA curve. Firstly, the weight of the sample decreases starting from 30 °C and ending at 150°C. Obviously, this is attributed to evaporation of the moisture absorbed in the fiber. The main loss at low temperatures is not significant. The second observation is a reduction of weight of the sample starting from 450°C. This may be attributed to the decomposition of the residual carbonate minerals in the fiber. There is further mass loss after this stage, but with lower gradient. It can be seen that the total weight loss of the sample is very small in the process of being heated from room temperature to 600°C. Basalt has excellent thermal stability during the TGA which implies that basalt fibers are almost flame resistant.

The thermograms of PP/PP show a two-stage weight loss. It can be noticed in the derivative weight-loss curve, the major decomposition rate of the PP appears at 230°C by a random scission process which yields no monomer up to about 300°C. As PP decomposition is a two-stage process characterized by a first step in the temperature range 230°C–450°C with a mass loss of 86 wt%, followed by second weight loss at 520°C and almost complete decomposition occurs around 600°C. PP has branch points on alternative carbon atoms. The availability of reactive tertiary H atoms initiates its thermal degradation. Polypropylene is liable to chain degradation from exposure to heat, Oxidation usually occurs at the tertiary carbon atom present in every repeat unit. A free radical is formed here, and then reacts further with oxygen, followed by chain scission to yield aldehydes and carboxylic acids. Melting temperature of PP is around 168°C which is observed by Stuart SMP3 and also verified by DSC as shown in Fig. 4.39(b).

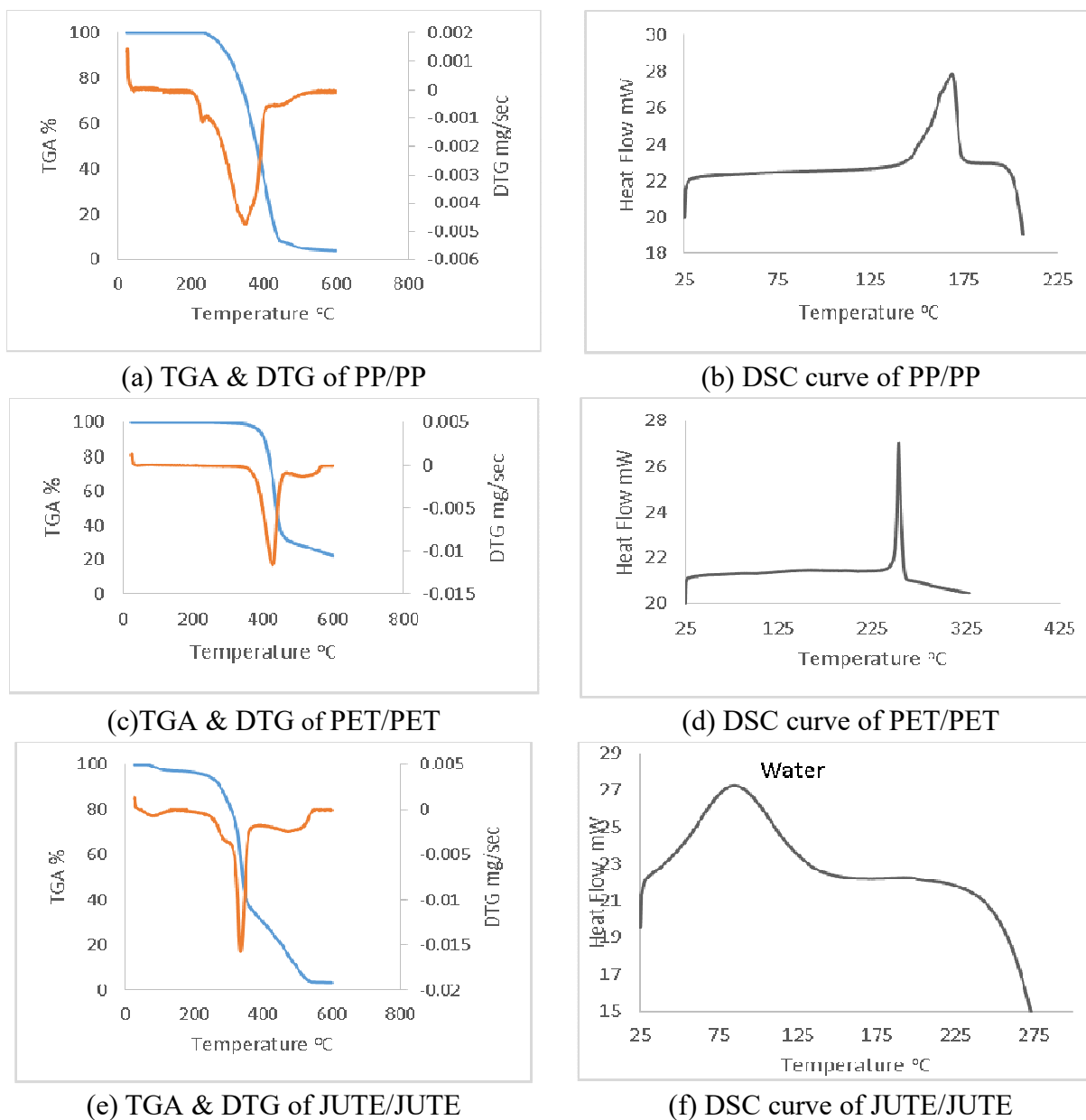


Figure 4.39: TGA, DTG and DSC curves for different structures.

It can be noticed that the polyester degradation follows a two-step reaction scheme characterized by a first step in the temperature range 250°C–450°C with a mass loss of 70 wt%, followed by a second decomposition step located in the range 450°C–600°C. This behavior is determined by random scission of the polyester backbone (ester linkage) and to the oxidation and the breakage of the secondary bonds. As a result, a large amount of low-molecular-weight volatiles (CO, CO₂, methane, ethylene) are released rather than char. Melting temperature of PET is around 253°C which is observed by Stuart SMP3 and also verified by DSC is as shown in Fig. 4.39(d). Thermoplastic fibers show peak at their melting point. Thermal degradation of PP woven

structures occurs earlier than PET woven structures because of its low melting temperature. At temperature above melting point, molecular movement increases a lot, the components of the long chain backbone of the polymer can begin to separate (molecular scission) and react with one another to change the properties of the polymer. So initiation of thermal decomposition starts earlier in PP based structures but PP is a long chain polymer so high bond dissociation energy is needed, its heat of decomposition is more than PET. Generally, the lower the respective T_c (combustion temperature) and usually T_d (decomposition temperature), the hotter the flame, the more flammable is the fiber (i.e 320-400°C for PP and 285-305°C for PET). The ignition temperature for PP is higher i.e 570°C as compared to PET (450°C) and its volatile gases which fasten the combustion process are less as compared to PET so its flammability is lower. For Jute/Jute, the first weight loss occurred due to moisture evaporation and second weight loss occurred due to degradation of light materials such as hemicellulose and cellulose at around 250°C, while 70% weight loss occurred due to decomposition of heavy material like lignin of the jute fiber at a temperature around 320°C. This is also observed by DSC of Jute Fig. 4.39(f).

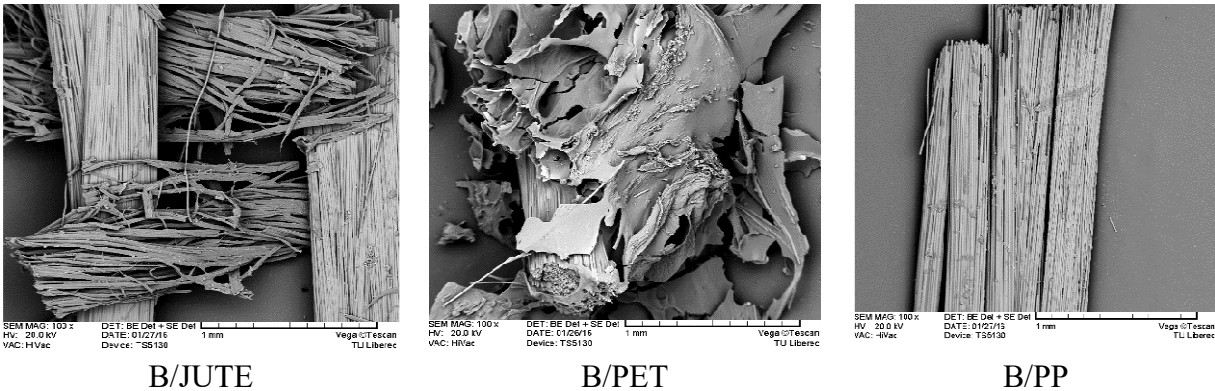


Figure 4.40: SEM images of hybrid fabrics after TGA.

After the removal of the free water, the degradation process began in the cellulose, hemicelluloses, lignin constituents, and the associated linked water. After 380°C, the quick decomposition of the jute fiber is found due to the complete depolymerization of the cellulose, hemicellulose, and lignin components. The thermal degradation in jute results in char formation rather than molten drip. The formation of char residues may involve initial physical desorption of water, intramolecular dehydration, formation of carboxyl and carbon-carbon double bonds, cleavage of glycosidic linkage and rupture of C-O and C-C bonds and condensation and aromatization of carbon atoms from each original pyranose ring to form discrete graphite layers. It can be seen from the result that the rate of weight loss of the hybrid samples was less than non-hybrid fabrics. TGA analysis of hybrid samples show that residue left at 600°C is more than that for non-hybrid fabrics. The effectiveness of using basalt yarn in hybrid structures may be indicated by shifting of decomposition stages to higher temperature and leaving more amount of residue at maximum temperature as compared to the non-hybrid samples where residue is almost nil at 600°C.

Chapter 5 - Summary and Conclusions

In this research work, new kind of yarns were run on the weaving machine and set of parameters for efficient weavability was developed. Parameters for weaving of basalt hybrid fabrics were optimized. The knowledge of mechanical properties is very important for development of a fabric for specific end use. The results reveal that the hybridization of basalt with polypropylene and polyester in different weaves leads to significant improvement in the static and dynamic mechanical properties of fabrics. When choosing a weave design for a particular product, one must consider the physical suitability of the weave as well as the desired properties. Structure of weave and fiber type have strong influence on static and dynamic mechanical properties of fabrics. Hybridization of basalt yarn in warp direction has more significant effect on mechanical properties. It is also established that the type of weave has a great influence on the tensile modulus of fabrics in warp direction among hybrid structures, matt weave has superior mechanical properties as compared to other weaves.

The comparison of predicted tensile properties from computation with *Wisetex* correlates reasonably with experimental data. Its correlation is only 70% as new kind of material was used for development of hybrid fabrics in this work.

Shear properties i.e ability of fabric to deform within its plane, which is important for molding of TRC (Textile reinforced concretes) was evaluated using picture frame tester. It showed good correlation with image analysis based evaluation of shear angle till buckling occurs.

The results reveal that the hybridization of basalt with polypropylene, polyester and jute in different weaves leads to significant improvement in thermal and transmission related characteristics. Structural parameters have strong influence on thermal properties. Structure of weave and fiber type have strong influence on conductivity. Plain weave has highest thermal conductivity and lowest thermal resistance values in all hybrid structures. Twill weave has highest air permeability and thermal resistance values overall. Thermal conductivity of other structures can be improved by adding basalt fiber for application as heat sinks. Thermal resistance of basalt structures can be improved by adding other fiber especially jute fiber for application as thermal insulation. The hybridization with Jute and PET significantly increases the thermal resistance. It is clear from the measurement that there are considerable differences in the results of measurement with two instruments, although correlation exists.

In this research, electrical behavior of different technical textile woven fabrics was analyzed according to fiber and weave type. Basalt, jute, polypropylene and polyester were used as warp or weft yarns. Combining different warp and weft yarns and using different weave patterns (plain, matt, twill) hybrid and non-hybrid structures with different porosity levels were prepared. Fabrics were evaluated according to their electrical resistance (volume and surface) with reference to structure (porosity).

It was confirmed that both material of fiber and structure, represented by porosity (different weave) show statistically significant effect on resulting electric resistance. The highest resistance was observed in samples made of 100% basalt fiber regardless of weave type. It can be

concluded that plain weave structures show lower electrical resistance compared to other non-plain weave patterns. This phenomenon is in agreement with the fact, that plain weave structures have higher cover factor compared to matt and twill weaves. From this analysis it was found that samples prepared in matt weave have higher electrical resistance value especially when basalt is used in warp. Electrical resistance higher than $4E+10 \Omega$ can be reached using either 100% basalt fabrics, or basalt/polypropylene fabrics, or basalt/jute fabrics or 100% jute fabric regardless of weave type.

It can be seen that fabrics with polyester fiber have better Noise Reduction Coefficient. The reason for better NRC of polyester fabrics is attributed finer fibers which results in higher number of fibers per unit weight of the material. This leads to higher total fiber surface area, and greater possibilities for a sound wave to interact with the fibers and ultimately dissipate inside the structure. By hybridization with basalt, the noise reduction coefficient increases as the combination of dissimilar yarns results in higher crimp of individual yarns and more porosity in the structure. Matt weave structures have highest value of NRC due to more porosity.

Specific acoustic impedance depends on elastic moduli of materials with linear relationship between them. As elastic modulus of material increases, impedance value increases i. e material can be good sound reflector, but not good sound absorber.

The thermal stability of the basalt fiber is excellent. When comparing TGA curves for hybrid samples it demonstrates that thermal stability of the samples containing basalt is much higher than the non-hybrid samples. Percentage weight loss is less in basalt hybrid samples as compared to non-hybrid samples. It is also confirmed from SEM images.

The degradation of fiber due to the alkalinity in the cement matrix seriously decreases the durability and may cause premature failure of the concrete composite. Calcium hydroxide is the primary cause of alkaline environment in cement. The weight loss increases with increasing treatment time, pH and use of stronger alkali (NaOH). The weight loss of basalt fiber is minimum as it is least affected by alkali followed by PP fiber. The tensile test results for the controlled samples are compared to the alkali treated samples in terms of applied maximum load versus elongation %. It can be noticed that ultimate tensile strain decreases in all the fiber types along with decrease in F_{max} . Reduction in mechanical properties in basalt yarn is minimum and maximum in Jute yarn and this is also verified by SEM images. The microstructure of yarn surfaces indicated that the jute fiber encountered the most severe alkali attack and precipitation of hydration products in the cement matrix.

It is very important that there is good adhesion between the reinforcing fibers and the concrete or cement matrix, otherwise debonding may take place. Bond strength may dominate the mechanical properties of fiber-reinforced concrete. Pull out test is most general test for this purpose. In case of basalt, very small slippage (displacement) is observed as they have good adhesion with cement matrix. In case of PP and PET, adhesion is not good and it can be viewed by high slippage/displacement/deformation.

So overall hybrid basalt structures have promising application in TRC.

Future scope for research:

Further research can be conducted for;

- Industrial large scale weaving operations may be carried out to optimize and further improve weavability of basalt based hybrid fabrics. Suitable surface finish may improve weaving efficiency.
- Suitable computational tools can be developed to predict mechanical properties of such industrial fabrics more accurately. Existing tools can be modified to predict other mechanical properties especially for industrial fabrics.
- Development of basalt and hybrid fabric reinforced concrete composites and their mechanical characterization in terms of compression, bending and impact tests. These tests can be done in room temperature and extreme conditions to check the durability of structures in case of high temperatures.
- Flammability behavior of basalt hybrid fabric reinforced concrete can be investigated. This investigation will provide fundamental information on behavior of TRC under different temperatures without and with preloading in form of temperature dependent stress-strain-relations under tensile, bending, shear and compressional deformation.
- Ductility behavior of basalt fabric reinforced concrete can be studied in details so as to develop futuristic material for earthquake resistance.

Research outputs

Publications in International Journals

1. **Hafsa Jamshaid**, Rajesh Mishra and Jiri Militky, “Thermo-Mechanical Characteristics of Basalt Hybrid & Non-hybrid Woven Fabric Reinforced Composites, published online in **Polymer Composites**, 2015.(**Impact factor=1.6332**)
2. **Hafsa Jamshaid**, Rajesh Mishra, Jiri Militky and Veronika Safarova, “Investigation of electrical properties of basalt and its hybrid structures”, published online in **Textile Research Journal**, 2016. (**Impact factor=1.599**)
3. **Hafsa Jamshaid**, Rajesh Mishra, Jiri Militky and Jan Novak, “End use performance characterization of novel fabrics”, **Fibers and Polymers**, published 16 (11), pp. 2477-2490, 2015.(**Impact factor=0.881**)
4. **Hafsa Jamshaid**, Rajesh Mishra and Jiri Militky, “A green material from Rock : A basalt fiber”, published in the **Journal of the Textile Institute**, 2015.(**Impact factor=0.722**)
5. **Hafsa Jamshaid**, Rajesh Mishra, Jiří Militký “Thermal and mechanical characterization of novel basalt woven hybrid structures published in the Journal of the Textile Institute. 107 (4), pp. 462-471,2015 (**Impact factor=0.722**).
6. **Hafsa Jamshaid**, Rajesh Mishra “Photoilluminance of different woven structure published in **Fiber & Polymer** 15 (5), pp. 950-953,2014. (**Impact factor=0.881**)
7. **Hafsa Jamshaid**, Rajesh Mishra, Jiří Militký “Characteristics of woven basalt and hybrid structures as composite reinforcement” is under review in JTI.(**Impact factor=0.722**)
8. **Hafsa Jamshaid**, Rajesh Mishra, Jiri Militky, Miroslava Pechociakova, Muhammad Tayyab Noman, “Mechanical, “Thermal and Interfacial Properties of Green Composites from Basalt and Hybrid Woven Fabrics” is under review in **Fibers & Polymers**.(**Impact factor=0.881**)
9. **Hafsa Jamshaid**, Rajesh Mishra, Jakub Weiner, Jiri Militky “New generation of flame-resistant woven fabrics from green material” is submitted in **Chemical Engineering Journal** (**Impact factor =4.16**)
10. **Hafsa Jamshaid**, Rajesh Mishra, Lubos Hes, Jiri militky, Sajid Hussain “ Sustainable textile materials for advanced thermal applications “is submitted in **JEFF**(**Impact factor =0.986**)
11. **Hafsa Jamshaid**, Rajesh Mishra, Jiri Militky, Miroslava Pechociakova, Muhammad Tayyab Noman, “Usability of Textile Reinforced Concrete: Structural Performance and Durability” is submitted in **Journal of Industrial textiles**.(**Impact factor =1.349**)
12. **Hafsa Jamshaid**, Rajesh Mishra, Jiri Militky “Investigation of basalt hybrid woven structures by optical method “ is under process. **Fibres & Textiles in Eastern Europe**(**Impact factor=0.667**)
13. Muhammad Tayyab NOMAN, Jakub WIENER, Jana SASKOVA, Muhammad Azeem ASHRAF & **Hafsa JAMSHAI**D Synthesis and Characterization of TiO₂ nanoparticles prepared from Ultrasonic Assisted Technique (UAT) is submitted in **Ultrasonic** (**Impact factor =1.94**)

14. Mohanapriya Venkataraman, **Hafsa Jamshaid**, Rajesh Mishra, Jiri Militky, Aerogel for high performance thermal insulation in textiles, **Textile progress**, Vol. 48, No. 2, 2016.

Book chapters

1. Hafsa Jamshaid, Rajesh Mishra, Jiří Militký, “Analysis of Electrical Properties of Basalt and its Hybrid Structures” in Recent Developments In Fibrous Material Science, ISBN 978-80-87269-45-9, 2015
2. Hafsa Jamshaid, Rajesh Mishra, Jiří Militký, “Thermal Properties of Basalt Hybrid Woven Fabrics” in Recent Developments In Fibrous Material Science, ISBN 978-80-87269-45-9. 2015
3. Hafsa Jamshaid, Rajesh Mishra, Jiří Militký, “Thermal Properties of Electrospun Nanofibres Embedded with Aerogel” in Recent Developments in Fibrous Material Science, ISBN 978-80-87269-45-9. 2015
4. Hafsa Jamshaid, Rajesh Mishra, Jiří Militký, “Acoustic Properties of Aerogel Embedded Nonwoven Fabrics” in Recent Developments in Fibrous Material Science, ISBN 978-80-87269-45-9. 2015
5. Hafsa Jamshaid, Rajesh Mishra, Jiří Militký “Effect of Washing Treatments and Blend Ratio on Comfort Properties of Denim Fabrics” in Recent Developments In Fibrous Material Science, ISBN 978-80-87269-45-9. 2015
6. Hafsa Jamshaid, Rajesh Mishra, Jiří Militký, Miroslava Maršálková and Rudolf Šrámek, “Basalt hybrid and non-hybrid fabric reinforced composites”, Progress in fibrous material science, ISBN 978-80-87269-40-4, 2014.
7. Hafsa Jamshaid, Mohanapriya Venkataraman, Rajesh Mishra et. Al, “Photoilluminance of Different Woven Structures By Treatment With Phosphorescent Pigment, Selected Properties Of Functional Materials,” ISBN 978-80-87269-28-2, 2013.
8. Hafsa Jamshaid, Mohanapriya Venkataraman, Rajesh Mishra, Jiri Militky, “Aerogels: Novel Materials For Insulative Textiles, Selected Properties Of Functional Materials”, ISBN 978-80-87269-28-2, 2013.
9. Hafsa Jamshaid, Mohanapriya Venkataraman, Rajesh Mishra, Jiri Militky, Aerogel Based Insulation Materials: Characterization of Thermal, Electrical And Electromagnetic Behavior, Selected Properties Of Functional Materials, ISBN 978-80-87269-28-2, 2013.

Publications in International Conferences

1. Hafsa Jamshaid, Rajesh Mishra, , Jiří Militký, “Mechanical & Functional Characterization of Basalt woven structures” in Fiber society, 25-27 May ,2016
2. Hafsa Jamshaid, Rajesh Mishra ,”Characteristics Of Woven Basalt Hybrid Composites” Textile institute conference -28April 2016
3. Hafsa Jamshaid, Rajesh Mishra, Jiří Militký “Investigation of Thermal Properties of Hybrid Structures ISERD conference 2016 ISBN 978-93-85973-41-3

4. Hafsa Jamshaid Seminar on “Advances in Material engineering” 1-2 December 2015, Technical University of Liberec, Czech Republic
5. R. Mishra, Hafsa Jamshaid, Performance utility of novel basalt woven hybrid fabrics, 6th international Technical Textile congress, Izmir, 14-16 October, 2015.
6. R. Mishra, Hafsa Jamshaid, Bio-based composite materials, Keynote lecture, International conference, CET, Bhubaneswar, 9th november, 2015.
7. R. Mishra, Hafsa Jamshaid, Basalt based hybrid woven stuctures and composites, Keynote lecture, INNOTEX-International conference, JNGEC, Sundernagar, Himachalpradesh, 7th November, 2015.
8. Hafsa Jamshaid, Rajesh Mishra, Thermal And Mechanical Characterization Of Basalt Hybrid Structures in 15th Autex world Textile conference 2015 is presented. ISBN; 978-606-685-275-3
9. Hafsa Jamshaid, Rajesh Mishra, “Thermo-Mechanical Characteristics of Hybrid Woven Structures” in Clotech 2015 is presented. ISBN ;978-83-7283-665-6
10. Hafsa Jamshaid, Rajesh Mishra, “Mechanical & Functional Characterization Of Unconventail Knitted Fabrics” in 5th SMARTEX , 2015.(Egypt)
11. Analysis if basalt fabrics: thermal and mechanical analysis, Svetlanka 2015 ,ISBN; 978-80-7494-229Hafsa Jamshaid, Rajesh Mishra,“Thermal and mechnical properties of woven Basalt fabric reinforced hybrid & non-hybrid composites“ presented in 6th International Istanbul conference on Future Technical textiles(FTT2014) ,15-17 October 2014.ISBN:978-975-400-386-4
12. Hafsa Jamshaid, Rajesh Mishra,“Thermal And Mechanical Properties Of Novel Basalt Woven Structures presented in 20th International conference STRUTEX 2014.
13. Hafsa Jamshaid, Rajesh Mishra, Thermo-Mechanical Characteristics of Hybrid Woven Structures in Clotech 2015 is presented.
14. Hafsa Jamshaid, Rajesh Mishra, Jan Novak, Jiri Militky, “Mechanical and functional characterization of unconventional knitted structures,” SMARTEX, World textile conference, Egypt, November 2015.
15. Hafsa Jamshaid, Rajesh Mishra,“Thermal and mechanical properties of woven Basalt fabric reinforced hybrid & non-hybrid composites“ presented in 6th International Istanbul conference on Future Technical textiles(FTT2014) ,15-17 October 2014.ISBN:978-975-400-386-4.
16. Hafsa Jamshaid, Rajesh Mishra, “Thermal And Mechanical Properties Of Novel Basalt Woven Structures presented in 20th International conference STRUTEX 2014.
17. Hafsa Jamshaid,Mohnapryia Vankataraman, Rajesh Mishra."Effect of temperature on mechanical properties of polymer fibers” Textile Science Conference 23-25 September 2013, Liberec, Czech Republic.

References:

- [1] Chaphalkar, P and Kelkar, A.D. "Classical laminate theory model for twill weave fabric composites". *Composites Part A: Applied Science and Manufacturing*, vol. 32, No. 9, pp. 1281-1289, 2001.
- [2] Potter, K.D. "Beyond the pin-jointed net: maximizing the deformability of aligned continuous fibre reinforcements". *Composites Part A: Applied Science and Manufacturing*, vol. 33, pp. 677-686, 2002.
- [3] Potter, K.D. "Bias extension measurements on cross-plyed unidirectional prepreg". *Composites Part A: Applied Science and Manufacturing*, vol. 33, pp. 63-73, 2002.
- [4] Potter, K.D. "In-plane and out of plane deformation properties of unidirectional preimpregnated reinforcement". *Composites Part A: Applied Science and Manufacturing*, vol. 33, pp. 1469-1477, 2002.
- [5] Potter, K.D. "The influence of accurate stretch data for reinforcements on the production of complex structural mouldings - Part 1. Deformation of aligned sheets and fabrics". *Composites*, vol. 10, No. 3, pp. 161-167, 1979.
- [6] Razera, A.T. and Frollini, E. "Composites based on jute fibers and phenolic matrices: properties of fibers and composites". *Journal of Applied Polymer Science*, vol. 91, No. 2, pp. 1077-1085, 2004.
- [7] Gassan, J. and Bledzki, A.K. "Possibilities for improving the mechanical properties of jute/epoxy composites by alkali treatment of fibers". *Composites Science and Technology*, vol. 59, No. 9, pp. 1303-1309, 1999.
- [8] Ray, D. et al. "Mechanical properties of vinyl ester resin matrix composites reinforced with alkali-treated jute fibers". *Composites Part A*, vol. 32, No. 1, pp. 119-127, 2001.
- [9] Ray, D. et al. "Fracture behavior of vinylester resin matrix composites reinforced with alkali treated jute fibers". *Journal of Applied Polymer Science*, vol. 85, No. 12, pp. 2588-2593, 2002.
- [10] Saha, K. et al. Saha, S. Das, D. Bhatta, and B. C. Mitra, "Study of jute fiber reinforced polyester composites by dynamic mechanical analysis". *Journal of Applied Polymer Science*, vol. 71, No. 9, pp. 1505-1503, 1999.
- [11] Dash, N. et al. "Novel, low-cost jute-polyester composites. Part 1: processing, mechanical properties, and SEM analysis". *Polymer Composites*, vol. 20, No. 1, pp. 62-71, 1999.
- [12] Rabinovich, F.N et al. "Stability of basalt fiber in a medium of hydrating cement". *Journal of Glass and Ceramics*, vol. 58, pp. 11-12, 2001.
- [13] Medvedyev and Tsybulya, Y.L. "The outlook for the use of basalt continuous fiber for composite reinforcement". *International Sample technical conference. Covina, CA: SAMPE*, 2004, pp. 275-279.
- [14] Wang, M.C. et al. "Chemical Durability and Mechanical Properties of Alkali-proof Basalt fibre and its Reinforced Epoxy Composites". *Journal of Reinforced Plastics and Composites*, vol. 27, pp. 393-407, 2008.
- [15] Matko, S. et al. "Fire retarded insulating sheets from recycled materials". *Macromolecular Symposia*, vol. 233, pp. 217-224, 2006.
- [16] Militky, J. et al. "Influence of thermal treatment on tensile failure of basalt fibre". *Engineering Fracture Mechanics*, vol. 69, pp. 1025-1033, 2002.
- [17] Dalinkevich, A.A. et al. "Modern basalt fibrous materials and basalt fibre-based polymeric composites". *Journal of Natural Fibers*, vol. 6, pp. 248-271, 2009.
- [18] Botev, M. et al. "Mechanical properties and viscoelastic behavior of basalt fibre-reinforced polypropylene". *Journal of Applied Polymer Science*, vol. 74, pp. 523-531, 1999.
- [19] Liu, Q. et al. "Investigation of basalt fibre composite mechanical properties for applications in transportation". *Polymer Composites*, vol. 27, pp. 41-48, 2006.
- [20] Palmieri, A. et al. "Basalt fibres for Reinforcing and Strengthening Concrete. In *Proceedings of the 9th International Symposium of the fibre-Reinforced Polymer Reinforcement for Reinforced Concrete Structures (FRPRCS-9)*". Adelaide, Australia, 2009, pp. 13-15.
- [21] Barbero, E.J. *Introduction to Composite Materials Design*. 2nd Ed. Taylor and Francis Group, LLC. 2011.
- [22] William, D.C and David, G.R. *Materials Science and Engineering, an Introduction*. 8th Ed. John Wiley & Sons, Inc. 2010.

- [23] Mishra, R. et al. "Modeling and simulation of 3D orthogonal fabrics for composite applications". *Journal of the Textile Institute*, vol. 103, No. 11, pp. 1255-1261, 2012.
- [24] Mishra, R. and Militky J. "Recycling of Textile Waste into Green Composites: Performance Characterization". *Polymer Composites*, vol. 35, No. 10, pp. 1960-1967, 2014.
- [25] Kalaprasad, G. et al. "Hybrid effect in the mechanical properties of short sisal/glass hybrid fiber reinforced low density polyethylene composites". *Journal of Reinforced Plastics and Composites*, vol. 15, pp. 48, 1996.
- [26] Sathishkumar T.P. et al. "Characterization of natural fiber and composites: a review". *Journal of Reinforced Plastics and Composites*, vol. 32, pp. 1446-1465, 2013.
- [27] Bunsell, A.R. and Harris, B. "[Hybrid carbon and glass fibre composites](#)". *Composites*, vol. 5, No. 4, pp. 157-164, 1974.
- [28] Jones, F.R. *Handbook of Polymer Composites*, Longman Scientific and Technical, 1994.
- [29] Burgueno, R. et al. "Hybrid Biofiber-Based Composites for Structural Cellular Plates". *Composites-Part A: Applied Science and Manufacturing*, vol. 36, No. 5, pp. 581-593, 2005.
- [30] Haq, M. et al. "Hybrid Bio-based Composites from Blends of Unsaturated Polyester and Soy Bean Oil Reinforced with Nanoclay and Natural Fibers". *Composites Science and Technology*, vol. 68, No. 15-16, pp. 3344-3351, 2008.
- [31] Jawaid M and Khalil, H.P.S.A. "Cellulosic/synthetic fiber reinforced polymer hybrid composites". *Carbohydrate Polymers*, vol. 86, pp. 1-18, 2011.
- [32] Muthuvel, M. et al. "Characterization study of jute and glass fiber reinforced hybrid composite material". *International Journal of Engineering Research & Technology*, vol. 2, pp. 335-344, 2013.
- [33] Shahzad, A. "Hemp fiber and its composites". *Journal of composite materials*, vol. 46, pp. 973-986, 2011.
- [34] Sathishkumar, T.P. et al. "Characterization of new cellulose sansevieria ehrenbergii fibers for polymer composites". *Composite Interfaces*, vol. 20, No. 8, pp. 575-593, 2013.
- [35] Sathishkumar, T.P. et al. "Tensile and flexural properties of snake grass natural fiber reinforced isophthalic polyester composites". *Composites Science and Technology*, vol. 72, pp. 1183-1190, 2012.
- [36] Mohanty, A.K. et al. "Biofibres, biodegradable polymers and biocomposites: an overview". *Macromolecular Materials and Engineering*, vol. 276-277, pp. 1-24, 2001.
- [37] Aoki, R. et al. "3D fabrics for composites". 15th Textile Research Symposium. Osaka: The Textile Machinery Society of Japan, 1984.
- [38] Sathishkumar, T.P. et al. "Hybrid fiber reinforced polymer composites – a review". *Journal of Reinforced Plastics and Composites*, vol. 33(5), pp. 454–471, 2014.
- [39] Chou, T.W. and Ko, F.K. *Textile Structural Composites*. Composite Materials Series, Amsterdam: Elsevier Science Publishers B.V., 1993.
- [40] Laroche, et al. "Forming of woven fabric composites". *Journal of Material Composites*, vol. 28, pp. 1825-1839, 1994.
- [41] Mohammed, U. et al. "Experimental studies and analysis of draping of woven fabrics". *Composites Part A: Applied Science and Manufacturing*, vol. 31, pp. 1409-1420, 2000.
- [42] Mishra, R. "Meso-scale finite element modeling of triaxial woven fabrics for composite inplane reinforcement properties". *Textile Research Journal*, vol. 83, pp. 1836-1845, 2013.
- [43] Wittek, T. and Tanimoto, T. "Mechanical properties and fire retardancy of bidirectional reinforced composite based on biodegradable starch resin and basalt fibers". *EXPRESS Polymer Letters*, vol. 2, No.11, pp. 810-822, 2008.
- [44] Woven fabric edited by Edited by Han-Yong Jeon, chapter 1. B. K. Behera, Jiri Militky, Rajesh Mishra and Dana Kremenakova, *Modeling of Woven Fabrics Geometry and Properties*, 2012.
- [45] Behera, B.K. and Mishra R. "3-Dimensional weaving". *Indian Journal of Fibre and Textile Research*, vol. 33, pp. 274-287, 2008.
- [46] R. A. Naik, "Failure analysis of woven and braided fabric-reinforced composites," *J. Compos. Mater.*, vol. 29, pp.2334-2363, 1995.
- [47] Jamshaid, H. and Mishra, R. "A green material from Rock: A basalt fiber". *Journal of the Textile*

Institute, vol.107,pp.923-937,2015.

[48] KamennyVek. (2009). Advanced basalt fiber.Basfiber. Internet: <http://www.basfiber.com>, Retrieved May9, 2012.

[49] Ross, A. (2006). Basalt fibers: Alternative to glass? *Composites World*. Internet: <http://www.compositesworld.com/articles/basalt-fibers-alternative-to-glass>, Retrieved July 2014.

[50] Sim, J. et al. “Characteristics of basalt fiber as a strengthening material for concrete structures”. *Composites Part B: Engineering*, vol. 36, No. 6-7, pp. 504-512, 2005.

[51] Piero De Fazio, Basalt fiber: from earth an ancient material for innovative and modern application. Internet: <http://www.enea.it>, Retrieved on July 2104.

[52] Kunalsingha. “A short review on Basalt fiber”. *International Journal of Textile Science*, vol. 1, No. 4, pp. 19-28, 2012.

[53] Militky, J. and Kovacic, V. “Ultimate Mechanical Properties of Basalt Filaments”. *Textile Research Journal*, vol. 66, No. 4, pp. 225-229, 1996.

[54] Wei, B. et al. “Tensile behavior contrast of basalt and glass fibers after chemical treatment. Materials and Design”. *The journal of Textile Institute*, vol. 31, pp. 4244-4250, 2010.

[55] Cook, J.G. *Handbook of Textile Fibre and Natural Fibres*, 4th edition, England, Morrow Publishing, 1968.

[56] Sezemanas, G. et al. “The alkali and temperature resistance of some fibers”. *Material Science*, vol. 11, pp. 29-35, 2005.

[57] Toropina, L.V. et al. “New cloth from basalt fibres”. *Fibre Chemistry*, vol. 27, pp. 67-68, 1995.

[58] Landucci, G. et al. “Design and testing of innovative materials for passive fire protection”. *Fire Safety Journal*, vol. 44, pp. 1103-1109, 2009.

[59] Liu, Q. et al. “Investigation of basalt fiber composite mechanical properties for applications in transportation”. *Polymer Composites*, vol. 27, pp. 478-483, 2006.

[60] Czigany, T. “Discontinuous basalt fiber-reinforced hybrid composites”. *Express Polymer Letters*, vol. 1, pp. 59-60, 2007.

[61] Czigany, T. et al. “Basalt fiber as a reinforcement of polymer composites”. *Periodical: Polytechnic of Mechanical Engineering*, vol. 49, pp. 3-14, 2005.

[62] Czigany, T. Discontinuous basalt fiber-reinforced hybrid composites. In K. Friedrich, S. Fakirov, & Z. Zhang (Eds.) *Polymer Composites: From Nano- to Macro-Scale* (pp. 309–328). London: Springer Science+Business Media.2005 ISBN: 978-0-387-24176-0 (Print) 978-0-387-26213-0 (Online)

[63] Dias, D.P. and Thaumaturgo, C. et al. “Fracture toughness of geopolymeric concretes reinforced with basalt fibers”. *Cement Concrete Composites*, vol. 27, pp. 49-54, 2005.

[64] Dorigato, A. and Pegoretti, A. “Fatigue resistance of basalt fibers-reinforced laminates”. *Journal of Composite Materials*, vol. 46, pp. 1773-1785, 2012.

[65] Novitskii, A.G. and Sudakov, V.V. “An unwoven basalt fiber material for the encasing of fibrous insulation: An alternative to glass cloth”. *Refractory Industrial Ceramics*, vol. 45, pp. 234-241, 2004.

[66] Sergeev, V.P. et al. “Basalt fibers: A reinforcing filler for composites. *Powder Metallurgy and Metal Ceramics*, vol. 33, pp. 555-557, 1994.

[67] Haeberle, D.C. et al. “Performance and interfacial stresses in the polymer wear surface/FRP deck bond due to thermal loading”. *Advanced Composite Materials in Bridges and Structures: 3rd International Conference*, Ottawa, Canada, 2000, pp. 13-15.

[68] Wang, Y. et al. “Concrete Reinforcement with Recycled Fibers”. *Journal of Materials In Civil Engineering*, vol. 12, pp. 314-319, 2000.

[69] Ochia, T. et al. “Development of recycled PET fiber and its application as concrete-reinforcing fiber”. *Cement and Concrete Composites*, vol. 29, No. 6, pp. 448-455, 2007.

[70] Karmaker, A.C. and Youngquist, J.A. “Injection Molding Of Polypropylene Reinforced With Short Jute Fibers”. *Journal of Applied Polymer Science*, vol. 68, No. 8, pp. 1147-1151, 1996.

[71] Chand, N. and Hashmi, S.A.R. “Mechanical Properties of Sisal Fiber at Elevated Temperature”. *Journal of Material Science*, vol. 28, pp. 6724-6728, 1993.

[72] Zastrau, B. et al. “The Analytical Solution of Pullout Phenomena in Textile Reinforced Concrete”.

- Journal of Engineering Materials and Technology*, vol. 125, No. 1, pp. 38-43, 2003.
- [73] Neville, A.M. “*Properties of Concrete*”. Pearson Education Asia Pvt. Ltd., London, 2000.
- [74] Gartner, E. M.et.al , “*Hydration Of Portland Cement Structure and Performance Of Cements*” ,Bensted, J. & Barnes, P. Eds. Spoon Press, London, 2002.
- [75] Keller, T. “Use of Fiber Reinforced Polymers in Bridge Construction”. *International Association for Bridge and Structural Engineering. Zurich*, 2003.
- [76] Gururaja M.N. and Rao, A.N.H. “A Review on Recent Applications and Future Prospectus of Hybrid Composites”. *International Journal of Soft Computing and Engineering*, vol. 1, No. 6, pp. 352-355, 2012.
- [77] Kawabata, S. et al. “The finite-deformation theory of plain weave fabrics. Part I: the biaxial-deformation theory”. *Journal of Textile Institute*, vol. 64, No. 1, pp. 21-46, 1973.
- [78]Kawabata, S. et al. “The finite-deformation theory of plain weave fabrics. Part II: the uniaxial-deformation theory”. *Journal of Textile Institute*, vol. 64, No. 2, pp. 47-61, 1973.
- [79]Kawabata, S. et al. “The finite-deformation theory of plain weave fabrics. Part III: the shear-deformation theory”. *Journal of Textile Institute*, vol. 64, No. 2, pp. 62-85, 1973.
- [80]King, M. et al. “A continuum constitutive model for the mechanical behavior of woven fabrics”. *International Journal of Solids and Structures*, vol. 42, No. 13, pp. 3867-3896, 2005.
- [81]Klosterhalfen, B. et al. “The lightweight and large porous mesh concept for hernia repair”. *Expert Review of Medical Devices*, vol. 2, No. 1, pp. 103-117, 2005.
- [82]Nadler, B. et al. “Multiscale constitutive modeling and numerical simulation of fabric material”. *International Journal of Solids and Structures*, vol. 43, No. 2, pp. 206-221, 2006.
- [83]Nayfeh, A. and Kress, G. “Non-linear constitutive model for plain-weave composites”. *Composites part B Engineering*, vol. 28, No. 5-6, pp. 627-634, 1997.
- [84]Röhrnbauer, B. and Mazza, E. “A non-biological model system to simulate the in vivo mechanical behavior of prosthetic meshes”. *Journal of the Mechanical Behavior of Biomedical Materials*, vol. 20, pp. 305–315, 2013.
- [85]Antonietti, P. et al. “Theoretical study and numerical simulation of textiles”. *Applied Mathematical Modelling*, vol. 35, No. 6, pp. 2669-2681, 2011.
- [86]Assidi, M. et al. “Equivalent properties of monolayer fabric from mesoscopic modelling strategies”. *International Journal of Solids and Structures*, vol. 48, No. 20, pp. 2920-2930, 2011.
- [87]Boubaker, B. et al. “Discrete woven structure model: yarn on-yarn friction”. *Comptes Rendus de l'Académie des Sciences-Series IIB-Mechanics-Physics-Astronomy*, vol. 335, No. 3, pp. 150-158, 2007.
- [88] Vandeurzen, P. et al. “Micro-stress analysis of woven fabric composites by multilevel decomposition”. *Journal of Composite Materials*, vol. 32, No. 7, pp. 632-651, 1998.
- [89] Gommers, B. et al. “The Mori-Tanaka method applied to textile composite materials”. *Acta Materials*, vol. 46, No. 6, pp. 2223-2235, 1998.
- [90] Lomov, S.V. and Truevtzev, N.N. “A software package for the prediction of woven fabrics geometrical and mechanical properties”. *Fibres & Textiles in Eastern Europe*, vol. 3, No. 2, pp. 49-52, 1995.
- [91] Lomov, S.V. et al. “Two-component multilayered woven fabrics: weaves, properties and computer simulation”. *International Journal of Clothing Science & Technology*, vol. 9, pp. 98-112, 1997.
- [92] Lomov, S.V. and Gusakov, A.V. “Mathematical modelling of 3D and conventional woven fabrics”. *International Journal of Clothing Science & Technology*, vol. 10, No. 6, pp. 90-91, 1998.
- [93] Lomov, S.V. et al. “Textile geometry preprocessor for meso-mechanical models of woven composites”. *Composites Science and Technology*, vol. 60, pp. 2083-2095, 2000.
- [94] Lomov, S.V. et al. “Mathematical modelling of internal geometry and deformability of woven preforms”. *International Journal of Forming Processes*, vol. 6, No. 3-4, pp. 413-442, 2003.
- [95] Lomov, S.V. et al. *Manufacturing and internal geometry of textiles. Design and manufacture of textile composites*. A. C. Long, Woodhead, 2005, pp. 1-60.
- [96] Lomov, S.V. and Verpoest, I. “Model of shear of woven fabric and parametric description of shear resistance of glass woven reinforcements”. *Composites Science and Technology*, vol. 96, pp. 919-993, 2006.

- [97] Hu, J. *Structure and mechanics of woven fabrics*. Woodhead Pub., ISBN 0-8493-2826-8, Cambridge, 2004.
- [98] Saville, B. *Physical testing of textiles*. Woodhead Publishing and CRC Press, ISBN 1- 85573-367-6, Cambridge, 2002.
- [99] Dai, X. et al. "Simulating Anisotropic Woven Fabric Deformation with a New Particle Model". *Textile Research Journal*, vol. 73, No. 12, pp. 1091-1099, 2003.
- [100] Kilby, W.F. "Planar stress-strain relationships in woven fabrics". *Journal of Textile Institute*, vol. 54, pp. 9-27, 1963.
- [101] Kovar, R. and Gupta, B.S. "Study of the Anisotropic Nature of the Rupture Properties of a Woven Fabric". *Textile Research Journal*, vol. 79, No. 6, pp. 506-506, 2009.
- [102] Lo, M.W. and Hu, J.L. "Shear Properties of Woven Fabrics in Various Directions". *Textile Research Journal*, vol. 72, No. 5, pp. 383-390, 2002.
- [103] Kilby, W.F. "Shear Properties in Relation to Fabric Hand". *Textile Research Journal*, vol. 31, pp. 72-73, 1961.
- [104] Vanclooster K. et al. "Investigation of interply shear in composite forming". *International Journal of Material Forming*, vol. 1, pp. 957-960, 2008.
- [105] Tyrone Lv. *Textile Processing and Properties Preparation, Dyeing, Finishing and Performance*. Elsevier. ISBN: 978-0-444-88224-0, 1994.
- [106] Long A.C. et al. "Characterizing the processing and performance of aligned reinforcements during preform manufacture". *Composites: Part A*, vol. 27, pp. 247-253, 1996.
- [107] Grosberg, P. and Park, B.J. "The mechanical properties of woven fabrics. Part V. The initial modulus and the frictional restraint in shearing of plain weave fabrics". *Textile Research Journal*, vol. 36, pp. 420-431, 1966.
- [108] Domskiene, J. and Strazdien, E. "Investigation of fabric shear behavior". *Fibres & Textiles in Eastern Europe*, vol. 13, No. 2(50), 2005.
- [109] Potluri, P. et al. Biaxial shear testing of textile performs for formability analysis. *16th International Conference on Composite Materials*. 2007
- [110] Basset, R. and Postle, R. "Experimental methods for measuring fabric mechanical properties: A review and analysis". *Textile Research Journal*, vol. 69, No. 11, pp. 866-875, 1999.
- [111] Zhu B, Yu TX and Tao XM. "Large deformation and slippage mechanism of plain woven composite in bias extension". *Compos Part A- Appl S*. vol. 38, pp. 1821-1828, 2007.
- [112] Willems A, Lomov SV, Verpoest I and Vandepitte D. "Picture frame shear tests on woven, textile composite reinforcements with controlled pretension". *In: 10th ESAFORM conference on material forming, Parts A and B 2007*: 999-1004.
- [113] Lin H, Clifford MJ, Long AC and Sherburn M. "Finite element modelling of fabric shear". *Model Simul Mater Sci* 2009; 17: 1-16.
- [114] Lyman, F. and Hollies, N.R.S. "Clothing Comfort and Function" in *Fiber Science Series*, L. Rebenfeld, Series Ed. Marcel Dekker Inc., New York. 1970
- [115] Hes L. "Recent Developments in The Field Of User Friendly Testing Of Mechanical And Comfort Properties Of Textile Fabrics And Garments" *World Congress Of The Textile Institute*, Cairo, March, 2002.
- [116] Xiao, X. et al. "Through-thickness air permeability of woven fabric under low pressure compression". *Textile Research Journal*, vol. 85, pp. 1732-1742, 2015.
- [117] Cha, J. et al. "Building Materials Thermal Conductivity Measurement and Correlation with Heat Flow Meter, Laser Flash Analysis and Tci". *Journal of Thermal Analysis and Calorimetry*, vol. 109, pp. 295-300, 2012.
- [118] Venkataraman, M. et al. "Novel Techniques To Analyse Thermal Performance Of Aerogel-Treated Blankets Under Extreme Temperatures". *The Journal of the Textile Institute*, vol. 106, No. 7, pp. 736-747, 2015.
- [119] Militký J. and Křemenáková D. "A Simple Methods for Prediction of Textile Fabrics Thermal Conductivity". *Hefat, 5th International Conference On Heat Transfer, Fluid Mechanics And*

Thermodynamics Sun City, South Africa ,Paper Number: Pj4, 2007.

[120] Ukponmwan, J.O. “The Thermal Insulation Properties of Fabric”. *Textile Progress*, vol. 24, No. 4, pp. 1-54, 1993.

[121] Bal, K. and Kothari, V.K. “A theoretical model to predict thermal resistance of plain woven fabric”. *Indian Journal of Fiber and Textile Research*, pp. 252-257, 2005.

[122] Kuvandykova, D. “A new transient method to measure thermal conductivity of asphalt”. *C-Therm Technologies*, vol. 7, pp. 1-10, 2010.

[123] Melling, A. “Tracer particles and seeding for particle image velocimetry”. *Measurement Science and Technology*, vol. 8, pp. 1406-1416, 1997.

[125] Bedeloglu, A. “Investigation Of Electrical, Electromagnetic Shielding, And Usage Properties Of Woven Fabrics Made From Different Hybrid Yarns Containing Stainless Steel Wires”. *The Journal of the Textile Institute*, vol. 104, No. 12, pp. 1359-1373, 2013.

[126] Hearle, J.W.S. “The electrical resistance of textile materials: I. The influence of moisture content”. *The Journal of the Textile Institute*, vol. 44, No. 4, pp. 117-143, 1953.

[127] Hearle, J.W.S. “Capacity, dielectric constant, and power factor of fiber assemblies”. *Textile Research Journal*, vol. 24, No. 4, pp. 307-321, 1954.

[128] Asanovic, K.A. et al. “Investigation of the electrical behavior of some textile materials”. *Journal of Electrostatics*, vol. 65, No. 3, pp. 162-167, 2007.

[129] Safárová, V. and Militký, J. “Electromagnetic shielding properties of woven fabrics made from high-performance fibers”. *Textile Research Journal*, vol. 84, pp. 1255-1267, 2014.

[130] AssagraI, Y.A.O. et al. “Laminated composite based on polyester geotextile fibers and polyurethane resin for coating wood structures”. *Material Research*, vol.16, No.5, 2013.

[131] Hogue, M.D. et al. “Triboelectric, Corona, and Induction Charging of Insulators as a Function of Pressure”. *Journal of Electrostatics*, vol. 65, No. 4, pp. 274-279, 2007.

[132] Aso, K. and Kinoshita, R. “Absorption of sound wave by fabrics, Part 1: Absorption mechanism”. *Textile Machinery Society of Japan*, vol. 8, No. 1, pp. 32-39, 1963.

[133] Aso, K. and Kinoshita, R. “Absorption of sound wave by fabrics, Part 3: Flow resistance”. *Textile Machinery Society of Japan*, vol. 10, No. 5, pp. 236-241, 1964.

[134] Aso, K. and Kinoshita, R. “Sound absorption characteristics of fiber assemblies”. *Textile Machinery Society of Japan*, vol. 10, No. 5, pp. 209-217, 1964.

[135] Na, Y.J. et al. “Sound absorption coefficients of micro-fiber fabrics by reverberation room method”. *Textile Research Journal*, vol. 77, No. 5, pp. 330-335, 2007.

[136] Lee, Y.E and Joo, C.W. “Sound absorption properties of recycled polyester fibrous assembly absorbers”. *AUTEX Research Journal*, vol. 3, No. 2, pp. 77-84, 2003.

[137] Marjanovic, L. et al. “Analysis of cement by inductively coupled plasma optical emission spectrometry using nebulization”. *Journal of Analytical Atomic Spectrometry*, vol. 15, pp. 983-985, 2000

[138] Lomov, S.V. and Truevtzev, N.N. “A software package for the prediction of woven fabrics geometrical and mechanical properties”. *Fibres and Textiles in Eastern Europe*, vol. 3, No. 2, pp. 49-52, 1995.

[139] Lomov, S.V. et al. “Textile geometry preprocessor for meso-mechanical models of woven composites”. *Composites Science and Technology*, vol. 60, pp. 2083-2095, 2000.